

**Advantages and limitations of spectroscopic,
chromatographic and electrophoretic methods for the
characterisation of synthetic cannabinoids and synthetic
cathinone derivatives**

Dissertation

der Mathematisch-Naturwissenschaftlichen Fakultät
der Eberhard Karls Universität Tübingen
zur Erlangung des Grades eines
Doktors der Naturwissenschaften
(Dr. rer. nat.)

vorgelegt von
Sonja Metternich
aus Koblenz

Tübingen
2020

Gedruckt mit Genehmigung der Mathematisch-Naturwissenschaftlichen Fakultät der Eberhard Karls Universität Tübingen.

Tag der mündlichen Qualifikation:

08.06.2020

Dekan:

Prof. Dr. Wolfgang Rosenstiel

1. Berichterstatter:

Prof. Dr. Carolin Huhn

2. Berichterstatter:

Prof. Dr. Jürgen Pomp

Table of contents

Table of contents	i
Abstract	3
Zusammenfassung	4
1 Introduction	5
1.1 New psychoactive substances - a never ending-story	5
1.1.1 Synthetic cannabinoids	6
1.1.2 Synthetic cathinone derivatives	8
1.2 NPS analytics - a challenging task in Forensic Science	9
1.2.1 Presumptive tests	10
1.2.2 Optical spectroscopy	12
1.2.3 Separation Techniques	14
1.2.4 Chiral analysis	15
2 Ion mobility spectrometry as a fast screening tool for synthetic cannabinoids to uncover drug trafficking in jail via herbal mixtures, paper, food, and cosmetics	17
2.1 Abstract	17
2.2 Introduction	17
2.3 Materials and Methods	21
2.3.1 Chemicals	21
2.3.2 Methodology: Characterization of NPS powders from seizures	23
2.4 Results	27
2.4.1 Characterization of NPS with UPLC, GC-MS and NMR	27
2.4.2 IMS measurements	31
2.5 Discussion	38
2.6 Conclusion	40
3 Discrimination of synthetic cannabinoids in herbal matrices and of synthetic cathinone derivatives by portable and laboratory-based Raman spectroscopy	41
3.1 Abstract	41
3.2 Introduction	41
3.3 Materials and Methods	43
3.3.1 Chemicals	43
3.3.2 Methodology	46
3.3.3 Data treatment and chemometrics	48
3.4 Results and discussion	49
3.4.1 Comparison of different Raman spectrometers	49
3.4.2 Principal Component Analysis	53
3.4.3 Characteristic Raman bands for both, synthetic cathinone derivatives and synthetic cannabinoids	56
3.4.4 Identification of synthetic cannabinoids in 60 herbal mixtures from casework samples	69
3.5 Conclusion	73
4 Terahertz spectroscopy for the contactless and non-destructive detection of synthetic cannabinoids to uncover drug trafficking	74
4.1 Abstract	74
4.2 Introduction	74
4.3 Materials and Methods	77
4.3.1 Chemicals	77

4.3.2	Methodology: Characterisation of NPS powders from seizures	78
4.4	Results	83
4.4.1	Characterisation of NPS with GC-MS and NMR	83
4.4.2	THz procedure	83
4.4.3	Model applications and matrix tolerance	91
4.5	Discussion	94
4.6	Conclusion.....	97
5	Structural similarity of synthetic cannabinoids in herbal mixtures allows to cross-calibrate analytes without reference material by UPLC-DAD	98
5.1	Abstract	98
5.2	Introduction	98
5.3	Materials and Methods	100
5.3.1	Chemicals	100
5.3.2	Methodology	103
5.4	Results and discussion.....	104
5.4.1	Characterisation of reference samples including NMR and GC-MS.....	104
5.4.2	Evaluation of the UPLC-DAD method	105
5.4.3	Application to casework samples	117
5.5	Conclusion.....	119
6	Chiral discrimination of NPS using CE-DAD: Enantioselective separation of synthetic cathinone derivatives by capillary electrophoresis with UV.....	120
6.1	Abstract	120
6.2	Introduction	120
6.3	Materials and Methods	123
6.3.1	Chemicals	123
6.3.2	Methodology	127
6.4	Results and discussion.....	128
6.4.1	Chiral separation optimisation	128
6.4.2	Selection of internal standard	133
6.4.3	Figures of merit	133
6.4.4	Applications	139
6.5	Discussion	142
6.5.1	Interaction of synthetic cathinone derivatives with HS- β -CD	142
6.5.2	Comparison of the screening method and high-throughput method with literature methods	144
6.6	Conclusion.....	147
7	Comparison of all analytical techniques applied.....	148
7.1	On site analysis - best choice for a presumptive test.....	148
7.2	Identification strength: the characterisation of unknowns	154
7.3	Quantification of NPS	155
7.4	Chiral discrimination of NPS	157
8	Conclusion.....	160
	References	163
	Supervision and Project partners	184
	Own contribution in the chapters	187
	Abbreviations	189
	Acknowledgement.....	191
	List of Publications and scientific contributions	192

Abstract

Over the last decade new psychoactive substances (NPS) flooded Europe and the challenging task for drug law enforcement is how to effectively respond to the dynamically and constantly changing drug market. NPS are regarded as legal alternatives to internationally controlled drugs of abuse. NPS are sold via the internet as, inter alia, “designer drugs”, “legal highs”, or “bath salts” in colourful and professionally designed packages mixed with herbal products or as pure powder. There is a persisting race between the legal prosecution and the producers of designer drugs as those strive to be one step ahead by rapidly generating new NPS products in reaction to new legislative measures. The rapid emergence of novel products means that developing and maintaining selective analytical methods and reference standards is challenging. Beside laboratory methods, the demand for portable analytics is high given the versatile distribution channels and the related particular risk for public institutions handling these products including postal delivery facilities, custom controls and prisons.

In this thesis, new analytical methods were developed for the detection of synthetic cannabinoids and synthetic cathinones, the most frequently seized NPS subgroups. An ion mobility spectrometry (IMS) method was developed as an in-field alternative presumptive test for the non-destructive and selective detection of NPS in different matrices by wiping the surface of a sample with a swab. The suitability of the method for on-site analysis was demonstrated in a prison in Rhineland-Palatinate. The contactless and non-destructive detection of NPS was investigated using THz radiation for the first time.

Fast characterisation of newly emerged and unknown substances was examined using portable and laboratory-based Raman spectrometers. Data analysis used a combination of a newly developed principal component analysis model and frequency tables. In addition, it was shown, that the analysis of herbal mixtures was possible using a simple solid/liquid extraction followed by precipitation of the synthetic cannabinoid constituents. New laboratory methods were developed to complement the screening techniques. The possibility to quantify NPS via the calibration curves of a small set of NPS, for which reference material is commercially available was demonstrated and validated via the analysis of seizures using ultra-performance liquid chromatography-diode array detection. Finally, capillary electrophoresis-diode array detection with a chiral selector was used for the chiral discrimination of NPS in the form of a general unknown screening method for mixtures and bulking agents on the one hand and a high throughput method for the fast analysis of single substances on the other hand. With the methods developed here, the analytical portfolio of NPS drug analysis was greatly expanded to meet the challenges of the dynamically and constantly changing drug market. All methods were successfully applied to real samples and partly in routine analysis in different criminal investigations offices and in public institutions (Wittlich prison).

Zusammenfassung

Seit Jahren halten neue psychoaktive Substanzen (NPS) Einzug in den europäischen Drogenmarkt und stellen die Drogenpolitik vor große Herausforderungen. NPS werden meist über das Internet als "Designerdrogen", "Legal Highs" oder "Badesalze" verkauft und gelten als legale Alternative zu international kontrollierten Drogen. Die Produkte werden meist in bunten und professionell gestalteten Verpackungen vermarktet, entweder als reines Pulver oder auf bestimmten Matrices wie Kräutermischungen. Es existiert ein Wettlauf zwischen dem In-Verkehr-Bringen immer neuer chemischer Varianten bekannter Stoffe und den anzupassenden strafrechtlichen Verfolgungen und die dynamische Verbreitung neuer NPS-Produkte fordert die Entwicklung selektiver Analysemethoden und Referenzstandards. Neben dem Einsatz von laborbasierten Methoden wächst die Nachfrage an portablen Analysetechniken in öffentlichen Einrichtungen wie z.B. Postverteilerzentren, Zollkontrollstellen und Gefängnissen, die meist unwissentlich mit diesen Produkten in Kontakt kommen. Die hier vorgestellte Arbeit beschreibt die Entwicklung neuer Methoden für die Analyse von synthetischen Cannabinoiden und synthetischen Cathinonen, der zwei am häufigsten sichergestellten NPS-Substanzklassen. Ein alternativer Schnelltest für den zerstörungsfreien und selektiven Nachweis von NPS in unterschiedlichen Matrices wurde mittels portablen Ionenmobilitätsspektrometrie entwickelt. Die Anwendung des Verfahrens wurde in einer rheinland-pfälzischen Justizvollzugsanstalt nachgewiesen. Außerdem wurde erstmals die berührungslose und zerstörungsfreie Analyse von NPS mittels THz-Strahlung diskutiert. Für die Anwendung portabler und laborbasierter Raman-Spektrometer wurde eine Referenzdatenbank, ein chemometrisches Hauptkomponenten-Modell und spezifische Raman Frequenztabellen entwickelt, die in ihrer Kombination eine schnelle und effektive Charakterisierung von bekannten, aber auch unbekanntem Substanzen ermöglichen. Es wurden laborbasierte Techniken zur Identifizierung und Quantifizierung von synthetischen Cannabinoiden und Cathinonen entwickelt. Eine effiziente Quantifizierung von synthetischen Cannabinoiden mittels Hochleistungsflüssigkeitschromatographie- Diodenarray Detektion wurde anhand sichergestellter Asservate demonstriert und validiert, indem Kalibrierkurven eines definierten Satzes ausgewählter und kommerziell verfügbaren Referenzsubstanzen verwendet wurden. Zum anderen wurden ein Screening Verfahren und eine High-throughput-Methode für die chirale Diskriminierung von synthetischen Cathinonen mittels Kapillarelektrophorese-Diodenarray-Detektion entwickelt. Mithilfe dieser Arbeit wurde das analytische Portfolio von Analysemethoden für die Charakterisierung von NPS stark erweitert, um somit den Herausforderungen des dynamischen Drogenmarkts gerecht zu werden. Alle Methoden wurden erfolgreich an Realproben getestet und werden teilweise in der Routineanalytik in verschiedenen Kriminalämtern und in öffentlichen Einrichtungen (Gefängnis Wittlich) eingesetzt.

1 Introduction

1.1 New psychoactive substances - a never ending-story

The continuous emergence of new psychoactive substances (NPS) on the recreational and illicit drug market has challenged law enforcement, executive apparatus, public health authorities and forensic and toxicological laboratories. The substances are marked as purportedly “legal” alternatives to internationally controlled drugs under various names such as “designer drugs”, “legal highs”, “herbal highs”, “bath salts”, “research chemicals” or “laboratory reagents”.¹ NPS have initially been designed to mimic established illicit drugs, such as cannabis, cocaine, amphetamine and LSD.^{2,3} The United Nations Office on Drugs and Crime (UNODC) established a clear terminology: “New psychoactive substances are substances of abuse, either in a pure form or a preparation, that are not controlled by the 1961 Single Convention on Narcotic Drugs⁴ or the 1971 Convention on Psychotropic Substances,⁵ but which may pose a public health threat. In this context, the term ‘new’ does not necessarily refer to new inventions but to substances that have recently become available”.⁶

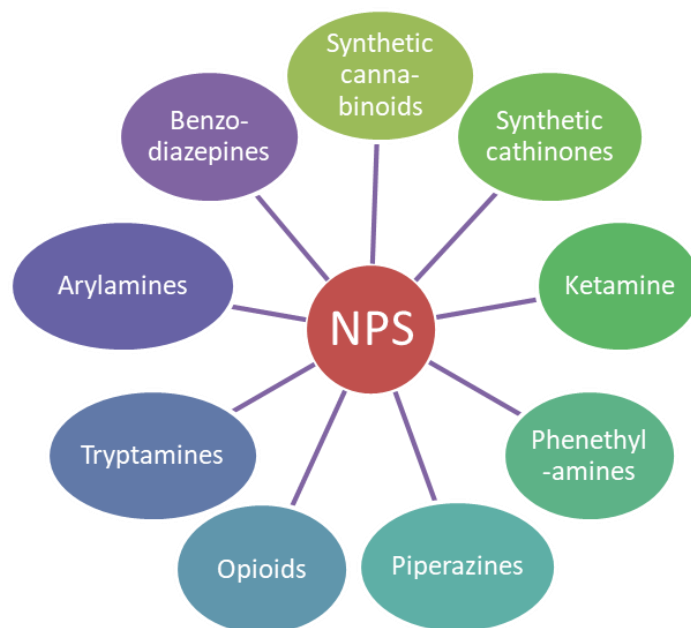


Figure 1-1 NPS subclasses⁷

The word NPS comprises several substance classes which are summarised in Figure 1-1. Synthetic cannabinoids and synthetic cathinones represented 51 % and 24 % of the most frequently seized new psychoactive substances in 2017, followed by benzodiazepines with 5 % and opioids with 2 %.⁸ These percentages challenge the legislative drug control authorities. In some European countries, only specific substances are listed in the drug law

and even small modifications in the chemical structure of such listed substances already allow circumventing existing law.⁹ Consequently there is a race between the legal prosecution and the producers as those strive to be one step ahead by generating new NPS-products. The physiological and psychological effects they have in NPS-consumers are unpredictable and sometimes fatal as there is no information about the active drug given on the product label.¹⁰⁻¹² National or international commissioning and support are required, hence, the European Monitoring Centre for Drugs and Drug Addiction (EMCDDA) implemented an early warning system¹³ in the European Union under the terms of a Council Decision 2005/387/JHA¹⁴ to guarantee a rapid exchange of information and provide a risk assessment for new psychoactive substances. By the end of December 2018, the EMCDDA described more than 700 new substances that have appeared on Europe's drug market over the past 20 years.

1.1.1 Synthetic cannabinoids

Synthetic cannabinoids are the largest group of new substances monitored by the EMCDDA and are becoming increasingly diverse with regard to their chemical structure. Synthetic cannabinoids were initially designed to mimic the effects of delta 9-tetrahydrocannabinol (THC) in cannabis products. Synthetic cannabinoids bind to the same cannabinoid receptors (CB1 and CB2) as THC which explains their psychotropic effects.³ The adverse events associated with synthetic cannabinoids include agitation and nausea and an abnormally fast, racing heartbeat. However, also serious adverse events were reported such as stroke, seizure, heart attack, breakdown of muscle tissue, kidney damage, psychosis and severe or prolonged vomiting and associated deaths.¹⁵



Figure 1-2 Packaging materials of herbal mixtures

The major manufacturers of the synthetic cannabinoids are chemical companies based in China.¹⁶ Substances are shipped as bulk powders to Europe using express mail and courier companies or air and sea cargo.¹⁵ Then, in Europe, synthetic cannabinoid powders are dissolved in a solvent such as acetone and sprayed onto the surface of dried plant material

upon stirring. The solvent is evaporated while a thin coating of synthetic cannabinoid is deposited.² Damiana (*Turnera diffusa*) and Lamiaceae herbs such as Melissa, Mentha and Thymus are commonly used as the plant base.^{15,16} Herbal mixtures are sold in colourful and professionally designed packages as substitutes for cannabis with misleading product descriptions such as “herbal incense” (see Figure 1-2).^{16,17} Due to the high potency of some synthetic cannabinoids, the amount of powder needed for each packet can be in the order of a few tens of milligrams. Synthetic cannabinoids have four major structural elements: tail, core, linker and linked group (see Figure 1-3). Common core groups are indole, indazole, carbazoles, azaindoles and gamma-carbolines. The structural variability leads to different synthesis routes of synthetic cannabinoids. For example, aminoalkylindoles are synthesised via Friedel-Crafts acylation at C3 followed by N-alkylation of a (substituted) indole represents and common precursors are 1-alkylindoles and 1-alkyl-2-methylindoles (alkyl: butyl, pentyl, hexyl or others, halogenated if applicable) or 1-naphthoyl chlorides (e.g. substituted at C4).²

In most cases the nomenclature is related to the components of the chemical structure which allows to identify a synthetic cannabinoid without knowing the IUPAC name. The proposed naming syntax follows the rule: LinkedGroup-Tail-Core-Linker. In Figure 1-3, the name AB-CHMINACA is an abbreviation from its chemical name: N-[(2S)-1-amino-3-methyl-1-oxobutan-2-yl]-1-(cyclohexylmethyl)indazole-3-carboxamide.

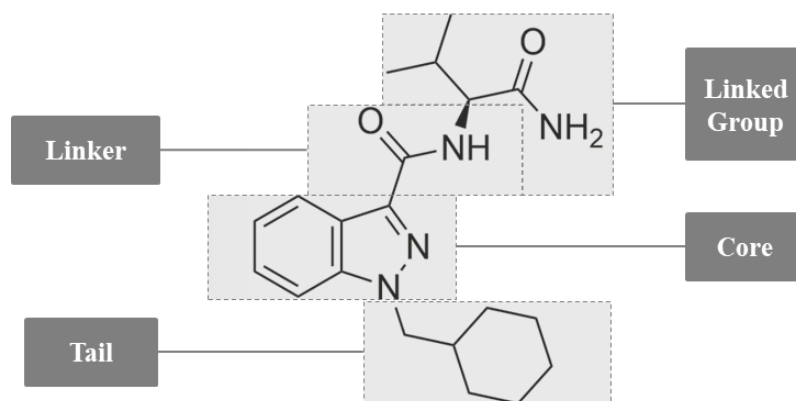


Figure 1-3 Structural elements of synthetic cannabinoids including the core, a linker, its linked group and the tail, exemplified for AB-CHMINACA

Some synthetic cannabinoids were named according to their inventors, e.g. “JWH” after John W. Huffman or “AM” after Alexandros Makriyannis. Alternatively, the institution or company where they were first synthesised like ‘HU’ series of synthetic cannabinoids being from the Hebrew University in Jerusalem, or ‘CP’ from Carl Pfizer. Some names follow marketing strategies like AKB-48, which is the name of a popular Japanese girl band, or XLR-11, which was named after the first liquid fuel rocket developed in the USA.¹⁵

1.1.2 Synthetic cathinone derivatives

Synthetic cathinone derivatives are chemically related to cathinone, the major active ingredient in the Khat plant.¹⁸ Synthetic cathinone derivatives are members of the phenethylamine family, which also includes amphetamine and methamphetamine. The essential distinctive characteristic for synthetic cathinone derivatives is the presence of a β -keto group at the side chain of the phenethylamine (see Figure 1-4). Typically, synthetic cathinone derivatives are amphetamine type analogues, i.e. cathinone, ephedrone, and methylone are structurally related to amphetamine, methamphetamine and MDMA (3,4-Methylenedioxyamphetamine), respectively, and thus show similar stimulant effects to common illicit drugs.¹⁹

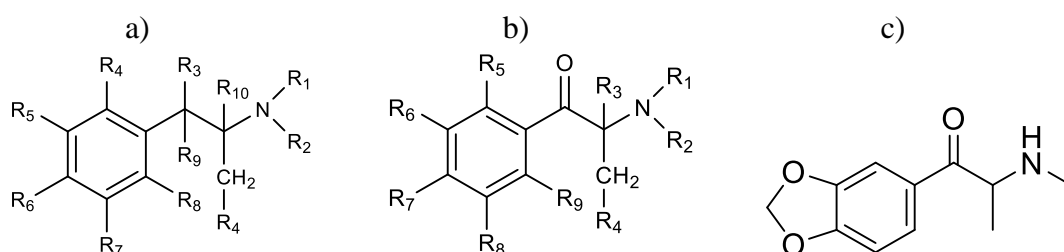


Figure 1-4 General chemical structures of a) phenethylamines, b) general structure of cathinones, and c) the synthetic cathinone methylone

Thus, stimulation of the central nervous system via effects on the levels and action of neurotransmitters such as serotonin, dopamine and noradrenaline was reported.¹⁹⁻²² Many synthetic cathinone derivatives have a single chiral centre and thus exist in two enantiomeric forms with differing potencies.²³ Synthetic cathinone derivatives show a variety of behavioural effects including cardiac, psychiatric, and neurological signs,²⁰ but also short-term adverse effects were reported including loss of appetite, blurred vision, anxiety, post-use depression, confusion, hallucinations, short-term psychosis and mania.^{24,25} Intoxication by synthetic cathinones derivatives may also lead to severe adverse effects, including acute liver failure, acute kidney injury, high blood pressure and tremor.²⁶ In contrast to synthetic cannabinoids, synthetic cathinones derivatives are usually marketed as powder, in pill or capsule form and sold as “research chemicals” or “bath salts”. Most synthetic cathinones derivatives appearing on the European market were synthesised outside Europe, with China and, to a lesser extent, India identified as the primary sources.²⁷

The synthesis of synthetic cathinone derivatives is analogous to the manufacture of amphetamine and MDMA-related substances including 1) reductive amination and 2) the Leuckart reaction, both with an aromatic ketone as precursor, 3) the use of aromatic aldehydes under Knoevenagel conditions²⁸ and 4) the oxidation of the readily available pharmaceuticals pseudoephedrine and ephedrine.^{27,29} The routes 1) and 2) are the most common production processes found in clandestine laboratories. Here, the precursors like ketones contain a

stereogenic center at the β -carbon of the ketone structure.^{5,30} In 1929, Saem de Burnaga Sanchez published a synthetic strategy for mephedrone as the first synthetic cathinone derivative starting with 1-tolylpropan-1-one as precursor, which was α -brominated and then reacted with methylamine to produce racemic 4-methylmethcathinone.³¹ Today, almost all synthetic cathinone derivatives exist as racemic mixtures.²⁶ Synthetic cathinone derivatives are taken by insufflation, orally or, less common, via injection.

1.2 NPS analytics - a challenging task in Forensic Science

From an analytical point of view, the constantly changing availability of new substances poses the challenge to develop new methods and techniques for the identification and quantification of NPS, partly in mixtures and/or different matrices. Beside the characterisation of substances, quantification of samples is essential to determine the active ingredient content relevant for prosecution. The demand for both laboratory-based and portable analytical techniques is constantly increasing. The emergence of new drugs has created a need for reference material in order to verify their identification and especially to enable their quantification by routine laboratory methods such as HPLC. The in-house production of reference material entails capital investment, running costs, as well as operation of advanced analytical instruments and data interpretation.³² Therefore, analytical data for various recently launched NPS are lacking which impedes the analysis of casework samples. Reference spectral libraries should constantly be updated to keep up with the vast variety of substances available. Only a few techniques are able to identify a substance without a reference standard e.g. nuclear magnetic resonance (NMR) and mass spectrometry (MS). In addition, NMR is an absolute method and therefore suitable for the quantification of substances.

A special problem, when no reference material is available, is the correct identification of positional isomers or enantiomers, which has been recognized to be of increasing relevance. This is due to the fact that their effects on humans are different and the level of legal penalties conforms to a specific isomer which is listed in drug laws. This also holds true for e.g. mass spectrometric analysis.³³ A particular challenge lies in the analysis of synthetic cannabinoids, as they are often added to herbal mixtures. Here, the strategy for analysis is different to classical herbal drugs such as cannabis or drugs in other processed forms such as heroin, cocaine and amphetamine-type-stimulants: special sample preparation techniques or analytic techniques without any further extraction process have to be designed to guarantee a simple and fast analysis of seized samples. Sufficiently sensitive methods are necessary due to the low concentrations (typically 5-30 mg/g) in the herbal matrix with possible interferences from matrix constituents.² In case of synthetic cathinone derivatives, the presence of bulking agents and extenders has to be taken into account already during method development. The following chapters provide insight into the current state of technology of NPS analytics.

1.2.1 Presumptive tests

The demand for rapid drug detection by police, customs, federal armed forces, prisons and other public institutions is growing.³⁴ However, the applicability of rapid drug testing for NPS is limited. In general, to uncover drug trafficking the police uses relatively simple presumptive tests with colour coding for specific drugs.



Figure 1-5 Typical police roadside presumptive tests used in Rhineland- Palatinate

Usually the Duquenois–Levine colour test is used for classical cannabinoids such as THC and the van Urk colour test is used for indole-containing drugs of abuse. However, both colour tests show negative results in the identification of synthetic cannabinoids. Isaac et al. tested an alternative colour test reagent, 2,4-dinitrophenylhydrazine, which reacts with a keto moiety. Therefore, it is capable of reacting with synthetic cannabinoids, such as the naphthoylindole, phenylacetylindole, benzoylindole, and cyclopropylindole classes. The analysis was carried out with substances either in powders or adsorbed onto plant material. No limits of detection (LOD) was given in the article, the solution tested contained at least 10 mg of synthetic cannabinoid powder suspended in 1 mL methanol.³⁵ Moreover, synthetic cannabinoids which do not contain a ketone did not react. Two further colour tests commonly applied are the Marquis test, which reacts with all nitrogen-containing drugs, and the Dragendorff test, which is positive for the JWH series. In addition, fast blue BB (4-benzamido-2,5-diethoxybenzene diazonium chloride hemi zinc salt) reacts with cyclohexylphenols.³⁶

The colour coding detection of synthetic cathinone derivatives differs from that of synthetic cannabinoids. The Marquis reagent, which reacts with all nitrogen-containing drugs, is negative for cathinones without substituents or having only a methyl-substitution at the benzene ring like in cathinone itself and in mephedrone. For synthetic cathinone derivatives with a methylenedioxy moiety, the test also gives positive results. LODs are not reported. Thus, generally the combination of more than one reagent is required including Marquis, Ehrlich, Simon, Lieberman-Burehand, and Mandelin reagents to detect synthetic cathinone derivatives in samples.³⁷⁻³⁹

In addition to colour coding tests, immunoassays based on an antibody-antigen interaction are applied. Some commercially available immunoassay kits have been developed for the detection of specific synthetic cannabinoids like the JWH-type substances in urine, available on the drug market for a rather long time now.⁴⁰ Every emerging synthetic cannabinoid would require a new and rather time-consuming development of a specified immunoassay.

No commercial immunoassay is available for synthetic cathinone derivatives. Some researchers studied the detection of synthetic cathinones in urine using immunoassay technology,^{41,42} but some of them obtained false-positive results. For example, MDPV (methylenedioxypropylvalerone) showed cross reactivity with phencyclidine.⁴³

Thin layer chromatography (TLC) is a technique commonly used for the separation and identification of illicit drugs in the laboratory and is not part of the portable analytical techniques portfolio. The identification is possible via the retention factor in comparison to reference standards, which have to be available.

Commonly, dissolved powders or extracts of herbal mixtures are prepared at a concentration of approximately 1 mg/mL in methanol. Afterwards 1 μ L spots, 2 μ L of the standard solutions and 2 μ L of solvent (as a negative control) are applied on the TLC plate.^{2,27} In some publications, retention factors for NPS were determined.^{2,27,36,44} Logan et al. described the limitations of this technique due to the fact that many of the standards give the same responses (R_f and colour) with multiple visualisation techniques, differentiation based on TLC was not always possible and complementary analytical techniques were necessary for identification.⁴⁴

In conclusion, it is possible to detect synthetic cannabinoids and synthetic cathinone derivatives with portable techniques including different reagents or immunoassays but these tests show significant limitations: They are unspecific. Possible cross reactivities with other substances including plant materials, flavours or bulking agents were not discussed in detail. The strongest limitation, however, stems from the great variety in the chemical structure within the substance class of the synthetic cannabinoids caused by the increasing NPS-market. This would require the constant production of new rapid drug tests. To conclude, most presumptive tests are unspecific and not suitable for the high number of emerging NPS. In Chapter 2, ion mobility spectrometry will be introduced as an alternative presumptive test with substance specific parameters including drift time and reduced ion mobility. The good resolution and separation efficiency give rise to selectivity high enough to identify most NPS commonly on the market despite the presence of complex matrices.

1.2.2 Optical spectroscopy

According to the recommendations of the scientific working group for the analysis of seized drugs (SWGDRUG), spectroscopic methods like NMR, Raman and Infrared (IR) spectroscopy as well as mass spectrometry are category A analytical techniques with maximum discriminating power.⁴⁵ In recent years, NMR spectroscopy has also been used for the characterisation of NPS in herbal mixtures or powders to achieve unambiguous structural elucidation and determine the purity of unknown compounds in seizures.⁴⁶⁻⁵⁸ Thus, NMR is a powerful method to provide structural information necessary for the large number of emerging and structurally related NPS. The complete functional group assignment of a molecule can be achieved using NMR experiments involving 1-dimensional proton (¹H) and carbon (¹³C) spectra and a combination of 2-dimensional correlation experiments including NOESY (Nuclear Overhauser Effect Spectroscopy), and HMQC (Heteronuclear Multiple-Quantum Correlation).²⁷ ¹H-NMR is also very useful for the discrimination of regioisomers: Para-substituted aromatic molecules show different splitting patterns than ortho or meta substituted aromatic ring systems. In contrast, it is difficult to discriminate between ortho and meta substituted aromatic substance without further complementary experiments.²⁷ The analysis of challenging matrices was described in several publications including the use of preparative LC or preparative TLC to purify the target, which is then analysed by NMR spectroscopy.⁵⁴⁻⁵⁸ Major disadvantages of this technique are its costs and the required technical expertise, which lead to a limited applicability in routine analysis.² In the field of portable analytics, spectroscopic methods like IR- and Raman spectroscopy are the techniques of choice for rapid analysis of NPS as several manufacturers produce handheld or portable IR and Raman devices for the direct on-site analysis of substances.⁵⁹⁻⁶¹ In contrast to presumptive tests, these techniques allow compound identification via spectral fingerprinting. For structure elucidation of unknown compounds, Raman and IR spectroscopy would be very useful to differentiate isomers when it is not possible using ion trap techniques (MSⁿ). One disadvantage is the difficulty in analysing synthetic cannabinoids in different interfering matrices like herbal mixtures, papers or tobaccos. IR-spectroscopy is more sensitive than Raman spectroscopy and with a further extraction step with methanol or acetone, it is possible to obtain a good IR spectrum after evaporating the extract directly on the ATR (attenuated total reflection) diamond cell.^{2,62,63} Pure powders or liquids can be analysed directly provided that there is a relative high concentration of the active ingredient in the sample. In recent years, Raman spectroscopy has been increasingly applied for the analysis of different illicit drugs including barbiturates,⁶⁴⁻⁶⁶ benzodiazepines,^{66,67} cocaine,^{66,68-75} amphetamine,^{71,72,74,76,77} MDMA,^{66,71,72,75,78,79} methamphetamine,^{66,77,80,81} 2,5-dimethoxy-4-bromoamphetamine,⁸² ketamine,⁷² morphine,⁸³ codeine,⁸³ hydrocodone,⁸³ heroin,^{66,74,75} and THC.⁷⁵ In case of NPS analytics, publications are limited to specific focal points.^{59,75,77,84-96}

One focus is the characterisation of NPS using different portable or benchtop Raman spectrometer at different wavelengths (785 and 1064 nm).^{59,84,86,90,93,96} Comparison of the Raman spectra generated by different Raman spectrometers or different operating conditions were evaluated using instruments' in-built algorithms to determine the Hit quality index (HQI)⁸⁶ or dissimilarity calculations.⁸⁵ These studies aimed at constructing and validating spectral libraries to guarantee a possible transfer of those databases to other (portable) Raman spectrometers, sometimes using chemometric models, especially principal component analysis (PCA).^{84,85,88,91} Another focal point represents the method development and application of surface enhanced Raman spectroscopy (SERS) for the trace analysis of NPS taking advantage of the reduced fluorescence in bulk samples.⁹²⁻⁹⁴

The identification power of spectroscopic methods depends on the actuality and quality of the reference libraries. The analysis of unknown substances that are not (yet) present in the reference library is challenging. Until now, only two publications concentrate on the structural characterisation and interpretation of specific Raman bands in spectra of NPS.^{89,95} Christie et al. described the differences of specific vibrations for regioisomers of synthetic cathinone derivatives⁸⁹ and Lobo et al. described Raman bands of 5F-AMB (methyl (2*S*)-2-[(1-(5-fluoropentyl)-1*H*-indazol-3-yl)formamido]-3-methylbutanoate) with a detailed table for all possible vibrational modes.⁹⁵ In addition, PCA models focused on the discrimination of substance classes but not on the distinction of substances within one substance class. The combination of frequency tables with PCA models can provide a lot of information to characterise even unknown samples.

In Chapter 3, the analysis of NPS using different Raman spectrometers with different operating conditions was evaluated. The focus is on the question if it is possible to use only one reference library which is then transferred to different portable Raman spectrometers? To answer this question, instrument in-built correlation algorithms and different pre-processing methods were tested. A PCA model together with new vibration frequency tables allows characterising unknown substances within different substance classes.

The demand for contactless analysis through packaging material or containers is rising. Therefore, another spectroscopic technique is discussed in Chapter 4: THz spectroscopy. For drug analysis, the use of the THz technology is not widespread and is currently limited to the detection of classical drugs. For NPS analytics, there are no publications and experimental data about the application of THz radiation. In this work a novel approach in case of uncovering drug trafficking was discussed: the detection of synthetic cannabinoids in postal packages using THz spectroscopy.

In contrast to the spectroscopic techniques presented above, UV/VIS spectroscopy is classified as category B analytical technique by SWGDRUG. Here the identification strength is lower in comparison to NMR, IR, Raman or Mass spectroscopy due to the fact that only the UV or VIS absorbance of a substance is measured which results in a broad band. Therefore

UV/VIS spectroscopy is used in combination with other chromatographic techniques. In Chapter 5, the quantification of synthetic cannabinoids is presented and in this context, the UV-spectra of several synthetic cannabinoids are discussed.

1.2.3 Separation Techniques

For the qualitative and quantitative analysis of NPS in laboratories, chromatographic techniques coupled to mass spectrometry are the most common methods used in routine forensic laboratories.⁹⁷ Gas chromatography-mass spectrometry is the most widely applied method for a general unknown screening or systematic toxicological analyses either in clinical or forensic toxicology.⁹⁸ Substances that are appropriate for GC with interfaces for electron or chemical ionisation were analysed either per se or after derivatisation. GC-MS analysis affords sample clean-up and purification of the analytes due to the fact that only organic extracts can be injected. Sample preparation is simple and more or less identical in nearly all publications: Powdered samples and samples in herbal mixtures are dissolved/suspended in an organic solvent e.g. methanol or ethanol (approximately 1 mg/mL analyte concentration) under ultrasonication for 10 min. After centrifugation, the solution is filtered and directly measured using GC-MS.^{99,100} Many studies deal with the identification of both synthetic cannabinoids^{36,44,54-58,62,100-107} and synthetic cathinone derivatives^{47,108-114} as pure substances or in different matrices by GC-MS. One major limitation is that some analytes are heat-unstable and may thus be degraded already in the injection port of the GC-instrument. This is the case especially for cyclopropyl or ester analoga like UR-144 or QUPIC. The reported LODs for GC-MS analysis of NPS range from 0.5–1.0 mg/L.¹⁰⁰ Synthetic cannabinoids^{101,115-132} and synthetic cathinone derivatives^{111,114,133-136} have also been analysed by LC-MS with the advantage of a higher matrix tolerance. The ability to inject aqueous samples makes the method suitable for a rapid, high throughput screening application (dilute and shoot). In most cases, the publications concentrate on the analysis of synthetic cannabinoids and synthetic cathinone derivatives in biological materials including oral fluid, urine, blood, serum and hair as, summarised by Namera et al.¹³⁷ Only a few publications deal with the analysis of powders or herbal mixtures using LC.^{47,114,133,138-141} Sample preparation steps for powders and herbal mixtures are similar to those for GC-MS analysis. The LODs obtained by LC-MS ranged from 2 ng/mL to 10 µg/mL with analysis times between 8 and 15 min.

In the field of NPS analytics, well-studied MS fragmentation pathways of synthetic cathinone derivatives^{36,101,111-114,133,142} and synthetic cannabinoids^{36,44,54-58,100-102,143} were studied and together with retention times allow identification of the analyte, especially when reference standards are available.

For unambiguous identification, GC-MS and LC-MS analysis depend on the availability of reference standards and the establishment of a reference library. In general, quantification of substances efforts time consuming calibration or a validation performances and the presence of reference standards independent of the applied analytical technique. At present, there are no alternatives published for fast and effective quantification of NPS independent of the availability of reference standard (except NMR analysis).

In Chapter 5, a quantitative screening method of synthetic cannabinoids is presented using UPLC-DAD with maximal retention times of 10 min. Here, the need for reference standards is lowered by evaluating cross calibration possibilities between different structurally related synthetic cannabinoids.

1.2.4 Chiral analysis

The chiral discrimination and the availability of stereoselective analytical methods gain in importance in medicinal chemistry, and forensic toxicology. In some cases, the level of penalties conforms to a specific enantiomer which is listed in drug laws. Synthetic cathinone derivatives have chiral centres; and the R and S enantiomers show significant differences in their pharmacodynamic activity and their pharmacokinetic properties due to differences in their affinity or intrinsic activity at receptor sites.^{144,145} Thus, the need for screening methods to investigate the chirality of unknown samples as well as the fast analysis of a large number of NPS samples is increasing.

The most common technique for chiral investigation is HPLC-UV with chiral stationary phases¹⁴⁶⁻¹⁵² or an achiral stationary phase with cyclodextrins (CDs) added to the mobile phase.¹⁵³ The use of GC-MS for chiral analysis of synthetic cathinone derivatives separating diastereomers after derivatisation with chiral trifluoroacetyl-L-prolyl chloride¹⁵⁴⁻¹⁵⁶ or α -methoxy- α -trifluoromethylphenylacetic acid¹⁵⁰ is rather time-consuming.

An alternative are capillary electrophoresis (CE-DAD or CE-MS) methods. The most common chiral selectors employed for the CE enantiomeric separations of low-molecular weight organic compounds are cyclodextrins. Especially the enantioselective separation of synthetic cathinone derivatives using capillary electrophoresis (CE-DAD or CE-MS) in combination with different CDs as chiral selector were published including β -CD,^{157,158} highly sulphated- β -CD (HS- β -CD),^{154,159} highly sulphated- γ -CD (HS- γ -CD).¹⁶⁰ In general, several alternative chiral selectors have been employed in chiral CE like crown ethers^{161,162}, proteins¹⁶³, or polysachcharides¹⁶⁴. In literature, the application of those chiral selectors for the analysis of cathinone derivatives is only described in connection with capillary electrochromatography with chiral stationary phases. Each of these non-CD selectors has decisive limitations compared to CDs: Crown ethers demand a separation electrolyte free of potassium or ammonium ions because they compete with the enantiomers for the cavity. This

increases requirements on the purity and composition of electrolyte systems and limits some applications. Low separation efficiency, adsorption to the capillary wall and high UV absorption were observed for the use of proteins as chiral selector.^{165,166} Linear and positively charged polysaccharides show low solubility and adsorption to the inner surface of the capillary.¹⁶⁷

The simultaneous analysis of a large number (< 12) of newly emerged NPS with and without bulking agents has not been discussed in literature. In Chapter 6, an effective and fast chiral screening method and a high-throughput method for the large number of 36 newly emerged synthetic cathinone derivatives is presented. The utility of this approach is demonstrated by the successful analysis of seized samples containing bulking agents.

2 Ion mobility spectrometry as a fast screening tool for synthetic cannabinoids to uncover drug trafficking in jail via herbal mixtures, paper, food, and cosmetics

2.1 Abstract

The greatest challenge for European drug policies is how to effectively respond to the dynamic and constantly changing market for new psychoactive substances (NPS). Even small modifications in the chemical structure of substances often allow circumventing existing laws. Also in prison, the consumption of NPS is rising and there is growing evidence that NPS are responsible for a large share of drug-related problems. Ion mobility spectrometry (IMS) is the technique of choice for trace analysis of illicit drugs or explosives at security points e.g. airports. Currently, databases of the reduced mobility (K_0) values are limited to classical drugs and should be completed with data of emerging NPS. In this paper, K_0 -values, LODs (0.7-3.6 ng) and drift times of 25 synthetic cannabinoids were evaluated. The data were added to existing databases of IMS which were then applied for fast screening in prison. The detection capability of the portable IMS technique was evaluated by the determination of intraday (0.089 %) and interday precision (0.004 to 0.14 %), systematic error (0.19 %) and separation capability for structurally related NPS. The applicability of the methodology was demonstrated by the successful analysis of 12 different pieces of paper impregnated with synthetic cannabinoids, 7 different cosmetics and 5 food samples (liquids), spiked with a mixture of narcotic drugs and a synthetic cannabinoid. In addition, 14 herbal mixtures and 36 different casework samples from prisons were analyzed provided by the State Office of Criminal Investigation Rhineland-Palatinate (Germany).

2.2 Introduction

Over the last decade a new generation of drugs flooded Europe and the challenging task for drug policies is how to effectively respond to the dynamic and constantly changing drug market.¹⁶⁸ The substances are known as “designer drugs”, “legal highs”, “herbal highs”, “bath salts”, “research chemicals” or “laboratory reagents”.¹ They are sold via internet in specialized shops in colorful and professionally designed packages of herbal products or of pure powder.^{16,17} The United Nations Office on Drugs and Crime (UNODC) established a clear terminology: “New psychoactive substances are substances of abuse, either in a pure

form or a preparation, that are not controlled by the 1961 Single Convention on Narcotic Drugs⁴ or the 1971 Convention on Psychotropic Substances,⁵ but which may pose a public health threat. In this context, the term ‘new’ does not necessarily refer to new inventions but to substances that have recently become available”.⁶

These NPS have initially been designed to mimic established illicit drugs, such as cannabis, cocaine, amphetamine and LSD.^{2,3} In reality, the effects for NPS-consumers are unpredictable and sometimes fatal¹⁰⁻¹² as there is no information about the active drug given on the product label. In some European countries, only specific substances are listed in the drug law and even small modifications in the chemical structure of such listed substances already allow circumventing existing law.⁹ There is a race between the legal prosecution and the producers as those strive to be one step ahead by generating new NPS-products. The rapid emergence of novel products means that developing supportive health intervention responses is challenging.⁷ The European Monitoring Centre for Drugs and Drug Addiction (EMCDDA) implemented an early warning system¹³ in the European Union under the terms of a Council Decision 2005/387/JHA¹⁴ to guarantee a rapid exchange of information and provide a risk assessment on new psychoactive substances. By the end of December 2017, the EMCDDA described more than 670 new substances that have appeared on Europe’s drug market over the past 20 years. In 2015 alone, there was an increase of NPS types by 25 % in comparison to 2014.¹⁶⁹

The use of NPS in prison settings is developing rapidly. There is growing evidence that NPS are responsible for a large share of drug-related problems in some European prisons and appropriate responses are mostly lacking.^{7,170} In 2017, the EMCDDA carried out a target rapid information assessment between August and December 2017 for 22 European countries to understand the prevalence and patterns of NPS use and to analyze NPS-related problems in prison settings.¹⁷⁰ The study discovered that synthetic cannabinoids are the most common NPS followed by synthetic cathinone derivatives. In the study presented here, the focus is on the analysis of synthetic cannabinoids. The supply routes range from the “throw-over“-method¹⁷⁰ of drugs over the prison wall to the manipulation of common foods with drugs. Another method for bringing NPS into prison was identified: the abuse of mail service. For this, the NPS are dissolved in a solvent such as acetone and sprayed onto a piece of paper, tobacco or textiles and sent as a postal package or letter to the prison. In most cases, the potential carrier substances are reduced to small pieces and then smoked or swallowed. The wide range of physical and mental health harms caused by the consumption of NPS¹⁰ also provides a challenge to prison officers.¹⁷¹ For an early and easy detection of NPS, there is a great demand for mobile techniques. They are inevitable to detect potential NPS in order to avoid their penetration into the prison.

From an analytical point of view the choice of rapid drug tests for NPS is limited, especially for synthetic cannabinoids.^{172,173} However, the demand for rapid drug detection for Police, customs, Federal armed forces and prisons is growing.³⁴

In general, to uncover drug trafficking the police uses relatively simple presumptive tests with color coding for specific drugs. In addition, immunoassays based on an antibody-antigen (drug) interaction are applied. These tests are commercially available for classical drugs like tetrahydrocannabinol, cocaine, amphetamine, lysergic acid diethylamide, heroin, buprenorphine, ephedrine, γ -hydroxybutyric acid, methamphetamine, MDMA, methadone, and ketamine. In most cases, test kits are used for the analysis of oral fluid¹⁷⁴ and urine^{40,175} samples. However, they are not suitable for the detection of synthetic cannabinoids¹⁷⁶ due to the normally low concentration of the analytes in herbal mixtures and possible interferences by the sample matrix.² Moreover, the differences in the chemical structure within the substance class of the synthetic cannabinoids caused by increasing NPS-market would require the constant production of new rapid drug tests.

Currently, mobile spectroscopic techniques like Infrared- and Raman spectroscopy are the techniques of choice for rapid characterization of synthetic cannabinoids.⁵⁹⁻⁶¹ In contrast to preliminary tests, these techniques allow compound identification. One disadvantage of these spectroscopic techniques is the difficulty in analysing synthetic cannabinoids in different interfering matrices like herbal mixtures, papers or tobaccos. A sample preparation step is required. In most cases the different matrices were dissolved in alcohols like methanol or acetone.^{2,62,63} Pure powders or liquids can be analyzed directly provided that there is a relative high concentration of the active ingredient in the sample matrix.

For the qualitative and quantitative analysis of NPS in laboratories, chromatographic techniques coupled to mass spectrometry are the most common methods used in routine forensic laboratories. There are many studies dealing with the identification of NPS in different matrices with the help of gas chromatography-mass spectrometry^{47,108-110} and liquid chromatography-mass spectrometry.^{123,134-136} The sample preparation has to be adapted to the specific matrices but for herbal mixtures or powders, the samples are mostly suspended in alcohol.² In the last few years, nuclear magnetic resonance spectroscopy (NMR) has also been used for the characterization of NPS in herbal mixtures or powders.⁴⁶⁻⁵³ It is a fast technique which allows unambiguous structural elucidation of unknown compounds. Disadvantages of this technique are the cost of NMR spectroscopy and the technical expertise required which leads to a limited applicability in routine analysis.²

Ion mobility spectrometry (IMS) is a powerful analytical method that is used for trace analysis of organics. Due to its high sensitivity (ng-range), analytes can be detected in different matrices with hardly any sample preparation. The analytes are collected by wiping the surface of the sample with a teflon membrane (swab). The fast analysis times of less than 10 s and the ease of sampling and handling allow applying mobile IMS at security points like

airports.^{177,178} The most common application of IMS is the detection of explosives and chemical warfare agents.¹⁷⁹⁻¹⁸⁴ In addition, there is a wide variety of analytical purposes including pharmaceutical applications (quality control,¹⁸⁵ cleaning verification,^{179,182,183} resolution of isomers¹⁸⁶⁻¹⁸⁸), environmental applications (air quality,^{189,190} water and liquid samples,¹⁹¹⁻²⁰¹ solids and aerosols^{202,203}), applications in the food and feed sector,²⁰⁴⁻²¹⁵ biomedical and clinical analyses (biomarkers in breath,²¹⁶⁻²²¹ urine,²²² blood and serum,^{223,224} lymph extracts²²⁵). Since 1990 IMS is frequently applied in forensic analysis. Especially for drug analysis, IMS proved to be very versatile and was applied for the analysis of classical drugs both in forensic science and forensic toxicology,²²⁶⁻²³² the analysis of psilocin and psilocybin in mushrooms,²³³ the analysis of MDMA, MDEA, methamphetamine, cocaine and clenbuterol in hair samples,²³⁴⁻²³⁶ analysis of volatile drug markers of cocaine, MDMA and THC in air samples²³⁷ and the analysis of benzodiazepines.²³⁸ In the last few years, a number of NPS have been successfully analyzed using IMS such as synthetic cathinone derivatives,²³⁹⁻²⁴² tryptamines,^{239,240,242} synthetic cannabinoids,^{2,241,242} and phenethylamines^{241,242}. The selectivity of the mobile IMS is limited and some publications reported that analytes with nearly identical chemical structure like the synthetic cannabinoids cannot be distinguished.^{2,181} With the high sensitivity of IMS, it is possible that disturbing matrix components are detected and generate an alarm due to a false positive result. Some publications are concerned with the reduction of false positive responses commonly encountered in the field when drugs and explosives are detected.^{243,244}

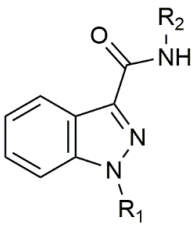
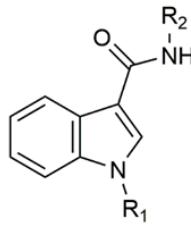
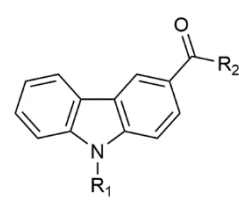
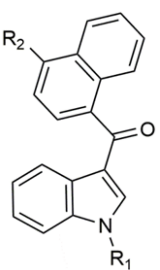
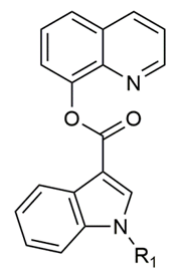
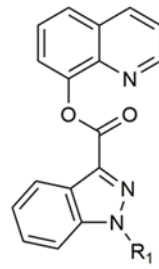
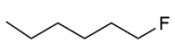
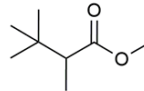
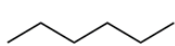
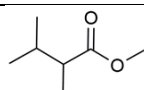
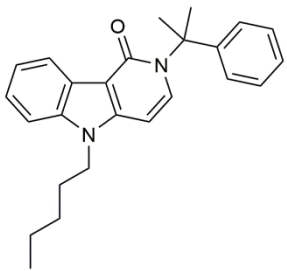
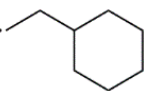
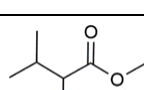
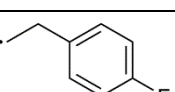
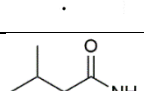
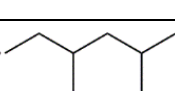


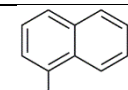
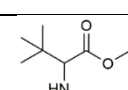
The topic of this paper is the fast and effective detection of synthetic cannabinoids in various samples such as herbal mixtures, papers (postal packages), cosmetics and foods using mobile IMS. IMS serves as a preliminary test for the detection of NPS in suspicious objects found in or around the prison. Current databases of reduced mobility values (K_0) are limited to classical drugs like amphetamine, methamphetamine, THC, heroine. In this study, the K_0 -values of 25 synthetic cannabinoids were determined. The selection of substances complies with the current state of synthetic cannabinoid distribution in Rhineland-Palatinate (Germany) and refers to the number of appearance of each synthetic cannabinoid in the State Office of Criminal Investigation Rhineland-Palatinate. In conjunction with criminal cases referring to prisons, only the 25 synthetic cannabinoids listed here were seized during the last years. The data are added to existing databases for other drugs of abuse and drug testing in prison. The utility and applicability of the IMS method is demonstrated by the analysis of seized samples like herbal mixtures, papers, foods products and cosmetics from real criminal cases.

2.3 Materials and Methods

2.3.1 Chemicals

The reference standards of 25 synthetic cannabinoids (powders) employed in this study were taken from criminal cases provided by the State Office of Criminal Investigation Rhineland-Palatinate (Germany) and listed in Table 2-1. These include 5F-ADB (N-[[1-(5-fluoropentyl)-1*H*-indazol-3-yl]carbonyl]-3-methyl-D-valine, methyl ester), 5F-AMB (N-[[1-(5-fluoropentyl)-1*H*-indazol-3-yl]carbonyl]-L-valine, methyl ester), 5F-PB-22 (1-(5-fluoropentyl)-8-quinolinyl ester-1*H*-indole-3-carboxylic acid), 5F-SDB-005 (naphthalene-1-yl 1-(5-fluoropentyl)-1*H*-indazole-3-carboxylate), AB-CHMINACA (N-[(1*S*)-1-(aminocarbonyl)-2-methylpropyl]-1-(cyclohexylmethyl)-1*H*-indazole-3-carboxamide), AB-FUBINACA (N-[(1*S*)-1-(aminocarbonyl)-2-methylpropyl]-1-[(4-fluorophenyl)methyl]-1*H*-indazole-3-carboxamide), AB-PINACA ((*S*)-N-(1-amino-3-methyl-1-oxobutan-2-yl)-1-pentyl-1*H*-indazole-3-carboxamide), AM-2201 ([1-(5-fluoropentyl)-1*H*-indol-3-yl]-1-naphthalenyl-methanone), APICA (N-(1-adamantyl)-1-pentyl-1*H*-indole-3-carboxamide), BB-22 (1-(cyclohexylmethyl)-8-quinolinyl ester-1*H*-indole-3-carboxylic acid), Cumyl-PeGaClone (2,5-dihydro-2-(1-methyl-1-phenylethyl)-5-pentyl-1*H*-pyrido[4,3-*b*]indol-1-one), EAM-2201 ((4-ethyl-1-naphthalenyl)[1-(5-fluoropentyl)-1*H*-indol-3-yl]-methanone), EG-018 (naphthalen-1-yl(9-pentyl-9*H*-carbazol-3-yl)methanone), EMB-FUBINACA (ethyl (1-(4-fluorobenzyl)-1*H*-indazole-3-carbonyl)-L-valinate), FDU-PB-22 (1-[(4-fluorophenyl)methyl]-1*H*-indole-3-carboxylic acid, 1-naphthalenyl ester), FUB-AMB (N-[[1-[(4-fluorophenyl)methyl]-1*H*-indazol-3-yl]carbonyl]-L-valine, methyl ester), JWH-018 (1-pentyl-1*H*-indol-3-yl)-1-naphthalenyl-methanone), JWH-122 ((4-methyl-1-naphthalenyl)(1-pentyl-1*H*-indol-3-yl)-methanone), MAB-CHMINACA (N-[1-(aminocarbonyl)-2,2-dimethylpropyl]-1-(cyclohexylmethyl)-1*H*-indazole-3-carboxamide), MDMB-CHMICA (N-[[1-(cyclohexylmethyl)-1*H*-indol-3-yl]carbonyl]-3-methyl-L-valine, methyl ester), MDMB-CHMCZCA (methyl N -[[9-(cyclohexylmethyl)-9 *H* -carbazol-3-yl]carbonyl]-3-methyl-L-valinate), MMB-2201 (N-[[1-(5-fluoropentyl)-1*H*-indol-3-yl]carbonyl]-L-valine, methyl ester), PB-22 (1-pentyl-8-quinolinyl ester-1*H*-indole-3-carboxylic acid), THJ-2201 ([1-(5-fluoropentyl)-1*H*-indazol-3-yl]-1-naphthalenyl-methanone), UR-144 ((1-pentyl-1*H*-indol-3-yl)(2,2,3,3-tetramethylcyclopropyl)-methanone). Each drug standard was dissolved in methanol p.A. (Geyer, Renningen, Germany) to prepare stock solutions of 0.05 mg/mL. For UPLC-DAD and GC-MS measurements, methanol (LC-MS-grade, Geyer, Rennigen, Germany) was used.

Table 2-1 Chemical structures of the synthetic cannabinoids evaluated in this study

Indazole			Indole			Carbazole		
								
Substance	R ₁	R ₂	Substance	R ₁	R ₂	Substance	R ₁	R ₂
5F-ADB	A	A	APICA	B	F	EG-018	B	G
5F-AMB	A	B	MDMB-CHMICA	C	A	MDMB-CHMCZCA	E	H
AB-CHMINACA	C	D	MMB-2201	A	B			
AB-FUBINACA	D	D	Naphtyl-Indole 	Naphtyl-Indole-carboxylate 				
AB-PINACA	B	D						
EMB-FUBINACA	D	C						
FUB-AMB	D	B						
MAB-CHMINACA	C	E						
Naphtyl-Indazole-carboxylate 			Substance	R ₁	R ₂	Substance	R ₁	
			AM-2201	A	-	BB-22	C	
			EAM-2201	A	I	5F-PB-22	A	
			JWH-018	B	-	FDU-PB-22	D	
			JWH-122	B	J	PB-22	B	
			THJ-2201	A	-			
Substance	R ₁		R ₁ A: 			R2A: 		
5F-SDB-005	A		R ₁ B: 			R2B: 		
Cumyl-PeGaClone 			R1C: 			R2C: 		
			R1D: 			R2D: 		
			R1E: 			R2E: 		
						R2F: 		
						R2G: 		
						R2H: 		
						R2I: CH ₃		
						R2J: C ₂ H ₅		

The following solvents were used for solid phase extraction (SPE): acetone p.A., acetic acid 100 %, sodium dihydrogen phosphate-1-hydrate, dichloromethane (Merck, Darmstadt, Germany), acetonitrile Rotisolv UV/IR grade $\geq 99,9$ %, ammonia solution Rotipuram 30-33 % (Carl Roth. KG, Karlsruhe, Germany), albumin from bovine serum (BSA) Cohn V fraction ≥ 96 % (Sigma Aldrich, Germany), 2-propanol p.a. 99,7 % (Th. Geyer, Germany).

For the NMR analysis, acetone-d₆ (purchased from Deutero, Kastellaun, Germany) and internal calibrant 3,5-dinitrobenzoic acid (Fluka, TraceCERT, 99.66 %) were used. The teflon membranes (swabs) for IMS measurements were provided by Smith Detection (Edgewood, USA). The drug mixture consisted of methadone hydrochloride ((RS)-6-(dimethylamino)-4,4-diphenylheptan-3-on), DL-amphetamine sulphate ((±)-1-phenylpropane-2-amine), buprenorphine hydrochloride ((α S,5 α ,7 α)-17-(cyclopropylmethyl)- α -(1,1-dimethylethyl)-4,5-epoxy-18,19-dihydro-3-hydroxy-6-methoxy- α -methyl-6,14-ethenomorphinan-7-methanol), fentanyl hydrochloride (N-(1-(2-phenylethyl)-4-piperidinyl)-N-phenylpropanamide) which were purchased from LGC-Standards (Wesel, Germany) except amphetamine sulphate which was purchased from Sigma Aldrich (St.Lous, MO, USA).

2.3.2 Methodology: Characterization of NPS powders from seizures

2.3.2.1 Gas chromatography-mass spectrometry

As not all NPS were commercially available during experimental work of this study, material from seizures was used as standards. Identity and purity of each seized drug powder were determined using a gas-chromatograph with mass spectrometric detection (GC-MS). GC was performed on an Agilent 7890B equipped with a 5977A MS (Agilent, Waldbronn, Germany). The separation column was a 19091S-433 HP-1MS from Agilent with a length of 30 m, an inner diameter of 250 μ m and a coating thickness of 0.25 μ m. The MS detector was operated with electron ionization (EI) with an ionization potential of 70 eV, a scan range of 50-550 amu and a data rate of 50 scans/s. The inlet heater temperature was 250 °C, the transfer line temperature was 270 °C, the ion source temperature was 230 °C and the quadrupole temperature was 150 °C. Helium served as the carrier gas at a flow rate of 0.8 mL/min. A split injection volume of 1 μ L was used at a split ratio of 50:1. The temperature program of the oven started at 100 °C (hold time 0 min), and increased at a rate of 20 °C/min to 300 °C (hold time 25 min). The mass spectrum derived for each compound was compared to libraries. Standards containing other substances than the drug of interest (e.g. cutting agents) were excluded from method optimization and database setup.

Five mg of powdered samples were dissolved in 1 mL methanol. For herbal mixtures or tobacco mixtures 200 mg of herbal mixture was suspended in 3 mL methanol. In cases, where less material was available, the amount of methanol was reduced until the whole material was covered with organic solvent. The solutions were filtered with syringe filters from Macherey-Nagel (Düren, Germany) with a pore size of 0.20 μ m and a diameter of 25 mm directly into

GC-MS vials for injection. Papers spiked with NPS were covered with methanol for extraction (10 min) in a glass vial. Afterwards, the solution was transferred into a second glass vial and evaporated to dryness. Then 100 μ L methanol were added to the glass vial and the solution was transferred to a GC-MS vial with a cone-shaped insert (Wicom, Heppenheim, Germany).

For the analysis of cosmetic products or foods, a solid-phase extraction (SPE) was done using octadecyl (C18) disposable extraction 3 mL SPE columns (Fisher Scientific, Schwerte, Germany). All extractions were performed using a vacuum manifold system (Carl Roth, Karlsruhe, Germany). For this, 0.5 g of the sample was suspended in 3 mL 0.1 M NaH_2PO_4 -buffer with 3 % BSA.

The SPE procedure was: (i) conditioning of the cartridge with 3 mL methanol; (ii) conditioning of cartridge with 3 mL 0.1 M phosphate buffer (pH = 6) (iii) loading 3 mL of the sample dissolved in BSA-phosphate buffer; (iv) washing with 3 mL bidest. water; (v) washing with 3 mL of a water:methanol mixture (80:20), (vi) washing with 1 mL 0.1 M aqueous acetic acid, (vii) evaporating to dryness under vacuum (-10 mm kPa) for 10 min; (viii) eluting the acidic target analytes with 3 mL of dichloromethane and acetone (1:1); (ix) eluting the basic target analytes with 3 mL of a mixture of dichloromethane:isopropanol:ammonia solution (33 %) (40:10:1); (x) evaporating the eluted extracts to dryness under a gentle stream of nitrogen at 50 °C; (xi) reconstituting the extract in 100 μ L of methanol. The reconstituted extracts were transferred into a GC-MS vial with an inlet conus.

2.3.2.2 NMR

The purity determination of NPS samples from seizures was conducted by quantitative NMR (qNMR) analysis. It is considered as a primary method being traceable to the SI unit mol. The number of nuclei is directly proportional to the signal intensity.⁴⁹ The measurements were carried out with the NMR spectrometer AVANCE III HD 500 (Bruker, Rheinstetten, Germany) equipped with a Bruker 5 mm broad band inverse probe with z-gradient. Approximately 10 mg of the seizures were weighed directly in an NMR tube on an analytical balance together with the internal calibrant and 0.5 mL acetone-d₆ were added as solvent. The measurements were performed without sample spinning. All quantifications were performed on the basis of a single pulse ¹H-NMR experiment. The observing frequency for ¹H was 500.13 MHz. The number of scans was 4 and a 90° pulse was used for four accumulated scans. The transmitter offset was 5.5 ppm and the spectral width 17 ppm. An exponential multiplication was applied with a line broadening of 0.2 Hz. The time domain was set to 128 k as well as the spectrum size. The purity of the analyte P_x (expressed in % g/g) was calculated from the NMR signal intensity via an internal calibrant (IC) with known purity P_{Std} :

$$P_x = \frac{I_x}{I_{\text{IC}}} \times \frac{N_{\text{IC}}}{N_x} \times \frac{M_x}{M_{\text{IC}}} \times \frac{m_{\text{IC}}}{m_{\text{sample}}} \times P_{\text{IC}}$$

where I is the integral value, N the number of spins belonging to the respective molecular unit, M the molar mass and m the weighed-in mass.⁴⁹

2.3.2.3 UPLC-DAD

For quantitative analysis of samples an ultra-performance liquid chromatography (UPLC) Acquity-System (Waters, Milford, MA, USA) equipped with a diode array detection (DAD) was utilized. The synthetic cannabinoids were separated on a Raptor Biphenyl column (2.7 μm , 150 x 2.1 mm) from Restek (Bad Homburg, Germany) using a gradient with methanol (A)/ammonium formate buffer (B) at a flow rate of 0.5 mL/min. The gradient was constructed as follow: (A) 70 %/(B) 30 % for 4 min, (A) 75 %/(B) 25 % for 2 min, (A) 80 %/(B) 20 % for 4 min, (A) 90 %/B 10 % for 3 min and return to the start conditions within 2 min. The scan range of DAD was set to 210-400 nm and the detection wavelength for all synthetic cannabinoids was set to 301 nm. The sampling rate was 20 points/s with a resolution of 1.2 nm. Powdered material (1 mg) and herbal mixtures (100 mg) were suspended in 10 mL methanol. The solutions were filtered with syringe filters from Macherey-Nagel (Düren, Germany) with a pore size of 0.20 μm diameter of 25 mm. Then, 100 μL of the filtered sample solution was mixed with 900 μL methanol directly into UPLC-vials for injection (injection volume 5 μL).

2.3.2.4 IMS procedure

For IMS analysis, the IONSCAN600 (Smith Detection, Hemel Hempstead, United Kingdom) was utilized for the qualitative analysis of 25 synthetic cannabinoids. The factory operating method “narcotics” was used as measuring mode (Table 2-2). The mean value of all 43 segments was calculated for determination of K_0 - and drift time values for one substance. A teflon membrane substrate (called swab) was used for sampling and sample application. For the analysis of reference standards, 50 ng (1 μL of 0.05 mg/mL solution of standard in methanol) was pipetted onto the swab. Before each measurement, the empty swab was conditioned in the thermal desorption chamber and a plasmagram was recorded to assure that no carry over effects from analytes or matrix components were present. Reduced mobility (K_0) and its tolerance window, drift time, threshold and full width at half maximum (FWHM) were considered during automatic data evaluation using a software detector controller (Smith Detection). A positive detection alarm was programmed. The limits of detection (LODs) were estimated using the function $\text{LOD} = y_{\text{blank}} + 3 \times \text{SD}_{\text{blank}}$ where y_{blank} represents the mean amplitude of the background ($n = 5$) and SD_{blank} the standard deviation of the amplitude of the background.²⁴⁵ These calculated LODs were 100 du on average and this value was set as the threshold for the alarm to avoid false positive alarms.

Table 2-2 IMS operating conditions (positive ionization mode)

Measuring mode	“Narcotics”, positive mode
ionization source	APCI, corona discharge
Sampling method	teflon membrane substrate (swab)
Drift tube length	8 cm
Positive calibrant	Nicotinamide
Electric field strength	+240 Vcm ⁻¹
Inlet temperature	180 °C
Drift tube temperature	170 °C
Flash Heater temperature	240 °C
Drift gas /carrier gas	Dried purified air
Drift flow	206 cc/min
Absolut pressure	102 kPa
Number of scans	43
Scan time	19 ms

Based on these values, the concentration range of a 5-point-calibration curve was set (1.0-8.0 µg/mL) using standards in methanol (n = 3). LODs were then calculated from slope and intercept.²⁴⁶ For analysis, 1 µL of each concentration level was spiked onto the swab. This equals 1-8 ng standard per analysis. For the analysis of herbal mixtures the surface of the plant material was touched with a wooden rod (n = 3) and the adherent particles were transferred to the swab. To simulate drug transport via paper, pieces of paper were impregnated with synthetic cannabinoids at concentrations correlating to current dosages as described on internet platforms (see Table 2-3).²⁴⁷ For each synthetic cannabinoid, 2 different working solutions differing in concentration were prepared in methanol (see Table 2-3) and spiked to papers, which were allowed to dry at room temperature. For sample preparation, the papers were directly stroked by the swab (n = 3). The cosmetics and food samples were prepared by mixing a standard of 6 different compounds in methanol: 5F-ADB, fentanyl hydrochloride, methadone, amphetamine, tetrazepam, buprenorphine (1 mg/mL each). Afterwards, 100 µL of the mixture were added to 1000 µL of the different liquid cosmetics and food samples homogenized via vortexing for 30 s. Then, 1 µL of the spiked sample was then applied to the swab for analysis (effective amount of 100 ng for each compound).

Table 2-3 Concentration levels based on different internet platforms published in ²⁴⁷ for the preparation of impregnated papers with synthetic cannabinoids

Substance	Dosage low concentration in mg	Dosage high concentration in mg
5F-ADB	0.02	0.2
5F-AMB	0.1	2
5F-PB-22	1	2
AB-CHMINACA	1	2
AB-FUBINACA	0.5	4
AB-PINACA	0.5	4
MAB-CHMINACA	0.25	0.5
AM-2201	0.5	3
APICA	2	5
BB-22	0.5	-
JWH-018	2	5
MDMB-CHMICA	0.1	0.3

2.4 Results

2.4.1 Characterization of NPS with UPLC, GC-MS and NMR

For standards, samples from seizures were used. The powders were characterized by UPLC-DAD, GC-MS and NMR to determine their purity and to exclude the presence of impurities. These substances served as reference material in this study. Initially, the powder material was analyzed via GC-MS and the retention times and the characteristic m/z values of each substance are reported in Table 2-4 (arranged according to their importance). For identification of the synthetic cannabinoids, the MS-spectra of the different samples were compared to MS libraries. In addition, each sample was characterized with UPLC-DAD. Measuring conditions are given in Section 2.3.2.3 and the on-column UV-spectra are shown in the publication of Metternich et al. (Figure S1).²⁴⁸ The retention times and the λ_{\max} are presented in Table 2-4 for each standard. The purity was determined using ¹H-NMR to be > 94.6 %, except FDU-PB-22 with only 76.4 %. This sample also contained diethylamine and ethanol, which did not impair IMS measurements. Other samples with impurities were not taken into consideration including cutting agents that could also be present as an active ingredient in seized samples like paracetamol, caffeine, sugars or other drugs like e.g. amphetamine, cocaine and THC.

Table 2-4 List of 25 synthetic cannabinoids with the data from GC-MS with fragment masses (m/z -values) and retention times (R_t), absorption maximum (λ_{\max}) of the UPLC-DAD measurements, sample purity as determined by NMR, drift times and reduced mobility K_0 of IMS analysis with reference, where available

Substance	MW in g/mol	GC-MS		UPLC- DAD	NMR	IMS		
		m/z	R_t in min	λ_{\max} in nm	Purity in %	Drift time in ms	K_0 in $\text{cm}^2\text{V}^{-1}\text{s}^{-1}$	Ref. K_0 in $\text{cm}^2\text{V}^{-1}\text{s}^{-1}$
5F-ADB	377.46	233, 145, 130, 289, 321	10.9	301	98.7	10.564	0.9917	0.984 ²⁴⁹
5F-AMB	363.44	233, 145, 304, 249, 131	10.9	301	98.5	10.288	1.0123	
5F-PB-22	376.43	232, 144, 116, 89, 376	18.2	215, 294	99.6	10.48	0.9995	
5F-SDB-005	376.4	233, 145, 115, 213, 115	15.2	301	97.3	10.696	0.9827	
AB- CHMINACA	356.47	241, 312, 145, 55, 131	13.5	300	95.2	10.528	0.9975	
AB- FUBINACA	368.41	109, 252, 324, 145, 83	13.4	301	94.9	10.396	1.0128	
AB-PINACA	330.41	215, 286, 145, 216, 131	11.8	302	96.3	10.064	1.0463	
AM-2201	359.45	359, 127, 284, 232, 144	15.2	217, 247, 315	99.8	10.288	1.0127	1.0163 ²
APICA	364.54	214, 144, 307, 364, 347	16.9	302	98.5	11.044	0.9508	0.9466 ²⁴¹

Substance	MW in g/mol	GC-MS		UPLC- DAD	NMR	IMS		
		m/z	R _t in min	λ _{max} in nm	Purity in %	Drift time in ms	K ₀ in cm ² V ⁻¹ s ⁻¹	Ref. K ₀ in cm ² V ⁻¹ s ⁻¹
BB-22	384.48	240, 144, 116, 241, 55	24.8	215, 294	97.2	11.116	0.9456	
Cumyl- PeGaClone	372.50	254, 197, 118, 91, 372	13.9	250, 324	98.6	10.822	0.9741	
EAM-2201	387.50	232, 287, 312, 144, 370	19.9	221, 315	98.5	10.924	0.9592	
EG-018	391.50	334, 391, 335, 127, 179	23.8	216, 276, 298, 340	94.6	11.284	0.9328	
EMB- FUBINACA	377.5	109, 253, 324, 269, 254	12.31	301	98.8	10.948	0.9571	
FDU-PB-22	395.44	109, 252, 253, 143, 83	22.8	218, 293	76.5	13.024	0.8069	
FUB-AMB	383.40	109, 253, 324, 254, 383	10.9	300	99.9	10.624	0.9884	
JWH-018	343.47	127, 341, 214, 284, 144	13.7	217, 247, 315	98.6	10.204	1.0301	1.0288 ²
JWH-122	355.48	355, 298, 215, 115, 338	15.0	221, 315	99.9	10.528	0.9970	0.9950 ²
MAB- CHMINACA	370.50	241, 326, 145, 131, 55	13.4	302	91.6	10.768	0.9724	

Substance	MW in g/mol	GC-MS		UPLC- DAD	NMR	IMS		
		m/z	R _t in min	λ _{max} in nm	Purity in %	Drift time in ms	K ₀ in cm ² V ⁻¹ s ⁻¹	Ref. K ₀ in cm ² V ⁻¹ s ⁻¹
MDMB- CHMICA	384.51	240, 144, 296, 328, 268	12.6	290, 216	97.0	11.128	0.9415	0.968 ²⁴⁹
MDMB- CHMCZCA	434.5	290, 434, 179, 346, 378	23.1	235, 277	98.3	12.256	0.8576	
MMB-2201	362.50	232, 248, 144, 362, 233	11.7	216, 289	96.6	10.432	1.0065	
PB-22	358.44	214, 144, 116, 89, 358	17.7	216, 294	98.2	10.564	0.9917	
THJ-2201	360.44	127, 271, 360, 259, 155	14.1	218, 320	97.2	10.156	1.0341	1.031 ²⁴⁹
UR-144	311.46	214, 144, 296, 311, 252	10.3	215, 245, 305	98.8	9.995	1.0511	1.042 ²⁴² 1.0484 ²⁴¹

2.4.2 IMS measurements

2.4.2.1 Determination of drift times and K_0 -values

A standard method preprogrammed for the IMS was used. All 25 synthetic cannabinoids were analyzed by IMS and the K_0 -values were calculated from drift times of analytes ($t_{d \text{ analyte}}$) and of nicotinamide ($t_{d \text{ cal}}$) as internal standard to correct for pressure and temperature changes using the following equation¹⁸¹:

$$K_{0 \text{ analyte}} = \frac{K_{0 \text{ cal}} \times t_{d \text{ cal}}}{t_{d \text{ analyte}}}$$

The drift times for synthetic cannabinoids were in the range of 9.995-13.024 ms corresponding to K_0 -values of 1.0511-0.8069 $\text{cm}^2\text{V}^{-1}\text{s}^{-1}$ as summarized in Table 2-4. The plasmagrams for each synthetic cannabinoid are shown in Figure 2-1. K_0 -values were reported for 8 synthetic cannabinoids in previously published studies corroborating the results in this study.^{2,241,242,249} To the best of our knowledge, for the other substances no reference values have been published. For alarm generation for the synthetic cannabinoids, a library with K_0 -values was built.

A positive result (an alert) was assumed with a specific tolerance range. This range was set in the following way: Drift times were determined at the peak's left and right inflection points of the smallest and the largest peak within the 43 segments during one analysis and K_0 -values were calculated for both points. These inflection points are based on the baseline intercepts of tangent lines to a Gaussian peak and are equivalent to the peak width at 13.4 % of the height. The tolerance range of K_0 is expressed as:

$$\text{tolerance range} = K_0 \pm \frac{K_{0 \text{ Ls}} + K_{0 \text{ Ll}}}{2} - \frac{K_{0 \text{ Rs}} + K_{0 \text{ Rl}}}{2}$$

where L means the position on the left flank and R the position of the right flank and s means the smallest and l the largest peak at $W_{0,1}$ (peak width at 13.4 % of peak height) within the 43 scans. The additional detection alarm parameters were defined as follows: full width at half maximum (FWHM) of 200-250 μs and threshold of 100 du in order to avoid false positive alarms.

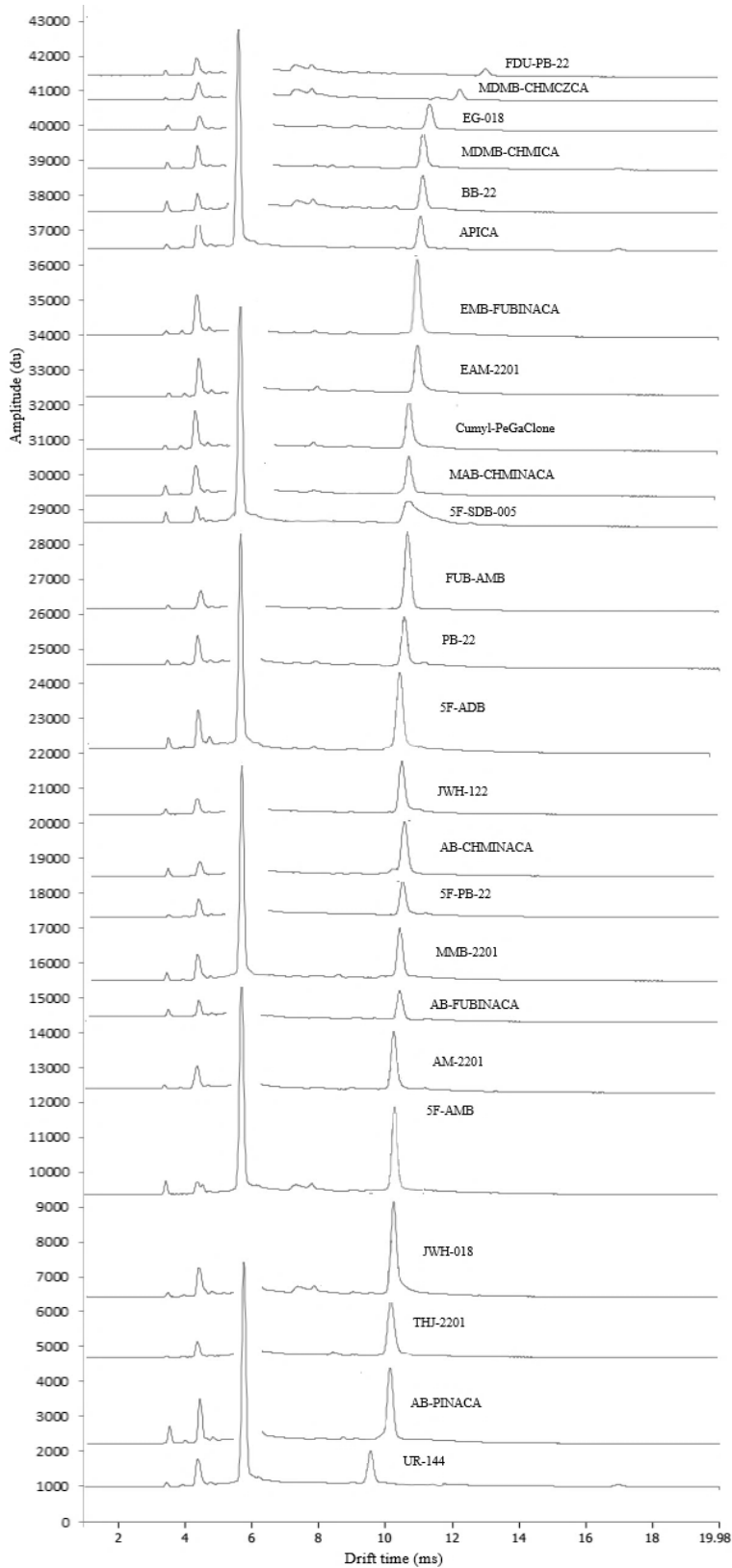


Figure 2-1 Plasmagrams of the 25 synthetic cannabinoids evaluated in this study applying 50 ng each on the swab (standard concentration of 0.05 mg/mL each), the signal at 5.959 ms stems from the internal calibrant nicotineamide

2.4.2.2 Figures of merit of the IMS method

In order to fully demonstrate the applicability of the IMS method, the precision, the separation capability and limits of detection were determined. The detection capability of the portable IMS technique was evaluated and the intra-day and inter-day precision of the K_0 -values are shown in Table 2-5. For intraday precision ($n = 5$) the RSD values were below 0.089 % and for interday precision ($n = 3$ on two different days at one week interval) the RSD values ranged from 0.004 to 0.14 %. The precision of the method and instrumentation presented here was similar to other studies.

Table 2-5 Precision, linearity and LOD values of the IMS analysis for the 25 synthetic cannabinoids injected separately

Substance	Intraday RSD in %	Interday RSD in %	Linearity R^2	LOD in ng	Reference LOD in ng
5F-ADB	0.0084	0.0121	0.9946	2.0	
5F-AMB	0.0044	0.1425	0.9937	1.5	
5F-PB-22	0.0071	0.0997	0.9778	1.6	
5F-SDB-005	0.0170	0.0170	0.9988	2.7	
AB-CHMINACA	0.0110	0.0385	0.9756	1.3	
AB-FUBINACA	0.0070	0.0450	0.9783	2.5	
AB-PINACA	0.0321	0.0321	0.9955	0.7	
AM-2201	0.0107	0.0760	0.976	3.6	
APICA	0.0120	0.0142	0.981	1.5	0.04-0.08 ²⁴¹
BB-22	0.0088	0.0088	0.9924	1.1	
Cumyl-PeGaClone	0.0245	0.0245	0.9945	2.0	
EAM-2201	0.0074	0.0483	0.9929	1.0	
EG-018	0.0117	0.0117	0.9939	2.0	
EMB-FUBINACA	0.0087	0.0087	0.9899	1.1	
FDU-PB-22	0.0055	0.0055	0.9893	3.0	
FUB-AMB	0.0000	0.0195	0.9923	2.4	
JWH-018	0.0053	0.0312	0.9928	2.7	
JWH-122	0.0090	0.0090	0.9894	1.5	
MAB-CHMINACA	0.0046	0.0287	0.995	0.7	
MDMB-CHMICA	0.0095	0.0170	0.9892	1.0	
MDMB-CHMCZCA	0.0082	0.0082	0.9891	2.0	
MMB-2201	0.0191	0.0529	0.9855	1.6	
PB-22	0.0115	0.0115	0.9629	2.6	
THJ-2201	0.0043	0.0043	0.9812	2.8	
UR-144	0.0707	0.0707	0.9967	0.7	0.02-0.08 ^{241,242}

The systematic error of the mobile IMS was also evaluated using the formula

$$D_t = \frac{l_d}{t_d} = K \times E$$

where the ion mobility K represents the proportional constant between the set value of the electric field strength E and the drift velocity D_t which is defined as the length of the drift distance l_d divided by the time t_d , which the ions need to reach the detector plate. Assuming that the electric field strength and the drift distance for the measuring system are nearly constant, the uncertainty of IMS measurements can be expressed by the following equation:

$$K \times t_d = \frac{l_d}{E} = \text{const.}$$

The uncertainty of the measurements was 0.19 % which corresponds to an absolute drift time deviation of ± 0.024 ms and an absolute deviation of the K_0 values of ± 0.0019 $\text{cm}^2\text{V}^{-1}\text{s}^{-1}$. The LODs of the 25 compounds are listed in Table 2-5 and range from 0.7-3.6 ng with an acceptable linearity of $0.9988 > R^2 > 0.9756$ (description of the determination of LODs in section “IMS Procedure”). Compared to literature (see Table 2-5) the evaluated LOD in this study were larger by a factor of 10-100. The dynamic range is limited by the ionization efficiency and thus by the consumption of reactant ions during the ionization process of analyte molecules. The range was in the ng to μg range for qualitative analysis of substances. Resolution was determined using the definition from chromatography. The drift time (and K_0) differences necessary to discriminate two analytes was > 0.15 ms (> 0.013 $\text{cm}^2\text{V}^{-1}\text{s}^{-1}$) at a resolution of $R = 0.75$, and was > 0.35 ms (> 0.024 $\text{cm}^2\text{V}^{-1}\text{s}^{-1}$) for baseline separation of two analytes ($R > 1.5$). Figure 2-2 demonstrates a mixture of 5 different synthetic cannabinoids analyzed via IMS with drift time differences > 0.15 ms. For samples with two or more synthetic cannabinoids the differences in drift times and reduced mobility values of < 0.15 ms (0.013 $\text{cm}^2\text{V}^{-1}\text{s}^{-1}$) led to an alarm for only the substance present at higher concentration in the sample.

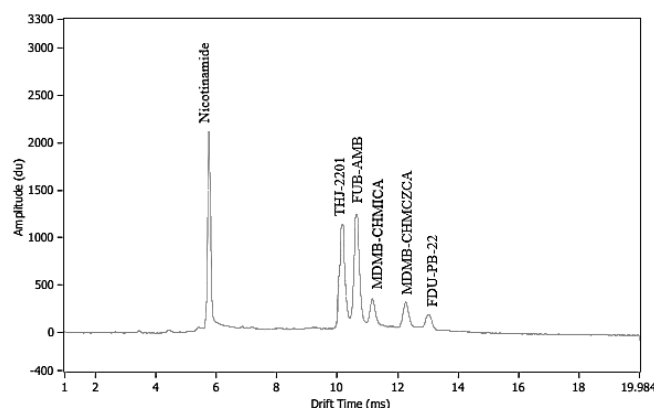


Figure 2-2 IMS plasmagram of a mixture of 5 different synthetic cannabinoids THJ-2201, FUB-AMB, MDMB-CHMICA, MDMB-CHMZCZA, FDU-PB-22 applying 50 ng each on the swab (standard concentration of 0.05 mg/ml each) and nicotinamide as internal calibrant

2.4.2.3 Model applications and matrix tolerance

The applicability of the method developed in this study was demonstrated by analyzing synthetic cannabinoids spiked to different matrices like herbal mixtures, impregnated papers, cosmetic products and liquid food samples. 14 herbal mixtures containing different synthetic cannabinoids (5F-ADB, 5F-AMB, 5F-PB-22, AB-CHMINACA, AB-FUBINACA, AM-2201, APICA, BB-22, EAM-2201, FUB-AMB, JWH-018, MAB-CHMINACA, MDMB-CHMICA, MMB-2201) were casework samples provided by State Office of Criminal Investigation Rhineland-Palatinate (Germany). The papers (standard copy papers 80 g/m²) were impregnated with different synthetic cannabinoids dissolved in methanol at the two concentration levels given in Table 2-3 referring to common dosages.²⁴⁷ For sample preparation of herbal mixtures and papers the swab was directly wiped over the sample surface. All synthetic cannabinoids could be detected by IMS without false alarms in these samples. Figure 2-3 shows the analyte 5F-ADB spiked into different matrices like papers, herbal mixtures and an herbal mixture with tobacco remains.

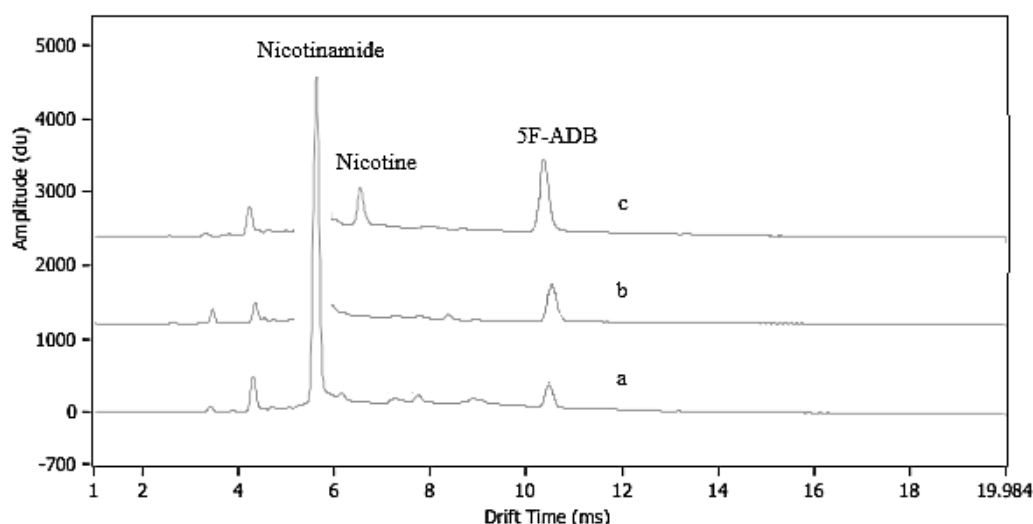


Figure 2-3 IMS-plasmagrams of 50 ng 5F-ADB a) spiked onto a paper, b) in a herbal mixture and c) in a herbal mixture with tobacco remains (casework Sample 5) and nicotinamide as internal calibrant

For the selection of cosmetic products and food samples, the product list of kiosk confectionery of a prison in Rhineland-Palatinate was used to choose potential matrices for drug trafficking. A mixture of 6 different compounds (5F-ADB, fentanyl hydrochloride, methadone, amphetamine, tetrazepam, buprenorphine) as representatives for different substance classes were spiked to several cosmetic products and food samples. These 6 compounds represent typical substances found in prison¹⁷⁰ and were included for the detection alarm system of the IMS. The following cosmetic products were analyzed: alcohol free mouth rinse, face cleansing lotion, face cleansing milk, contact lens solution, nasal spray, liquid soap and toothpaste. The analysis of food samples was limited to liquids including cola, orangeade, milk, coffee and peppermint tea. The analysis revealed positive alarms for 6 compounds in all

matrices except in liquid soap and toothpaste (false negative). For those two matrices only methadone, amphetamine and tetrazepam were detected with IMS (Figure 2-4).

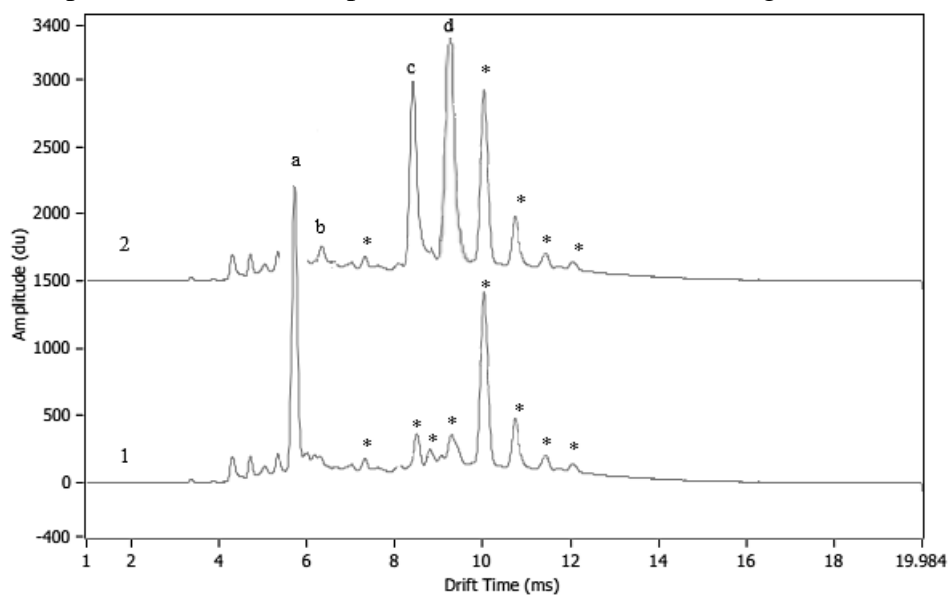


Figure 2-4 Plasmagrams of 1) the toothpaste (blank) with * signals deriving from the toothpaste matrix and a) internal calibrant nicotinamide and 2) the toothpaste spiked a mixture of 6 different compounds (5F-ADB, fentanyl hydrochloride, methadone, amphetamine, tetrazepam, buprenorphine), only b) amphetamine, c) tetrazepam and d) methadone were detected with IMS

Overall, IMS measurements provided a selectivity which was high enough to discriminate all 25 different synthetic cannabinoids taken up in the database.

2.4.2.4 Application to casework samples

The developed IMS method with automated detection alarm system was applied to prison settings in order to uncover drug trafficking. In total, 36 suspicious samples were analyzed via IMS. Results were verified by GC-MS analysis. The results are summarized in Table 2-6. In 35 out of 36 cases the IMS alarm generation reached a hit quality of > 89 %. The hit quality is calculated by the mean value of all K_0 -values of the analyte within the 43 segments per scan subtracted from the K_0 -value entered into the database.

The identification corresponded well to the GC-MS results. The major limitation of the method is the inability to detect more than one analyte in a sample which is shown in Case 6 and Cases 28-30 (Table 2-6). Only the active ingredient of higher peak intensity was identified. However, for the application in prison settings, the detection of only one analyte is sufficient to start hazard prevention. Nicotine is an analyte often detected in casework sample. To characterize nicotine with IMS, a nicotine standard was dissolved in methanol (0.5 mg/mL) and 1 μ L (effective amount 50 ng) was pipetted onto the swab ($n = 5$). The K_0 -value of nicotine was $1.5632 \text{ cm}^2\text{V}^{-1}\text{s}^{-1}$ and the drift time was 6.565 ms. Thus, there are no interferences with any analyte. Moreover, 11 commercially available tobacco brands were tested by striking the swab over the tobacco. Each tobacco sample revealed a nicotine signal

at 6.565 ± 0.0042 ms and 1.5632 ± 0.0007 cm²V⁻¹s⁻¹. Since nicotine is not relevant under criminal law, it was not included in the IMS database to avoid alarm generation.

Table 2-6 IMS and GC-MS results of the measurement of casework samples from prisons

Case	Description	IMS	Hit in %	GC-MS
1	plastic foil with herbal mixture	Cumyl PeGaClone	97	Cumyl-PeGaClone
2	Finely grounded tobacco remains	FUB-AMB	95	FUB-AMB, nicotine
3	Piece of paper	No alarm	-	Nicotine
4	4 self-made cigarettes, tobacco remains	No alarm	-	Nicotine
5	Remains of 2 self-made cigarettes	5F-ADB	96	5F-ADB, nicotine
6	Yellow pieces of paper	5F-ADB	94	AB-CHMINACA, APINAC, 5F-ADB MMB(N)-2201, caffeine
7	tobacco	No alarm	-	Nicotine
8	Piece of paper	No alarm	-	Nicotine
9	Remains of 1 self-made cigarette	No alarm	-	Nicotine
10	Tobacco in plastic foil	No Alarm	-	Nicotine
11	Tobacco in plastic foil	No Alarm	-	Nicotine
12	4 Self-made cigarettes	5F-ADB	-	5F-ADB, nicotine
13	2 Self-made cigarette	No Alarm	-	Nicotine
14	Piece of paper	No Alarm	-	No signals
15	Yellow piece of paper	No Alarm	-	Nicotine
16	Yellow piece of paper	No Alarm	-	Nicotine
17	Yellow piece of Paper	No Alarm	-	Palmitic acid, Leucocrystal violet
18	Remains of herbal mixture in plastic foil	Cumyl-PeGaClone	97	Cumyl-PeGaClone
19	Herbal mixture and tobacco	Cumyl-PeGaClone	93	Cumyl-PeGaClone, nicotine
20	Fine tobacco	FUB-AMB	95	FUB-AMB, nicotine
21	Piece of paper	No Alarm	-	Nicotine
22	4 Self-made cigarettes	FUB-AMB	-	FUB-AMB, nicotine
23	Envelope with two dark spots (from a liquid)	No Alarm	-	Glycerol
24	10 Pieces of paper	No Alarm	-	Leucocrystal violet
25	Photo	No Alarm	-	No signals
26	Envelope of greeting card	No Alarm	-	Palmitic acid

Case	Description	IMS	Hit in %	GC-MS
27	Greeting card	No Alarm	-	No signals
28	Brown herbal mixture	5F-ADB	-	5F-ADB, FUB-AMB, nicotine
29	Brown herbal mixture	5F-ADB	-	5F-ADB, FUB-AMB, nicotine
30	Brown herbal mixture	5F-ADB	94	5F-ADB, PB-22, nicotine
31	Envelope	No Alarm	-	Palmitic acid
32	Handwritten letter	Cocaine*	89	Cocaine, caffeine paracetamol
33	Vial with transparent colorless liquid	Methadone	99	Methadone
34	Eye drops	No Alarm	-	No signals
35	Eye and nasal ointment	Methadone	95	Dexpanthenol
36	Eye and nasal ointment	No Alarm	-	Cholesterol

*substances from the general database from Smith Detection, they are no part of the database for synthetic cannabinoids which was developed during the study

2.5 Discussion

The portable IMS is a powerful analytical method for the application in prisons to uncover NPS drug trafficking. This thesis is supported by the key figures shown in this study. Due to the rapid emergence of novel NPS products the demand for rapid and simple drug detection is growing.³⁴ In prisons, the wide range of physical and mental health harms caused by the consumption of NPS¹⁰ is also challenging for prison officers.¹⁷¹ IMS offers the decisive advantage over other mobile analysis techniques, that the analysis of synthetic cannabinoids in different matrices is possible with high sensitivity. In this study no false negative alarms were generated when analyzing synthetic cannabinoids in different matrices. Each synthetic cannabinoid was successfully detected. In addition, the analysis is fast (less than 10 s), easy to use and non-destructive, which is important for daily work for prison officers especially also for paper samples. Color coding tests or immunoassays are rapid, sensitive, inexpensive and easy but they lack specificity. There is a risk of false positive results due to cross-reactivity with other non-targeted drugs of similar chemical structure. In case of more than one cannabinoid with close drift times in a sample the selectivity is limited to the detection of only one substance. Due to the fast changing drug market of NPS, the development of new test kits is constantly required. Other portable techniques like IR- or Raman spectroscopy are not able to examine synthetic cannabinoids in different matrices like herbal mixtures, papers, cosmetics or food samples.⁵⁹⁻⁶¹ In seizures, the concentration of an active ingredient is too low and the matrix impairs the spectral quality.⁵⁹ A further sample preparation step is thus

necessary.^{62,63} In the case of pure powders, the unique identification of an active compound is given by its spectral fingerprint. An unambiguous assignment is not possible with IMS, because it is a preliminary test which gives a hint to a possible active ingredient based on the size and shape of the ion with the reduced mobility as the only parameter available for preliminary identification. In order to fully demonstrate the applicability of the IMS method in prison, the precision, the separation capability and limits of detection were determined. The estimated LODs for the synthetic cannabinoids are in the range of 0.7-3.6 ng. The evaluated LOD in previously published studies were 10-100 times lower than the LOD determined in this study [55]. This could be attributed to the fact, that the threshold was set to 100 du in this study to avoid false positive alarms. In contrast, Gwak et al.²⁴¹ set a threshold of 2.5 du and demonstrated lower LOD. Higher LODs are also due to different ionization techniques. Gwak et al.²⁴¹ and Armenta et al.²⁴² used a ⁶³Ni ionization source whereas in this study, a corona discharge ionization source based on APCI was used. However, for criminal investigations or to uncover drug trafficking in prisons, the LOD in the ng-range is sufficient. From common dosages described in different platforms we know, that there is a realistic value for the detection of consumable amounts of synthetic cannabinoids especially in herbal mixtures or on impregnated papers.²⁴⁷ A higher threshold and thus a lower sensitivity were accepted to avoid generation of false positive results in prison.

Some publications reported that analytes with nearly the same chemical structure like the synthetic cannabinoids cannot be distinguished.^{2,181} In this study, all synthetic cannabinoids in demand were successfully detected by IMS when present as single substances independent of the matrix. The selectivity of the IMS was not always sufficient as shown for cases with two or more active ingredients with close K_0 values. The necessary resolution $R > 0.75$ of mobile IMS for identification was estimated to require differences in drift times and reduced mobility values of > 0.15 ms (> 0.013 cm²V⁻¹s⁻¹). Smaller differences led to an alarm only for the substance present at higher concentration. The active ingredients 5-F-ADB, AB-CHMINACA, FUB-AMB and PB-22 from casework Samples 6, 28-30 show smaller differences in drift time and reduced mobility values. The limitation of portable IMS was the analysis of active ingredients in highly viscous matrices (toothpaste or liquid soap) and medicinal products (casework Sample 35). This was caused by the poor solubility and inhomogeneous distribution of the analytes in the cosmetic products. The latter was due to the high viscosity of the matrices. Methadone, amphetamine and tetrazepam could be detected but not 5F-ADB, buprenorphine and fentanyl HCl. In general, it seems that only liquids with a low viscosity are amenable for the detection of synthetic cannabinoids. Medicinal products contain an active ingredient. The selectivity of the mobile IMS is limited and may lead to false positive alarms. In these cases, chromatographic techniques coupled to mass spectrometry represent the analytical techniques of choice due to their high separation

capability and identification power, however, at the cost of speed, simplicity costs and especially the necessity of a laboratory environment and personnel.^{47,108-110,123,134-136}

2.6 Conclusion

In this study, 25 different synthetic cannabinoids were successfully characterized by IMS in a rapid screening. For most of them, K_0 -values (1.0511 - $0.8069 \text{ cm}^2\text{V}^{-1}\text{s}^{-1}$) and drift times (9.995 - 13.024 ms) were reported for the first time. LODs were sufficient to detect these analytes with regard to common dosages. The IMS software was programmed to generate alarms to allow prison staff to quickly test suspicious samples for illicit drugs. The applicability of this study is demonstrated by the analysis of several seized drug samples including 14 different herbal mixtures (from real cases of the Detection Centre of Rhineland Palatinate), 12 papers and 36 cases from prisons from Rhineland Palatinate. Of all sample types tested, on highly viscous matrices and medicinal products could not be analyzed successfully. This new IMS approach is an effective and non-destructive presumptive test with a direct indication of the presence of synthetic cannabinoid. The IMS guarantees a fast operation with a simple sample application by wiping the surface of a sample with a swab. It can easily be used by prison officers without requirement of special skills. Therefore, IMS is suitable for mobile usage in prisons.

3 Discrimination of synthetic cannabinoids in herbal matrices and of synthetic cathinone derivatives by portable and laboratory-based Raman spectroscopy

3.1 Abstract

One of the greatest challenges for European drug police and customs forces is how to effectively respond to the dynamically changing market for new psychoactive substances (NPS). Due to the NPS phenomenon, there is an increasing demand by customs or drug enforcement organisations for rapid and portable analytical techniques to characterise unknown samples, such as Raman spectroscopy, which are frequently used as first indicative techniques to detect controlled substances like illicit drugs. In this study, the effective discrimination of 28 synthetic cannabinoids and 15 synthetic cathinone derivatives using three different Raman spectrometers with different excitation wavelengths (532, 785 and 1064 nm) was investigated. The results show a high comparability of the Raman spectra from different spectrometers using spectral pre-processing methods. A PCA model allows assigning a substance to a specific substance class and additionally provides information on the nature of structural building blocks of the synthetic cathinone derivatives or synthetic cannabinoids being in the focus of this study. Characteristic group frequencies for synthetic cannabinoids and cathinone derivatives are summarised in tables to support future identification in other studies and in police and customs forensic case work. Combining both the use of chemometrics and Raman frequency tables has been shown as a successful tool to improve the characterisation of 60 seized herbal mixtures containing synthetic cannabinoids as active ingredients.

3.2 Introduction

The appearance of new psychoactive substances (NPS) on the European drug market is not a new phenomenon, but they still cause serious harm to consumers and represent a persisting challenge to drug enforcement organisations.^{6,250} The distribution channels for NPS partly differ from those of classical drugs and the ordinary mail service is frequently used for the transport of hazardous NPS. The online market differentiates between three different selling strategies: shops offering NPS in the surface web 1) under their actual chemical names as “research chemicals”, 2) as blended and branded products in categories like “designer drugs,”

“legal highs,” “herbal highs,” “bath salts, ”Spice”¹ or 3) shops offering NPS in the dark web.²⁵¹ NPS have initially been designed to mimic established illicit drugs, such as cannabis, cocaine, amphetamine and lysergic acid diethylamide (LSD).^{2,3} In most cases no specific information on the active substance is given on the product label, thus the effects for NPS consumers are unpredictable and sometimes fatal.¹⁰⁻¹² According to the versatile distribution channels, there is also a particular risk for public institutions handling these products including postal delivery facilities, custom controls and prisons.²⁵² The term NPS comprises a wide variety of several types of psychotropic compounds with different effects including predominantly synthetic cannabinoids, synthetic cathinone derivatives, new synthetic opioids (e. g. fentanyl derivatives) and designer benzodiazepines.¹⁷⁰

The focus of this study is on the most common NPS in the European Union, that are represented by synthetic cannabinoids with 45 % of all seizures followed by synthetic cathinone derivatives with 33 %.²⁵⁰ Synthetic cannabinoids were initially designed to mimic the effects of delta 9-tetrahydrocannabinol (THC) in cannabis products. Therefore, pure synthetic cannabinoids are dissolved in a solvent such as acetone and sprayed onto the surface of dried plant material while stirring and sold in colourful and professionally designed packages as “herbal incense”.^{16,17} In contrast, synthetic cathinone derivatives are generally sold in powder form, they are chemically related to cathinone, the major active ingredient in the Khat plant¹⁸ and have similar effects to amphetamine and other stimulant drugs.¹⁹ Only few European countries list specific synthetic cathinone derivatives and cannabinoids in their drug law⁹, but the discrimination of new substances with often only small modifications in the chemical structure require selective analytical methods, which can easily comprise further compounds.⁷

Currently, inherently portable spectroscopic methods like Infrared- and Raman spectroscopy are the techniques of choice for rapid and mobile on-site analysis of NPS due to their high identification potential via spectral fingerprinting.^{59-61,253} According to the recommendations of the scientific working group for the analysis of seized drugs (SWGDRUG), Raman and IR spectroscopy are category A analytical techniques with maximum discriminating power along with other typically laboratory-based techniques (such as NMR- and mass spectrometry).⁴⁵

An important feature of portable Raman instruments compared to IR spectrometers is the possibility of direct analysis of packaged substances. Plastic bags and glass bottles are often transparent to the laser radiation of Raman spectrometers and a direct contact of the operator with hazardous and highly potent materials such as fentanyl derivatives is avoided.⁷⁴

Several publications evaluated the use of Raman for NPS products with different focal points.^{59,75,77,84-95} In some publications, the effect on Raman spectra generated using different excitation wavelengths including 785 nm and 1064 nm were discussed.^{86,90,96} Major limitations in NPS analysis with these techniques, however, may arise from matrix components, especially herbal mixtures in case of synthetic cannabinoids due to low active

ingredient contents. Comparison of the Raman spectra generated by different Raman spectrometers or different operating conditions were evaluated using instruments' in-built algorithms to determine the Hit quality index (HQI)⁸⁶ or dissimilarity calculations.⁸⁵ These studies aimed at constructing and validating spectral libraries to guarantee a possible transfer of those databases to other (portable) Raman spectrometers, sometimes using chemometric models, especially principal component analysis (PCA). Hargreaves et al. described the identification of classical drugs including cannabis, cocaine, amphetamine, MDMA and heroine using PCA.⁷¹ Regarding NPS, Omar et al. described the prediction potential when assigning an unknown substance to a substance class, whose spectrum is not present in a reference library, originally recorded for fentanyl derivatives, synthetic cathinone derivatives and synthetic cannabinoids.⁸⁴ Mohammadi et al. expanded the investigated substances classes with aminoindanes and diphenidines using surface enhanced Raman scattering.⁹¹ The potential of dual laser excitation wavelengths (785 and 1064 nm) was discussed in the work of Assi et al., where aminoindanes, benzodiazepines, synthetic cathinone derivatives, phenmetrazine derivatives, phenidate derivatives and methamphetamine derivatives.⁸⁸ Calvo-Castro et al. demonstrated the predictive potential of representative libraries and their PCA models for structurally related NPS subgroups.⁸⁵ Mostly, PCA models focus on substance classes but not on the distinction of substances within one substance class.

For further characterisation within the class of cathinone derivatives and synthetic cannabinoids, a detailed interpretation of Raman spectra is necessary with a clear assignment of specific bands to a group frequency for NPS, especially for synthetic cannabinoids. Lobo et al. described Raman bands of 5F-AMB with a detailed table for all possible vibrational modes.⁹⁵ For criminal investigations, it would be of interest to be able to identify the different core structures, linkers and linked group by Raman spectroscopy. This aspect is envisaged in the study presented here. Furthermore, we show for the first time that a straightforward sample preparation procedure using solid/liquid extraction followed by precipitation of the contained synthetic cannabinoids allows their identification in herbal products. We here combine PCA models with frequency tables from the reference library to more deeply characterise synthetic cannabinoids and cathinone derivatives using both benchtop and portable Raman spectrometers. The applicability of this approach was proven by the successful analysis of 60 herbal mixtures from police seizures.

3.3 Materials and Methods

3.3.1 Chemicals

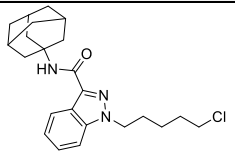
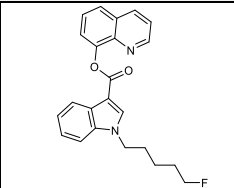
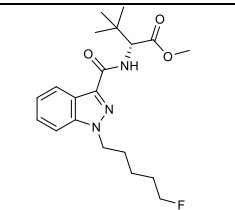
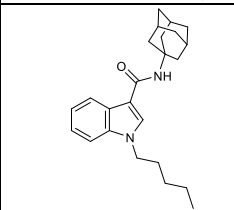
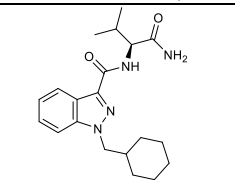
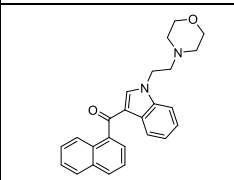
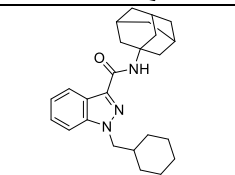
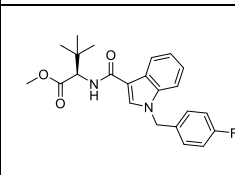
The reference material of 43 NPS (powders) employed in this study was provided by the EU-project "ADEBAR", which was co-funded by the Internal Security Fund of the European Union (IZ25-5793-2016-27). It is a cooperation project of the Federal Criminal Police Office,

seven State Bureaus of Criminal Investigation and German Customs. Seized samples are used to generate analytical standards not commercially available otherwise. Thus, new drugs appearing on the illicit drug market in Germany from 07/2017 to 07/2019 from various sources were identified by different analytical techniques (e.g. $^1\text{H-NMR}$). Technical information, the sample preparation steps and method parameters of the purity determination of NPS samples from seizures which was conducted by quantitative NMR (qNMR) are described by Schoenberger.⁴⁹ In Chapter 2 and in the publication of Metternich et al., the details of NMR analysis are summarised.²⁴⁸

Table 3-1 shows all 43 reference standards of this study, 28 synthetic cannabinoids and 15 synthetic cathinone derivatives. Exemplarily, Figure 1-3 shows the structure of the synthetic cannabinoid AB-CHMINACA with specific components core, linker and linked group.¹⁵

60 herbal mixtures from police seizures with 10 different synthetic cannabinoids as active ingredients were provided by the State Office of Criminal Investigation Rhineland-Palatinate.

Table 3-1 Chemical structures of the reference standards (powders) including a) synthetic cannabinoids and b) synthetic cathinone derivatives evaluated in this study with information of the corresponding source ADB (EU-project ADEBAR) or RLP (seized samples provided by State Office of Criminal Investigation Rhineland-Palatinate)

substances	Chemical structure	MW in g/mol	substances	Chemical structure	MW in g/mol
Synthetic cannabinoids					
Indazole-cores			Indole and azaindole-cores		
5-Cl-AKB-48		399.21	5F-PB-22		376.43
5F-ADB		377.21	APICA		364.53
AB-CHMINACA		356.47	JWH-200		384.48
A-CHMINACA		391.56	MDMB-FUBICA		396.46

substances	Chemical structure	MW in g/mol	substances	Chemical structure	MW in g/mol
ADB-CHMINACA		370.50	MMB-CHMICA		379.49
ADB-FUBINACA		382.44	SDB-006		306.41
AKB-48		362.52	UR-144		325.50
AMB-FUBINACA		383.42	XLR-11		329.46
THJ-2201		360.43	AB-5F-P7AICA		348.42
THJ-018		342.44	MDMB-5F-P7AICA		377.46
Carbazole and gamma-carboline-cores					
AB-FUBINACA		368.41	Cumyl-5F-P7AICA		367.47
5F-AMB		363.43	EG-018		391.51
5F-AKB-48		383.51	MDMB-CHMCZCA		448.61

substances	Chemical structure	MW in g/mol	substances	Chemical structure	MW in g/mol
Cumyl-4-CN-BINACA		360.46	Cumyl-PeGaClone		372.51
Synthetic cathinone derivatives					
Benzyl-cathinones			3,4-methylenedioxybenzene-cathinones		
alpha-PiHP		245.37	dibutylone		235.28
alpha-PPP		203.29	ephylone		249.31
buphedrone		177.25	MDPHP		289.38
1-(4-methylphenyl)-cathinones			1-(4-chlorophenyl)-cathinones		
4-methylpentedrone		205.30	4-Cl-butylcathinone		239.74
N-ethyl-4-methylnorpentedrone		219.33	4-Cl-ethcathinone-HCl		211.69
N-ethylnorhexedrone		233.36	4-Cl-N,N-dimethylcathinone		211.69
N-methylbenzedrone		267.37	4-Cl-pentadone-HCl		225.72
			4Cl-PVP-HCl		265.78

3.3.2 Methodology

3.3.2.1 Raman spectroscopy

The analysis of the reference standards was carried out with three different Raman spectrometers including one benchtop and two portable devices. Seized herbal mixtures were analysed using only the benchtop spectrometer with microscope. Identical operating conditions were used for powders and extracts from herbal mixtures.

Spectrometer 1: A benchtop Bruker (Ettlingen, Germany) Senterra Infinity 1 Raman spectrometer with a laser wavelength of 532 nm and a laser power of 10 mW was used. The operating software was OPUS 7.0. The reference standards were prepared by placing 1-5 mg onto a glass slide. Solid/liquid extraction of 100 mg herbal mixture with 1 mL

dichloromethane (Merck, Darmstadt, Germany) was accomplished, followed by filtration with syringe filters from Macherey-Nagel (Düren, Germany) with a pore size of 0.20 μm and a diameter of 25 mm and precipitating the synthetic cannabinoids by adding 2 mL ice cold water to the organic extract while keeping plant constituents in the organic phase. The precipitate was collected by decantation and dried directly on a glass slide under a flow of nitrogen at 45 °C and then placed under the microscope of the Raman spectrometer. The sample spectra were acquired with a runtime of 30 s with 10 scans/spectrum and stored in a database (OPUS 7.0). The wavelength resolution was set to 3-5 cm^{-1} with a scan range of 150-3400 cm^{-1} . All microscope data were collected using a 20x objective with a pinhole-type aperture of 50 μm . For each sample, 3 measuring points were sampled to check the spatial consistency of the spectral profiles. Homogeneity of the samples was verified by overlaying the 3 generated Raman spectra and a visual comparison of the spectral quality. Thus, for further analysis, averaged spectra were used.

Spectrometer 2: The first portable Raman spectrometer, a Progeny ResQ from RIGAKU (Neu-Isenburg, Germany) was equipped with a 1064 nm Nd:YAG laser. The Raman spectra were recorded at the maximum laser power of 490 mW with a wavelength resolution of 8-11 cm^{-1} and a scan range of 200-2 500 cm^{-1} . Each Raman spectrum was collected in the “auto mode”, which means that the scans/spectrum (1-3) and the duration of a scan (1 000-3 000 ms) were set automatically by the system.

Spectrometer 3: The second portable Raman spectrometer from BWTek LLC (Newark, USA) was an i-Raman Plus system with a BWS465-785S spectrometer, which was equipped with a laser emitting at a wavelength of 785 nm. The scan range was 174-3200 cm^{-1} and the wavelength resolution was set to 4.5 cm^{-1} . All microscope data were recorded using a 20x objective with BAC151B Raman Video Microsampling System (camera: active pixels: 1 280 x 1 024) using: BWSpec 4.03_23_C software. The integration time (in ms) was chosen and adjusted in a way that a relative intensity preferably above 45 000 for the most intensive peak was reached. The laser power was set to 207 mW, the integration time ranged from 5 000-250 000 ms. 10 scans/spectra were recorded. The powdered material was measured directly through a grip-bag or on a cap with the Video Microsampling System.

3.3.2.2 UPLC-DAD

The quantitative analysis of synthetic cannabinoids in 60 herbal mixtures from seizures were carried out using an UPLC Aquity-System (Waters, Milford, MA, USA) equipped with diode array detection (DAD). Further technical information, method parameters are given in Chapter 2.3.2.3 and in the publication of Metternich et. al.²⁴⁸

The quantification of herbal mixtures was carried out using a 7-point-calibration ($n = 3$) in the range of 0.25-0.005 mg/mL (in methanol) with the appropriate reference standard. 100 mg of the herbal mixture were suspended in 10 mL methanol for 20 min. The solutions were filtered with syringe filters from Macherey-Nagel (Düren, Germany) with a pore size of 0.20 μm and

a diameter of 25 mm. Subsequently, 100 μL of the filtered sample solution were transferred into UPLC vials and diluted with 900 μL methanol for injection (injection volume 5 μL). For recovery calculations of the solid/liquid-extraction (described in Section 2.2.1.1), the precipitate was dissolved in methanol (Merck, Darmstadt, Germany) to achieve a concentration of 1 mg/mL. Subsequently, 100 μL of the filtered sample solution were transferred into UPLC vials and diluted with 900 μL for injection (injection volume 5 μL).

3.3.3 Data treatment and chemometrics

Raman spectra of Spectrometer 1 were recorded directly with OPUS 7.0 software and saved in spc-format. Data from the portable Spectrometers 2 and 3 were exported as spc-files and imported into OPUS 7.0 software. Data pre-treatment was independent of the instrument.

3.3.3.1 Baseline correction

All spectra were baseline corrected using the “concave rubberband correction” algorithm (patented method by Bruker (Ettlingen, Germany)) with 10 iterations and 60 baseline points. This method divided the spectra into 60 wavenumber ranges (= baseline points) of equal size and the intensity minima of each range are determined. These minimal baseline points were connected by straight lines.

3.3.3.2 Algorithm for spectral comparison

The comparison of the Raman spectra recorded by spectrometers against the reference library (recorded by Spectrometer 1) is achieved by a Min-Max normalisation. This normalisation method performs a linear transformation on the data by transferring the minimum value of a band to 0 and the maximum value to 1. All other values were transformed to a decimal between 0 and 1. The maximum and minimum of a value x (\min_x and \max_x) for each band are calculated to get normalised data point x' :

$$x' = \left[\frac{(x - \min_x)}{(\max_x - \min_x)} \right]$$

Afterwards, the algorithm “spectra correlation” (OPUS 7.0) was applied to show the comparability of Raman spectra recorded by different instruments. Here, the sum of the squared deviations between the library spectrum (Lib_m) (from Spectrometer 1) and the spectrum (Unkn_m) from Spectrometer 2 or 3 for each data points is calculated. The Hit quality (HQ) is calculated as follows:

$$HQ = \left[1 - \frac{(\text{Lib}_m * \text{Unkn}_m)^2}{(\text{Lib}_m * \text{Unkn}_m)(\text{Unkn}_m * \text{Unkn}_m)} \right] * 100$$

$$Lib_m = Lib - \left[\frac{\sum_{i=1}^n Lib_i}{n} \right]$$

$$Unkn_m = Unkn - \left[\frac{\sum_{i=1}^n Unkn_i}{n} \right]$$

A HQ of 100 % indicates identity to the library spectrum. In this study, the threshold for a positive hit was set to 85 % for all spectrometers.

3.3.3.3 PCA

Principal component analysis (PCA) was conducted using the software “Unscrambler X” by CAMO Analytics (Trondheim, Norway) after import of baseline corrected Raman spectra (concave rubber band method) in the spc-file format.

PCA requires a prior normalisation step of all spectra, which was performed by a standard normal variate (SNV).²⁵⁴ This algorithm centre and scale individual spectra to removes scatter effects from spectral data without smoothing the spectra information.

3.4 Results and discussion

3.4.1 Comparison of different Raman spectrometers

All Raman spectra generated by Spectrometers 2 and 3 were matched against the reference library (recorded by Spectrometer 1) to determine the Hit qualities. The Raman spectra (pre-processed) of all reference sample recorded by Spectrometer 1 are shown in the publication of Metternich et al. (Figure S1).²⁵⁵ Both, non-processed (without any chemometric data treatment) and pre-processed (for details see Section 2.3 Data treatment and chemometrics) Raman spectra were investigated. Figure 3-1 a, b and c show the effects of the pre-processing steps for the Raman spectra of a representative cathinone (4-chlorobutylcathinone).

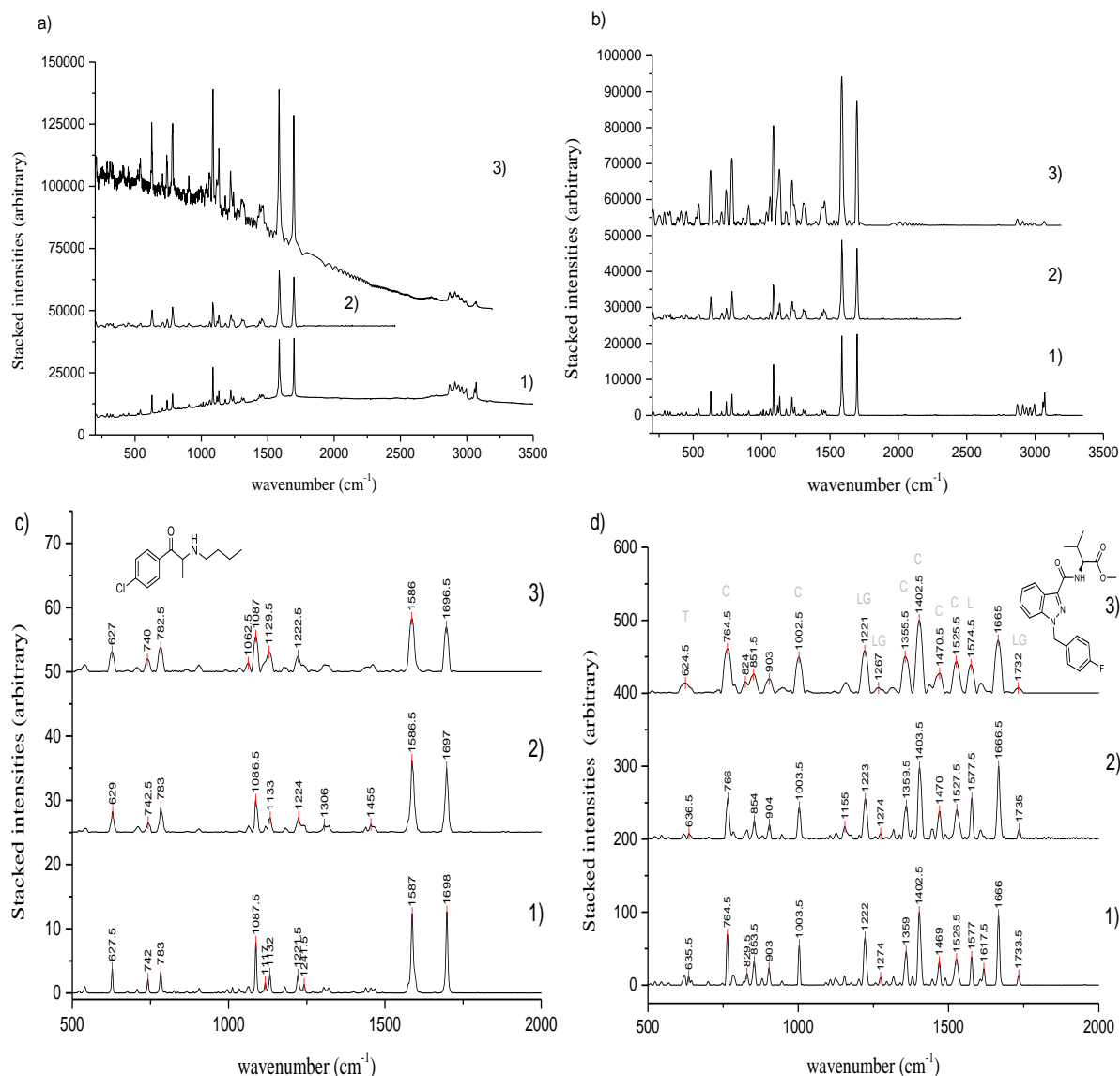


Figure 3-1 Comparison of Raman spectra (Trace 1 recorded with Spectrometer 1, Trace 2 recorded with Spectrometer 2 and Trace 3 recorded with Spectrometer 3) of a)-c) 4-chlorobutylcathinone and d) AMB-FUBINACA including Raman spectra a) without any chemometric pre-treatment, b) after baseline correction and c) after baseline correction and normalisation d) normalised and baseline-corrected with T, C, L and LG which indicate characteristic bands for tail, core, linker and linked group

Both, non-processed (without any chemometric data treatment) and pre-processed (for details see Section 2.3 Data treatment and chemometrics) Raman spectra were investigated. Figure 3-1 a), b) and c) show the effects of the pre-processing steps for the Raman spectra of a representative cathinone (4-chlorobutylcathinone). Despite differences in exposure time, laser power, resolution and laser wavelength, the frequencies and the relative intensities of specific Raman bands were similar for the three Raman spectrometers. Clearly, resolution decreases for Spectrometer 1 to 3. In addition, signal-to-noise (S/N-) ratios differ with Spectrometer 1 showing an S/N of 101-592, Spectrometer 2 of S/N = 30-107, and Spectrometer 3 of S/N = 18-48. A similar result is obtained for synthetic cannabinoids as shown in Figure 3-1d

for AMB-FUBINACA, demonstrating also that the chosen spectral pre-processing with baseline correction and normalisation is suitable. Especially, the concave rubberband baseline correction was advantageous for spectra recorded with Spectrometer 3 in particular, where fluorescence was observed. To guarantee that no information is lost upon pre-processing, processed Raman spectra were matched against non-processed spectra recorded with Spectrometer 1. Hit qualities above 98 % were obtained. Further normalisation tools were tested, which were offered by OPUS 7.0. Among them, Min-Max normalisation revealed better Hit qualities than vector normalisation. Regarding correlation of spectra, we observed that the correlation algorithm was better suited for the comparison of the Raman spectra than the “Euclidean distance algorithm” (OPUS 7.0 software). However, we experienced it to be less tolerant to slight peak shifts ($> 2 \text{ cm}^{-1}$), differences in the peak width at half height as well as relative intensities which could be present due to the use of different spectrometers. Thus, for further analysis, the correlation algorithm was preferred. Table 3-2 summarises the Hit qualities between the reference spectra (Spectrometer 1) and spectra from the two portable Raman devices of non-processed and pre-processed spectra for the 43 reference standards. The Hit quality ranged between 87-96 % with a threshold set to 85 %. This threshold value is recommended by the manufacturer of the applied portable Raman spectrometers and is also preferred in forensic institutions in Germany, which is further justified with regard to the different operating parameters of the instruments. Guirguis et al.⁸⁶ described correlations between internet products with NPS signature with Hit qualities that ranged from 57.0 to 84.1 % using an excitation wavelength of 785 nm and from 60.0 to 91.3 % using a laser excitation wavelength of 1064 nm. The authors showed that every tested standard was correctly identified with the help of the reference library, also with Hit qualities < 90 %.

Overall, “Spectrometer 3” showed better Hit qualities (by 2 % on average) for non-processed Raman spectra. This is due to the facts that the S/N ratio was a factor of 10 smaller than for Spectrometer 1. Other baseline correction methods provided by OPUS 7.0 like scattering correction and normal rubber band correction revealed the same Hit qualities. In contrast, the Hit quality obtained in the comparison with spectra from “Spectrometer 2” was largely independent of the data pre-treatment: non-processed spectra showed similar results. It can be concluded that the determination of Hit qualities of Raman spectra between different spectrometers requires test measurements and the evaluation of different chemometric models to enhance comparability.

Table 3-2 List of 28 synthetic cannabinoids and 15 synthetic cathinone derivatives with the data from UPLC-DAD measurements with the absorption maximum (λ_{max}), sample purity as determined by NMR, Hit quality values of the portable Raman spectrometers (Spectrometers 2 and 3) against the reference database generated with Spectrometer 1 for both pre-processed and non-processed spectra

Substance	Hit quality (Portable Spectrometers against reference library)			
	"Spectrometer 2"		"Spectrometer 3"	
	Pre-processed spectra in %	Non-processed spectra in %	Pre-processed spectra in %	Non-processed spectra in %
5-Cl-AKB-48	93	93	91	91
5F-ADB	94	92	86	92
5F-PB-22	87	87	88	92
5F-AMB	91	90	90	91
5F-AKB-48	91	90	89	90
AB-5F-P7AICA	93	92	87	89
AB-CHMINACA	92	92	87	88
A-CHMINACA	93	93	90	89
ADB-CHMINACA	91	90	87	87
AB-FUBINACA	90	89	89	90
ADB-FUBINACA	88	87	87	90
AKB-48 (APINACA)	94	94	88	92
AMB-FUBINACA	96	92	87	93
APICA	89	88	90	93
Cumyl-4-CN-BINACA	95	94	87	91
Cumyl-5F-P7AICA	93	90	89	90
Cumyl-PeGaClone	92	92	90	91
EG-018	97	97	90	93
JWH-200	87	87	87	90
MDMB-5F-P7AICA	96	87	90	94
MDMB-CHMCZCA	86	88	90	91
MDMB-FUBICA	94	93	87	88
MMB-CHMICA	90	90	88	89
SDB-006	90	90	88	89
THJ-018	93	92	89	92
THJ-2201	93	93	87	90
UR-144	91	91	88	91
XLR-11	92	93	87	91
4-chlorobutylcathinone	93	92	89	90
4-chloroethcathinone-HCl	95	95	91	91
4-chloro-N,N-dimethylcathinone	91	92	90	88
4-chloropentedrone-HCl	92	91	90	89
4Cl-PVP-HCl	92	93	88	87
4-methylpentedrone	90	91	86	86
alpha-PiHP	91	90	87	89
alpha-PPP	93	94	88	86
buphedrone	92	91	87	95
dibutylone	90	94	90	94
ephylone	93	92	93	96
MDPHP	90	90	86	88
N-ethyl-4-methylnorpedrone	92	91	87	88
N-ethylnorhexedrone	92	92	88	92
N-methylbenzedrone	94	94	84	91

3.4.2 Principal Component Analysis

PCA was carried out with all spectroscopic data of the 43 reference standards recorded by the three Raman spectrometers. A common region of interest (ROI) of 550-1750 cm^{-1} of the Raman spectra was selected. This ROI provided the most reliable information in the fingerprint region with a large number of bands being significant for discrimination (see discussion below). In addition, especially Spectrometer 3 showed noisy baselines in the spectral region of 200-550 cm^{-1} as visible in Figure 3-1. Figure 3-2 and Figure 3-3 show the score and loadings plots for synthetic cathinone derivatives (Figure 3-2a and b) and synthetic cannabinoids (Figure 3-3a-f). The variances covered by the first two principal components (PCs) are relatively low (49 % for synthetic cathinone derivatives and 37 % for synthetic cannabinoids) because all data points of the Raman spectra in the range of 550-1750 cm^{-1} were considered for PCA. Differences in signal intensities, resolution, noise and S/N-ratios of the three Raman spectrometers further induce variances. Nevertheless, the first two PCs provided sufficient information for the discrimination of structural features for both substance classes as visible from Figure 3-2 and Figure 3-3 (see discussion below). Similarly, Omar et al. grouped fentanyls, synthetic cannabinoids and synthetic cathinone derivatives using PCA with PC-1 and PC-2 contributing only to 37 % among the data. They also successfully used the whole Raman spectra for comparison in the range of 680–1725 cm^{-1} .⁸⁴ The use of the whole Raman spectrum is advantageous with regard to the ease of application in fast screening scenarios. The Raman spectra generated by different Raman spectrometers (and thus different operation conditions) showed a high degree of similarity which is corroborated by PCA. Synthetic cathinone derivatives with a 3,4-methylenedioxybenzene group and indazole-type synthetic cannabinoids form clusters plotting PC-1 vs. PC-2 (see Figure 3-2a and Figure 3-3a).

In Figure 3-2a, the score plot of PC-2 versus PC-1 for synthetic cathinone derivatives is shown. Four clusters are visible without overlap, which can mainly be assigned to the different substituents on the benzene ring. The 3,4-methylenedioxybenzene (MDB) cathinone derivatives are described by negative scores on PC-1 and positive scores on PC-2 with characteristic loadings at $\sim 1354 \text{ cm}^{-1}$, $\sim 1600 \text{ cm}^{-1}$ (PC-1) and 1680 cm^{-1} (PC-1 and PC-2) marked with MDB in Figure 3-2b. The 1-(4-chlorophenyl)-cathinones show positive scores on PC-1 and PC-2 with a large impact by bands of $\sim 1088 \text{ cm}^{-1}$ (PC-2), $\sim 1690 \text{ cm}^{-1}$ and $\sim 1588 \text{ cm}^{-1}$ (PC-1 and PC-2) according to the loadings plot in Figure 3-2b, labelled with Cl. The substitution on the benzene ring influences the frequency of molecular vibration. Whereas the 1-(4-methylphenyl)-cathinones have scores on PC-1 and PC-2 close to zero (not explicitly shown in Figure 3-2b), the benzyl group itself leads to negative scores on PC-2 (marked with Benz in Figure 3-2b). Responsible for this shift is the band near 1000 cm^{-1} , representing a band with the highest loadings for PC-2. Only negligible differences are induced by methyl substituents.

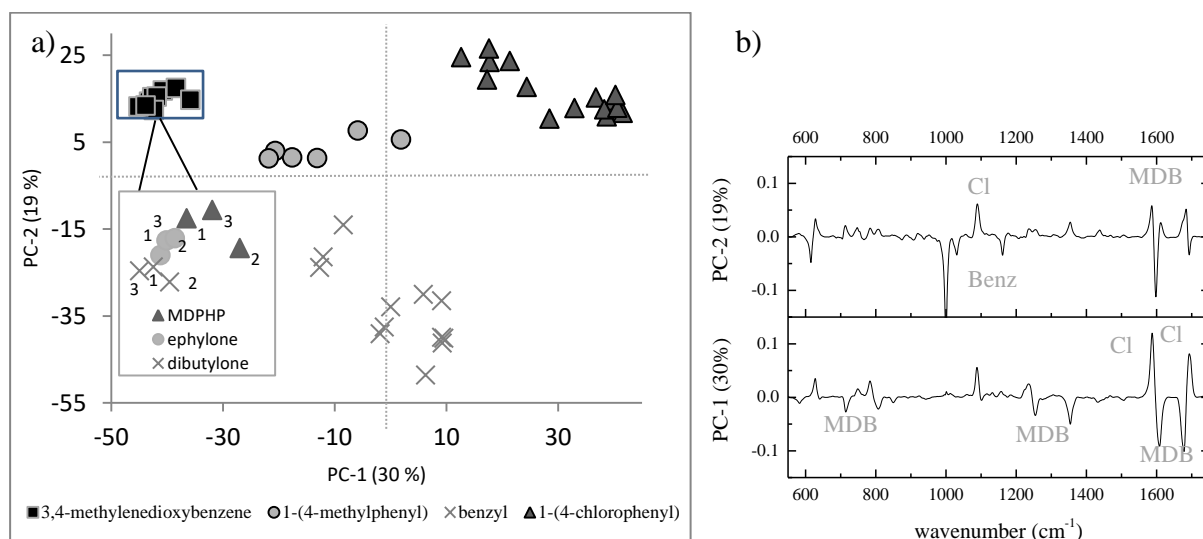
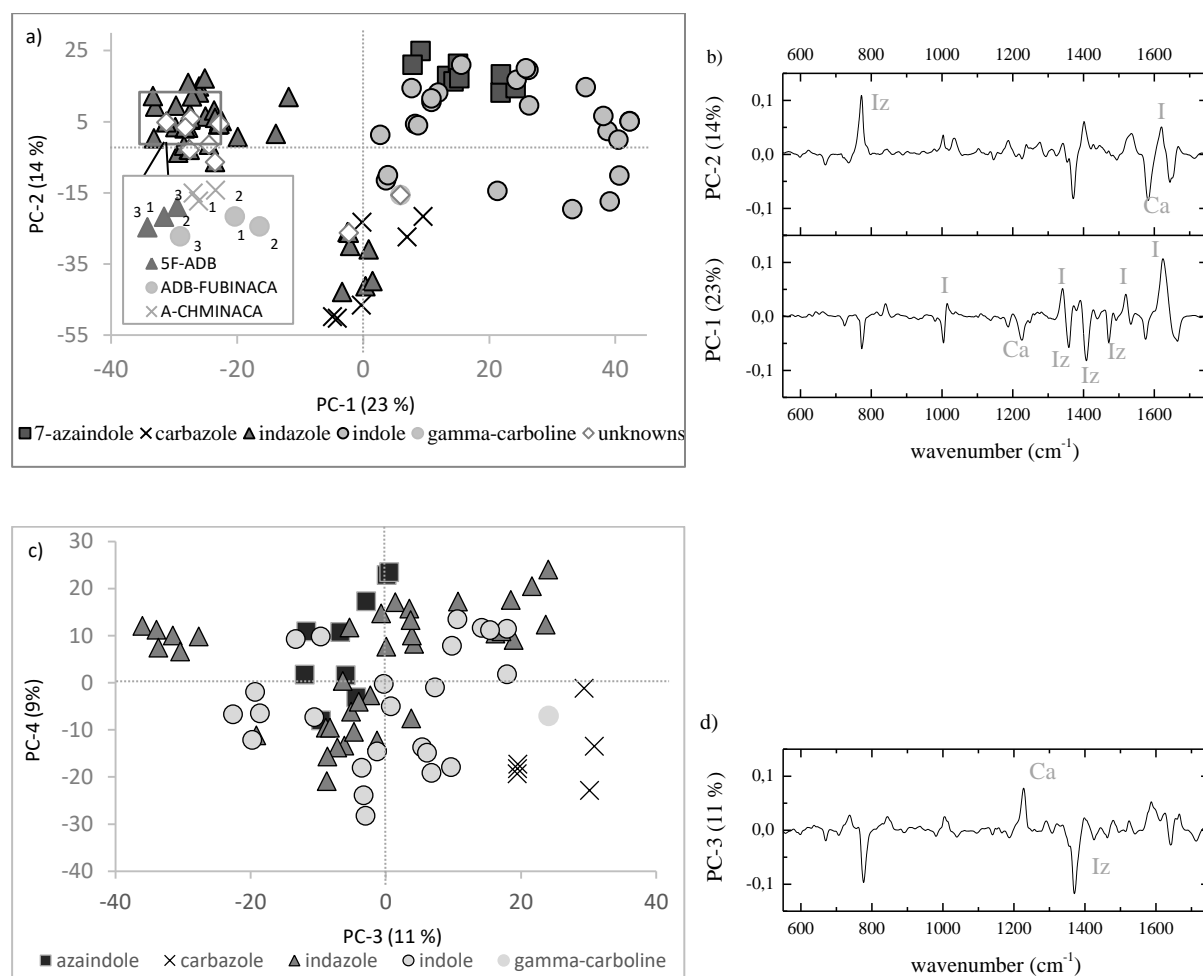


Figure 3-2 PCA score plots and loading plots computed for the Raman spectra of all reference samples measured with three different Raman spectrometers (including one benchtop-spectrometer ("Spectrometer 1") and two portable devices ("Spectrometer 2 and 3"), with a) all synthetic cathinone derivatives with the degree of similarity between pre-processing Raman spectra recorded on different Raman spectrometers (1-3) for selected substances with b) loadings plot of PC1,2 with characteristic loadings for MDB = 3,4-methylenedioxybenzene cathinones, Cl = 1-(4-chlorophenyl)-cathinones and Benz = benzyl-cathinones

In Figure 3-3a, the scores plot of PC-1 versus PC-2 for synthetic cannabinoids, labelled according to their core structure, is shown. The aromatic system is well described by the first five PCs (63 % of the variance explained on total). Two clusters of synthetic cannabinoids with an indazole core structure can be observed. The larger cluster consisting of nine different cannabinoids (overall 27 data points for the three different Raman spectrometers) shows negative scores on PC-1 and positive scores on PC-2 with characteristic loadings for 1405 cm^{-1} , 1350 cm^{-1} , 1470 cm^{-1} (PC-1) and 775 cm^{-1} (PC-2), marked with Iz in Figure 3-3b. The second smaller cluster consists of two indazole-based synthetic cannabinoids, THJ-2201 and THJ-018, with overall 6 data points for the three different Raman spectrometers. These substances show negative scores for PC-2 similar to synthetic cannabinoids with carbazole core structure. These two substances have a keto group as a linker connected to a naphthyl-moiety as a linked group as in EG-018 (see Table 3-1), producing relatively similar Raman spectra. In Figure 3-3c, a graph of PC-4 versus PC-3 is shown, which provides information to distinguish between these substances. Specific wavelengths of carbazole core structures can be identified by negative scores on PC-2 at 1570 cm^{-1} (Figure 3-3b) and PC-3 at 1220 cm^{-1} (Figure 3-3d).

Overall, indazoles can well be discriminated from indoles and azaindoles due to the N-N stretching vibration in the region of 1405 cm^{-1} (see loadings plot for PC-1 in Figure 3-3b) in the indazole ring system). The indoles and azaindoles are primarily described by positive scores on PC-1 and PC-2 with loadings at 1620 cm^{-1} (PC-1 and PC-2), 1520 cm^{-1} , 1340 cm^{-1} and 1010 cm^{-1} (PC-1), labelled with I in Figure 3-3b. The classes of azaindoles and indoles have overlapping clusters when plotting PC-2 vs. PC-1. However, comparing PC-5 versus

PC-2 (20 % variance explained) allows further distinguishing between these classes due to large positive scores on PC-5 (see Figure 3-3e and f) for azaindoles evoked by the band at 775 cm^{-1} marked with Az in the corresponding loadings plot. A relatively wide cluster of indole compounds can be observed due to the high variety in the linker group including amide, keto and ester-linkages. The amide linkage shows positive scores only for PC-1 whereas keto-linkage shows positive scores for both PC-1 and PC-2. In addition, the indole compound 5F-PB-22 is the only substance that carries an ester-group as a linker. This substance has both PC-1 and PC-2 values close to zero. No influence by the tail group was observed on cluster formation (data not shown explicitly). It was illustrated that for synthetic cannabinoids and synthetic cathinones derivatives, the assignment to a specific group according to their cores was very efficient using PCA. However, the application is limited in case of structurally closely related substances. The close-ups in Figure 3-2a and Figure 3-3a demonstrate that for MDPHP (Figure 3-2a) and AMB-FUBINACA (Figure 3-3a) the differences in PC-1 and PC-2 are too small to be discriminated when different spectrometers are used. This shows that PCA alone is not capable to identify unknown substances when using different spectrometers, but has to be supported by a reference library.



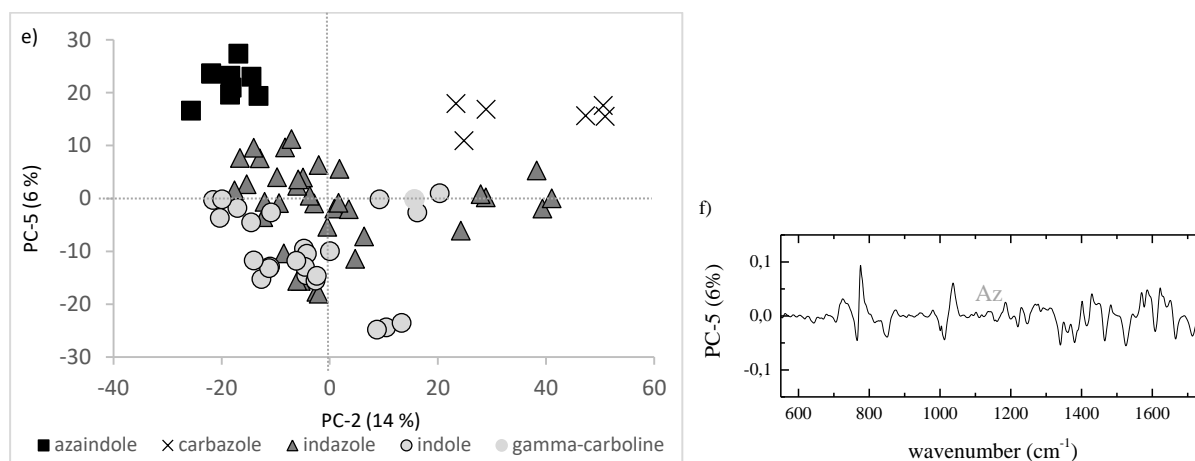


Figure 3-3 PCA score plots and loading plots computed for the pre-processed Raman spectra of all reference samples measured with three different Raman spectrometers (including one benchtop-spectrometer (“Spectrometer 1”) and two portable devices (“Spectrometer 2 and 3”), with a-f) synthetic cannabinoids with the degree of similarity between Raman spectra recorded on different Raman spectrometers (1-3) for selected substances with a) PC-2 vs. PC-1 and c) PC-5 vs. PC-2 and e) PC-4 vs. PC-3 with characteristic loadings (b, d, f) for I = indoles and azaindoles, Iz = indazoles, Ca = carbazoles and Az = azaindoles (to distinguish between indoles)

3.4.3 Characteristic Raman bands for both, synthetic cathinone derivatives and synthetic cannabinoids

Only a few publications have interpreted Raman spectra of synthetic cathinone derivatives and synthetic cannabinoids with regard to group frequencies.^{77,89,95} In our study, we identified discriminating and characteristic structural vibrations of NPS based on the PCA results, especially the loadings plots (see Tables 3-7). Raman spectra for representative substances are presented in Figure 3-4, where the main vibrational frequencies are marked. The Raman spectra of all reference sample (pre-processed as described in Section 2.3 Data treatment and chemometrics) recorded by Spectrometer 1 are shown in the publication of Metternich et al. (Figure S1).²⁵⁵ The Tables include the observed wavenumbers of the vibration, the intensity (recorded with Spectrometer 1) and a tentative assignment to the associated functional group and the characteristic values derived from the loadings plot for all NPS analysed. These Tables served as a powerful tool for substance identification in seized samples as demonstrated in section 3.4.4.

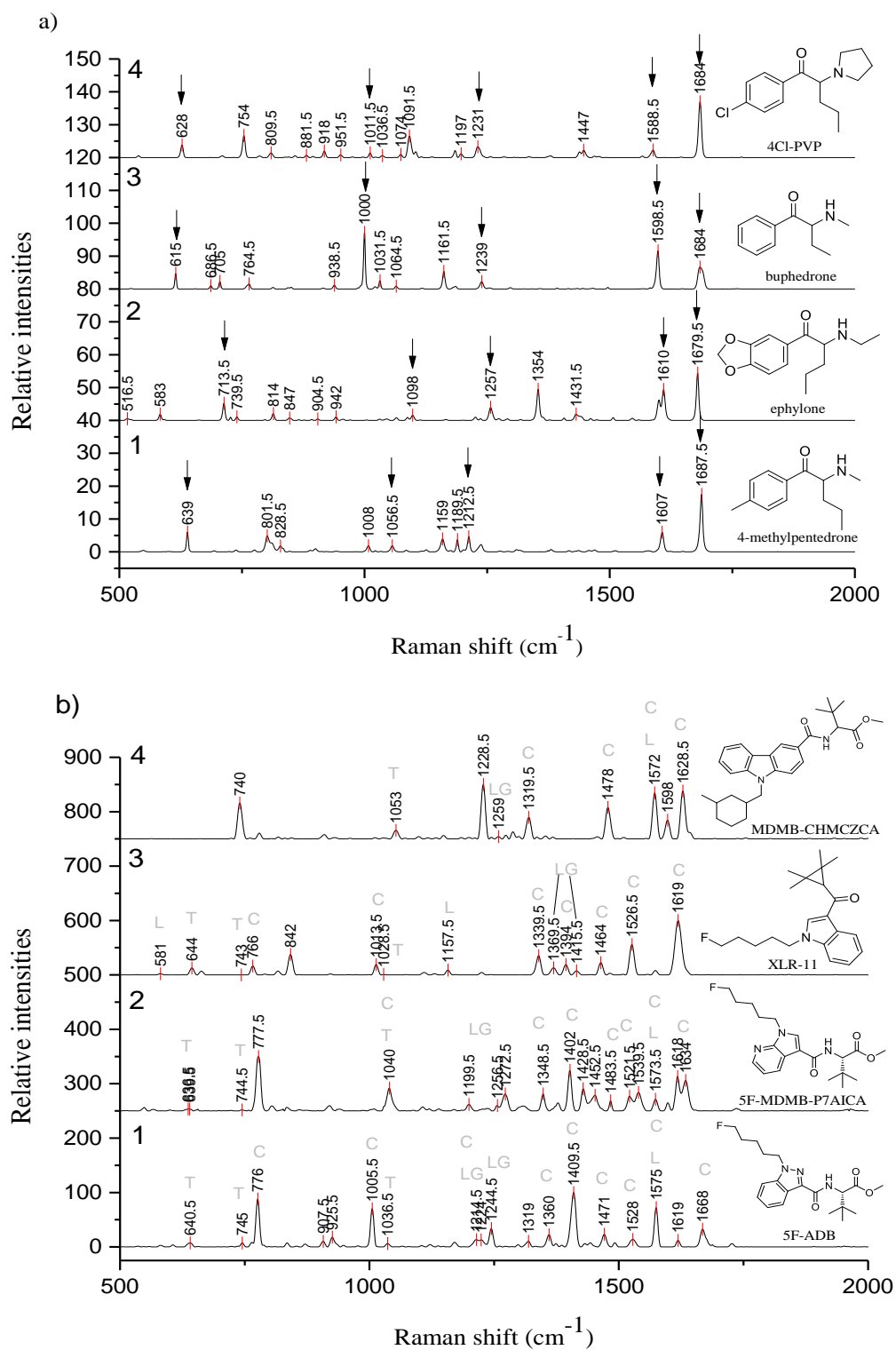


Figure 3-4 Raman spectra (baseline corrected and normalised) recorded with Spectrometer 1 with specific vibrational frequencies of a) four representative synthetic cathinone derivatives, each with different substituents on the benzyl-group, with 1 = 4-methylpentredone, 2 = ephylone, 3 = buphedrone, 4 = 4-Cl-PVP (with arrows labelled bands are discussed in the text) and b) four representative synthetic cannabinoids, each with different core-groups including 1 = 5F-ADB, 2 = MDMB-5F-P7AICA, 3 = XLR-11 and 4 = MDMB-CHMCZCA

3.4.3.1 Raman bands specific for synthetic cathinone derivatives

In Table 3-3, the Raman bands of four classes of synthetic cathinone derivatives are described differing in the substitution at the aromatic ring: benzyl-cathinones without an additional functional group, 3,4-methylenedioxybenzene-cathinones and 1,4-disubstituted-cathinones possessing either a methyl group (1-(4-methylphenyl)-cathinones) or a chloro-atom (1-(4-chlorophenyl)-cathinones). The spectrum of one representative of each class is given in Figure 3-4a. Benzyl-cathinones experience a strong in-plane ring deformation at $1010 \pm 10 \text{ cm}^{-1}$ assigned as Wilson mode ν_{12} , which involves displacing alternating carbon atoms around the ring. The modes give rise to the most intense bands in the Raman spectra of *N*-ethylnorhexedrone, alpha-PiHP, alpha-PPP and buphedrone (all benzyl-cathinones) as also visible in the loadings plot of PC-2. This band is specific for benzyl-cathinones (see Figure 3-2a and b) as this breathing motion is independent of the substituent as long as the substituents are located at the 1-, 1,3-, or 1,3,5-position. When the benzene is 3,4- or 1,4-disubstituted both groups of alternating carbon atoms in the aromatic ring are substituted and the band corresponding to Wilson mode ν_{12} is shifted from 1010 cm^{-1} to $1056\text{-}1101 \text{ cm}^{-1}$. The following trend was observed: benzyl-cathinones ($998\text{-}1000 \text{ cm}^{-1}$) < 1-(4-methylphenyl)-cathinones ($1056\text{-}1073 \text{ cm}^{-1}$) < 1-(4-chlorophenyl)-cathinones ($1087\text{-}1091 \text{ cm}^{-1}$) < 3,4-methylenedioxybenzene-cathinones ($1095\text{-}1101 \text{ cm}^{-1}$), see also Table 3-3. Obviously, beside steric effects and mass differences, electron-accepting moieties (Cl, methylenedioxy) increase the double-bond character of the aromatic ring system and thus increase the frequency of the bond-vibration. Two further strong bands for synthetic cathinone derivatives were identified from their high loadings on PC-1 at $1596 \pm 11 \text{ cm}^{-1}$ and $1684 \pm 14 \text{ cm}^{-1}$ (see Figure 3-2b) in the spectra of all synthetic cathinone derivatives being strongest for 3,4- and 1,4-disubstituted benzenes. The first band at ca. 1596 cm^{-1} is distinct and assigned to the $\nu_{8\beta}$ mode. The intensity of second band around 1684 cm^{-1} from aromatic C=C stretching is enhanced compared to benzyl cathinones due to the conjugated carbonyl stretching vibration. MDPHP, ephylone and dibutylone show an additional band at $1610\text{-}1623 \text{ cm}^{-1}$, representing a useful marker for the 3,4-methylenedioxy substituted-cathinone derivatives not present for any other NPS (marked MDB in PC-2 in Figure 3-2b). This distinguishing feature has also been reported to be present in the Raman spectrum of MDMA⁷⁷. Another region of interest is $1206\text{-}1257 \text{ cm}^{-1}$ where bands are observed from aromatic C-H in-plane deformation vibrations. There is a clear shift in wavenumbers according to the substitution on the benzene ring: 1-(4-methylphenyl)-cathinones ($1205\text{-}1212 \text{ cm}^{-1}$) < benzyl-cathinones ($1208\text{-}1238 \text{ cm}^{-1}$) < 1-(4-chlorophenyl)-cathinones ($1230\text{-}1241 \text{ cm}^{-1}$) < 3,4-methylenedioxybenzene-cathinones ($1252\text{-}1257 \text{ cm}^{-1}$). The C-H out-of-plane deformation vibrations in the region of $580.2\text{-}811.3 \text{ cm}^{-1}$ show an opposite trend in the shift in wavenumbers: 1-(4-methylphenyl)-cathinones ($801\text{-}811 \text{ cm}^{-1}$) > benzyl-cathinones ($752\text{-}772 \text{ cm}^{-1}$) > 1-(4-chlorophenyl)-cathinones ($744\text{-}754 \text{ cm}^{-1}$) > 3,4-methylenedioxybenzene-cathinones ($580\text{-}584 \text{ cm}^{-1}$).

Bands at 614-638 cm^{-1} arise from aromatic C-C in-plane deformation vibration. Typically, this vibration is assigned to benzene as a medium strong band near 606 cm^{-1} (benzyl cathinones at 615 cm^{-1}), which becomes shifted to higher wavenumbers upon substitution (vibration called ν_{6b} mode). Strong shifts to 626-638 cm^{-1} are observed for para-substituted benzenes and even further to 713 cm^{-1} in case of 3,4-methylenedioxy-cathinones (see Figure 3-2b). Para-substituted cathinone derivatives, including 1-(4-methylphenyl)-cathinones and 1-(4-chlorophenyl)-cathinones, can be distinguished due to ring breathing coupled with C-Cl stretching vibrations with a typical band of strong-to-medium intensity in the region 265-385 cm^{-1} due to C-Cl in-plane deformation vibration. The substances 4-chloro-*N,N*-dimethylcathinone, 4Cl-PVP, 4-chloroethcathinone, 4-chloropentedrone and 4-chlorobutylcathinone show weak bands at 289-300 cm^{-1} with overtone bands of medium intensity at 1510-1450 cm^{-1} . The 1-(4-chlorophenyl)-cathinones have a weak band between 1453-1468 cm^{-1} , described to be characteristic for these compounds by Christie et al.¹⁰³ and Stewart et al.^{77,89} and also visible in Table 3-3 (specific for benzyl-cathinones, 3,4-methylenedioxybenzene-cathinones and those with a methyl or fluoro-moiety on the benzene ring).

3.4.3.2 Raman bands specific for synthetic cannabinoids

In Tables 4-7, the group frequencies of specific structural elements with the highest intensity in the spectra of synthetic cannabinoids (shown in bold) are summarised with the core (Table 3-4), the linker (Table 3-5), the linked group (Table 3-6) and the tail (Table 3-7). These structural elements are depicted in Figure 1-3. One spectrum for a representative synthetic cathinone derivative of each class of ring substitution is given in Figure 3-4b.

a) Core group

The identification of synthetic cannabinoids via characteristic Raman bands of the indole-core is supported by studies on indole and tryptophan by Miura et al. and Takeuchi et al. and summarised from this study in Table 3-4. In total, eighteen fundamental vibrations due to the plane vibrations (W1-W18) of the indole ring were visible in our spectra^{256,257}. The bands W1-W6 appear in the region of 1624-1379 cm^{-1} . Indole-rings show C-H stretching vibrations in the wavenumber region 1463-1471 cm^{-1} (W5) and C-H out-of-plane deformation vibrations at 763-774 cm^{-1} (W18). The strongest bands in the Raman spectrum are observed at 1612-1627 cm^{-1} and 1572-1574 cm^{-1} , both caused by aromatic C-C stretching vibrations of the indole ring with the highest potential energy for C7-C8 (W1). These bands also have a strong impact on the PCA causing high values for PC-1. Other ring stretching vibrations were observed at 1480-1497 cm^{-1} (C8-C9), 1338-1342 cm^{-1} (C2-C3) and 1012-1020 cm^{-1} (C5-C6). Two bands were observed from vibrations involving the nitrogen-atom of the indole ring, identified from a N1-C stretching vibration at 1515-1528 cm^{-1} and from N-H in-plane deformation vibration at 1379-1403 cm^{-1} .²⁵⁶

Several vibrations in indazole-cores were similar to indole-core vibrations. Indazole ring C-H stretching vibrations appeared in the region of 3052-3074 cm^{-1} and 1447-1471 cm^{-1} , C-H in-plane deformation vibration at 1483-1494 cm^{-1} and 1413-1398 cm^{-1} and C-H out-of-plane deformation vibrations at 764-779 cm^{-1} . Ring (C-C) stretching vibrations were visible at 1616-1622 cm^{-1} , 1569-1578 cm^{-1} , 1345-1359 cm^{-1} and 1002-1009 cm^{-1} .²⁵⁸ Two bands were observed which stem from vibrations including the nitrogen-atom of the indole ring at 1522-1538 cm^{-1} (an N1-C2 stretching) and at 1369-1379 cm^{-1} (N-H in-plane deformation vibration). In the region of 1494-1398 cm^{-1} there are several perceptible vibrations are observed involving nitrogen atoms including N2-C3, N1-C5 and N1-N2 stretching vibrations and N1-H10 in-plane deformation vibrations.

A discrimination between indole- and indazole-based synthetic cannabinoids is possible via the strongest bands in the spectra (see also Table 3-4): (1) bands specific for indazoles were observed at 1413-1398 cm^{-1} from stretching vibrations of N2-C3, N1-N2 and C-C of the phenyl ring, in-plane deformation vibrations of N1-H10, C7-H13 and C6-H12 and 764-779 cm^{-1} which arise from C-H out-of-plane deformation vibration, and (2) bands specific for indoles at 1612-1627 cm^{-1} and 1572-1574 cm^{-1} , both caused by aromatic C-C stretching vibrations of the indole ring with the highest potential energy for C7-C8 (W1). Both findings are supported by the PCA and the loadings plots of PC-1 and PC-2.

The synthetic cannabinoids MDMB-5F-P7AICA, AB-5F-P7AICA and Cumyl-5F-P7AICA contain azaindole (a pyrrolo[2,3-b]pyridine) as a core, but the vibrations are closely related to those of indoles, so that PC-1 and PC-2 do not allow discriminating between them (see Figure 3-3a). Here, plotting PC-5 versus PC-2 provides additional discrimination power, so that the band around 775 cm^{-1} can be used for distinction with azaindoles having the strongest band at 775 cm^{-1} whereas the strongest band for indoles is located around 1622 cm^{-1} .

The third core-group of synthetic cannabinoids are carbazoles and their specific vibrations were characterised by Anandhi et al.²⁵⁹ Carbazoles show C-C stretching vibrations at 1628-1623 cm^{-1} , 1572-1584 cm^{-1} , 1456-1465 cm^{-1} , 1334-1340 cm^{-1} , 1288-1228 cm^{-1} , 1291-12272 cm^{-1} and 1011-1014 cm^{-1} . There are also C-H deformation vibrations at 1477-1481 cm^{-1} , 1320-1325 cm^{-1} and 1149-1146 cm^{-1} . The band at 1288-1291 cm^{-1} stems from C-N stretching vibrations which have a lower potential energy. With these bands, a discrimination from other core groups is possible.

Table 3-3 Main vibrational bands and their intensities (vs (very strong = 90-100 %), s (strong = 90-70 %), m (medium = 70-30 %) and w (weak = 30-10 %) in the spectra of different synthetic cathinone derivatives and their assignments (ν = stretching vibration, δ = in-plane deformation vibration, γ = out-of-plane deformation vibration measured with Spectrometer 1, compared to literature values, characteristic vibrational frequencies with dominant contribution to the components in loadings plots of PCA analysis

Substance	Aromatic ν C-H	ν C=O	Aromatic ν C=C	Aromatic δ C-H	δ Ring	Aromatic δ C-C	γ C-H	ν C-Cl	γ C-Cl
	in cm^{-1}								
benzyl-cathinones									
Intensity	(m)	(s)	(s) PC-1	(m)	(vs) PC-2	(m)	(w)		
N-ethylnorhexedrone	3061	1692	1598	1228	998	615	752		
alpha-PiHP	3065	1678	1595	1226	1000	614	762		
alpha-PPP	3063	1689	1596	1208	999	614	772		
buphedrone	3062	1685	1598	1238	1000	614	763		
3,4-methylenedioxybenzene-cathinones									
Intensity	(m)	(vs) PC-1	(s) (m) PC-1	(m) PC-1	(m)	(m)	(w)		
MDPHP	3065	1680	1603 1611	1255 1354	1095	713	580		
ephylone	3061	1681	1600 1609	1257 1353	1098	713	583		
dibutylone	3062	1673	1606 1623	1252 1364	1101	715	584		

Substance	Aromatic ν C-H	ν C=O	Aromatic ν C=C	Aromatic δ C-H	δ Ring	Aromatic δ C-C	γ C-H	ν C-Cl	γ C-Cl
	in cm^{-1}								
1-(4-methylphenyl)-cathinones									
Intensity	(w)	(vs)	(s)	(m)	(m)	(m)	(m)		
<i>N</i> -ethyl-4- methylnorpentedrone	3064	1690	1606	1211	1056	638	802		
<i>N</i> -methylbenzedrone	3057	1674	1602	1205	1073	637	811		
4-methylpentedrone	3065	1650	1607	1212	1056	638	801		
1-(4-chlorophenyl)-cathinones									
Intensity	(m)	(vs) PC-1	(s) PC-2	(m)	(m) PC-1	(m)	(m)	(w)	(w)
4-chloro- <i>N,N</i> -dimethylcathinone	3057	1691	1587	1235	1090	626	744	1457	293
4Cl-PVP	3060	1684	1588	1230	1091	627	754	1468	300
4-chloroethcathinone	3060	1685	1587	1240	1088	627	747	1453	289
4-chloropentedrone	3069	1690	1589	1237	1087	627	749	1468	290
4-chlorobutylcathinon	3057	1698	1587	1241	1087	627	749	1467	290
Literature values									
fluorophenyl-, methylphenyl-, benzyl-, methylenedioxy-cathinones ⁸⁹	-	-	~1600	~1250	1000	-	690	-	-
β -ketophenethylamine ⁷⁷	-	1700	1605	1220	1001	~626	737	1458	-

Table 3-4 Main vibrational bands and their intensities (vs (very strong = 90-100 %), s (strong = 90-70 %), m (medium = 70-30 %) and w (weak = 30-10 %) of different cores in the spectra of synthetic cannabinoids and their assignments (ν = stretching vibration, δ = in-plane deformation vibration, γ = out-of-plane deformation vibration measured with Spectrometer 1, compared to literature values of related structures,* characteristic vibrational frequencies with dominant contribution to the components in loadings plots of PCA analysis)

Indoles										
Substance	ν C-H	Aromatic ν C7-C8 ν C5-C6 ν C8-C9	Aromatic ν C9-C4 ν C6-C7 ν C7-C8	ν N1-C2 δ C2-H δ N1-H	Aromatic ν C8-C9 δ C4-H δ C7-H	ν C-H ν C8-N ν C4-C5	δ N-H ν C2-C3 δ C6-H	Aromatic ν C2-C3 ν C8-N δ C6-H	Aromatic ν C5-C6 ν C6-C7 ν C4-C5	γ C2-H γ C2-N γ N-H
Intensity	(m)	(vs) PC-1	(w)	(s) PC-1	(m)	(w)	(m)	(m)	(m)	(s) PC-2 PC-5
JWH-200	--	-	-	1517	1484	1463	1390	1342	1013	767
XLR-11	3067	1619	1573	1526	1482	1464	1393	1339	1013	766
UR-144	3070	1627	1573	1521	1483	1465	1392	1342	1012	768
SDB-006	3076	-	1573	1520	1480	1465	1398	1341	1012	763
APICA	3069	1624	1573	1518	1483	1466	1397	1341	1012	767
MMB- CHMICA	3067	1619	1574	1520	1482	1463	1394	1339	1013	768
MDMB- FUBICA	3069	1613	1572	1515	1487	1471	1403	1338	1020	771
5F-PB-22	-	-	-	1528	1497	1465	1379	1342	1013	774
AB-5F- P7AICA	3052	1622	1569	1530	1483	1447	1399	1345	1002	778
Cumyl-5F- P7AICA	3052	1622	1569	1517	1481	1455	1402	1344	1003	775
MDMB-5F- P7AICA	3057	1618	1573	1522	1483	1451	1401	1348	1008	777
Ref. Indoles ²⁵⁶	-	1616 (W1)	1576 (W2)	1509 (W3)	1487 (W4)	1455 (W5)	1412 (W6)	1352 (W7)	1010 (W16)	767 (W18)
Ref. Tryptophan ²⁵⁷	-	1620	1577	1543	1491	1460	1430	1350	1010	760

Indazoles											
Substance	ν C-H	Aromatic ν C7-C8	Aromatic ν C9-C4	ν N1-C2	ν N2 C3 δ C-H δ N1-H	ν N2-C3 ν N1-C5 ν C-C ν C-H	ν N2-C3 ν N1-N2 ν C-C δ N1-H δ C-H	δ N-H	Aromatic ν C5-C4	Aromatic ν C7-C8 ν C6-C7 ν C8-C9	γ C2-H
Intensity	(m)	(m)	(s)	(m)	(m)	(m)	(m)	(vs) PC-1	(m) PC-1	(s)	(vs) PC-2
in cm^{-1}											
5F-ADB	3063	1618	1574	1528	1492	1470	1409	1374	1359	1005	776
5F-AMB	3062	1620	1576	1520	1492	1472	1404	1376	1360	1004	780
AB-FUBINACA	3066	1636	1572	1536	1492	1472	1402	1372	1356	1004	764
AMB-FUBINACA	3064	1617	1576	1526	1489	1469	1403	1379	1358	1003	764
AB-CHMINACA	3072	1618	1575	1530	1491	1470	1407	1379	1358	1004	778
ADB-FUBINACA	3074	1619	1577	1535	1494	1469	1398	1379	1359	1004	766
ADB-CHMINACA	3068	1618	1575	1530	1491	1470	1407	1379	1357	1004	778
AKB-48	3068	1617	1576	1534	1492	1471	1404	1373	1358	1004	773
5F-AKB-48	3067	1652	1572	1536	1492	1472	1404	1384	1360	1004	772
5Cl-AKB-48	3073	1615	1573	1538	1491	1470	1408	1374	1359	1004	773
A-CHMINACA	3069	1617	1571	1533	1492	1470	1413	1376	1359	1003	771
THJ-2201	-	1616	1578	-	1493	1464	1400	1369	1354	1009	778
THJ-018	-	1616	1576	-	1494	1469	1391	1370	1354	1005	779
4-CN-BINACA	3062	1615	1572	1533	1489	1476	1416	1379	1357	1003	778
Ref. 1 <i>H</i> -indazole ²⁶⁰ Ref. 1 <i>H</i> -indazole ²⁵⁸	3071	1626	1588 1601	-	1488	1444	1391 1405	-	1355	1003	769 775

Carbazole											
Substance	ν C-C δ C-H	ν C-C δ C-H	δ C-H ν C-C	ν C-C δ C-H	δ C-H ν C-C	ν C-C δ C-H	δ C-H ν C-C	ν C-C δ C-H	ν C-C δ C-H δ C-C	δ C-H ν C-C δ C-C	ν C-C δ C-H δ C-C
in cm^{-1}											
Intensity	(vs)	(s)	(w)	(w)	(m)	(w)	(m)	(w)	(s)	(w)	(m)
MDMB-CHMCZCA	1628	1572	1477	1456	1334	1320	1288	1228	1149	1011	
EG-018	1623	1584	1481	1465	1340	1325	1291	1227	1146	1014	
Ref. <i>N</i> -ethylcarbazole ²⁵⁹	1627	1577	1491	1458	1344	1313	1283	1219	1153	1015	
Ref. carbazole ²⁶¹	1625	1576	1481	1449	1334	1313	1288	1217	1183	1012	
Gamma-Carboline											
Substance	ν C-C δ C-H	ν C-C δ C-H	δ C-H ν C-C	ν C-C δ N1-H δ C-H	δ C-H ν C-C	ν C-H	ν (N11C) δ CH ν (C-CH3)	δ C-H	Aromatic ν C-C	γ C-H	
in cm^{-1}											
Intensity	(s)	(m)	(s)	(vs)	(m)	(w)	(m)	(w)	(s)	(s)	
Cumyl-PeGaClone	1636	1572	1472	1404	1356	1316	1260	1136	1004	788	
Ref. Harmane ²⁶²	1627	1577	1484	1405	1373	1311	1264	1139	1012	-	

b) Linker

Table 3-5 summarises the characteristic vibrations of the different linkers found in synthetic cannabinoids. C-O-C asymmetric stretching vibrations at 1249 and 1222 cm^{-1} are due to ester-linkages.²⁶⁰ Ketones show an asymmetric C-CO-C stretching vibration at 1152-1164 cm^{-1} . Aliphatic ketones have a strong in-plane deformation of the C-CO-C group at 630-620 cm^{-1} . The band is shifted to lower frequencies of 580-565 cm^{-1} , if alpha-branching occurs,²⁶⁰ visible in the Raman spectra of cannabinoids with a band at 593-601 cm^{-1} (e.g. JWH-200, XLR-11, UR-144, THJ-2201, THJ-018). However, most of the synthetic cannabinoids have an amide-linkage. A strong band at 1569-1577 cm^{-1} is due to aromatic C-C stretching vibrations of the indole or indazole-core but also due to N-H deformation vibration of secondary amide linker.

Table 3-5 Main vibrational bands of different linker in the spectra of synthetic cannabinoids and their assignments (ν = stretching vibration, δ = in-plane deformation vibration, as = asymmetric) measured with Spectrometer 1

Amide		Ester		
Substance	δ N-H in cm^{-1}	Substance	(as) ν C-O-C in cm^{-1}	(as) ν C-O-C in cm^{-1}
SDB-006	1573	5F-PB-22	1249	1222
APICA	1573	Ketone		
MMB-CHMICA	1574	Substance	(as) ν C-CO-C in cm^{-1}	(as) δ C-CO-C in cm^{-1}
MDMB-FUBICA	1572	JWH-200	1164	593
5F-ADB	1574	XLR-11	1157	581
5F-AMB	1576	UR-144	1152	595
AMB-FUBINACA	1576	THJ-2201	1152	598
MDMB-5F-P7AICA	1573	THJ-018	1164	601
AB-CHMINACA	1575			
AB-FUBINACA	1572			
ADB-FUBINACA	1577			
ADB-CHMINACA	1575			
AKB-48	1576			
5F-AKB-48	1572			
5Cl-AKB-48	1573			
A-CHMINACA	1571			
4-CN-BINACA	1572			
MDMB-CHMCZCA	1572			
AB-5F-P7AICA	1569			
Cumyl-5F-P7AICA	1569			

c) Linked group and tail

The substances evaluated in this study show different linked groups including ester (ν C=O and ν C-O-C 1800-1700 cm^{-1} and 1300-1000 cm^{-1}), amides (ν C=O \sim 1650 cm^{-1} , δ N-H \sim 1570 cm^{-1} and \sim 620 cm^{-1}), naphthalenes (ν C=C \sim 1510 cm^{-1} , γ C-H \sim 796 cm^{-1}), quinolines

(ν C=C \sim 1470 cm^{-1}), cyclopropyl-groups (γ C-H \sim 1400 cm^{-1}) or adamantyl-group (with many characteristic bands ²⁶¹) (see Table 3-6).

Table 3-6 Main vibrational bands of different linked group in the spectra of synthetic cannabinoids and their assignments (ν = stretching vibration, δ = in-plane deformation vibration, as = asymmetric) measured with Spectrometer 1

Ester		Vibrational band in cm^{-1}								
Substance	ν C=O	(as) ν C-O-C	(s) ν C-O-C							
MMB-CHMICA	1734	1258	1199							
MDMB-FUBICA	1725	1254	1199							
5F-ADB	1727	1244	1214							
5F-AMB	1740	1240	1216							
AMB-FUBINACA	1733	1257	1222							
MDMB-5F-P7AICA	1736	1256	1199							
MDMB-CHMCZCA	1737	1258	1228							
Amido		Vibrational band in cm^{-1}								
Substance	ν C=O	δ N-H	γ C=O							
AB-CHMINACA	1652	1575	617							
AB-FUBINACA	1636	1572	620							
ADB-FUBINACA	1655	1577	616							
ADB-CHMINACA	1651	1575	628							
AB-5F-P7AICA	1650	1569	623							
Naphthyl		Vibrational band in cm^{-1}								
Substance	ν C=C	γ C-H	δ Ring							
JWH-200	1517	798	645							
THJ-2201	1507	795	643							
THJ-018	1510	795	644							
EG-018	1506	795	646							
Cyclopropyl		Vibrational band in cm^{-1}								
Substance	γ C-H ₂	γ C-H								
XLR-11	1415	1369								
UR-144	1411	1369								
Quinolinyl		Vibrational band in cm^{-1}								
Substance	ν C=C	γ C-H	ν C-C	δ C-H						
5F-PB-22	1510	787	1486	1465						
Adamantyl		Vibrational band in cm^{-1}								
	δ H-C-H	δ H-C-C				ν C-C		δ C-C-C		
APICA	2922	2851.9	1438	1311	123	1103	977	942	644	450
AKB-48	2922	2852	1438	1315	1247	1101	979	944	644	453
5F-AKB-48	2922	2850	1436	1315	1244	1104	980	944	644	460
5Cl-AKB-48	2939	2847	1437	1310	1250	1102	980	943	644	460
A-CHMINACA	2923	2849	1436	1313	1248	1102	979	943	644	450

Also the tail, attached to the core of the synthetic cannabinoid (see Figure 1-3) shows characteristic vibrations as summarised in Table 3-7. Tails are similar in structure to the linked group, but further moieties including fluorobenzenes and fluoropentanes, (ν C-H

$\sim 3000\text{ cm}^{-1}$, $\gamma\text{ C-H } \sim 635\text{ cm}^{-1}$, $\sim 750\text{ cm}^{-1}$, $\sim 330\text{ cm}^{-1}$), chloropentanes ($\nu\text{ C-Cl } \sim 790\text{ cm}^{-1}$, $\sim 365\text{ cm}^{-1}$) and cyclohexanes ($\nu\text{ C-C } \sim 1055\text{ cm}^{-1}$) can be present. Exemplarily, the Raman spectrum of AMB-FUBINACA is presented in Figure 3-1b. This synthetic cannabinoid contains an ester group as a linked group and a fluorobenzene as a tail. Characteristic vibrations for the ester group include 1733 cm^{-1} , 1257 cm^{-1} and 1222 cm^{-1} and for the amide linker 1576 cm^{-1} .²⁶¹

Table 3-7 Main vibrational bands of different tails in the spectra of synthetic cannabinoids and their assignments (ν = stretching vibration, δ = in-plane deformation vibration, as = asymmetric) measured with Spectrometer 1

Fluorobenzene	Vibrational band in cm^{-1}			
Substance	$\nu\text{ C-H}$	$\delta\text{ C-F}$	$\delta\text{ C-H}$	Aromatic $\delta\text{ C-F}$
MDMB-FUBICA	2996	754	635	332
AMB-FUBINACA	3008	748	635	329
ADB-FUBINACA	3008	749	636	331
AB-FUBINACA	3007	764	620	332
Fluoropentane	Vibrational band in cm^{-1}			
Substance	$\nu\text{ C-H}$	$\delta\text{ C-F}$	$\delta\text{ C-H}$	
XLR-11	1028	743	644	
5F-ADB	1036	745	639	
5F-AMB	1020	748	620	
5F-AKB-48	1044	748	633	
MDMB-5F-P7AICA	1039	744	638	
5F-PB-22	1027	749	631	
THJ-2201	1024	735	643	
AB-5F-P7AICA	1034	750	623	
Cumyl-5F-P7AICA	1037	763	621	
Chloropentane	Vibrational band in cm^{-1}			
Substance	$\nu\text{ C-Cl}$	$\delta\text{ C-Cl}$		
5Cl-AKB-48	791	365		
Cyclohexane	Vibrational band in cm^{-1}			
Substance	$\nu\text{ C-C}$			
MMB-CHMICA	1053			
AB-CHMINACA	1053			
ADB-CHMINACA	1053			
A-CHMINACA	1060			
MDMB-CHMCZCA	1051			

Due to the structural similarity to other structural elements of synthetic cannabinoids, the identification of the tail and the linked group proved to be challenging. For example, the linker may possess an amide-group which is also present in some linked groups, e.g. in AB-CHMINACA. MMB-CHMICA has an ester group in the linked group, but an amide-linker giving rise to four specific Raman bands (1734 cm^{-1} , 1258 cm^{-1} , and 1199 cm^{-1}) for the ester

as a linked groups and one (1574 cm^{-1}) for the amide linker so that further bands have to be considered for a full discrimination or reference spectra must be available. In contrast, the absence of certain Raman bands from a spectrum assures the absence of a functional group with high certainty.²⁶²

3.4.4 Identification of synthetic cannabinoids in 60 herbal mixtures from casework samples

Synthetic cathinone derivatives normally seized in pure form without any bulking agents (according to statistical data from State Office of Criminal Investigation Rhineland-Palatinate, Germany) can well be identified by Raman spectroscopy.^{59,77,89,93} In contrast, synthetic cannabinoids are present in herbal mixtures making their identification by Raman spectroscopy challenging or even impossible as discussed by several authors, due to the low concentration of the active ingredient⁵⁹ and problems with fluorescence generation from herbal matrix components after laser excitation.^{59,94,95} In our study, we developed a simple sample preparation step to successfully remove (fluorescent) matrix components (see 2.2.2 UPLC-DAD). This included solid/liquid extraction with dichloromethane followed by precipitation of the cannabinoid upon addition of water. Results are given in Table 3-8 showing that ten different synthetic cannabinoids could be identified as active ingredients in the herbal mixtures. Identification was verified by UPLC-DAD (see Section 2.2.2 UPLC-DAD). A preliminary assignment to a specific substance class of the casework samples was possible using the PCA model including 10 spectra, which were averaged (for better visualisation on scores plot) and pre-processed (baseline subtraction and SNV-normalisation). In Figure 3-3a, all 10 synthetic cannabinoids in the 60 casework samples were correctly assigned to the cluster of synthetic cannabinoids with an indazole core (labelled as unknowns). As already observed for the reference substance, Cumyl-PeGaClone, the only substance with a gamma-carboline-core, had PC-1 and PC-2 values close to zero, so PCA did not support identification.

In a second step, the spectra of the ten different active agents (shown in Figure 3-5) were more closely investigated using Hit qualities and the reference library (see Table 3-8). It was demonstrated, that the band position and intensity were consistent but spectra of the herbal mixtures showed S/N ratios of 110-244 being lower by a factor 2-3 compared to the library spectra (385-309).

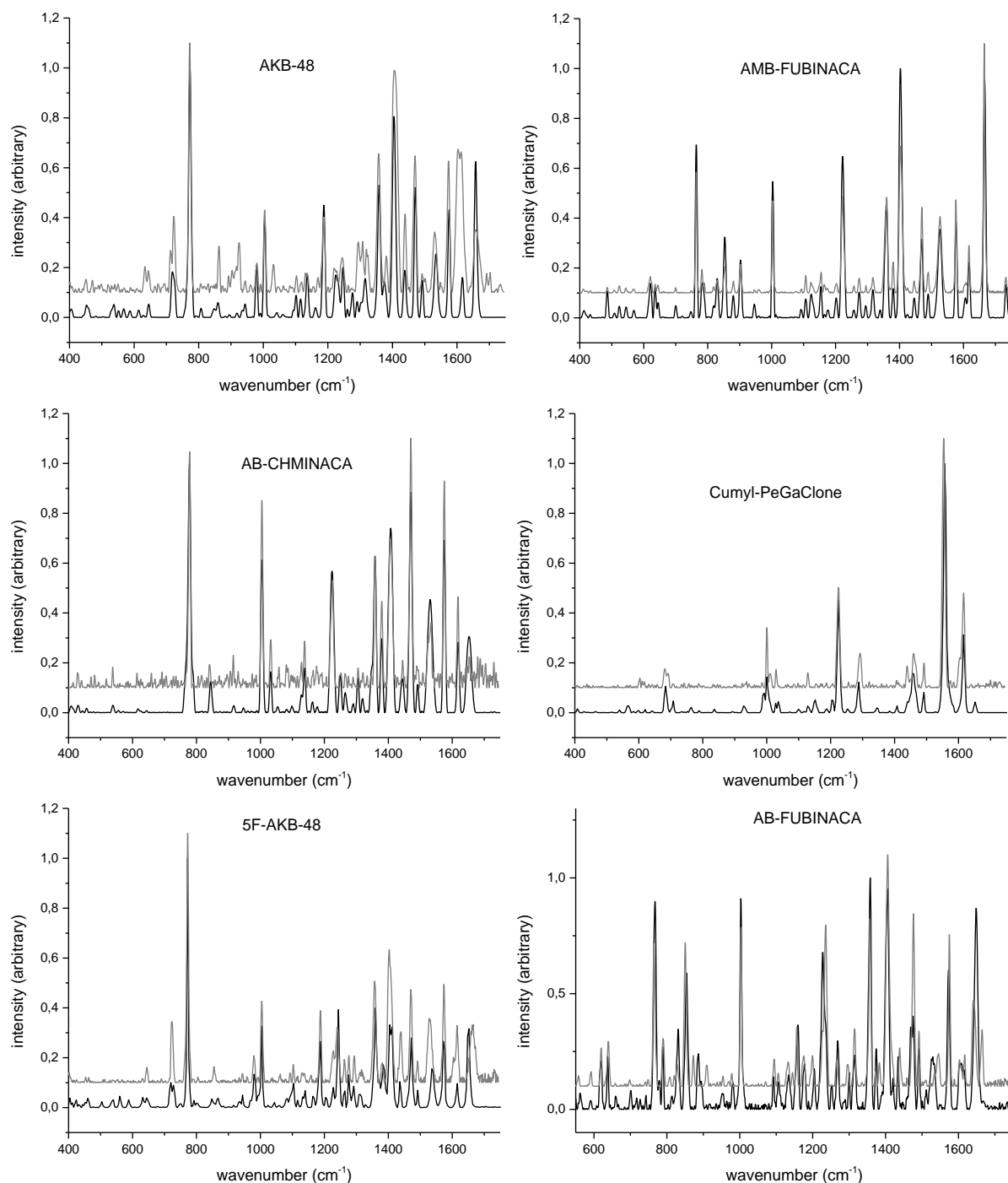


Figure 3-5 Raman spectra of six synthetic cannabinoids (exemplary) purified from herbal mixtures according to the protocol described in Section 2.2.1.1 Benchtop Raman spectrometer with microscope. Each plot shows the library spectrum (black) and the spectrum of the herbal mixture (grey) of a specific substance, generated both with Spectrometer 1 (spectra are normalised and baseline corrected according to Section 2.3 Data treatment and chemometrics)

Hit qualities ranged from 87.6 to 92.6 % (see Table 3-8) demonstrating that the combination of sample preparation and Raman spectroscopy can well be used for the characterisation of seizures. The observed bands were consistent with the characteristic group frequencies in Tables 4-7.

Table 3-8 Results of 60 casework samples (herbal mixtures) with UPLC-DAD data including λ_{max} , R^2 deriving from the calibration lines, content of the active ingredient in the herbal mixture determined and the recovery data with the absolute extracted amount and corresponding active ingredient content in the methanolic extract (see Section 2.2.2 UPLC-DAD) and Hit qualities of the Raman spectra against the reference library measured with Spectrometer 1

Casework sample	UPLC-DAD					Raman
	λ_{max} in nm	R^2	Active ingredient content herbal mixture in %	Recovery		Hit Quality in %
				Extracted amount in mg	Active ingredient content in extract in %	
Cumyl-PeGaClone						
1	221, 315	0.9998	1.0	1.35	26.2	90.7
2			1.5	1.69	32.1	92.7
3			3.8	1.05	54.2	92.2
4			3.8	1.18	50.9	92.0
5			0.5	0.93	23.0	87.8
6			3.4	1.72	45.6	87.7
7			3.3	5.22	45.5	93.8
8			0.9	1.70	28.2	80.3
9			3.3	1.48	50.8	92.2
10			2.9	1.82	41.8	92.7
AMB-FUBINACA						
11	301	0.9996	9.3	5.60	77.1	87.2
12			16.3	9.42	76.8	87.4
13			18.3	9.61	70.2	87.4
14			15.0	9.90	75.6	88.5
15			15.5	6.30	79.9	92.6
16			20.1	6.89	77.3	89.0
17			11.3	4.15	70.5	87.2
18			12.1	7.75	77.9	87.3
19			10.7	4.87	69.8	87.7
20			8.3	2.63	63.1	92.7
5F-ADB						
21	301	0.9999	2.10	0.554	73,6	87.4
22			3.61	2.081	24,7	87.7
23			1.81	1.896	26,2	87.1
24			3.82	3.078	23,8	87.9
25			3.63	2.746	44,9	86.5
26			2.24	1.451	25,6	85.9
27			5.02	2.758	30,8	88.5
28			1.50	1.409	21,8	87.3
29			4.11	2.245	33,8	88.3
30			3.30	2.389	36,4	90.6
AB-CHMINACA						
31	302	0.9997	1.91	1.43	24.3	87.9
32			1.72	1.59	29.9	87.5
33			24.0	9.40	61.6	92.9
34			4.22	2.06	29.8	90.4
35			6.57	-	-	-
36			3.12	1.48	31.2	88.0
37			1.87	1.57	24.3	88.9

Casework sample	UPLC-DAD					Raman
	λ_{\max} in nm	R ²	Active ingredient content herbal mixture in %	Recovery		Hit Quality in %
				Extracted amount in mg	Active ingredient content in extract in %	
38			24.0	9.26	62.1	93.8
39			2.13	1.64	17.2	88.1
40			2.93	2.56	31.8	87.2
ADB-CHMINACA						
41	301	0.9998	3.82	2.23	42.9	87.6
42			2.12	1.23	39.3	90.1
43			1.91	1.75	20.9	87.4
44			1.02	1.64	12.2	87.1
45			0.55	1.21	7.1	87.3
46			1.68	1.99	18.7	87.0
47			1.28	1.42	13.0	90.0
48			1.34	1.30	19.2	87.8
49			0.93	0.95	18.7	87.0
50			5.58	1.31	53.9	89.7
AB-FUBINACA						
51	301	0.9999	11.41	3.52	75.5	88.0
52			9.11	4.22	63.1	87.2
THJ-018						
53	218, 320	0.9997	6.92	3.83	49.9	88.9
54			6.22	2.33	38.1	89.9
5F-AMB						
55	301	0.9998	12.5	3.91	53.1	91.3
56			12.3	5.01	62.3	92.7
AKB-48						
57	301	0.9995	1.61	1.71	22.0	91.2
58			2.62	1.82	28.1	91.7
5F-AKB-48						
59	301	0.9995	9.11	2.13	52.8	92.5
60			8.92	1.82	53.7	92.6

However, some limitations of the approach are still present: When the concentration of the active ingredient was below 0.5 % (due to low concentration in sample or insufficient extraction), no Raman spectra could be recorded. This concentration may be found for highly potent synthetic cannabinoids (dose of 5 mg/g).²⁴⁷ However, when screening the literature on quantitative results for synthetic cannabinoids in herbal mixtures^{44,63,263,264} concentrations ranged from 5 to 446 mg/g in 765 samples investigated on total. Angerer et al. described the analysis of 342 herbal mixtures covering different brands, where 14 products showed active ingredients of one synthetic cannabinoid < 4 mg/g, sometimes with two or more additional active ingredients present in one sample (total content then > 5 mg/g).²⁶⁵ Together with the 60 herbal mixtures investigated during this study, the total content of active ingredient of synthetic cannabinoids < 4 mg/g is particular rare according to the statistics. Thus, the

estimated limit of detection of about 5 mg/g is suitable for most seizures. Otherwise, further preconcentration or more sensitive surface enhanced Raman spectroscopy or portable ion mobility spectrometry²⁴⁸ would be an alternative.

Besides the analysis with Raman spectroscopy, the dried precipitate also quantified via UPLC-DAD to determine the recovery of the sample preparation (see Table 3-8). The concentration range in the 60 herbal mixtures was very broad with 0.5-24 % active ingredient present. 0.5-9.9 mg active agent was recovered on the glass slide after sample preparation from 100 mg sample giving rise to recoveries between 7.1 and 79.9 %. In general, that low initial active ingredient contents were linked to low recoveries.

3.5 Conclusion

We here show that Raman spectroscopy is well suited to characterise seizures of synthetic cannabinoids and synthetic cathinone derivatives. Problems with regard to excitation of fluorescence with synthetic cannabinoids in plant matrix were solved using a simple solid/liquid extraction of only 100 mg herbal material in dichloromethane followed by precipitation of the active agent in water with recoveries high enough for subsequent Raman analysis down to a concentration of the synthetic cannabinoid in the sample of only 0.5 %.

We here showed that portable Raman instruments can be used for the identification of NPS, which is a great advantage for field analytics at border controls or in the area of policing. This was even possible using reference spectra generated by a benchtop instrument as proven by chemometry. Thus, only one spectral reference library proved to be necessary for the discrimination of unknown substances which can be transferred to the portable Raman system evaluated in this study. A PCA model was developed with corresponding loadings plots which was used to identify Raman bands characteristic for synthetic cathinone derivatives and synthetic cannabinoids but also to discriminate typical structural elements of the NPS including core, linker and linked group. Based on the PCA loadings, specific group frequencies of NPS were summarised in Tables that enable the assessment of a possible chemical structure. We successfully applied the combination of PCA and characteristic frequencies and a reference library (established using purified standards obtained from seizures) to characterise the active compound in various (herbal) seizures. The results demonstrate the high capability of the presented approach for forensic investigations both in laboratory but also on-site using portable devices. The benefits of Raman spectroscopy justify the application in public institutions, including the high discrimination power, the ability of portable usage of Raman devices, the analysis through packaging material and the safe handling of hazardous drugs for on-site operators.

4 Terahertz spectroscopy for the contactless and non-destructive detection of synthetic cannabinoids to uncover drug trafficking

4.1 Abstract

The demand for analytical techniques to uncover exploitation of the mail service for the transport of hazardous substances like explosives or drugs is still rising. Especially new psychoactive substances (NPS) are sold via internet in specialised shops and frequently sent via the ordinary mail service to the customer. The supply chains may stay unrevealed during the security inspection in postal facilities and pose a potential health risk presented by the unknowingly handling of drugs. We tested a method to detect NPS in postal packages using terahertz time domain spectroscopy (THz-TDS). Spectroscopic data of 16 synthetic cannabinoids were recorded including the centre frequency of the feature, FWHM and the cut-off frequency. Synthetic cannabinoids providing the same structural components show similar specific features, thus class identification is feasible. Synthetic cannabinoids containing an indazole-core showed centres of features at 1.2 THz and indole-cores at 1.3 THz. The indazole-based synthetic cannabinoids with a pentyl-group as a tail generated an additional feature at 2.4 THz. Naphthylindole-synthetic cannabinoids with an ester linkage showed significant features around 0.8 THz and 1.3 THz whereas a ketone-linkage showed five significant features at 0.8, 1.2, 2.2, 2.4-2.5, 3.7-3.9 THz. Naphthylindazole-synthetic cannabinoids (THJ-2201) possess nearly the same features with 0.8, 1.2, 2.1, 2.8 and 3.5 THz but two additional features were observed at 1 and 1.8 THz. Transillumination images of packed materials simplified and accelerated the selection of a grid of measurement points.

4.2 Introduction

At present, the rise in worldwide threats like terrorism, drug smuggling and assassination attempts calls for increased security measures. Public institutions are particularly at risk including custom controls, prisons, authorities, embassies, banks and political institutions.²⁵² The ordinary mail service is frequently misused for the transport of hazardous substances, especially for drugs.

Since 2004, a new phenomenon has arisen besides the use of classical drugs like amphetamine, cocaine, heroin or THC: the production of new psychoactive substances (NPS). The substances are sold as “designer drugs”, “legal highs”, “bath salts”, “research chemicals”

or “laboratory reagents”.¹ The United Nations Office on Drugs and Crime (UNODC) established a clear terminology: “New psychoactive substances are substances of abuse, either in a pure form or a preparation, that are not controlled by the 1961 Single Convention on Narcotic Drugs⁴ or the 1971 Convention on Psychotropic Substances,⁵ but which may pose a public health threat. In this context, the term ‘new’ does not necessarily refer to new inventions but to substances that have recently become available”.⁶ NPS have initially been designed to mimic established illicit drugs, such as cannabis, cocaine, amphetamine and LSD.^{2,3} Their effects are unpredictable for NPS-consumers and sometimes fatal¹⁰⁻¹² as there is no information about the active drug given on the product label. Synthetic cannabinoids represent the most common subgroup of NPS.¹⁶⁸ They are primarily sold via internet in specialised shops in colourful and professionally designed packages of herbal products or of pure powders.^{16,17} The selling of pure powders (in most cases at a scale of > 3 g according to data of State Office of Criminal Investigation Rhineland-Palatinate) is an indication of a subsequent processing of the synthetic cannabinoids (to for example herbal mixtures or e-liquids) and thus a dealer network. Currently, the security inspection in postal facilities stays unrevealed. Another fact that has to be taken into account is the potential health risk present due to handling of drugs. These challenges are not limited to postal facilities but also refer to other public institutions.

Several inspection techniques have been used such as x-ray scanning, canine detection, trace detections, ion mobility spectrometry (IMS), millimetre wave imaging and Raman or infrared imaging. In case of the detection of drugs, these techniques show some limitations.²⁶⁶ The ability of x-ray scanners is limited to the identification of the shape of for example a plastic bag but not the type of the drug or material and its elemental composition.²⁶⁷ The utilisation of trace detection techniques like portable ion mobility spectrometry makes sense only if there are detectable amounts of the concealed drugs outside the envelope.²⁴⁸ Millimetre wave imaging is limited to a spatial resolution of several millimetres and does not provide spectral information.²⁶⁶ Therefore, the characterisation of a drug type is difficult to realise. Spectroscopic techniques like infrared or Raman spectroscopy are invincible in the field of identification of unknown substances due to the chemical fingerprint region in the spectra. One disadvantage of these techniques is the high degree of absorption and scattering in paper which prevents an accurate analysis of the paper samples such as with NPS impregnated papers. Papers are used as a matrix in order to bring NPS into prisons by post. Therefore, NPS are dissolved in a solvent such as acetone and sprayed onto a piece of paper, tobacco or textiles and sent as a postal package or letter to the prison. The potential carrier substances are reduced to small pieces and then smoked or swallowed.²⁴⁸

As a result, the demand of an alternative technique is tremendous to detect and characterise NPS and related drug trafficking.

The THz frequency radiation possesses a combination of desirable properties for the detection of drugs in postal packages.²⁶⁸ The contactless THz-measurement principle is non-destructive, due to the low energy THz-waves, which do not induce a change in the chemical structure of the material under investigation. Moreover, THz-radiation is non-ionising and therefore not dangerous for human beings.²⁶⁹

THz radiation is located in the far infrared range from 0.1 to 10 THz between the microwave and the infrared portion of the electromagnetic spectrum with respective wavelengths from 3 mm to 30 μm .^{269,270} The properties of the THz radiation are characterised by a combination of the characteristics of both adjacent spectral ranges: Nonpolar and nonmetallic materials and dielectrics such as paper, clothes, wood and ceramics that are usually opaque at optical wavelength, are transparent to THz radiation.²⁷¹ The same phenomenon is observed for microwaves. THz radiation cannot penetrate metal and is strongly attenuated in water.

The IR range provides spectroscopic data with structural information of a substance due to spectral fingerprint region. In a medium, THz radiation primarily excites inter- and intramolecular oscillations but also rotational transitions.²⁷² Intramolecular oscillations describe the collective movement of molecules within a crystal lattice around their equilibrium state. Amorphous substances and liquids do not show any signatures, since intermolecular lattice oscillations are not excited in the crystal due to the near-order.²⁷³ In the last two decades, the extensive research in the field of THz radiation paved the way for the application in the field of science and technology.²⁷⁴ There is a wide variety of analytical purposes including communication,²⁷⁰ biology and medical sciences,^{275,276} pharmaceutical settings^{272,277,278} and space instrumentation.²⁷⁹ Since common packaging materials are dielectric, THz imaging is interesting in the field of defence and security for the inspection of sealed packages in public institutions without violating postal secrecy.²⁸⁰

The most common application of THz radiation in forensic science is the detection of explosives and chemical warfare agents.^{268,280} For drug analysis, the THz technology is hardly applied and is currently limited to the detection of classical drugs.

In principal, the analysis of different drugs can be carried out in packaging material like plastic bags and / or papers (envelopes) including methamphetamine,^{266,271,281-283} 3,4-methylenedioxyamphetamine (MDMA),^{266,271,283-285} 3,4-methylenedioxyamphetamine (MDA),^{283,284} cocaine,^{271,286} morphine,^{284,286} heroine,^{271,284} acetylcodein,²⁸⁴ acetaminophen,²⁷¹ terefindine²⁷¹ and ketamine.^{284,285} New innovations were demonstrated using cryogenic cooling with temperatures below -150°C and exchange of ambient air by the application of nitrogen. This reveals multiple spectral features that were not reported previously in room-temperature terahertz studies.^{281,284} In addition, the use of the solid-state density functional theory to correlate spectral features with molecular vibrations for methamphetamine, ketamine and 3,4-methylene-dioxyamphetamine.^{281,282,285,287}

This paper presents first tests for uncovering NPS drug trafficking of synthetic cannabinoids in postal packages using THz spectroscopy. The time domain and frequency domain spectra of 15 synthetic cannabinoids are presented. Furthermore, the experimental data are evaluated for each synthetic cannabinoid including the centre frequency of the feature, FWHM and die cut-off frequency which could serve as parameters in databases. The utility of the THz spectroscopy is successfully demonstrated by the analysis of synthetic cannabinoids in postal packages like plastic bags and envelopes. In addition, papers and herbal mixtures impregnated with synthetic cannabinoids were evaluated. We found out, that THz radiation is less sensitive than other spectroscopic techniques like Raman or IR spectroscopy to detect the synthetic cannabinoids due to the interfering matrix.

4.3 Materials and Methods

4.3.1 Chemicals

The reference standards of 16 synthetic cannabinoids (exclusively powders) employed in this study were taken from criminal cases provided by the State Office of Criminal Investigation Rhineland-Palatinate (Germany) and listed in Table 4-1. These include 5F-AB-PINACA (*N*-[[*(2S)*]-1-amino-3-methyl-1-oxobutan-2-yl]-1-(5-fluoropentyl)indazole-3-carboxamide), 5F-ADB (*N*-[[1-(5-fluoropentyl)-1*H*-indazol-3-yl]carbonyl]-3-methyl-*D*-valine, methyl ester), 5F-ADB-PINACA (*N*-(1-amino-3,3-dimethyl-1-oxobutan-2-yl)-1-(5-fluoropentyl)-1*H*-indazole-3-carboxamide), 5F-AMB (*N*-[[1-(5-fluoropentyl)-1*H*-indazol-3-yl]carbonyl]-*L*-valine, methyl ester), 5F-PB-22 (1-(5-fluoropentyl)-8-quinolinyl ester-1*H*-indole-3-carboxylic acid), 5F-UR-144 ((1-(5-fluoropentyl)-1*H*-indol-3-yl)(2,2,3,3-tetramethylcyclopropyl)methanone), AB-FUBINACA (*N*-[[*(1S)*]-1-(aminocarbonyl)-2-methylpropyl]-1-[(4-fluorophenyl)methyl]-1*H*-indazole-3-carboxamide), ADB-PINACA (*N*-(1-amino-3,3-dimethyl-1-oxobutan-2-yl)-1-pentyl-1-*H*-indazole-3-carboxamide), AM-2201 ([1-(5-fluoropentyl)-1*H*-indol-3-yl]-1-naphthalenyl-methanone), EG-018 (naphthalen-1-yl(9-pentyl-9*H*-carbazol-3-yl)methanone), FDU-PB-22 (1-[(4-fluorophenyl)methyl]-1*H*-indole-3-carboxylic acid, 1-naphthalenyl ester), JWH-018 (1-pentyl-1*H*-indol-3-yl)-1-naphthalenyl-methanone, THJ-2201 ([1-(5-fluoropentyl)-1*H*-indazol-3-yl]-1-naphthalenyl-methanone). For GC-MS and UPLC-DAD measurements, methanol (LC-MS-grade, Geyer, Rennigen, Germany) was used. For NMR analysis, acetone-*d*₆ (purchased from Deutero, Kastellaun, Germany) and internal calibrant 3,5-dinitrobenzoic acid (Fluka, TraceCERT, 99.66 %) were used.

Table 4-1 List of 16 synthetic cannabinoids with the data from GC-MS with fragment masses (m/z -values) and retention times (R_t) and the sample purity as determined by NMR

Substance	MW in g/mol	GC-MS		NMR
		m/z	R_t in min	Purity in %
5F-ADB	377.46	233, 145, 130, 289, 321	10.9	98.7
5F-AMB	363.44	233, 145, 304, 249, 131	10.9	98.5
5F-PB-22	376.43	232, 144, 116, 89, 376	18.2	99.6
5F-UR-144	329.45	232, 144, 314, 116, 247	10.7	98.5
5F-AB-PINACA	348.42	233, 304, 145, 234, 131	12.3	98.7
5F-ADB-PINACA	362.50	233, 318, 145, 131, 289	12.5	97.6
AB-FUBINACA	368.41	109, 252, 324, 145, 83	13.4	94.9
AB-PINACA	330.41	215, 286, 145, 216, 131	11.8	96.3
ADB-PINACA	344.51	215, 300, 144, 130, 271	11.9	97.9
AM-2201	359.45	359, 127, 284, 232, 144	15.2	99.8
EG-018	391.50	334, 391, 335, 127, 179	23.8	94.6
FDU-PB-22	395.44	109, 252, 253, 143, 83	22.8	76.5
JWH-018	343.47	127, 341, 214, 284, 144	13.7	98.6
ADB-CHMINACA	370.50	241, 326, 145, 131, 55	13.4	91.6
MDMB-CHMICA	384.51	240, 144, 296, 328, 268	12.6	97.0
THJ-2201	434.5	290, 434, 179, 346, 378	23.1	98.3

4.3.2 Methodology: Characterisation of NPS powders from seizures

4.3.2.1 Gas chromatography-mass spectrometry

As not all NPS were commercially available during the experimental work of this study, material from seizures was used as standards. Identity and purity of each seized drug powder were determined using a gas chromatograph with mass spectrometric detection (GC-MS). Information on the technical parameters, a detailed explanation of the sample preparation and the method parameters used are described in Chapter 2.3.2.1 and the corresponding publication.²⁴⁸ 5 mg of powdered samples were dissolved in 1 mL methanol. Papers spiked with NPS were covered with methanol for extraction (10 min) in a glass vial. Afterwards, the solution was transferred into a second glass vial and evaporated to dryness. Then, 100 μ L methanol were added to the glass vial and the solution was transferred to a GC-MS vial with a cone-shaped insert (Wicom, Heppenheim, Germany). The mass spectrum derived for each compound was compared to in-house libraries. Standards containing other substances than the drug of interest (e.g. cutting agents) were excluded from method optimisation and database setup.

4.3.2.2 NMR

The purity determination of NPS samples from seizures was conducted by quantitative NMR (qNMR) analysis. Technical information, the sample preparation steps and method parameters are described by Schoenberger.⁴⁹ In Chapter 2 and in the publication of Metternich et al., the details of NMR analysis are summarised.²⁴⁸

4.3.2.3 Terahertz time domain spectroscopy

In this study, a multipurpose Terahertz spectrometer T-spectralyzer TRF (Hübner, Kassel, Germany) was used. This technique is a time domain spectroscopy system (THz-TDS) based on infrared pulse transmission via optical single-mode fibers. A Ti:sapphire laser was applied to pump and detect THz waves, with the central wavelength of 810 nm, pulse duration of 100 fs, repeat frequency of 82 MHz and output power of 980 mW. The measurements were performed in the linear stage-based measurement mode and with reflection mode. For each measurement of pellets or powders, a grid of measurement points was chosen with defined number of points in x- (10 points) and y-direction (10 points). 2 mg of the powdered material were pressed into disks of 13 mm in diameter with a force of 7.5 tons with a hand hydraulic press (max. 25 t) from Specac (Orpington, UK) resulting in thicknesses of about 1.5-3 mm and a diameter of about 13 mm. The limit of detection was examined for EG-018 using 5 pellets with decreasing tablet thicknesses of 1.7 (~200 mg), 1.5 (~180 mg), 1.0 (~120 mg) and 0.6 mm (~70 mg).

To imitate real samples, one gram of each drug standard was packed in a plastic bag. Moreover, the plastic bag was additionally packed into a paper envelope to imitate postal packages. Herbal mixtures were provided by the State Office of Criminal Investigation Rhineland-Palatinate. The papers (standard copy papers 80 g/m²) were impregnated with different synthetic cannabinoids dissolved in methanol at two concentration levels (see Table 2-3) referring to common dosages.²⁴⁷

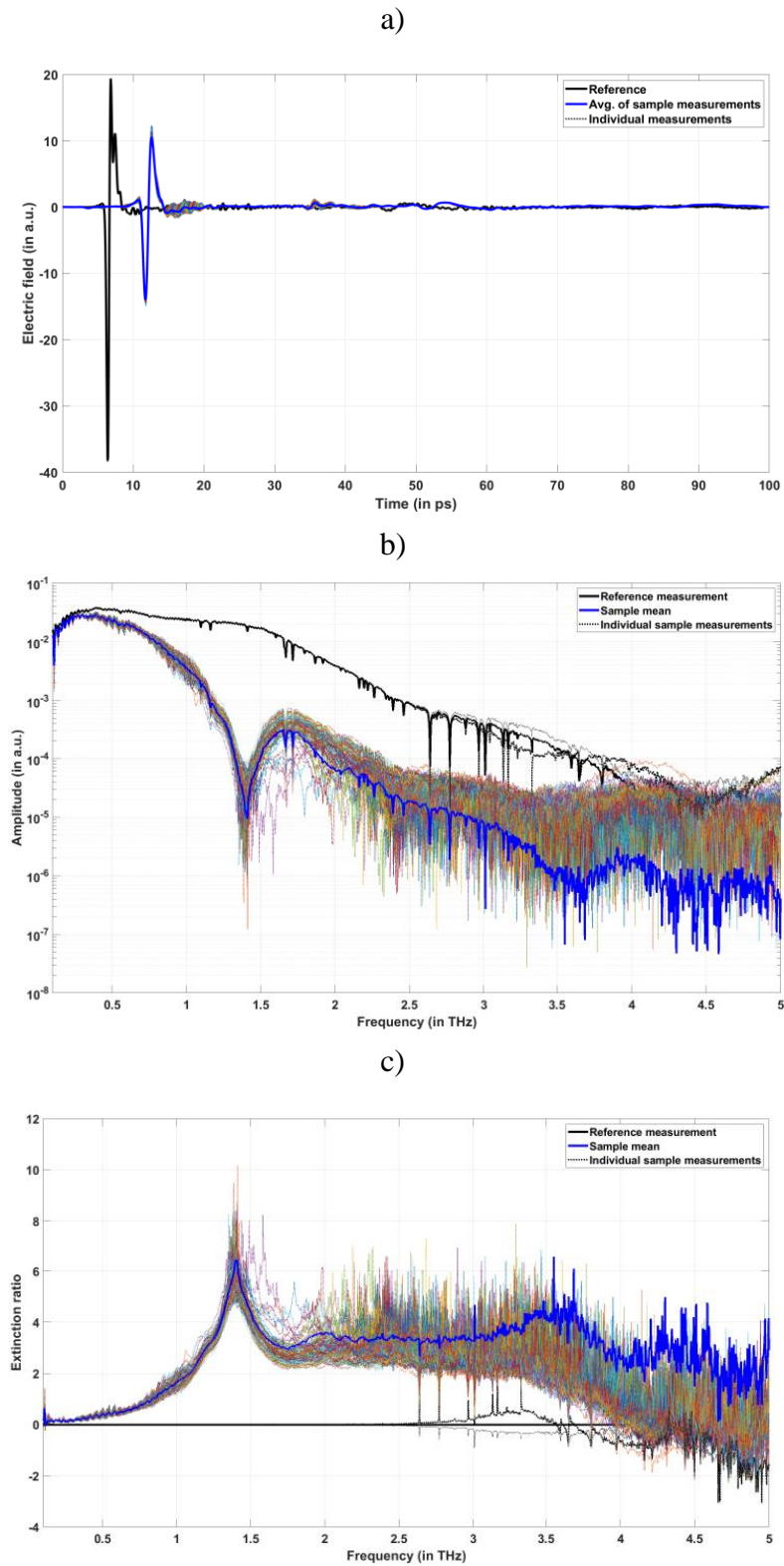


Figure 4-1 THz data of EG-018 depicted as a) the signals in the time domain for the reference (background measurement) and the average of sample measurements b) the corresponding curve in the frequency domain after FFT and c) the calculated extinction with a feature at 1.4 THz

The raster-scan THz imaging was performed by defining a rectangle with a representative area of interest. The THz image was superimposed on the optical image. The system automatically provides a “pixel” preview and an expected resolution.

Use the mouse to draw a rectangle, representing the area of interest, which you want to image. You will get a “pixel” preview, giving you an estimate of the resolution you can expect. One major advantage of THz technology is its ability to measure amplitude and phase of the electric field and not only the intensity of a THz wave. The interaction of the THz pulse with a sample leads to an attenuation and shift of the original THz pulse. Primarily, this provides information on a substance by the complex refractive index including the absorption by the sample. A mode-locked laser (e.g. fiber laser or Ti:sapphire) generated ultrashort laser pulses with typical pulse durations of about 100 fs and a respective THz range of 0.1 to 4 THz. The THz pulse is splitted at the beam splitter and transferred by optical fibers to the emitter and to the detector. The key of this technique is the synchronisation of the emitter and the detector, resulting in a repetitive measurement of the same section of the THz pulse and not statistically varying sections. The detector is only active for a very short period of time (less than one picosecond). Therefore, a specific section of the electric field of the THz pulse is recorded.

By varying the optical path length in the detector arm with e.g. a delay line, the section in which the detector is active changes. Therefore, the complete THz pulse is realised. The higher the delay line the longer the distance until the THz pulse reaches the detector. As the detector is only active for a very short time period, it responds only to a small fraction of the THz electric field, which is then seen as a quasi-DC field. These DC values are acquired and numerically assigned to the corresponding time delays. The measurement outcome is the sampled electric field as a function of time (delay) as shown in Figure 4-1a. This information can be transformed into a spectrum by fast Fourier transformation (FFT) (Figure 4-1b) or as an extinction function (Figure 4-1c).

4.3.2.4 UPLC-DAD

The quantitative analysis of synthetic cannabinoids in 26 herbal mixtures from seizures were carried out using an UPLC Aquity-System (Waters, Milford, MA, USA) equipped with diode array detection (DAD). Further technical information, method parameters are given in Chapter 2.3.2.3 and in the publication of Metternich et. al.²⁴⁸ The quantification of herbal mixtures was carried out using a 7-point-calibration ($n = 3$) in the range of 0.25-0.005 mg/mL (in methanol) with the appropriate reference standard. 100 mg of the herbal mixture were suspended in 10 mL methanol for 20 min. The solutions were filtered with syringe filters from Macherey-Nagel (Düren, Germany) with a pore size of 0.20 μm and a diameter of 25 mm. Subsequently, 100 μL of the filtered sample solution were transferred into UPLC vials and diluted with 900 μL methanol for injection (injection volume 5 μL). The results are shown in Table 4-2.

Table 4-2 Results of 26 casework samples (herbal mixtures) with UPLC-DAD data including λ_{\max} , R^2 deriving from the calibration lines and the content of the active ingredient in the herbal mixture (see Section 2.2.2 UPLC-DAD)

Casework samples	UPLC-DAD		
	λ_{\max} in nm	R^2	Active ingredient content in %
5F-ADB			
1	301	0.9999	2.11
2			3.63
3			1.80
4			3.82
5			3.65
6			2.29
7			5.07
8			1.53
9			4.17
10			3.33
ADB-CHMINACA			
11	301	0.9998	3.82
12			2.12
13			1.91
14			1.02
15			0.55
16			1.68
17			1.28
18			1.34
19			0.93
20			5.58
AB-FUBINACA			
21	301	0.9999	11.41
22			9.11
THJ-018			
23	218, 320	0.9997	6.92
24			6.22
5F-AMB			
25	301	0.9998	12.51
26			12.31

4.4 Results

4.4.1 Characterisation of NPS with GC-MS and NMR

For standards, samples from seizures were used. The powders were characterised by GC-MS and NMR to determine their purity and to exclude the presence of impurities. These substances served as reference material in this study. Initially, the powder material was analysed by GC-MS and the retention times and the characteristic m/z values of each substance are reported in Table 4-1 (arranged according to their importance). For identification of the synthetic cannabinoids, the MS spectra of the different samples were compared to in-house MS libraries. In addition, each sample was characterised with UPLC-DAD. The retention times and the λ_{\max} values are presented in Table 4-1 for each standard. The purity was determined using $^1\text{H-NMR}$ to be $> 94.6\%$, except FDU-PB-22 with only 76.4% . This sample also contained diethylamine and ethanol, which did not impair THz measurements. Other samples with impurities were not taken into consideration. Impurities included cutting agents that could also be present as an active ingredient in seized samples like paracetamol, caffeine, sugars or other drugs like e.g. amphetamine, cocaine or tetrahydrocannabinol.

4.4.2 THz procedure

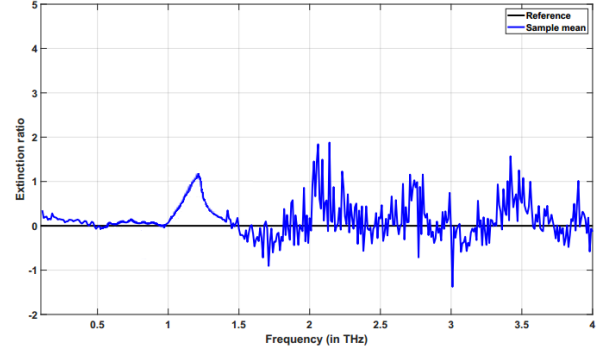
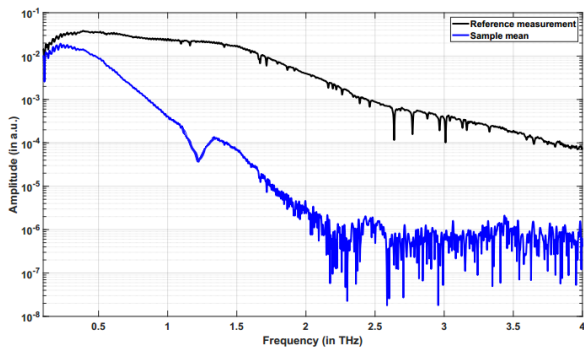
Table 4-3 summarises the corresponding characteristic parameters from the spectral data like the centre frequency of the feature, FWHM and the cut-off frequency.

The centre frequencies of synthetic cannabinoids ranged from 0.6 to 3.7 THz, with FWHM of 0.1-0.5 THz. No correlation between the cut-off frequencies of the synthetic cannabinoids, which ranged from 1.4 to 3.9 THz, and the thickness of a pellet was observed. Based on the THz spectroscopic data, some similarities in frequency domain spectra were emerged for structurally related compounds.

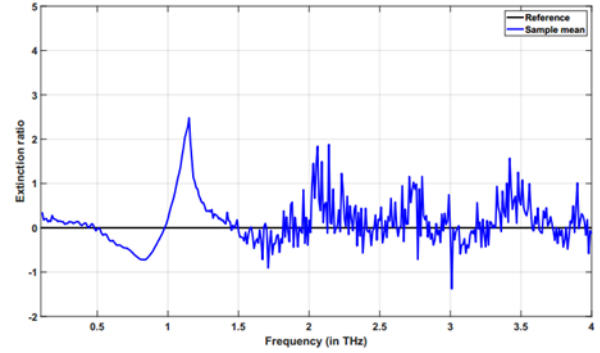
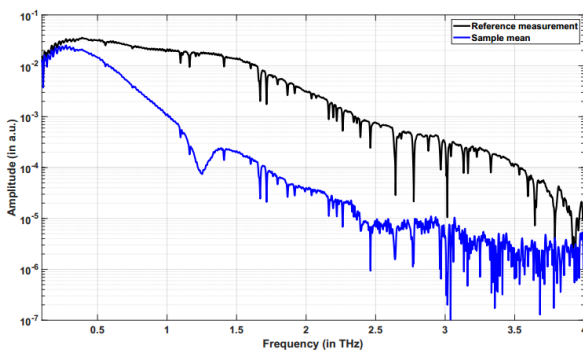
In this study, the indole-based synthetic cannabinoids 5F-PB-22, 5F-UR-144, AM-2201, FUB-PB-22, JWH-018 and MDMB-CHMICA show a feature around 1.3 THz (Table 4-3).

The centre frequency of the main feature for indazole-based synthetic cannabinoids is located around 1.2 THz. This includes the substances 5F-ADB, 5F-AMB, 5F-ADB-PINACA, 5F-AB-PINACA, AB-FUBINACA, AB-PINACA, ADB-PINACA, ADB-CHMINACA and THJ-2201. The indazole-based synthetic cannabinoids which possess a pentyl-group as a tail show an additional feature around 2.4 THz. Figure 4-1 presents the spectra of 5F-ADB PINACA and 5F-AB-PINACA, which show only one feature around 1.2 THz, whereas in the spectra of ADB-PINACA and AB-PINACA an additional strong and sharp feature around 2.4 THz were observed.

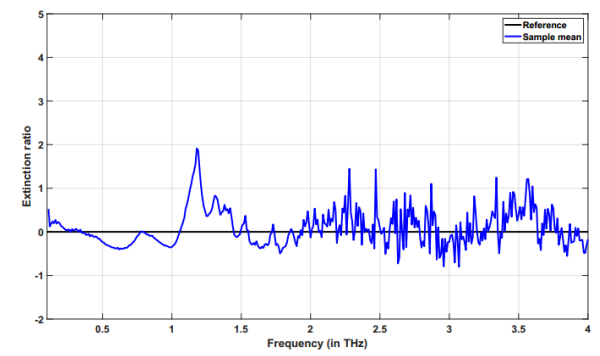
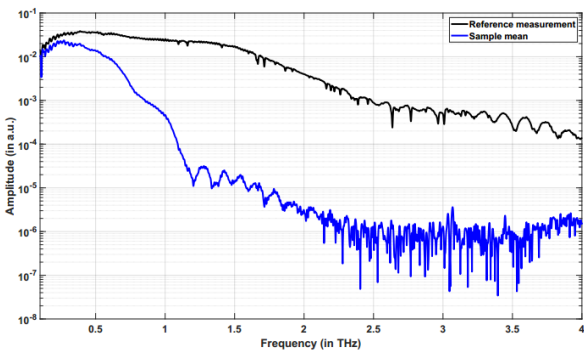
5F-ADB-PINACA



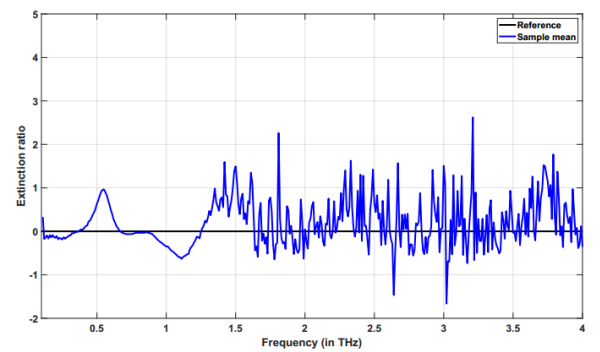
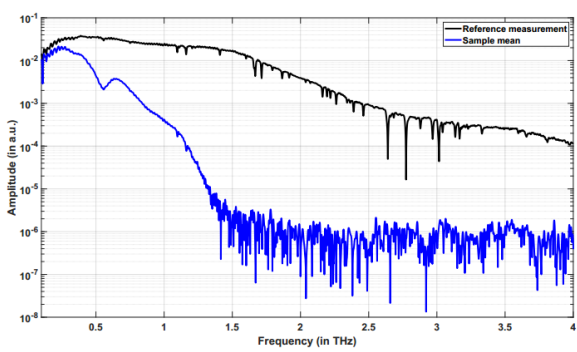
5F-ADB



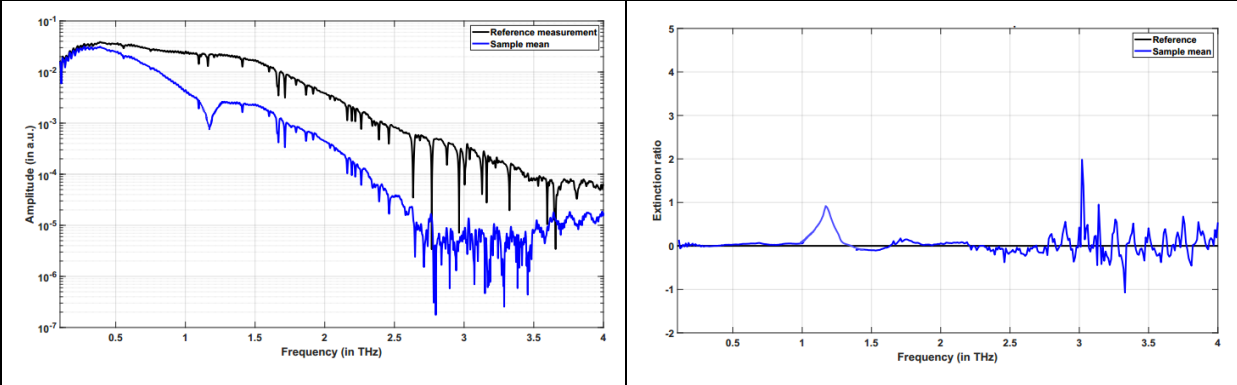
5F-PB-22



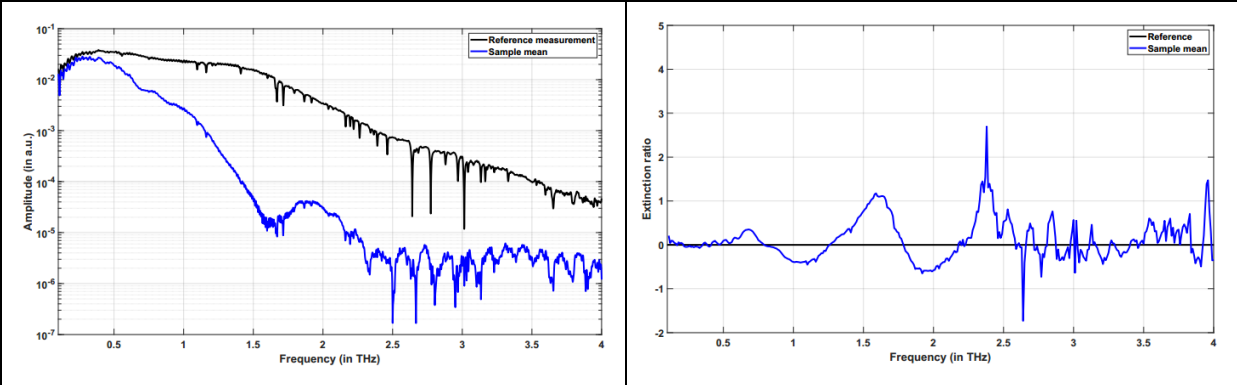
5F-UR-144



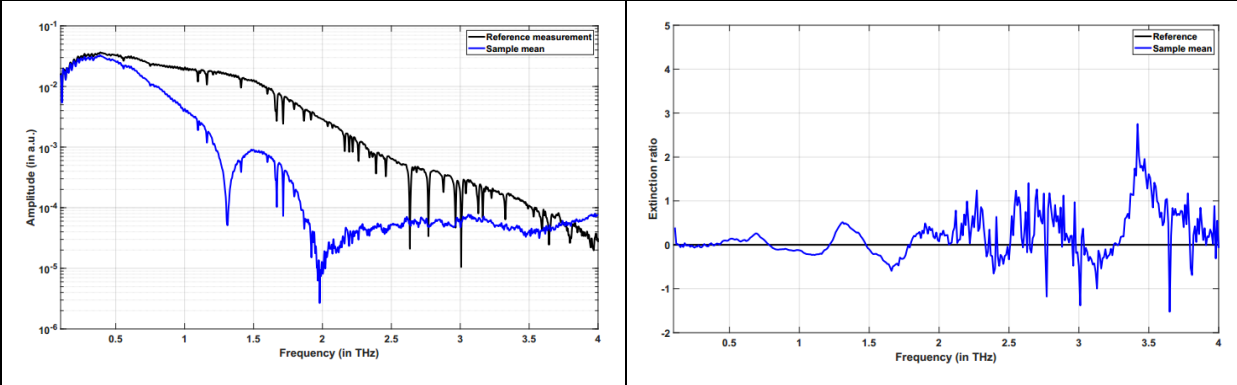
AB-FUBINACA



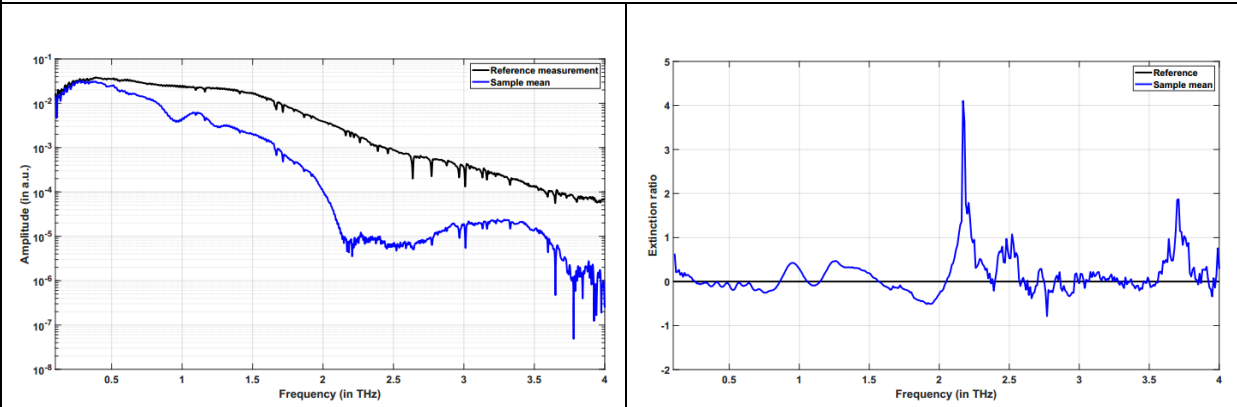
AM-2201



FUB-PB-22



JWH-018



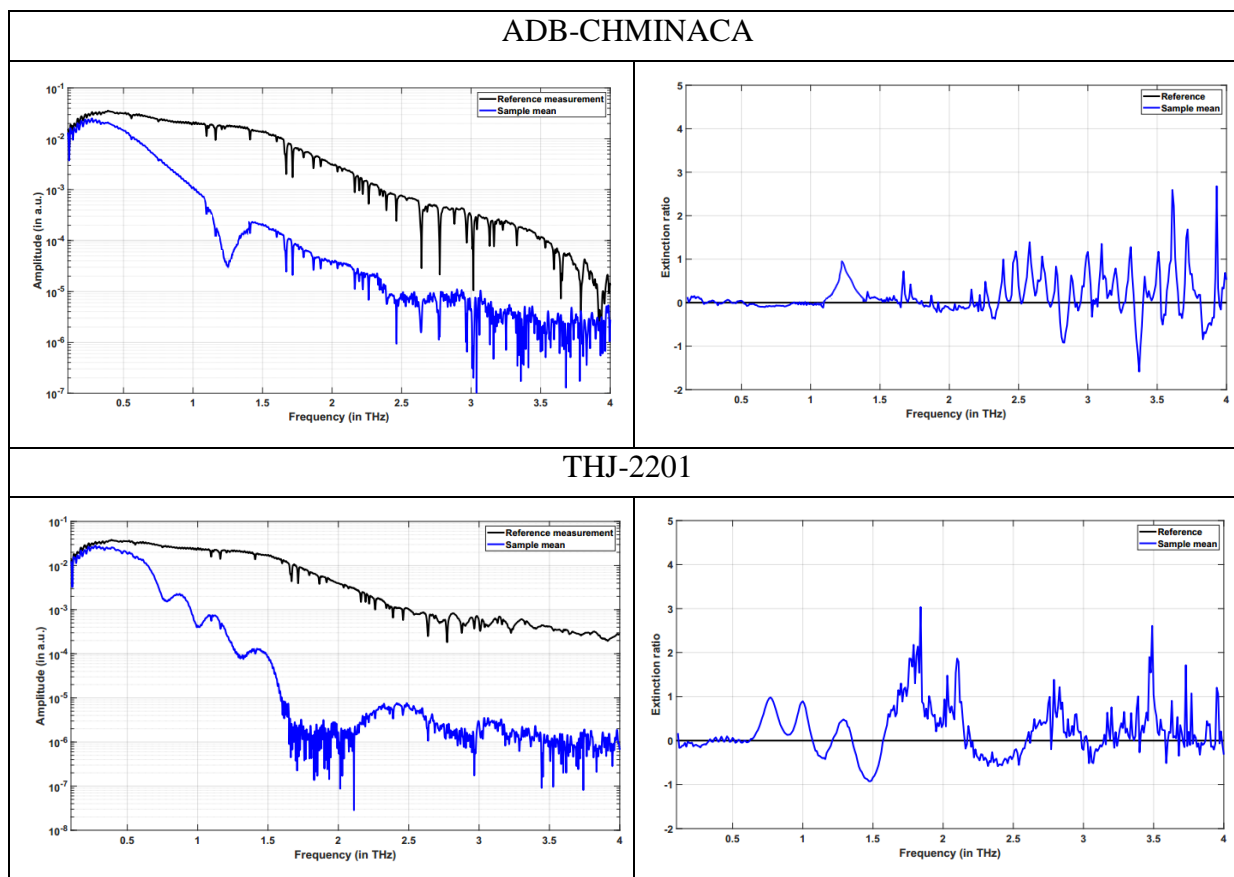
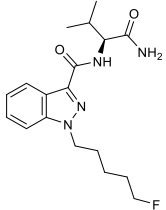
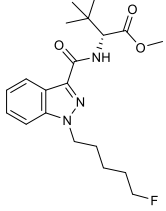
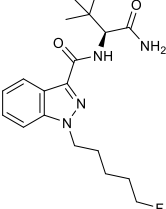
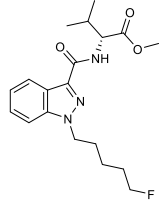
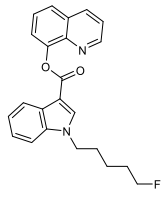
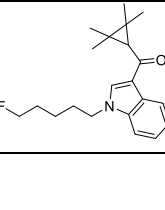


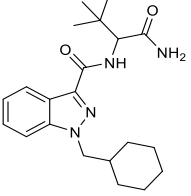
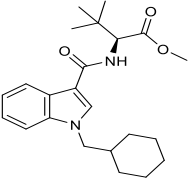
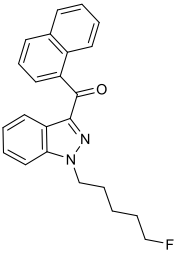
Figure 4-2 THz data of 10 of the investigated substances with frequency domain curve (left) and extinction curve (right)

Some of the investigated substances are naphthylindole-synthetic cannabinoids, where the indole core group is connected via an ester- or a ketone-linkage to a naphthyl-group as a linked group. 5F-PB-22 and FUB-PB-22 belong to the class of naphthylindole-synthetic cannabinoids with an ester linkage and show two significant features around 0.8 THz and 1.3 THz. Naphthylindole-synthetic cannabinoids with a ketone-linkage including AM-2201 and JWH-018 show five significant features at 0.8, 1.2, 2.2, 2.4-2.5, 3.7-3.9 THz. Naphthylindazole-synthetic cannabinoids (THJ-2201) revealed nearly the same features with 0.8, 1.2, 2.1, 2.8 and 3.5 THz but two additional features were observed at 1 and 1.8 THz. EG-018 is the only carbazole-based synthetic cannabinoid and shows a broad feature at 1.4 THz with a FWHM of 3.5 THz.

Table 4-3 Spectroscopic evaluation of THz measurements of synthetic cannabinoids including their chemical structure, die thickness of the pellet, the centre frequency of the feature, FWHM and die cut-off frequency

Sample	Chemical structure	Pellet thickness in mm	Centre frequency of feature in THz	FWHM in THz	Cut-off frequency in THz
5F-AB-PINACA		0.6	0.4	0.3	2.2
			1.2		
5F-ADB		1.9	1.2	0.2	1.7
5F-ADB PINACA		1.9	1.2	0.3	2.2
5F-AMB		1.7	1.2	0.1	1.6
5F-PB-22		3.0	0.8	0.2	2.1
			1.2	0.1	
			1.3	0.1	
5F-UR-144		3.0	0.6	0.2	1.4

Sample	Chemical structure	Pellet thickness in mm	Centre frequency of feature in THz	FWHM in THz	Cut-off frequency in THz
AB-FUBINACA		1.7	1.2	0.2	2.7
AB-PINACA		1.7	1.2	0.3	2.7
			2.4	0.1	
ADB-PINACA		1.6	1.25	0.3	2.7
			2.4	0.1	
AM-2201		1.5	0.8	0.1	2.5
			1.6	0.5	
			2.2	0.1	
			3.9		
EG-018		1.7	1.4	0.2	3.6
FUB-PB-22		1.8	0.8	0.1	3
			1.3		
			2	0.3	
JWH-018		1.1	0.8	0.2	3.9
			1.3	0.3	
			2.2	0.1	
			2.5	0.2	
			3.7	0.2	

Sample	Chemical structure	Pellet thickness in mm	Centre frequency of feature in THz	FWHM in THz	Cut-off frequency in THz
ADB-CHMINACA		0.8	1.2	0.2	2.4
MDMB-CHMICA		1.1	1.3	0.2	2.5
THJ-2201		2.1	0.8	0.2	3.5
			1	0.1	
			1.2	0.2	
			1.8	0.3	
			2.1	0.1	
			2.8	0.4	
			3.5	0.1	

The sensitivity of the method was investigated with 5 different pellets of EG-018 with decreasing tablet thicknesses of 1.7, 1.5, 1.0 and 0.6 mm. The extinction spectra recorded with samples of different tablet thicknesses are shown in Figure 4-3: At a pellet thickness of only 0.6 mm, no signal was observed.

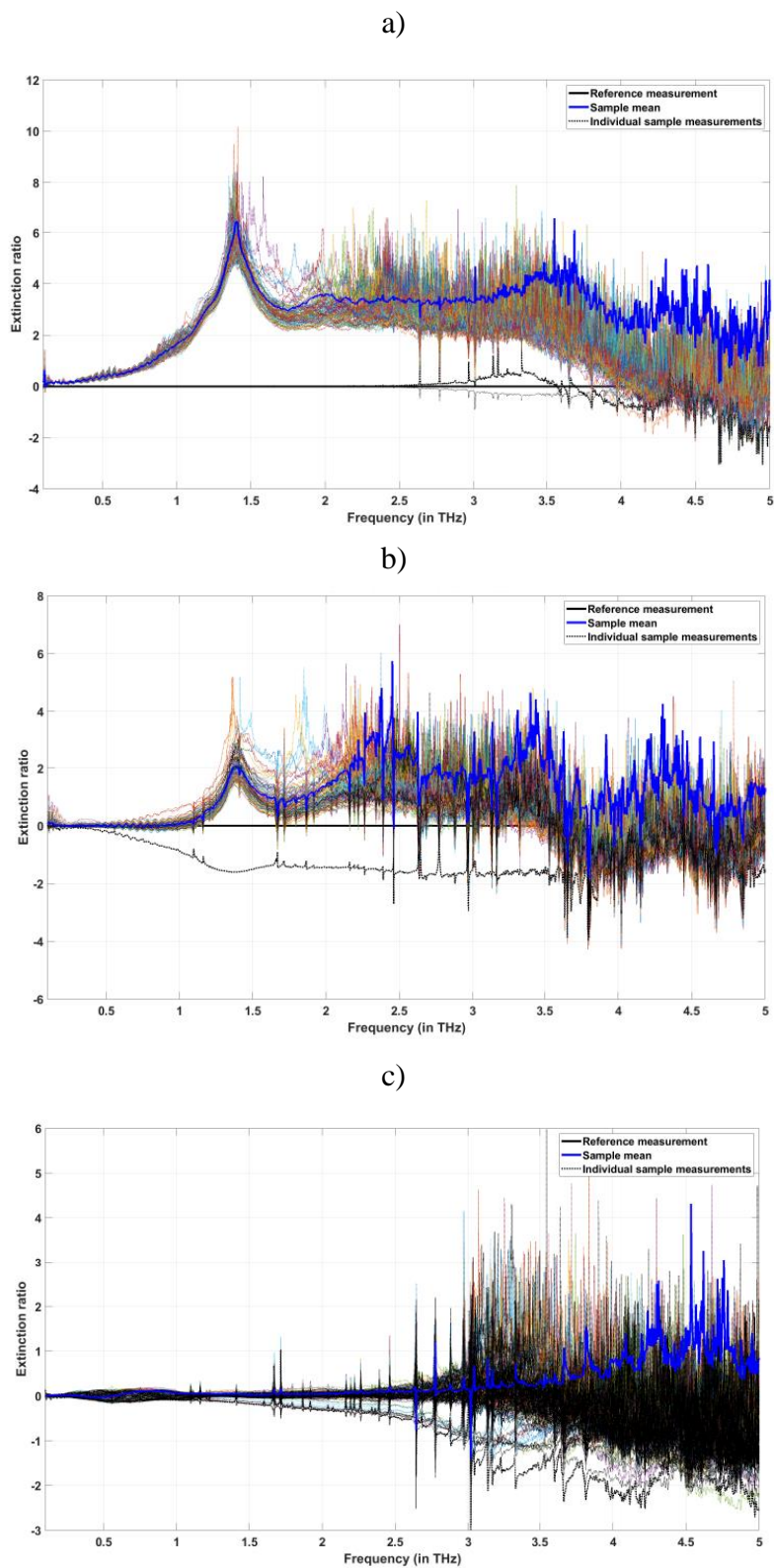


Figure 4-3 Different extinction plots for EG-018 with different pellet thicknesses including a) 1.7 mm, b) 1 mm and c) 0.6 mm

4.4.3 Model applications and matrix tolerance

In this study, samples with different matrices were analysed to investigate the matrix tolerance for THz spectroscopy including powders in packaging material, herbal matrices and papers, which were impregnated with synthetic cannabinoids. The grid chosen for these measurements is shown in Figure 4-4.

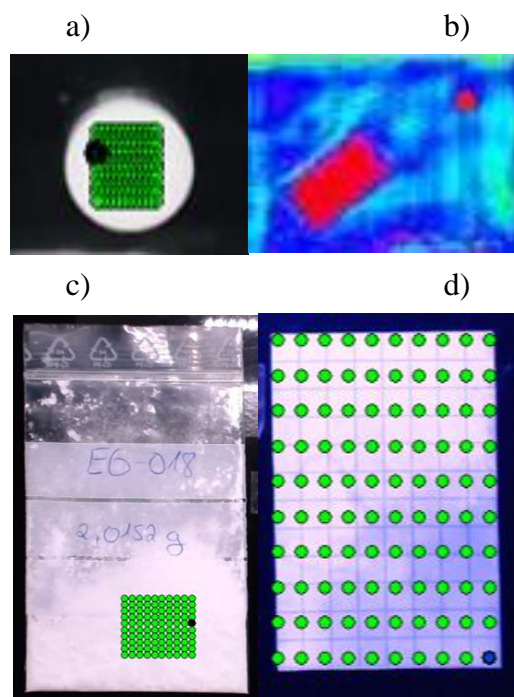


Figure 4-4 Imaging window of a) a tablet with a grid of measurement points (10x10), b) a transillumination images of an envelope containing a plastic bag with powder and a tablet, c) a plastic bag with powder and a grid of measurement points (10x10) and d) a paper (24 cm²) impregnated with EG-018 and a grid of measurement points (10x10)

THz spectra of analytes in pellet and powder samples were compared. For this purpose, EG-018 and UR-144 were chosen as representative substances. The pure powder was analysed in a grip bag and as a tablet. The spectra are shown in Figure 4-5. The centre of frequency, FWHM and the cut-off frequency for tablets coincides with those for powders, except the intensity of the feature, which is lower for powders. The lower intensity is due to scattering phenomena: It is standard practice in far-infrared (THz) spectroscopy to press samples into pellets due to the fact that powders often have grain sizes comparable to the THz wavelength. Then, strong scattering of the THz radiation occurs.

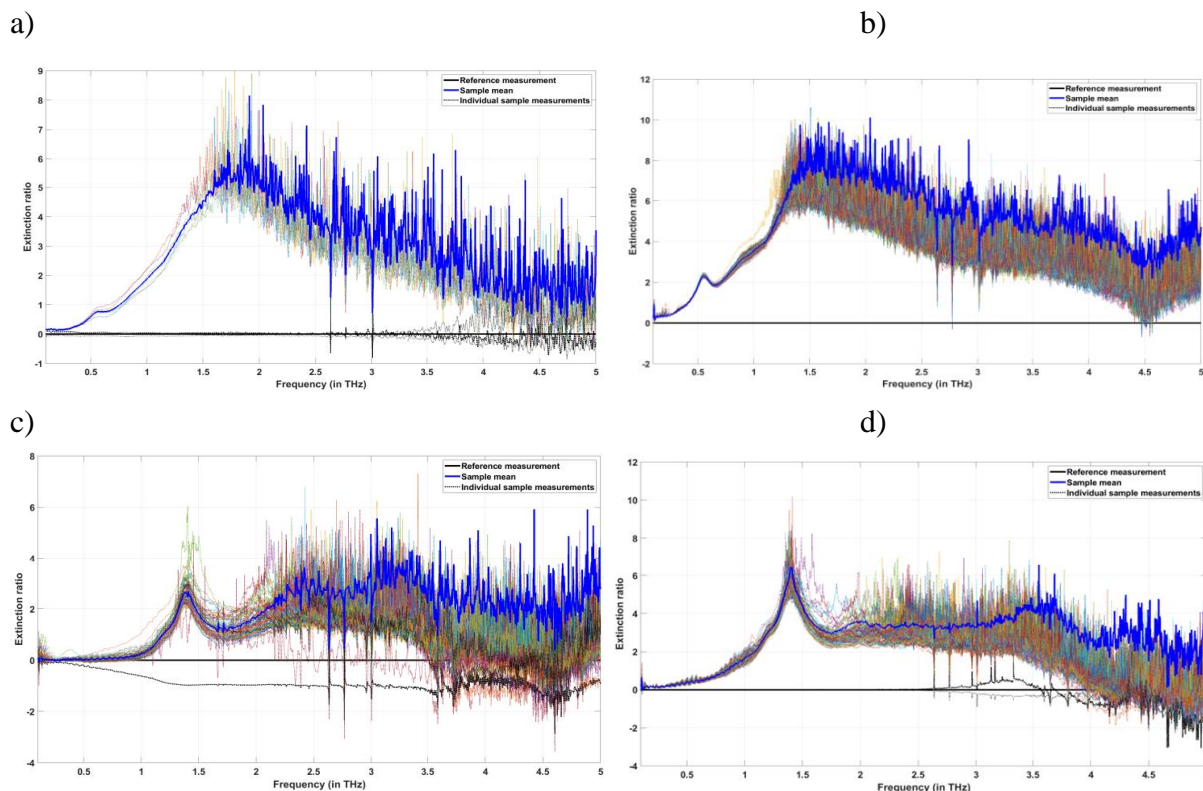


Figure 4-5 Extinction plots for a) UR-144 (powder), b) UR-144 (tablet), c) EG-018 (powder) and d) EG-018 (tablet)

The THz wavelengths are 10's to 100's of microns in scale and thus rough surfaces or interfaces between materials or the granular nature of substances can cause frequency-dependent scattering with the potential to alter or obscure signatures. The scattering effects are influenced by a number of factors including the angle of incidence and scattering, the operating frequency, the material contrast, the viewing geometry, and the statistics of the surface height variation.²⁸⁸ In Figure 4-6, this phenomenon is depicted: In case of a flat surface/interface (Figure 4-6), the reflected wave will be perfectly phase coherent and will appear only in the specular direction or the direction where the scattered angle is equal to the incident angle. For a rough surface with random height profile, energy from the incident wave will be redistributed in other directions, decreasing the coherent reflection, and producing incoherent (diffuse) scattering at non-specular angles.²⁸⁸

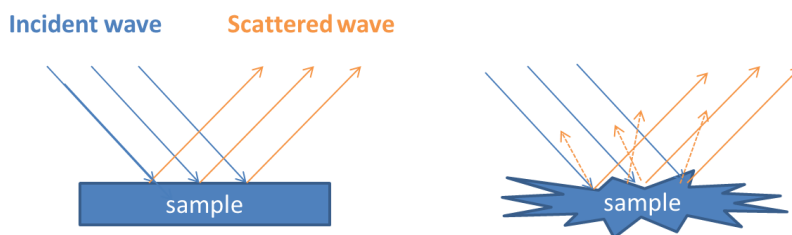


Figure 4-6 Left-hand side shows coherent specular scattering from a flat surface versus rough surface scattering (right-hand side) containing both coherent and incoherent scattering

Postal packages in mail services were simulated by packing tablets and powders of the synthetic cannabinoids into a plastic grip bag, which was additionally packed into a paper envelope. A pre-screening step of the envelope was carried out to obtain a transillumination image to avoid measuring the whole packaging material. In Figure 4-4b the transillumination image of an envelope containing a grip bag with a powder and a tablet is shown. The analysis demonstrated that materials like plastic or paper do not interfere with the measurements and the features generated were similar to those without any packaging material (data not shown, because spectra are similar to those of Figure 4-2).

In addition, herbal matrices containing different synthetic cannabinoids were quantified by THz spectrometry. In Table 4-2, UPLC-DAD data including the λ_{\max} , R^2 of the corresponding calibration line and the active ingredient contents of the synthetic cannabinoids in the herbal mixture are shown. The active ingredient contents ranged from 0.5 to 12.5 %, which are common percentages found in herbal mixtures.²⁶⁵ No signals of the NPS present in the herbal matrices were observed by THz spectroscopy. This is due to the fact, that synthetic cannabinoids were dissolved in an organic solvent and sprayed onto the plant material, resulting only in a thin coating of the active ingredient on the dried plant material. The THz spectrometer employed in this study was not sensitive enough to detect synthetic cannabinoids and to trigger specific intramolecular vibrations. The same applied to impregnated papers: To simulate drug transport via paper, pieces of paper were impregnated with synthetic cannabinoids at concentrations correlating to current dosages as described on internet platforms (Table 2-3). Here again, no spectral information were gathered. In order to estimate limits of detection, the dosage concentration for one EG-018, which shows a strong THz feature, was increased to 2 mg/cm², 4 mg/cm² and 8 mg/cm². Even at the highest dose, only 1 % of all measurements (n = 100) revealed a feature (Figure 4-7).

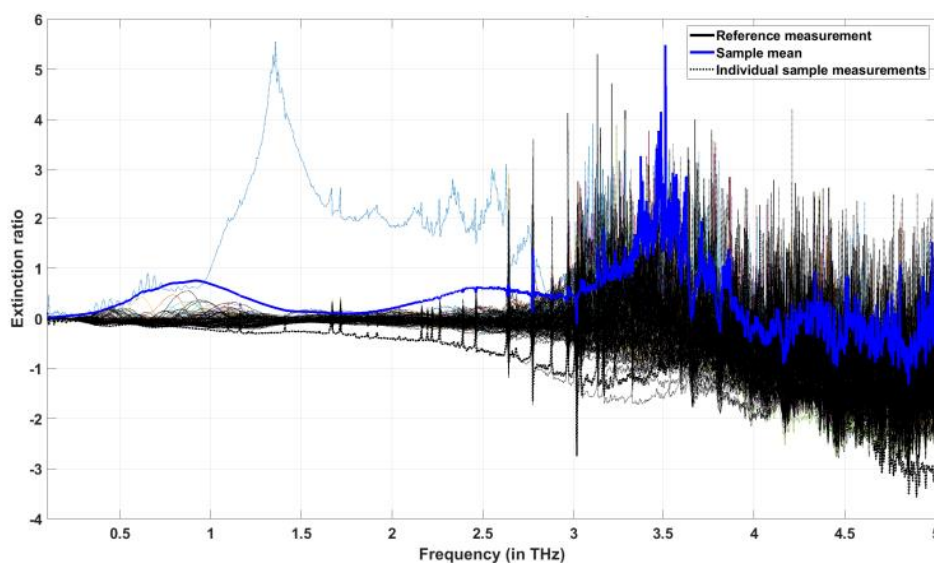


Figure 4-7 Extinction plot of EG-018, impregnated onto a paper at a concentration of 8 mg/cm²

4.5 Discussion

THz spectroscopy is an analytical technique only rarely applied in forensics. Currently, the relatively high costs of such systems impede their routine application in diverse institutions and limits research. For drug analysis THz spectroscopy is not widespread,²⁸⁰ because of the constant changes in chemical structures of NPS. THz spectroscopy provides information on the intramolecular rotational vibrations and the intermolecular constitution of a substance but does not provide information on specific structural components.²⁸⁹ In addition, THz spectroscopy is a lab-based technique, whereas other spectroscopic devices are also available as portable techniques, e.g. IR and Raman spectroscopy.

In this study, the features of synthetic cannabinoids were examined. Synthetic cannabinoids with identical core-structures and linked-groups showed similar features in the THz spectra. A distinction between substances with very similar structural components was not possible. In comparison, with Raman spectroscopy (Chapter 3), the analysis of structurally closely related substances was possible according to the spectral fingerprint region in the spectra. For example, AB-CHMINACA and ADB-CHMINACA differs only in the addition of one methyl-group in the linked group and show clear differences in the Raman spectrum. Therefore, THz-spectroscopy is suitable for the detection of substance classes but not for the identification of a substance. Regarding selectivity towards other drugs-of-abuse, synthetic cannabinoids show different features in the THz spectra compared. Table 4-4 summarises the THz features of classical drugs like cocaine, methamphetamine, MDMA, MDA diamorphine, morphine and ketamine. Each proscribed drug is characterised by a different absorption spectrum with sharp absorption peaks located within the Terahertz frequency range. Morphine is the only substance, which shows a feature at 1.25 THz similar to some synthetic cannabinoids. Here, the calculation of the exact centre of frequency with supporting chemometric methods is essential to distinguish between the feature of synthetic cannabinoids with indole-core of 1.3 THz, indazole core of 1.2 THz and morphine.

Table 4-4 A collection of feature band centre position frequency of some Drugs with the corresponding reference

Substance	Centre frequency of feature in THz	Reference
Cocaine HCl	1.54, 2.1, 2.6	286
Cocaine free base	1.54, 2.25, 2.5	267
methamphetamine	1.2, 1.7, 1.8, 2.4	280,282,283
MDMA	1.2, 1.4, 1.7, 1.9, 2.4	280,285
MDA	1.39, 1.68, 2.21	283
Diamorphin (Heroin)	1.42, 3.94	267
morphine	1.25	286
ketamine	1.16, 1.35, 1.52, 1.93, 2.40	285

Besides classical drugs, street samples contain cutting agents and impurities and these materials are often crystalline organic materials such as caffeine, lactose, or other pharmaceutical products, which will have spectral features in the THz range.^{267,286} Based on the statistical data of the State Office of Criminal Investigation Rhineland-Palatinate, synthetic cannabinoids appear as pure powders without any accompanying substances.

The rare application of THz spectroscopy in forensic science can be explained by several facts: The THz spectrum of a substance could be affected by different factors like different classes of multicomponent molecular crystals of drugs. Davies et al. described the influence of different matrices on the feature of cocaine. The THz-TDS spectra of cocaine free base and cocaine hydrochloride showed clear differences with only one common peak at 1.54 THz (see Table 4-4. Cocaine hydrochloride has a considerably larger absorption coefficient probably owing to the large Cl counter ion, which increases the magnitude of the dipole moment and thus the change in dipole moment during a normal mode vibration.²⁶⁷ Synthetic cannabinoids do not occur in salt form or other crystal forms but as it can be seen in Figure 4-2, the features are relatively weak and broad and tend to be masked by the combined effects which are explained as follows.²⁹⁰ But also different packaging materials and therefore the attenuation properties of the covering layers,^{291,292} the scattering effects related to the morphology and inhomogeneity of the substance surface,^{288,293} changes in the atmospheric humidity due to strong attenuation properties of water vapor during the measurements²⁹⁴ lead to low repeatability of this method.

In most publications and also predominant in this study, THz-TDS were performed on tablets, neglecting the scattering and diffraction phenomena. In addition, water features tend to fluctuate in strength and slightly in position. This leads to imprecision in the determination of the THz features from the quotient of the reference and the sample.²⁹⁴ To avoid absorption features within the spectral range caused by atmospheric water vapor, some publications used a dry-air box in which the optical setup was encapsulated.^{285,294,295} In this study, humidity was not considered, but should be controlled for future measurements.

Another challenge is the analysis of more than one sample in a package that complicates to extract the fingerprint of each of them. Moreover, THz spectroscopy is not very sensitive. The analysis of synthetic cannabinoids in different matrices like herbal mixtures, e-liquids or papers was not possible due to amounts of active ingredient in the matrix below limits of detection. The analysis of (pure) powders or pellets at a thickness of > 0.6 mm was possible. Similar measurement procedures for the analysis of drugs were used in most literature studies. Usually, the powders under investigation were pressed into a pellet in order to measure the THz transmission spectra. Most publications mixed the analyte material with an inert matrix or filler material which is typically transparent for THz radiation, such as polyethylene (PE)^{280,282,284,296} or PTFE^{267,281,296}. This allows to dilute concentrations of a highly absorbing agent to be measured. As the presence of matrix material can influence the measured THz

spectra, the use of a matrix material with an index of refraction that closely matches that of the powder can minimize the scattering by reducing the effect of the dielectric mismatch in the THz range. In reality, smugglers are not going to prepare their samples with specific matrix materials and so we decided to carry out the measurements of the synthetic cannabinoids in realistic form, as powders and pellets without filling material. In this study, the limit of detection was determined on the basis of the pellet thickness. To the best of our knowledge, the LOD of drugs-of-abuse were not discussed in other publications. In general, the sample thickness was described ranging between 0.5 and 3 mm.^{277,281,284-286} LODs were given in studies for pharmaceuticals pressed into pellets with nearly same thicknesses of approximately 2 to 3 mm.²⁹⁷ For each pharmaceutical, different pellets were prepared by mixing the pharmaceutical powder with PE at different concentrations from 0 to 100 % w/w.^{277,294,297} LODs ranged between 4-10 % w/w,^{277,294} but in most cases, a detection below 1 % w/w was impossible.²⁹⁷ In case of the detection of powders of synthetic cannabinoids, information about the minimal detection thickness is decisive since those substances show almost no addition of cutting agents.

The advantages of THz spectroscopy can only be taken, when several grams of powders are present in packaging material, many nonmetallic and nonpolar materials do not absorb THz radiation.²⁶⁹ This enables the spectral analysis of materials concealed within dry packaging, such as paper, plastics, cardboard, and enabling the imaging of concealed objects.²⁷¹ In this study, the spatial distribution of synthetic cannabinoids concealed in a plastic bag and an envelope, is obtained from terahertz multispectral transillumination images and absorption spectra. To avoid measuring the whole packaging material, a pre-screening step is proposed, by first detecting the presence of powders in the envelopes and then defining the grid of measurement points (Figure 4-4). Kawase et al. demonstrated the successful detection and discrimination of methamphetamine, MDMA, aspirin, where the substances were hidden in a plastic bag or envelope,²⁶⁶ whereas Fischer et al. described the analysis of cocaine and morphine through a plastic bag.²⁸⁶

Competing detection technologies such as x-rays and millimetre wave imaging were not able to provide a spectral fingerprint in their respective electromagnetic frequency ranges to distinguish illicit drugs from legal drugs.^{266,267} In Raman spectroscopy, the radiation may also transmit materials like glass⁸⁸ and polymer packaging⁶⁸ but not paper materials. Like Raman spectroscopy, IR imaging has the capability to distinguish different drugs based on fingerprint spectra in the infrared region, but most packaging are opaque for IR radiation.²⁸⁰

Thus, THz-technology shows some advantages as a complementary preliminary test at security points or mail service and can provide a first hint on the NPS subclass. It can thus uncover drug trafficking of NPS powders by a contactless and non-destructive measurement technology. Before reaching a final conclusion on a future relevance of THz spectroscopy in forensic science, further tests should be carried out including the in-field testing under

different atmospheric conditions and influences of air humidity, measurements in different packaging materials, the analysis of a large number of different powders to gain a better understanding of possible scattering effects.

4.6 Conclusion

The analysis of synthetic cannabinoids using THz-TDS was described. Previous studies concentrated on the characterisation of classical drugs like cocaine and amphetamine but not on the analysis of NPS. Based on different core-structures and linked groups, spectroscopic data of 16 synthetic cannabinoids were recorded including the centre frequency of the feature, FWHM and the cut-off frequency. Specific substance identification is not possible due to the fact that synthetic cannabinoids providing the same structural components show similar specific features. Thus, class identification is feasible. The strength of this technique lies only in the analysis of powders and not in the analysis of various matrices containing different active ingredients like herbal mixture and impregnated papers. Here, THz technique is not sensitive enough for the concentrations observed in field work. THz spectroscopy could be used in security institutions or mail centres due to desirable properties like the contactless and non-destructive measurement to get a first hint on possible illegal substance like drugs in packages and envelopes and the possibility of transillumination images of packed materials. Further in-field analysis should be performed with a large number of different samples. This could reveal the importance of interfering parameters such as humidity in air, medium, salt form.

5 Structural similarity of synthetic cannabinoids in herbal mixtures allows to cross-calibrate analytes without reference material by UPLC-DAD

5.1 Abstract

The steady appearance of new psychoactive substances (NPS) on the European drug market represents a challenge for analytical forensic investigations. The determination of the active ingredient in casework samples is one of the main tasks in forensic institutes due to specific punishment corresponding to different types and quantities of drugs. Problems arise from the fact that only for older NPS, reference substances are available. The traditional approaches and timescales of reference material production and certification are being increasingly challenged by the appearance of ever new substances. The effort required may become questionable given the short lifetime of many NPS on the market. In this study, the need for reference materials was circumvented by evaluating the possibility of cross calibrations of 20 synthetic cannabinoids using a small set of reference substances as calibrants for other NPS. This was possible due to the structural similarity of synthetic cannabinoids grouped into classes based on the core structure: eight indole-core, ten indazole-core and two carbazole-core synthetic cannabinoids could be quantified with one common calibration curve for each class. Bias values < 4.9 % were obtained with best results ranging from -1.5-1.0 % for pairs of substances containing similar linker- and tail-groups attached to the core-group.

5.2 Introduction

The phenomenon of new psychoactive substance (NPS) poses great challenges for the legislative, executive and forensic laboratories. By the end of 2018, the European Monitoring Centre for Drugs and Drug Addiction (EMCDDA) summarised more than 730 new psychoactive substances, 55 of which were detected for the first time in Europe in 2018.⁸ According to the dynamically changing NPS market, the availability of suitable reference material poses a major challenge for forensic institutions with regard to both identification and quantification of NPS. The traditional and time consuming production of reference material often requires several months, which is not appropriate for the rapidly changing drug market. Alternative approaches are required to produce materials of a suitable quality to satisfy the requirements of a robust quality system²⁹⁸ and also for quantification as described by Archer et al.³² The production of in-house reference materials requires significant effort

and synthetic as well as analytical capability and is not not feasible for routine laboratories. However, the identification and the quantification of the active ingredient content of casework samples is one of the main tasks in forensic institutes due to specific punishments corresponding to different types and quantities of drugs.

The methods most commonly employed for the quantitative routine analysis of NPS in forensic laboratories are chromatographic techniques coupled to mass spectrometry, mostly gas chromatography-mass spectrometry and liquid chromatography-mass spectrometry. Some publications describe the utilisation of LC in combination with UV-detection.^{2,140} The published LC-applications focus on the analysis of synthetic cannabinoids in biofluids including urine,^{103,117,124-126,128} hair,¹²⁰ oral fluids^{118,119} and serum/blood.^{115,121,123,127,130} Simple liquid-liquid extraction followed by LC-MS is usually used for sample preparation because of the high hydrophobicity of the drugs. The LODs reported ranged from 6-2000 ng/L. GC-MS applications mostly concentrate on the analysis of herbal mixtures with simple sample preparation steps, e.g. mixing the herbal material with an organic solvent and filtering the supernatant.^{100,102} LODs of 0.5-1.0 mg/L are usually higher than in LC-MS analysis. Another disadvantage of GC-MS analysis is its inability to identify cyclopropyl or ester analogs, such as UR144 or PB-22 (see Table 5-1) because cyclopropyl analogs have a low thermal stability and are easily degraded already in the injection port of the GC instrument.^{299,300} GC-MS with chemical or electron ionisation provides information on structural elements, whereas LC-ESI-MS would need specialised instrumentation for MS/MS analysis. For all chromatographic techniques, quantification is only possible via calibration with reference standards.

In the last few years, NMR has been established for the characterisation of NPS in herbal mixtures or powders.⁴⁶⁻⁵³ It is a fast technique which allows unambiguous structural elucidation of unknown compounds. In contrast to most other analytical methods, the use of standard references for the determination of the purity of a sample is not necessary. Quantification of a substance is based on integration of the analyte signal correlated to the signal of an internal calibrant. A detailed explanation on the determination of standard sample purity using high precision ¹H-NMR was given by Schoenberger.⁴⁹ A prerequisite is the selection of an appropriate internal standard so that the integral regions in the spectrum must be completely free of impurity or analyte signals. A structural similarity between the internal calibrant and the analyte is not necessary in NMR. Disadvantages of this technique are the high costs and the required technical expertise which limits the applicability in routine analysis.² At present, there are no alternative methods to NMR published for the fast and effective quantification of NPS, which allow the quantification independent of reference standards.

In this study, we investigated, if it is possible to use an NPS, for which reference material is commercially available, as a cross calibrant for other NPS. The procedure was tested for 20 synthetic cannabinoids using UPLC-DAD. For this, we discuss the required structural

crosslinks between indole-, indazole- and carbazole-core synthetic cannabinoids via two Quality Control (QC) samples for each synthetic cannabinoid to establish calibration curves for different NPS. The feasibility of cross calibration was judged using bias values. The methodology was validated in terms of accuracy, precision and sensitivity and its applicability proven by the analysis of 24 herbal mixtures with known active ingredient content.

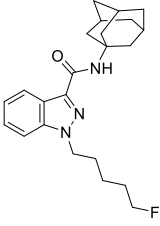
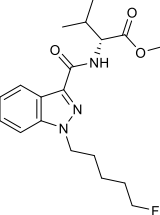
5.3 Materials and Methods

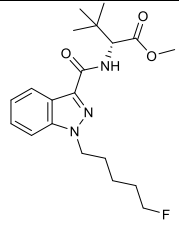
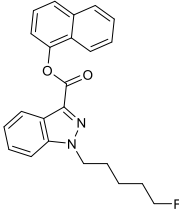
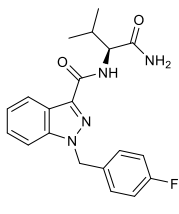
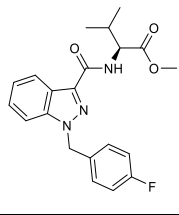
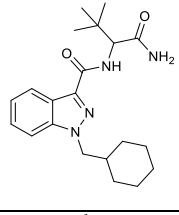
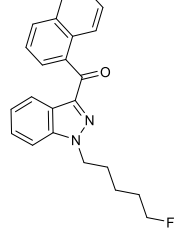
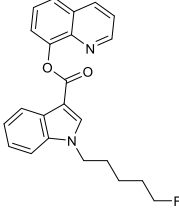
5.3.1 Chemicals

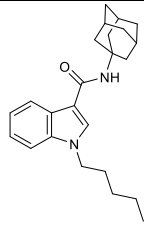
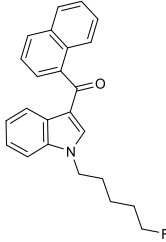
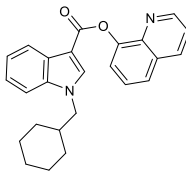
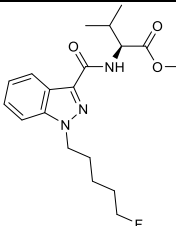
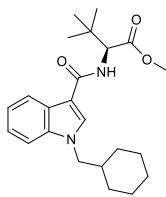
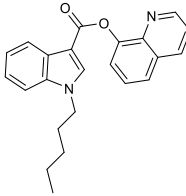
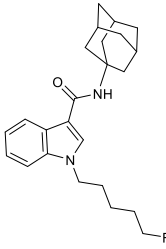
All reagents were of analytical grade. Ultrapure water was used throughout this work. For UPLC-DAD and GC-MS measurements, methanol from Th. Geyer (Renningen, Germany) was used. NMR analysis was carried out using acetone-d₆ (purchased from Deutero, Kastellaun, Germany) and the internal calibrant 3,5-dinitrobenzoic acid (Fluka, TraceCERT, 99.66 %).

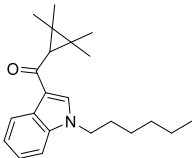
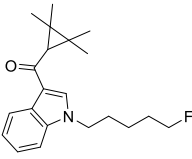
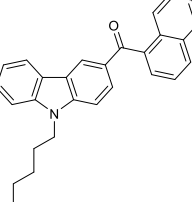
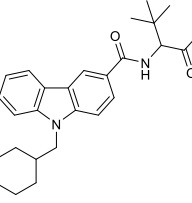
The reference standards of 20 synthetic cannabinoids (powders) employed in this study were taken from criminal cases provided by the State Office of Criminal Investigation Rhineland-Palatinate (Germany) and are listed in Table 5-1. The purity of the reference samples was investigated using ¹H-NMR and GC-MS. The herbal mixtures analysed in this study were provided by the State Office of Criminal Investigation Rhineland-Palatinate (Germany). The samples were taken from caseworks and corresponding IUPAC names and structural formulas are summarised in Table 5-1.

Table 5-1 Chemical structures, IUPAC names, purity determined by NMR and GC-MS parameters retention time *R_t* and *m/z* values of the reference standards (powders) evaluated in this study including synthetic cannabinoids containing indazole-, indole- and carbazole-core structures.

Substance	Chemical structure	IUPAC name	NMR	GC-MS	
			Purity in %	R _t in min	<i>m/z</i>
Indazoles					
5F-AKB-48		<i>N</i> -(adamantan-1-yl)-1-(5-fluoropentyl)-1 <i>H</i> -indazole-3-carboxamide	99.7	8.3	233 145 294 365 383
5F-AMB		Methyl-(2 <i>S</i>)-2-([1-(5-fluoropentyl)-1 <i>H</i> -indazol-3-yl]formamid)-3-methylbutanoate	98.5	10.9	233, 145, 304, 249, 131

Substance	Chemical structure	IUPAC name	NMR	GC-MS	
			Purity in %	Rt in min	m/z
5F-ADB		Methyl-(<i>S</i>)-2-[1-(5-Fluoropentyl)-1 <i>H</i> -indazole-3-carboxamido]-3,3-dimethylbutanoate	98.7	10.9	233, 145, 130, 289, 321
5F-SDB-005		Naphthalene-1-yl 1-(5-fluoropentyl)-1 <i>H</i> -indazole-3-carboxylate	97.3	15.2	233, 145, 115, 213, 115
AB-FUBINACA		<i>N</i> -[(1 <i>S</i>)-1-(aminocarbonyl)-2-methylpropyl]-1-[(4-fluorophenyl)methyl]-1 <i>H</i> -indazole-3-carboxamide	94.9	13.4	109, 252, 324, 145, 83
FUB-AMB		<i>N</i> -[[1-[(4-fluorophenyl)methyl]-1 <i>H</i> -indazol-3-yl]carbonyl]- <i>L</i> -valine, methyl ester	99.9	10.9	109, 253, 324, 254, 383
MAB-CHMINACA		<i>N</i> -[(2 <i>S</i>)-1-amino-3,3-dimethyl-1-oxobutan-2-yl]-1-(cyclohexylmethyl) indazole-3-carboxamide	91.6	13.4	241, 326, 145, 131, 55
THJ-2201		[1-(5-fluoropentyl)-1 <i>H</i> -indazol-3-yl](1-naphthyl)methanone	97.2	14.1	127, 271, 360, 259, 155
Indoles					
5F-PB-22		1-(5-fluoropentyl)-8-quinolinyl ester-1 <i>H</i> -indole-3-carboxylic acid	99.6	18.2	232, 144, 116, 89, 376

Substance	Chemical structure	IUPAC name	NMR	GC-MS	
			Purity in %	Rt in min	m/z
APICA		<i>N</i> -(1-adamantyl)-1-pentyl-1 <i>H</i> -indole-3-carboxamide	98.5	16.9	214, 144, 307, 364, 347
AM-2201		[1-(5-Fluoropentyl)-1 <i>H</i> -indol-3-yl]-1-naphthalenyl-methanone	99.8	15.2	359, 127, 284, 232, 144
BB-22		1-(Cyclohexylmethyl)-8-quinolinyl ester-1 <i>H</i> -indole-3-carboxylic acid	97.2	24.8	240, 144, 116, 241, 55
MMB-2201		(<i>S</i>)-Methyl-2-(1-(5-fluoropentyl)-1 <i>H</i> -indole-3-carboxamido)-3-methylbutanoate	96.6	11.7	232, 248, 144, 362, 233
MDMB-CHMICA		Methyl-(2 <i>S</i>)-2-([1-(cyclohexylmethyl)-1 <i>H</i> -indol-3-yl]formamido)-3,3-dimethylbutanoate	97.0	12.6	240, 144, 296, 328, 268
PB-22		1-Pentyl-1 <i>H</i> -indole-3-carboxylic acid 8-quinolinyl ester	98.2	17.7	214, 144, 116, 89, 358
STS-135		<i>N</i> -(adamantan-1-yl)-1-(5-fluoropentyl)-1 <i>H</i> -indole-3-carboxamide	98.9	11.1	232, 144, 307, 382, 264, 116

Substance	Chemical structure	IUPAC name	NMR	GC-MS	
			Purity in %	Rt in min	m/z
UR-144		(1-Pentylindol-3-yl)-(2,2,3,3-tetramethylcyclopropyl) methanone	98.8	10.3	214, 144, 296, 311, 252
XLR-11		(1-(5-Fluoropentyl)-1H-indol-3-yl)(2,2,3,3-tetramethylcyclopropyl) methanone	97.1	11.1	232, 144, 314, 329, 270
Carbazoles					
EG-018		Naphthalen-1-yl-(9-pentyl-9H-carbazol-3-yl)-methanone	94.6	23.8	334, 391, 335, 127, 179
MDMB-CHMCZCA		Methyl-(S)-2-(9-(cyclohexylmethyl)-9H-carbazole-3-carboxamido)-3,3-dimethylbutanoate	98.3	23.1	290, 434, 179, 346, 378

5.3.2 Methodology

5.3.2.1 Gas chromatography-mass spectrometry

As not all NPS standards were commercially available during the experimental phase of this study, material from seizures was used. Identity and purity of each seized drug powder or herbal mixture were determined by GC-MS. Information on the technical parameters, a detailed explanation of the sample preparation and the method parameters used are described in Chapter 2.3.2.1 and the corresponding publication.²⁴⁸

The samples were prepared as follows: Five mg of powdered samples were dissolved in 1 mL methanol. 200 mg of herbal or tobacco mixtures were suspended in 3 mL methanol. In cases, where less material was available, the amount of methanol was reduced until the whole material was covered with organic solvent. The solutions were filtered with syringe filters from Macherey-Nagel (Düren, Germany) with a pore size of 0.20 µm and a diameter of 25 mm directly into GC-MS vials for injection.

5.3.2.2 NMR

The purity determination of NPS samples from seizures was conducted by quantitative NMR (qNMR) analysis. Technical information, the sample preparation steps and method parameters are described by Schoenberger.⁴⁹ In Chapter 2 and in the publication of Metternich et al., the details of NMR analysis are summarised.²⁴⁸

5.3.2.3 UPLC-DAD

A UPLC Aquity-System (Waters, Milford, MA, USA) equipped with DAD was used for the quantitative analysis of 20 synthetic cannabinoids. Information on the technical parameters, a detailed explanation of the sample preparation and the method parameters used are described in Chapter 2.3.2.1 and the corresponding publication.²⁴⁸

Two samples of herbal mixtures, 100 mg each, were suspended in 10 mL methanol. The suspensions were filtered with syringe filters from Macherey-Nagel (Düren, Germany) with a pore size of 0.20 µm and a diameter of 25 mm. Then, 100 µL of the filtered sample solution were mixed with 900 µL methanol directly in UPLC vials for injection.

5.3.2.4 Cross calibration

The cross calibration of synthetic cannabinoids was carried out using a 7-point-calibration (n = 3) in the range of 5-100 mg/L (in methanol) with different reference standards. Two quality control (QC) samples, one with a low (10 mg/L) and one with a high concentration (75 mg/L), were prepared daily, called QC1 and QC2. The evaluation was carried out using the program Valistat 2.0 by Avercon (Walldorf, Germany).

5.4 Results and discussion

5.4.1 Characterisation of reference samples including NMR and GC-MS

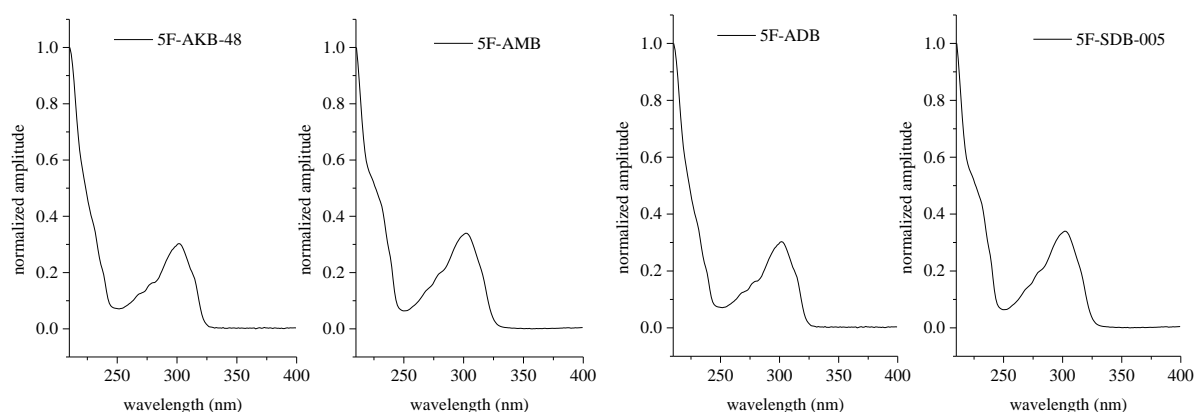
The reference standards used in this study were samples from seizures and the purity was determined using ¹H-NMR and GC-MS. Initially, the powder material was analysed via GC-MS to investigate the overall composition of the samples and identify active ingredient via the in-house GC-MS library. The retention times and the characteristic m/z values of each substance are reported in Table 5-1 (arranged according to their signal intensity). Afterwards, the purity was determined using ¹H NMR to be > 91.6 %. Samples with significant impurities such as cutting agents (paracetamol, caffeine, sugars) or other drugs (e.g. amphetamine, cocaine or THC) were not taken into consideration.

5.4.2 Evaluation of the UPLC-DAD method

5.4.2.1 UV-Spectra

The UV absorption spectra of compounds are highly characteristic and sensitive to changes upon substitution at the chromophore-region. The UV spectra of the synthetic cannabinoids investigated during this study are shown in Figure 5-1 and the corresponding chemical structures are summarised in Table 5-1. Generally, UV spectra of indoles have intense bands at 216, 262 and 280 nm.³⁰¹ The band near 262 nm can be shifted or even absent for many substituted indoles. E.g., alkylation of the indole nitrogen leads to bathochromic shifts of up to 10 nm.³⁰¹ In case of 1-acetylindole the band around 280 nm is shifted to 290 nm. All investigated indole-core synthetic cannabinoids that contain an amide or ester linkage show bands around 216 nm and 290 nm in their UV spectra as already described.³⁰² An exception was observed for indole-core synthetic cannabinoids having an adamantyl-group attached to the linker with only one band around 301 nm as can be seen for STS-135 and APICA. Indole-core synthetic cannabinoids which possess a keto-linker show intense bands at 216 nm, 245 nm and 305 nm like in UR-144 and XLR-11 (see Figure 5-1). The latter was shifted from 290 to 305 nm due to the aromatic system being extended by the double bond.

The UV spectrum of 1H-indazole shows two characteristic bands around 250 and 290 nm (see Figure 5-1). *N*-methylation shifts the latter band to ~300 nm as visible for many indazole-core synthetic cannabinoids with an amide- and ester-linker. The linked group naphthalene in THJ-2201, AM-2201 leads to an additional band at ~220 nm. The spectrum of carbazole shows bands at 236 nm, 277 nm, 340 nm and the presence of a naphthalene group (e.g. in EG-018, see Figure 5-1) even show a band around 220 nm.



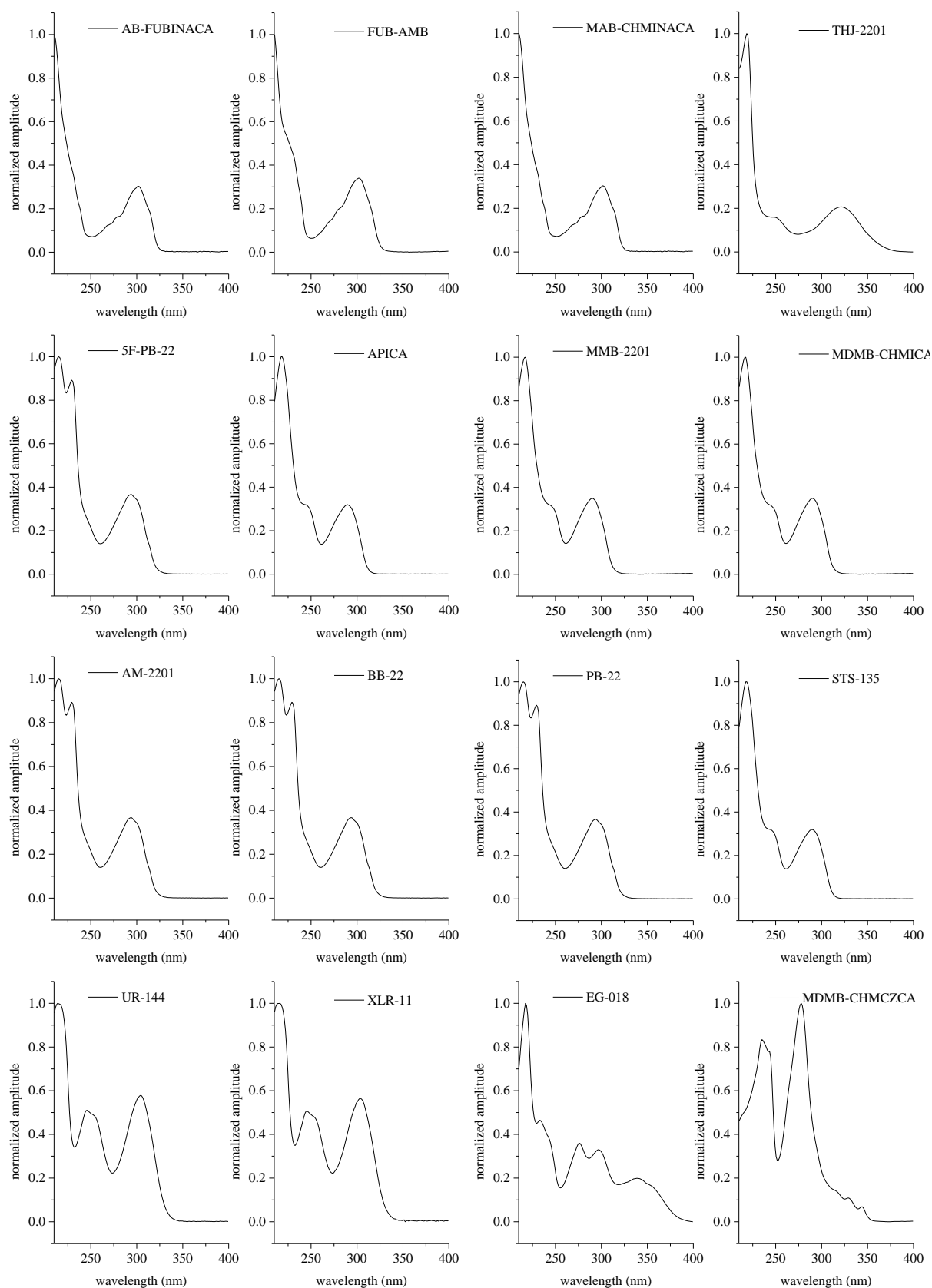


Figure 5-1 UV spectra of the synthetic cannabinoids investigated during this study, recorded during UPLC-DAD. Separation parameters given in Materials and Methods

5.4.2.2 Figures of merit

Table 5-2 summarises the figures of merit from the validation of the method in terms of linearity, sensitivity and precision. In addition, the wavelengths of the maxima in the spectrum, UV_{max} , and the retention times of the analytes are summarised in Table 5-2. Figure 5-2 shows a chromatogram of all synthetic cannabinoids investigated during this study.

Examination of linearity was performed by the analysis of three calibrations each consisting of seven calibrators spread over the substance-specific calibration range. In Table 5-2, the calibration equation and the corresponding correlation coefficients with $R^2 > 0.997$ for all analytes are listed. Sensitivity calculations including limit of detection (LOD) and limit of quantification (LOQ) were conducted according to DIN 32645. LODs and LOQs were in the range of 0.49-4.17 mg/L and 1.57-10.1 mg/L, respectively. The precision was determined with two quality control samples (QC) of high and low concentration, which were analysed daily ($n = 2$) on eight consecutive days. The intraday and interday imprecision was $\leq 2.21\%$ and $\leq 5.11\%$ (for QC1 and QC2).

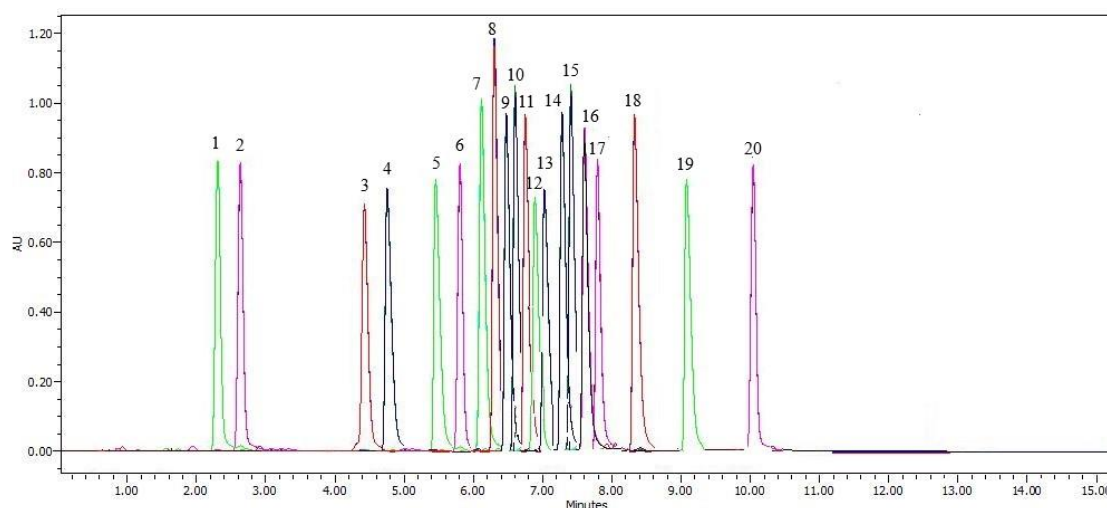


Figure 5-2 UPLC-DAD chromatograms (overlay) of the synthetic cannabinoids investigated during this study (1 = AB-FUBINACA, 2 = 5F-AMB, 3 = FUB-AMB, 4 = MAB-CHMINACA, 5 = XLR-11, 6 = 5F-ADB, 7 = 5F-PB-22, 8 = MDMB-CHMICA, 9 = UR-144, 10 = STS-135, 11 = PB-22, 12 = MMB-2201, 13 = THJ-2201, 14 = 5F-SDB-005, 15 = APICA, 16 = AM-2201, 17 = 5F-AKB-48, 18 = BB-22, 19 = MDMB-CHMCZCA, 20 = EG-018; Separation parameters given in Materials and Methods

5.4.2.3 Possibility of quantification of analyte classes with a common calibrator

The possibility to cross calibrate synthetic cannabinoids with other substances of the same substance class with regard to the core of the synthetic cannabinoid was evaluated using 7-point calibrations of each reference standard. Peak area was used to reduce impairments from peak broadening. Two QC samples of each substance were measured and the bias (%) of the calculated concentration was evaluated with the calibration data of all other synthetic cannabinoids (Table 5-2).

The synthetic cannabinoids are subdivided into 3 classes to study the effect of structural analogies on the feasibility of cross calibration: indazoles, indoles and carbazoles (Table 5-1). In the State Office of Criminal Investigation Rhineland-Palatinate (Germany), a general measurement uncertainty of 10 % is accepted for quantification. This value stems from empirical values of quantifications of classical drugs which allow a maximum deviation of 5 % during measurements. Consequently, the scope of uncertainty was established to be a twofold deviation of 5 %. The calculated bias must therefore be less than 5 %, all deviations above this value indicate that the possible cross-calibrator substance is unsuitable for the quantification of the analyte of interest.

In this study, eight different indazole-core synthetic cannabinoids were evaluated. Table 5-3 summarises the bias of the QC-samples for each pair of analyte and cross-calibrator. The fields marked in blue show the results when the analyte concentration is determined by its own calibration curve. Green fields mark bias values < 5 %, where cross calibration is feasible with the respective cross-calibrator. The following trend was observed: synthetic cannabinoids with same linker connected to the indazole-core group show a bias < 4.9 % and quantification within this substance class is possible. E.g. THJ-2201 and 5F-SDB-005 have a keto- and an ester-linkage, respectively. The different linkers lead to elevated bias values of 5.2 to 37.5 %, which is unacceptable for precise quantification. Best results with bias values that ranged from -1.5-1.0 % were recognised for pairs of substances additionally containing similar tail-groups such as the pair AB-FUBINACA and FUB-AMB or the pair 5F-ADB with 5F-AMB. The linked group was observed not to influence quantitative results. E.g. AB-FUBINACA possesses an amido- and FUB-AMB an ester-group, but similar bias values were observed.

In contrast, the tail plays a subordinate role in comparison to the linker which is illustrated by the substance pair of 5F-AKB-48 and MAB-CHMINACA. For 5F-AKB-48 containing a fluoro-pentyl-group the best cross-calibrator was FUB-AMB with a fluorobenzyl-group. For MAB-CHMINACA with a cyclopentyl-group best results were obtained with 5F-AMB containing a fluoro-pentyl group (see Table 5-1 and Table 5-3). For indazole-core synthetic cannabinoids, the UV spectra were very similar with UV_{max} around 300 nm except for THJ-2201, a substance with a keto linkage with UV_{max} of 218 and 320 nm. 5F-SDB-005 shows a band at ~300 but an ester-linker and thus, could not be quantified using the calibration data of any other substance.

Clearly, similar UV spectra themselves are not decisive but the slope of the calibration curve. Table 5-2 summarises the equations of the calibration curves and similar slopes represent an indication for possible cross links between substances. E.g., the indazole-core synthetic cannabinoids show values of $m = 17134.7-18610.4 \mu V \cdot sec \cdot L \cdot kg^{-1}$. THJ-2201 and 5F-SDB-005 have different slope values with $m = 1633.2$ and $m = 22256.1 \mu V \cdot sec \cdot L \cdot kg^{-1}$,

respectively (see Table 5-2). Thus, the slope is a reliable indicator for cross calibration possibilities between substances.

A similar evaluation of the data for ten indole-core synthetic cannabinoids (see Table 5-4) revealed similar trends as for the indole-core cannabinoids: Three different linker types including amide-, keto- and ester-linkage allowed cross calibration within these substance classes. Across the classes, unacceptable bias values of -62.4 to 152.1 % were obtained (see Table 5-4). For the class with an amide-linker including MDMB-CHMICA, STS-135, APICA and MMB-2201 cross calibration was possible with bias values < 4.9 % despite differences in the UV-spectra: the spectra of MDMB-CHMICA and MMB-CHMICA have bands at 216 and 290 nm, whereas STS-135 and APICA spectra show only one band at around 300 nm. The values of the slope are similar, ranging from $m = 11939.1\text{-}12734.1 \mu\text{V}\cdot\text{sec}\cdot\text{L}\cdot\text{kg}^{-1}$. AM-2201, UR-144 and XLR-11 belong to the class with a keto linkage and are feasible for cross calibration (bias values < 4.4 %). AM-2201 show the highest bias values of these three substances and the slope value of $m = 19420.1 \mu\text{V}\cdot\text{sec}\cdot\text{L}\cdot\text{kg}^{-1}$ differs from that of UR-144 ($m = 18224.3 \mu\text{V}\cdot\text{sec}\cdot\text{L}\cdot\text{kg}^{-1}$) and XLR-11 ($m = 18976.1 \mu\text{V}\cdot\text{sec}\cdot\text{L}\cdot\text{kg}^{-1}$). The last class with an ester-linkage includes PB-22, 5F-PB-22 and BB-22. Bias < 5 % were observed here (Table 5-4) with values of the slope that ranged from $m = 29391.6\text{-}28526.7 \mu\text{V}\cdot\text{sec}\cdot\text{L}\cdot\text{kg}^{-1}$.

As expected, structurally similar substances showed best cross calibration results with lowest bias values: e.g., STS-135 and APICA are structurally very similar except the fluoro atom attached to the pentyl tail in STS-135. The same applies to PB-22 with 5F-PB-22 and UR-144 with XLR-11. These substances show best cross calibration results with lowest bias values ranging from 0.3 to -1.6 %. Cross calibration of PB-22 with 5F-PB-22 achieved bias values < 1.6 % whereas bias values for BB-22 ranged from -5.0 to -3.6 % (see Table 5-4).

Only few carbazole-core synthetic cannabinoids have appeared on the NPS drug market so far. In this study only two representative substances were investigated including EG-018 and MDMB-CHMZCZA differing in linker, tail and linked group. Accordingly, cross calibration was not feasible with bias values > 300 % (data not shown), showing the limitations of the cross calibration approach for this class of cannabinoids.

We further tested, if a cross calibration between indole- and indazole-core synthetic cannabinoids is possible. Bias values ranged from -0.1 % to 95.9 % (see Table 5-5 and Table 5-6) and slopes of the calibration curve often differed. Cross calibration was shown to be possible only for indole-core synthetic cannabinoids with a keto-linker (UR-144 and XLR-11 and AM-2201) with indazole-core synthetic cannabinoids containing an amide-linkage with bias values that range from -4.9-4.5 %.

For quantification of casework samples in forensic applications, some general rules were deducted: The most important prerequisite for possible cross calibration are same core- and linker-groups present in the synthetic cannabinoids leading to a similar sensitivity given by

the slope of the calibration curve. Similarities in the tail-group can be advantageous but are not a precondition.

Indazole-core synthetic cannabinoids with an amide linkage represent the most common chemical structure of NPS and FUB-AMB and 5F-ADB show the lowest bias values in cross calibration with other synthetic cannabinoids of this group and can be regarded as suitable cross calibrants for the whole class. In the case of indole-core synthetic cannabinoids, for every linker type one substance is observed to reveal low bias values including 5F-PB-22 (ester-linker), STS-135 (amide-linker), UR-144 (keto-linker). For these substances, reference material is commercially available. Overall, only five synthetic cannabinoids standards are thus required for precise quantification via only a few cross calibrations, which also considerably reduces the effort and working time.

Table 5-2 Validation of synthetic cannabinoids evaluated in this study including linearity, sensitivity and precision, UV_{max} and retention time R_t .) with quality control samples QC1 (10 mg/L) and QC2 (75 mg/L)

Substance	UV_{max} in nm	R_t in min	Linearity		Sensitivity	Precision				
			Calibration curve	R^2		QC1		QC2		
						LOD	LOQ	Intra day	Inter day	Intra day
in mg/L					in %					
Indazole										
5F-AKB-48	301	7.82	$y = 17482.7x + 6810.0$	0.999	2.01	8.06	0.63	3.10	2.21	4.32
5F-AMB	301	3.77	$y = 18202.9x + 16234.3$	0.999	2.78	9.68	1.18	2.93	1.41	5.01
5F-ADB	301	4.99	$y = 17694.4x - 2068.4$	0.999	0.56	2.03	1.08	2.38	0.74	1.93
5F-SDB-005	301	7.26	$y = 22256.1x + 4991.3$	0.999	1.31	5.29	0.57	2.14	0.67	2.80
AB-FUBINACA	301	2.34	$y = 17997.7x + 4007.3$	0.999	1.22	4.22	0.90	1.05	0.15	1.15
FUB-AMB	300	4.50	$y = 18610.4x - 13352.2$	0.999	1.41	4.98	1.34	2.89	1.32	4.90
MAB- CHMINACA	302	4.54	$y = 17134.7x + 791.07$	0.999	0.50	1.79	0.85	1.17	0.65	2.88
THJ-2201	218, 320	7.05	$y = 1633.2x + 426.93$	0.999	0.49	1.57	1.00	2.28	0.70	1.95

Substance	UV _{max} in nm	R _t in min	Linearity		R ²	Sensitivity		Precision				
			Calibration curve			LOD	LOQ	QC1			QC2	
								Intra day	Inter day	Intra day	Inter day	in %
Indole												
5F-PB-22	215, 294	6.28	y = 29391.6x – 5157.2		0.998	2.91	5.22	0.41	2.63	1.30	3.90	
APICA	302	7.37	y = 12176.7x + 513.40		0.997	3.01	10.10	0.26	2.89	0.17	3.84	
AM-2201	217, 247, 315	7.68	y = 19420.1x – 9718.8		0.999	0.49	2.02	1.44	3.09	1.54	3.03	
BB-22	215, 294	8.33	y = 28526.7x – 22684.0		0.999	1.67	5.89	1.22	3.20	0.61	3.70	
MMB-2201	216, 290	6.95	y = 12734.5x – 14998.2		0.998	0.68	2.33	1.08	3.28	1.67	2.92	
MDMB-CHMICA	216, 290	6.49	y = 11939.1x – 12923.2		0.999	2.09	7.33	1.42	3.03	1.67	5.11	
PB-22	216, 294	6.81	y = 29265.3x – 3602.9		0.999	4.17	7.34	0.40	2.62	0.40	3.85	
STS-135	301	6.5	y = 12624.3 x – 15887.5		0.999	0.86	3.52	1.94	2.98	2.10	4.20	
UR-144	215, 245, 305	6.49	y = 18224.3x – 9956.7		0.997	0.71	2.90	0.24	1.17	0.61	2.30	
XLR-11	215, 245, 305	4.91	y = 18976.1x – 8453.8		0.999	0.66	2.70	1.27	3.49	0.70	2.80	
Carbazole												
EG-018	216, 276, 298, 340	11.68	y = 30.06x – 1.75		0.998	0.55	2.24	1.56	3.49	1.20	4.01	
MDMB- CHMCZCA	235, 277	9.04	y = 90.12x – 5.31		0.997	1.23	5.23	1.89	4.56	1.87	4.65	

Table 5-3 Bias values in % of the cross calibration of indole-core synthetic cannabinoids (blue = origin calibration, green = possible cross calibration partner with bias < 5)

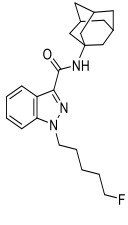
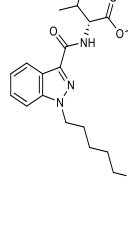
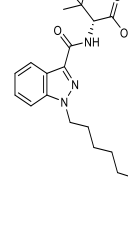
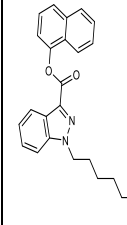
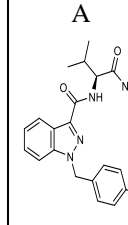
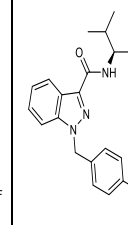
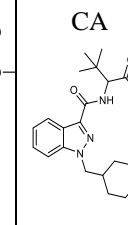
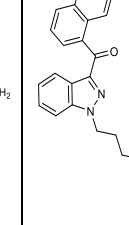
THJ-2201	Substances for cross calibration							
	MAB-CHMINACA	FUB-AMB	AB-FUBINACA	5F-SDB-005	5F-ADB	5F-AMB	5F-AKB-48	Active ingredient of QC-samples
-7.2	3.2	3.9	2.1	30.6	4.3	-2.3	-0.5	5F-AKB-48 
-8.0	4.8	2.8	1.5	26.1	4.6	-3.2	-2.0	5F-AMB 
-8.2	0.8	4.7	2.9	28.7	-1.0	-0.1	2.5	5F-ADB 
-7.9	1.4	4.9	2.7	23.2	-0.7	-0.5	2.3	5F-SDB-005 
-7.2	-1.9	2.5	2.7	27.5	-0.7	1.0	0.7	AB-FUBINACA A 
-7.3	-1.8	1.7	3.8	21.6	0.1	-0.7	0.6	FUB-AMB 
-28.1	24.2	-20.6	-19.7	-0.6	-22.5	-22.7	-22.1	MAB-CHMINACA CA 
-28.3	-24.3	-21.0	-19.6	-2.3	-22.6	-23.3	-22.4	THJ-2201 
-10.7	-5.5	-1.5	-0.2	23.2	3.8	3.5	1.7	
-11.0	-6.0	2.2	-0.2	17.4	-3.9	3.8	3.7	
8.2	-2.5	1.4	0.3	24.9	2.2	2.3	-0.7	
-8.0	-2.0	1.7	2.0	19.5	2.6	-0.8	0.2	
6.1	0.1	4.7	10.75	30.6	2.3	2.1	2.7	
-5.3	0.2	4.2	5.4	24.5	2.2	1.5	2.6	
-0.4	5.2	10.3	-19.5	37.2	7.4	7.2	7.9	
-0.5	5.3	9.4	11.5	30.8	7.4	6.7	7.8	

Table 5-4 Bias values in % of the cross calibration of indazole-core synthetic cannabinoids (blue = origin calibration, green = possible cross calibration partner with bias < 5)

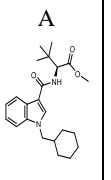

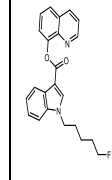
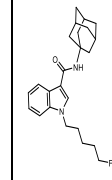
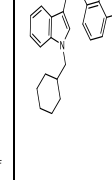
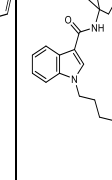
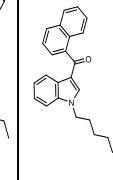
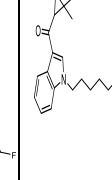
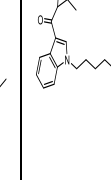
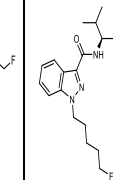
Active ingredient of QC-samples	Substances for cross calibration									
	MDMB-CHMICA	PB-22	5F-PB-22	STS-135	BB-22	APICA	AM-2201	UR-144	XLR-11	MMB-2201
	1.2	148.6	152.1	4.5	135.6	4.1	65.7	61.7	56.0	4.3
	2.1	147.6	150.3	4.5	135.5	4.6	64.8	60.7	55.2	4.9
	-62.4	-1.6	-0.3	-59.1	-4.3	-59.5	-35.9	-36.7	-39.9	-59.7
	-60.0	-0.6	0.1	-57.2	-3.8	-58.9	-35.2	-35.7	-39.1	-58.8
	-60.3	-0.8	0.6	-58.3	-5.0	-57.5	-34.5	-35.8	-38.4	-58.0
	-61.6	-0.7	0.3	-57.6	-4.0	-57.6	-34.4	-35.9	-38.3	-57.7
	-1.8	136.7	140.0	0.7	123.9	0.7	58.3	54.2	49.1	2.9
	-1.7	135.4	137.9	0.6	124.0	0.3	57.0	53.7	47.9	2.2
	-54.9	6.3	7.9	-54.5	0.2	-52.0	-28.4	-30.5	-32.4	-53.0
	-52.9	5.3	6.5	-54.7	0.7	-53.2	-29.3	-30.8	-33.4	-53.7
	-3.5	137.4	138.6	-1.5	125.7	-0.6	54.8	52.1	45.8	-1.7
	-2.4	41.4	139.6	-1.1	123.9	-0.1	56.1	52.7	46.7	-0.1
	-38.6	51.4	53.0	-34.6	44.1	-34.1	0.8	-1.5	-4.2	-35.0
	-37.8	54.6	53.0	-35.8	43.7	-34.7	0.5	-1.2	-4.4	-35.0
	-37.8	54.6	56.2	34.6	46.7	-33.0	2.7	1.5	-3.4	33.8
	-37.5	54.2	56.7	-38.8	46.7	-33.5	2.5	0.5	-3.5	-33.6
	-34.2	61.4	63.1	-31.6	53.2	-29.6	7.5	5.1	1.2	-30.7
	-35.3	63.8	62.5	-37.7	55.1	-30.3	7.2	5.1	0.9	-29.8
	-3.1	133.0	135.5	-0.5	121.8	3.4	56.4	52.5	46.3	1.0
	-2.1	133.0	132.8	-0.1	122.2	1.7	55.3	52.5	47.4	1.2

Table 5-5 Bias values in % for the cross calibration of indazole-core synthetic cannabinoids with indole-core synthetic cannabinoids, green columns indicate possible cross calibration partners

THJ-2201	MAB-CHMINACA	FUB-AMB	AB-FUBINACA	5F-SDB-005	5F-ADB	5F-AMB	5F-AKB-48	Substances for cross calibration												
								MDBM-CHMICA	PB-22	5F-PB-22	STS-135	BB-22	APICA	AM-2201	UR-144	XLR-11	MMB-2201			
43.9	53.2	58.4	61.5	95.7	55.7	54.6	54.2													
43.3	-42.2	58	60	95.9	55.8	54.8	52.3													
-45.1	-42.2	-39.7	-38.8	-23.9	-40.9	-41.3	-41.2													
-45.3	-42.5	-39.8	-38.1	-23.9	-40.8	-41.8	-40.2													
-43.2	-39.9	-37.6	-36.4	-22.4	-39.9	-39.2	-39.3													
-43.3	-39.9	-37.8	-35.8	-22.9	-39.3	-39.8	-40.1													
37.7	46.8	51.4	54.6	86.8	48.7	48.7	47.4													
36.3	46.2	51.9	55.2	81.9	48.8	48	47.2													
-37.4	-33.1	-31.2	-29.7	-15.6	-32.3	-32.5	-32.2													
-36.3	-33.2	-31.3	-29.2	-15.9	-32.2	-32.2	-38.2													
33.5	40.9	46.3	50.6	83.8	43.6	42.6	43.7													
33.3	40.2	46.8	50.8	81.9	43.2	42.8	43.7													
-12.7	-7.2	-4.3	-2	19.1	-5.9	-6.4	-6.4													
-13.3	-7.2	-4.9	-2.2	19.9	-5.3	-6.2	-6.8													
-11.1	-5.5	-2.2	-0.2	21.4	-4.2	-4.6	-4.7													
-11.6	-5.5	-2.3	-0.1	21.9	-4.8	-4.4	-4.8													
-6.9	-1	2.5	4.6	27	0.4	-0.7	-0.2													
-7	-1.5	2.2	4.1	27.9	0.8	-0.4	-0.3													
36	45	49.6	52.7	84.8	46.6	46.2	45.8													
37	42.3	50.1	53.6	85	45.3	46.3	46.2													

Table 5-6 Bias values in % for the cross calibration of indole-core synthetic cannabinoids with indazole-core synthetic cannabinoids, green columns indicate possible cross calibration partners

MMB-2201	XLR-11	UR-144	AM-2201	APICA	BB-22	STS-135	5F-PB-22	PB-22	MDMB-CHMICA	Substances for cross calibration										
										AKB-48	5F-AMB	5F-ADB	5F-SDB-005	AB-FUBINACA	FUB-AMB	Mab-CHMINACA	THJ-2201			
-30.9	1.3	4.5	7.9	-31.4	57.0	-31.5	65.6	64.6	-35.6											
-32.1	1.4	4.2	8.0	-32.3	56.3	-32.2	64.2	63.2	-36.3											
-29.6	1.8	4.1	8.1	-29.5	55.0	-30.9	65.5	64.5	-34.5											
-30.1	2.0	4.3	8.3	-30.0	54.2	-32.1	64.1	63.1	-33.8											
-30.1	1.9	4.1	8.4	-30.4	56.8	-30.9	65.5	64.5	-34.5											
-31.4	2.2	4.0	9.0	-29.8	54.5	-31.2	64.8	65.2	-35.0											
-45.4	-20.1	-16.8	-14.9	-45.8	23.6	-46.0	30.4	29.6	-49.9											
-46.7	-22.0	-15.7	-13.2	-42.3	24.2	-45.2	31.2	30.1	-43.3											
-32.4	-1.0	3.1	4.3	-32.8	53.0	-33.0	61.5	60.4	-36.7											
-32.8	-1.3	2.9	4.4	-33.4	53.4	-33.2	62.3	61.2	-36.8											
-31.6	-1.0	3.2	4.2	-31.6	51.1	-32.6	59.6	58.5	-35.7											
-32.1	-1.3	3.4	4.5	-33.1	52.2	-33.1	60.0	57.3	-35.9											
-28.4	4.6	9.0	11.3	-28.7	61.3	-29.1	70.3	69.2	-33.4											
-29.4	4.7	8.6	12.0	-32.1	62.4	-30.2	69.4	70.2	-33.0											
-24.8	9.8	14.4	16.9	-25.1	69.3	-25.5	78.7	77.6	-29.2											
-25.9	10.2	12.3	17.1	-24.8	70.2	-24.1	80.0	77.5	-29.2											

5.4.3 Application to casework samples

The applicability of the studied crosslinks for quantification was examined analysing 24 herbal mixtures with synthetic cannabinoids as active ingredient. First, GC-MS analyses were performed to determine the of the active ingredient of the samples. Afterwards, quantification was carried out via UPLC-DAD. Incense materials were purchased by the State Office of Criminal Investigation Rhineland-Palatinate (Germany) and the results which were obtained by UPLC-DAD were summarised in Table 5-7. Generally, identification was via retention time and UV spectra. First, the content of the active ingredient in the sample was calculated with the corresponding calibration curve of the target synthetic cannabinoid using the reference standard characterised previously by NMR. In addition, the active ingredient contents were calculated with other possible calibration curves of synthetic cannabinoids that were proven to be suitable for cross calibration (see Table 5-3 -, Table 5-6) by structural similarity and the slopes of the calibration curves. In Table 5-7, the name of the product, the active ingredient, the active ingredient content and the possible cross calibration with a synthetic cannabinoid are summarised together with the associated bias for each cross calibration. The calculated bias values were < 4.3 % and correspond well to the bias values given in Table 5-3 and Table 5-4. The five synthetic cannabinoids, that were identified to be suitable for general cross calibrations (5F-ADB, FUB-AMB, STS-135, PB-22, UR-144) during the method validation, showed acceptable bias values that ranged from -2.0-2.4 %, so that this small set of NPS can be regarded suitable for a broader application. In case of a newly emerged synthetic cannabinoids, the developed general procedure for cross calibration is: First, the active ingredient has to be identified with regard to its chemical structure with core, the linker and the tail by suitable methods (here, NMR and GC-MS. Second, based on this information, one of the five cross calibrators is chosen based on the highest structural similarity. Third, the analyte is quantified by UPLC-DAD. In general, the higher the similarity in the chemical structures (core, linker, linked group and tail), the higher the quantitative precision. Indazole-core synthetic cannabinoids with an amide-linker could be cross calibrated with FUB-AMB or 5F-ADB. Indole-core synthetic cannabinoids show a higher availability of possible linkers on the drug market and therefore, three different substances could be considered for cross calibration: PB-22 (ester-linker), STS-135 (amide-linker), UR-144 (keto-linker). Due to the low number of substances with a carbazole-core synthetic cannabinoid investigated during this study, possible cross links could not be obtained. In case of unknown samples, which were not further characterised, the UV_{max} values give a first insight of the presence of an indazole, indole or carbazole-core synthetic cannabinoid.

Table 5-7 Cross calibration for casework samples (herbal mixtures) with active ingredient content of the substance investigated with the corresponding calibration line, the package label and the concentrations determined from the calibration curves of other cross calibrators with bias values (mean value); performance of the analysis of herbal mixtures using UPLC-DAD as explained in Section Materials and Methods

ingredient content in%	Package label	Concentration (in %) determined from calibration curves of the cross-calibrators				
5F-ADB		5F-AKB-48	5F-AMB	AB-FUBINACA	FUB-AMB	MAB-CHMINACA
6.57	Trank	6.41	6.52	6.32	6.73	6.71
4.73	Amnesia	4.62	4.70	4.55	4.83	4.83
1.28	Abduccion	1.25	1.27	1.23	1.31	1.31
1.12	Armageddon	1.09	1.11	1.08	1.14	1.14
0.89	Hexen Sabbat	0.87	0.88	0.87	0.91	0.91
4.82	Trank	4.70	4.78	4.64	4.94	4.93
3.16	Diablo 4 g	3.09	3.13	3.05	3.22	3.22
4.52	Hexen Sabbat	4.41	4.50	4.35	4.63	4.62
0.87	Hexenmeister	0.85	0.86	0.84	0.89	0.88
8.31	Diablo 4g	8.14	8.24	7.99	8.51	8.49
Bias (%) (mean value)		-2.5	-0.8	3.8	2.4	2.2
MDMB-CHMICA		STS-135	APICA	MMB-2201		
0.61	Grazy Monkey	0.60	0.59	0.59		
0.70	ICE Dragon	0.69	0.68	0.68		
0.73	No name	0.72	0.71	0.71		
4.34	Deadman Walking	4.27	4.20	4.22		
3.88	Deadly Cobra	3.81	3.78	3.76		
1.39	Hexen Sabbat	1.38	1.36	1.35		
2.38	Deadly Cobra	2.34	2.30	2.31		
3.45	Joker	3.43	3.35	3.34		
4.89	No name	4.81	4.72	4.76		
1.23	No name	1.21	1.19	1.19		
Bias (%) (mean value)		< -1.7	< -3.5	< 3.1		

ingredient content in%	Package label	Concentration (in %) determined from calibration curves of the cross-calibrators				
5F-AMB		AB-FUBINCA	5F-AKB-48	5F-ADB	FUB-AMB	MAB-CHMINACA
0.90	No Name	0.88	0.89	0.93	0.92	0.93
Bias (%)		-3.2	-2.2	2.5	1.0	1.8
FUB-AMB		AB-FUBINCA	5F-AKB-48	5F-AMB	5F-ADB	MAB-CHMINACA
1.44	Alabama Wildfire	1.42	1.48	1.50	1.47	1.50
Bias (%)		-1.5	3.0	4.5	2.0	4.3
MAB-CHMINACA		5F-AKB-48	5F-AMB	5F-ADB	FUB-AMB	
0.83	Keep calm and show middle finger	0.86	0.84	0.82	0.81	
Bias (%)		3.3	0.9	-1.8	-2.0	
MMB-CHMICA		MDMB-CHMICA	STS-135	APICA		
3.88	Bob Marley	4.05	3.96	3.86		
Bias (%)		4.3	2.1	-0.5		

5.5 Conclusion

A UPLC-DAD method has been developed for the quantification of synthetic cannabinoids via cross calibration using only five calibrators to circumvent the quantification problem, when reference material of new occurring NPS products is not available. This approach represents a powerful tool for forensic toxicological applications. The sudden appearance and sometimes brief lifetime in the market of many of these novel legal highs or research chemicals does not justify organic synthesis or large-scale purification of reference material. Our study clearly indicates that similarities in the core, the linker and the tail structure of a synthetic cannabinoid were decisive for possible cross calibration with acceptable bias values $\leq 5\%$. We showed that only 5 cross-calibrator substances for indoles (5F-PB-22, STS-135, UR-144) and for indazoles (5F-ADB, FUB-AMB) were required. However, for carbazole-based synthetic cannabinoids, the current number of seizures is too low to be able to define suitable cross-calibrators. The applicability of the study was proven by the successful quantification of 24 herbal mixtures containing synthetic cannabinoids as active ingredient using the cross calibrators defined during method development. The transferability of the method to new NPS will be carried out with the help of round robin testing (Germany) in the future.

6 Chiral discrimination of NPS using CE-DAD: Enantioselective separation of synthetic cathinone derivatives by capillary electrophoresis with UV

6.1 Abstract

Chiral discrimination of new psychoactive substances (NPS) and the related development of stereoselective analytical methods gain in importance in medicinal chemistry and forensic toxicology. Since R and S enantiomers contain the same substituent atoms or groups, they may have different affinity and intrinsic activity at receptor sites. Many synthetic cathinone derivatives are on the market as racemic mixtures due to the use of racemic precursors during the manufacturing process.

In this study, the effective and fast enantioselective separation and detection of racemic mixtures of 36 synthetic cathinone derivatives using capillary electrophoresis with diode array detection is demonstrated. Two analytical methods were developed for different applications: First, a screening method for the simultaneous chiral analysis of synthetic cathinones was developed using reversed polarity and long-end injection mode with a maximum migration time of 26 min. The second method allows the fast determination of the enantiomeric excess of single synthetic cathinone derivative samples using normal polarity and short-end injection mode with an overall migration time of only 6 min. Both methods were validated using a suitable internal standard. The utility of this approach is demonstrated by the successful analysis of seized samples containing synthetic cathinone derivatives as active ingredients present in different bulking agents.

6.2 Introduction

Over the last decade, new psychoactive substances (NPS) have rapidly emerged in the European drug market as a “legal” alternative to conventional controlled substances.²⁵⁰ A challenging task for drug policies is how to effectively respond to the dynamic and constantly changing market of narcotics.⁶ Only a small number of NPS is controlled under drug law or equivalent legislation in European countries and even small modifications in the chemical structure of such listed substances already allow circumventing existing law.^{1,7} This circumstance induced a race between the legal prosecution and the producers as those strive to be one step ahead by generating new NPS products.

NPS have initially been designed to mimic established illicit drugs by imitating both appearance and consumption as well as the psychotropic effects. They are primarily sold via the internet as, inter alia, “research chemicals”, “designer drugs”, “legal highs” or “bath salts” and are usually manufactured as powder, pills or capsules.^{27,251} The focus of this study is on synthetic cathinone derivatives, the second most frequently seized group of new psychoactive substances, accounting for almost one-third of the total number of seizures in 2018.²⁵⁰ The five most frequently seized cathinone derivatives in 2016 were α -PVP, 4-CMC, 3-CMC, 4-methyl-*N,N*-dimethylcathinone and 3-MMC (for abbreviations see Section 2.1.2 Reference materials).²⁵⁰ Synthetic cathinone derivatives are β -ketoamphetamines and chemically related to cathinone, a naturally occurring stimulant in the khat plant (*Catha edulis*).⁶ In contrast to a classical drug class, the group of synthetic cathinone derivatives covers a broad spectrum of psychotropic effects caused by a multitude of possible chemical modifications in their chemical structures.¹¹ Synthetic cathinone derivatives predominantly act as central nervous system stimulants to inhibit the actions of monoamine transporters such as dopamine transporter (DAT), noradrenaline transporter (NAT), and serotonin transporter (SERT) like amphetamine, methamphetamine, MDMA and cocaine.^{11,27,303,304}

Synthetic cathinone derivatives without a substitution on the benzene ring (e.g. methcathinone) show similar stimulant effects to amphetamine acting as an inhibitor of DAT and NAT.²⁴ Synthetic cathinone derivatives containing a methylenedioxy substitution in the benzene ring like methylone, ethylone, and butylone show actions similar to cocaine and MDMA.³⁰⁵ The non-selective inhibition of the monoamine reuptake is similar to the one of cocaine, which shows greater affinity to DAT than SERT. The inhibition of SERT by synthetic cathinone derivatives is similar to MDMA.^{22,24,303,306-308} Alongside of a stimulating effect, synthetic cathinone derivatives also show entactogenetic effects. Methamphetamine inhibits the preferential reuptake of catecholamines and liberation of dopamine, the same applies to synthetic cathinone derivatives with an alkyl or halogen substituent at any possible position of the aromatic ring (for example 4-MMC, flephedrone, and 4-CMC).^{24,306} Cutting agents can mimic, enhance, or potentiate the effects of controlled drugs of abuse. The most common reported cutting agents in synthetic cathinone derivative products are benzocaine, lidocaine and caffeine.^{21,112,113,309}

The synthesis of synthetic cathinone derivatives is analogous to the manufacture of amphetamine and MDMA-related substances including 1) reductive amination and 2) the Leuckart reaction, both with an aromatic ketone as precursor, 3) the use of aromatic aldehydes under Knoevenagel conditions²⁸ and 4) the oxidation of the readily available pharmaceuticals pseudoephedrine and ephedrine.^{27,29} The routes 1) and 2) are the most common production processes found in clandestine laboratories. Here, the precursors like ketones contain a stereogenic center at the β -carbon of the ketone structure.^{5,30} In 1929, Saem de Burnaga Sanchez published a synthetic strategy for mephedrone as the first cathinone starting with

1-tolylpropan-1-one as a precursor, which was α -brominated and then reacted with methylamine to produce racemic 4-methylmethcathinone.³¹ Today, almost all synthetic cathinone derivatives exist as racemic mixtures.²⁶

The R and S enantiomers show significant differences in their pharmacodynamic activity and their pharmacokinetic properties due to differences in their affinity or intrinsic activity at receptor sites.^{144,145}

As a consequence, chiral discrimination and the availability and development of stereoselective analytical methods gain in importance in medicinal chemistry, and forensic toxicology. The most common technique is HPLC-UV with chiral stationary phases¹⁴⁶⁻¹⁵² or an achiral stationary phase with cyclodextrins (CDs) added to the mobile phase.¹⁵³ Few studies used GC-MS for the chiral analysis of synthetic cathinone derivatives separating diastereomers after derivatization with chiral trifluoroacetyl-L-prolyl chloride¹⁵⁴⁻¹⁵⁶ or α -methoxy- α -trifluoromethylphenylacetic acid.¹⁵⁰ Several publications deal with the enantioselective separation of synthetic cathinone derivatives using capillary electrophoresis (CE-DAD or CE-MS) in combination with different CDs as chiral selector including β -CD,^{157,158} highly sulphated- β -CD (HS- β -CD),^{154,159} highly sulphated- γ -CD (HS- γ -CD).¹⁶⁰ Capillary electrochromatography with chiral stationary phases was also applied for the analysis of synthetic cathinone derivatives.^{149,310}

The chiral separation of synthetic cathinone derivatives was demonstrated to be feasible with further publications and different analytical techniques.^{154,157-159} In order to cope with the constant changes in NPS, screening methods have to be developed which are applicable to a large number of structurally different synthetic cathinone derivatives. To the best of our knowledge, no further publication demonstrated the simultaneous separation of a large number of analytes including the discrimination of enantiomers of structurally closely related substances like regioisomers which differ only in the C4 or C5 position of a halogen-atom in a pentyl-chain. The reported analysis times of HPLC-methods range from 12-85 min,^{147,150-153} of GC-MS of 21-40 min¹⁵⁴⁻¹⁵⁶ and CE of 16-22 min.^{154,157-159} Analysis times may be shortened significantly when only one enantiomer pair is analysed (4-6 min) as shown e.g. by Weiß et al. and Aboul et al.^{146,150}

Besides the need for screening methods, the demand of fast methods (< 10 min) increases to enable high-throughput of a large number of samples to obtain a fast estimate of the enantiomeric excess of one substance. Furthermore, almost no publication thematises the analyses of seized samples with possible bulking agents. Silva et al. described the analysis of real samples with presence of bulking agents but without demonstrating that the selectivity is high enough to discriminate between bulk and active agent.¹⁵²

The aim of this study is the effective and fast enantioselective separation and detection of 36 newly emerged synthetic cathinone derivatives using CE-DAD. First, a chiral screening method for a large number of synthetic cathinone derivatives was developed using reversed

polarity after long-end injection. The utility of this approach was demonstrated by the successful analysis of seized samples containing bulking agents. Second, a high-throughput method enabling the fast determination of the enantiomer ratio for specific cathinone derivatives using short-end injection and normal polarity mode was established.

6.3 Materials and Methods

6.3.1 Chemicals

All reagents were of analytical grade. Ultrapure water, purified by a Milli-Q gradient system (18.2 M Ω) from Millipore (Bedford, MA, USA), was used throughout this work. HS- β -CD (β -cyclodextrin, highly sulphated sodium salt with 12-15 mol per mol β -CD) was purchased from Sigma Aldrich (Steinheim, Germany) and β -CD, HP- β -CD (2-hydroxypropyl)- β -cyclodextrin) and HP- γ -CD ((2-hydroxypropyl)- γ -cyclodextrin) from Fluka (Buchs, Switzerland). During this study, two different lots of HS- β -CD were used without a significant influence on the separation behaviour and strength. Sodium dihydrogenphosphate dihydrate (NaH₂PO₄·2H₂O) and aqueous ortho-phosphoric acid 85 % (H₃PO₄) were obtained from Fluka (Buchs, Switzerland) and Riedel-de Hën, (Seelze, Germany). Aqueous sodium hydroxide solution (c = 1.0 M) was delivered by Agilent Technologies, Waldbronn and methanol from Merck (Darmstadt, Germany).

6.3.1.1 Buffer preparation

Phosphate buffers used for CE experiments were prepared daily and a pH of 2.3 was adjusted with 0.1 M orthophosphoric acid.

For long-end injection, 2.5 % HS- β -CD were dissolved in 25 mM phosphate buffer whereas 3.5 % HS- β -CD were dissolved in 35 mM phosphate buffer for short-end injection. All electrolyte solutions for the CE separation were stored in glass bottles at +4°C.

6.3.1.2 Reference samples

Reference material in this study partly derived from the EU-project "ADEBAR". It is a Cooperation Project of the Federal Criminal Police Office, seven State Bureaus of Criminal Investigation and German Customs. Within this project, new drugs appearing on the illicit drug market in Germany from 07/2017 to 07/2019 were structurally characterised with different analytical techniques (1H-NMR, LC-MS, GC-MS, infrared spectroscopy, Raman spectroscopy) in order to generate analytical standards. This includes the synthetic cathinone derivatives dibutylone, 3-CMC, α -PiHP, DMC, MDPHP, methylone, 3-MMC, buphedrone, 4-Cl-pentedrone, NEH. The other synthetic cathinone derivatives were obtained either by the Australian Government National Measurement Institute (Canberra, ACT, Australia) including

methedrone and NEC, or Lipomed (Cambridge, MA, USA) including MDBD, ethylone, which are shown in Table 6-1.

Stock standard solutions of 1000 mg/L of each compound were prepared in ultrapure water and stored at +4 °C. From these standard solutions, working standard solutions with lower concentrations of all compounds were prepared daily by dilution with water and stored at 4 °C.

6.3.1.3 Casework samples

The seizures analysed in this study derived from the EU-project “ADEBAR” including 3,4-DMMC, 4-BMC, 4-CBC, 4-CEC, 4-CMC, 4-MEC, 4MMC, 4-M- α -PPP, 4CI-PVP, α -PHP, butylone, ephylone, methcathinone, NEHP and NEMNP. The samples α -PBP, α -PVP, pentedrone, MDPV, mexedrone and flephedron and mixtures of synthetic cathinone derivatives were taken from criminal cases provided by the State Office of Criminal Investigation Rhineland-Palatinate (Germany). All substances are summarised in Table 6-1.

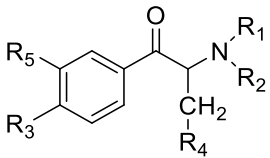
Several cutting agents were analysed including lidocaine (2-(diethylamino)-*N*-(2,6-dimethylphenyl) acetamide), caffeine (1,3,7-trimethylpurine-2,6-dione) from Sigma-Aldrich, (Steinheim, Germany) and benzocaine (ethyl-4-aminobenzoate) from Fluka (Buchs, Switzerland). Each compound was dissolved in water (1000 mg/L) and working solutions were prepared by diluting in water:phosphate buffer (2:8), with the addition of the internal standard 1-(2-chlorophenylpiperazin (oCPP). Table 6-1 shows all synthetic cathinone derivatives investigated in this study.

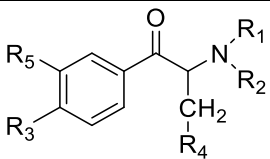
The enantiomeric excess (ee) determination was carried out using working solutions of 50 mg/L in water:phosphate buffer (2:8) of each synthetic cathinone derivatives.

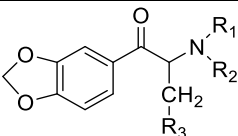
6.3.1.4 Internal standards

Different internal standards (1 mg/mL) were tested including 1-(3-chlorophenylpiperazin) monohydrochloride (mCPP), 1-(2-chlorophenylpiperazin) monohydrochloride (oCPP); (1-(4-chlorophenylpiperazin) monohydrochloride (p-CPP) each with a purity of 98 %, which were purchased by Alfa Aesar (Karlsruhe, Germany)), phentermine, phenethylamine and chinin ((*R*)-(6-methoxyquinolin-4-yl)[(1*S*,2*S*,4*S*,5*R*)-5-vinylquinuclidin-2-yl]methanol) (Sigma Aldrich, Steinheim, Germany). Finally, oCPP was chosen (see Section 3.3 Selection of internal standard).

Table 6-1 Chemical structures of synthetic cathinone derivatives evaluated in this study

						
Substance	IUPAC names	R1	R2	R3	R4	R5
3,4-DMMC	(<i>RS</i>)-1-(3,4-dimethylphenyl)-2-(methylamino)propan-1-one,	CH ₃	H	CH ₃	H	CH ₃
3-CMC	(<i>RS</i>)-1-(3-chlorophenyl)-2-(methylamino)-1-propanone	CH ₃	H	H	H	Cl
3-MMC	(<i>RS</i>)-2-(methylamino)-1-(3-methylphenyl)propan-1-one	CH ₃	H	H	H	CH ₃
4-BMC	(<i>RS</i>)-1-(4-bromophenyl)-2-(methylamino)propan-1-one	CH ₃	H	Br	H	H
4-CBC	(<i>RS</i>)-1-(4-chlorophenyl)-2-(butylamino)propan-1-one	C ₄ H ₉	H	Cl	H	H
4-CEC	(<i>RS</i>)-1-(4-chlorophenyl)-2-(ethylamino)-1-propanone	C ₂ H ₅	H	Cl	H	H
4-Cl-pentedrone	(<i>RS</i>)-1-(4-chlorophenyl)-2-(methylamino)pentan-1-one	CH ₃	H	Cl	C ₂ H ₅	H
4-Cl-PVP	(<i>RS</i>)-1-(4-chlorophenyl)-2-(1-pyrrolidinyl)-1-pentanone	pyrrolidinyl		Cl	C ₂ H ₅	H
4-CMC	(<i>RS</i>)-1-(4-chlorophenyl)-2-(methylamino)-1-propanone	CH ₃	H	Cl	H	H
4M- α -PPP	(<i>RS</i>)-2-(pyrrolidin-1-yl)-1-(p-tolyl)propan-1-one	pyrrolidinyl		CH ₃	H	H
4-MEC	(<i>RS</i>)-2-ethylamino-1-(4-methylphenyl)propan-1-one	C ₂ H ₅	H	CH ₃	H	H
4-MMC	(<i>RS</i>)-2-methylamino-1-(4-methylphenyl)propan-1-one	CH ₃	H	CH ₃	H	H
α -PBP	(<i>RS</i>)-1-phenyl-2-(1-pyrrolidinyl)-1-butanone)	pyrrolidinyl		H	CH ₃	H
α -PHP	(<i>RS</i>)-1-phenyl-2-(pyrrolidin-1-yl)hexan-1-one	pyrrolidinyl		H	C ₃ H ₇	H
α -PiHP	(<i>RS</i>)-4-methyl-1-phenyl-2-(pyrrolidin-1-yl)pentan-1-one	pyrrolidinyl		H	C ₃ H ₇	H
α -PPP	(<i>RS</i>)-1-phenyl-2-(1-pyrrolidinyl)-	pyrrolidinyl		H	H	H

						
Substance	IUPAC names	R1	R2	R3	R4	R5
	1-propanone					
α -PVP	(<i>RS</i>)-1-phenyl-2-(1-pyrrolidinyl)-1-pentanone	pyrrolidinyl		H	C ₂ H ₅	H
buphedrone	(<i>RS</i>)-2-(methylamino)-1-phenylbutan-1-one	CH ₃	H	H	CH ₃	H
DMC	(<i>RS</i>)-2-(dimethylamino)-1-phenyl-1-propanone	CH ₃	CH ₃	Cl	H	H
flephedrone	(<i>RS</i>)-1-(4-fluorophenyl)-2-(methylamino)propan-1-one	CH ₃	H	F	H	H
MDPHP	(<i>RS</i>)-1-(2H-1,3-benzodioxol-5-yl)-2-(pyrrolidin-1-yl)hexan-1-one	pyrrolidinyl		H	C ₃ H ₇	H
methcathinone	(<i>RS</i>)-2-(methylamino)-1-phenylpropan-1-one	CH ₃	H	H	H	H
mexedrone	(<i>RS</i>)-3-methoxy-2-(methylamino)-1-(4-methylphenyl)propan-1-one	CH ₃	H	CH ₃	OCH ₃	H
methedrone	(<i>RS</i>)-1-(4-methoxyphenyl)-2-(methylamino)propan-1-one	CH ₃	H	OCH ₃	H	H
NEC	(<i>RS</i>)- <i>N</i> -ethylcathinone, (2-(ethylamino)-1-phenylpropan-1-one	C ₂ H ₅	H	H	H	H
NEH	(<i>RS</i>)- <i>N</i> -ethylhexedron, (<i>RS</i>)-2-(ethylamino)-1-phenylhexan-1-one	C ₂ H ₅	H	H	C ₃ H ₇	H
NEHP	(<i>RS</i>)- <i>N</i> -ethyl-heptedrone or, 2-(ethylamino)-1-phenylheptan-1-one	C ₂ H ₅	H	H	C ₄ H ₉	H
NEMNP	(<i>RS</i>)-2-(ethylamino)-1-(4-methylphenyl)-1-pentanone	C ₂ H ₅	H	CH ₃	C ₂ H ₅	H
pentedrone	(<i>RS</i>)-1-phenyl-2-(methylamino)pentan-1-one	CH ₃	H	H	C ₂ H ₅	H

				
Substance	IUPAC names	R1	R2	R3
butylone	(<i>RS</i>)-1-(1,3-benzodioxol-5-yl)-2-(methylamino)butan-1-one	CH ₃	H	CH ₃
dibutylone	(<i>RS</i>)-1-(benzo[d][1,3]dioxol-5-yl)-2-(dimethylamino)butan-1-one	CH ₃	CH ₃	CH ₃
ethylone	(<i>RS</i>)-1-(1,3-benzodioxol-5-yl)-2-(ethylamino)propan-1-one	C ₂ H ₅	H	H
ephylone	(<i>RS</i>)-1-(1,3-benzodioxol-5-yl)-2-(ethylamino)pentan-1-one	C ₂ H ₅	H	C ₂ H ₅
MDPV	(<i>RS</i>)-1-(1,3-benzodioxol-5-yl)-2-(pyrrolidin-1-yl)pentan-1-one	pyrrolidinyl		C ₂ H ₅
methylone	(<i>RS</i>)-1-(1,3-benzodioxol-5-yl)-2-(methylamino)propan-1-one	CH ₃	H	H
MDBD*	(<i>RS</i>)-(1-(1,3-benzodioxol-5-yl)- <i>N</i> -methylbutan-2-amine	CH ₃	H	CH ₃

*(this substance does not contain a keto group on α -carbon)

6.3.2 Methodology

The separation of synthetic cathinone derivative standards and seized drug samples was performed using the capillary electrophoresis system G1600 from Agilent Technologies (Waldbronn, Germany) equipped with a diode array detector (CE-DAD). Measurements were performed in 50 μ m id uncoated fused silica capillaries with a total length of 68.5 cm and an effective length of 60.0 cm from Polymicro Technologies (Phoenix, AZ, USA). New capillaries were preconditioned by rinsing at 1 bar with 1.0 M NaOH for 15 min, water for 20 min and electrolyte for 20 min. At the beginning of a measurement series, the capillary was conditioned by flushing at 1 bar for 10 min with 1 M NaOH, 15 min with water and 15 min with BGE. CE-UV detection was performed on-column using a wavelength of 230 nm. The column temperature was maintained at 20°C.

The screening method was performed with hydrodynamic long-end injection mode (conventional injection) (50 mbar \times 5 s). A constant voltage of -20 kV was applied so that the anode was located at the capillary outlet at the detector (reversed polarity) with a resulting current of 49 μ A. Between runs, the capillary was equilibrated with BGE for 2 min.

The high-throughput method was performed using a short-end injection mode by applying vacuum at the inlet (-50 mbar \times 5 s) for sample injection. So the sample was injected from the end of the capillary nearest to the detector. The CE instrument was operated with positive

polarity (detection-end electrode was the cathode) with a voltage of +16 kV and a resulting current of 49 μ A.

6.4 Results and discussion

6.4.1 Chiral separation optimisation

6.4.1.1 Screening method

The dynamically changing drug market and the generation of more and more structurally similar NPS necessitates highly efficient and selective analytical methods for the discrimination of structurally closely related compounds as envisaged in this study of cathinones. Cathinones differ in the substitution at their benzyl-ring (alkyl-, bromo-, chloro- or fluoro-substitutions), at the α and β -carbon atoms or with regard to *N*-alkylations. In some cathinones, the nitrogen atom is part of a pyrrolidino ring. As cathinones can easily be ionised at the nitrogen atom, capillary electrophoresis is well suited to enable the separation of structurally closely related compounds. Upon addition of chiral selectors to the BGE, also chiral analysis is possible. The initial conditions for the separation were adapted from a previous study developed in this laboratory for the separation of (RS)-methamphetamine, (RS)-pseudo-ephedrine and (RS)-ephedrine.³¹¹ These compounds were separated within 30 min using a 100 mM phosphate buffer at pH 2.5 with 2.5 % (w/v) HS- β -CD as chiral selector.³¹¹ For the analysis of synthetic cathinone derivatives, buffer concentration and pH, type and concentration of CD, and temperature were optimised.

In prestudies, different CDs were tested to achieve baseline resolution of enantiomers using a mixture of four representative synthetic cathinone derivatives (DMC, dibutylone, MDPHP, α -PiHP). Separations were carried out using a 100 mM phosphate buffer (pH 2.3) containing 0.5 %, 1.0 % and 1.5 % native CDs (β -CD and γ -CD), 1.0 %, 1.5 % and 2.0 % hydroxypropyl- β -CDs (HP- β -CD and HP- γ -CD) and one highly sulphated CD (HS- β -CD) with concentrations of 1.5 %, 2.0 %, 2.5 % and 3.0 %. In case of γ -CD and HP- γ -CD, no separation of enantiomers was observed. β -CD and HP- β -CD were incapable to separate the enantiomers of DMC and dibutylone. Only the racemic mixture of synthetic cathinone derivatives where the nitrogen atom is part of the pyrrolidino ring (MDPHP and α -PiHP) showed different host-guest stability constants of R and S enantiomers resulting in different migration times and/or differences in the effective electrophoretic mobility of the diastereomeric complexes.³¹² HS- β -CD proved to be the CD of choice because all enantiomer pairs were separated. This combination of oppositely charged CDs and analytes proved to be successful in several other studies.^{159,313-316} At the acidic pH (2.3) chosen, the EOF is negligible and with the reversed separation polarity the anionic chiral selector migrates towards the anode, while the free analytes migrate towards the cathode. At a CD

concentration of 2.0 %, the equilibrium is shifted to the negatively charged CD-analyte complex so that the observed electrophoretic mobility is towards the anode.³¹⁷ Thus, a complexation of the analytes with the negatively charged HS- β -CD leads to a net migration towards the detector. Hence, short migration times indicate strong interaction with HS- β -CD.³¹⁸

Afterwards, the adjustment of the buffer composition, pH and the HS- β -CD concentration were varied simultaneously. In order to avoid excessive Joule heating with noisy baselines due to refractive index changes of the electrolyte,³¹⁹ 75 mM, 50 mM and 25 mM phosphate buffers with 3.0 %, 2.5 %, 2.0 % and 1.5 % (w/v) HS- β -CD were examined using a mixture of 14 different racemic synthetic cathinone derivatives, listed in Table 6-2. The electropherograms for BGEs with different buffer concentrations are shown in Figure 6-1a-c. With increasing buffer concentration, the migration times increase accompanied by decreasing number of theoretical plates (N) with 150°000 for 75mM, 190°000 for 50 mM and 210°000 for 25 mM each with 2.5 % HS- β -CD. Not all racemates could be resolved at buffer concentrations of 75 mM and 50 mM. The concentration of the HS- β -CD has a marked effect on both the resolution and the migration times as visible in Figure 6-1d-g. Higher concentrations of HS- β -CD resulted in increased migrations times and at 2.5 % HS- β -CD in a BGE of 25 mM phosphate all enantiomer pairs were at least partially separated (see Figure 6-1f).

Table 6-2 Comparison of enantiomeric excess *ee*, the separation efficiency of long-end injection and short-end injection in terms of resolution *R* and plate number *N* determined for each enantiomer of synthetic cathinone derivatives

Substance	ee in %	Long-end injection mode			Short-end injection mode		
		Time in min	R	N	Time in min	R	N
3-CMC	0.43	11.9	19.18	180000	3	7.34	13000
		13.5		150000	3.5		13300
3-MMC	0.40	14.3	4.13	95000	3.9	1.64	10200
		14.8		140000	4		13100
4-Cl-pentedrone	2.56	16.9	39.21	210000	5	12.76	12700
		21.1		214000	6.6		14600
α -PiHP	2.89	12.9	35.7	140000	3.2	9.75	4600
		16.4		167000	4.6		6600
buphedron	0.37	15.3	13.15	148000	4.2	5.86	10900
		16.7		163000	4.9		12000
dibutylone	2.83	10.3	11.21	131000	2.4	4.46	10000
		11.2		153000	2.7		12500
DMC	3.16	13.6	11.28	237000	3.5	3.21	10400
		14.4		331000	3.8		11300
ethylone	2.25	11.5	4.29	228000	3.9	1.44	2000
		11.8		191000	4.2		1900
MDBD	0.01	9.1	4.12	93000	2.1	1.55	6700
		9.4		83000	2.2		7800
MDPHP	0.35	13.8	11.78	161000	3.6	4.75	10400
		14.9		157000	4.1		12600
methylone	0.39	11.3	1.52	177000	2.7	1.43	11200
		11.4		190000	2.8		17000
methedrone	0.64	10.5	3.53	100000	2.6	1.36	10300
		10.8		130000	2.7		12500
NEC	1.39	15.1	10.23	142000	4.2	3.49	9100
		16.1		172000	4.6		9700
NEH	0.96	23.5	27.29	204000	5.7	10.57	9700
		27.7		185000	6.4		7700

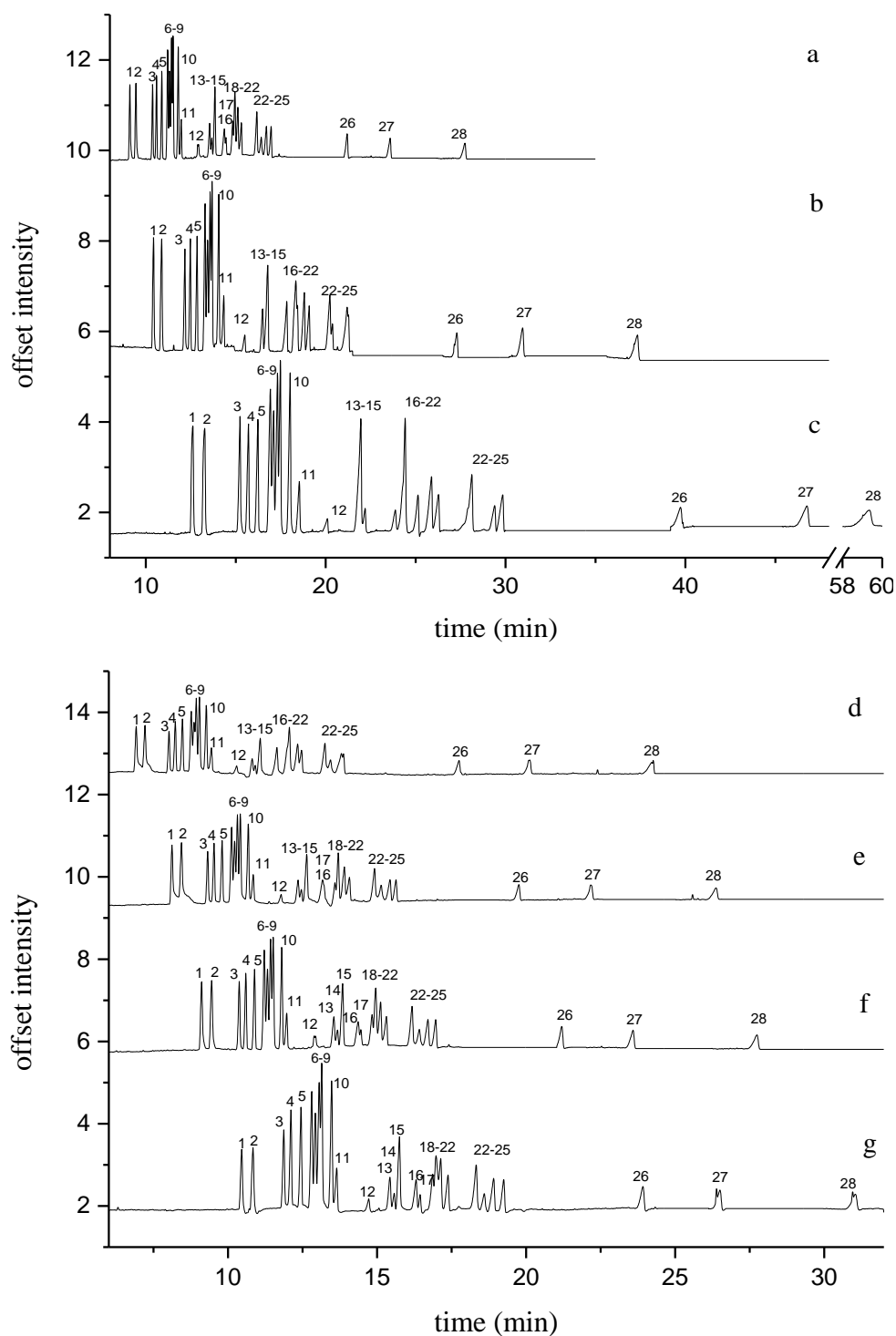


Figure 6-1 Electropherograms of 14 racemic mixtures of synthetic cathinone derivatives using the screening method (1+2 = (R/S)-MDD, 3+6 = (R/S)-dibutylone, 4+5 = (R/S)-mephedrone, 7+10 = (R/S)-methylon, 8+9 = (R/S)-ethylone, 11+13 = (R/S)-3-CMC, 12+23 = (R/S)- α -PiHP, 14+17 = (R/S)-DMC, 15+19 = (R/S)-MDPHP, 16+18 = (R/S)-3-MMC, 20+22 = (R/S)-NEC, 21+24 = (R/S)-buphedrone, 25+26 = (R/S)-4-Cl-pentredone, 27+28 = (R/S)-NEH) with a) 25 mM, b) 50 mM and c) 75 mM phosphate buffer concentration (pH 2.3) with 2.5 % HS- β -CD and d) 1.5 %, e) 2.0 %, f) 2.5 % and g) 3.0 % HS- β -CD in 25 mM phosphate buffer (pH 2.3), long end-injection (50 mbar \times 5 s), -20 kV, detection wavelength 230 nm, sample concentration of 50 mg/L in water/phosphate buffer (2:8)

Different temperatures were investigated including 20, 25, 30, 35 and 40 °C. With increasing temperature, the enantiomers of synthetic cathinone derivatives migrated faster through the capillary due to viscosity changes in the BGE, but a loss of separation efficiency and resolution was observed as well as elevated migration times (data not shown). For further experiments, the temperature was kept at 20 °C. The high separation selectivity reached in the final method came at the expense of a separation time of 26 min.

6.4.1.2 High-throughput method

Fast analysis of enantiomers or racemates in samples that contain only one active ingredient was accomplished using short end injection at normal polarity (vacuum injection). The effective and total length of the capillary were 8.5 and 68.5 cm. Using the optimised BGE from long end injection, the analysis time decreased from 27.7 to 6.4 min (factor 4.3), however at the cost of separation efficiency and resolution.³²⁰ Plater numbers decreased by a factor of 16.

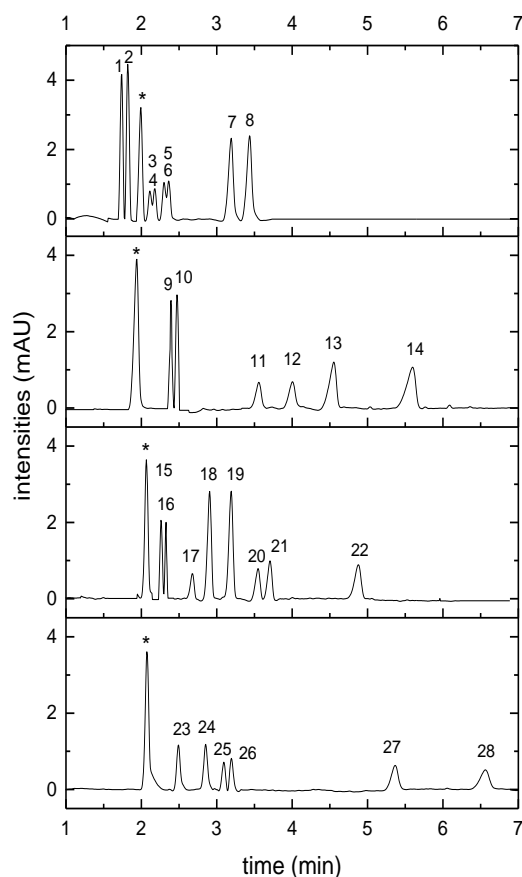


Figure 6-2 Electropherograms of 4 mixtures of the 14 racemic mixtures of synthetic cathinones derivatives using the high-throughput method without comigration events (1+2 = (R/S)-MDBD, 3+4 = (R/S)-mephedrone, 5+6 = (R/S)-ethylone, 7+8 = (R/S)-NEC, 9+10 = (R/S)-methylone, 11+12 = (R/S)-DMC, 13+14 = (R/S)-buphedron, 15+16 = (R/S)-dibutylone, 17+20 = (R/S)- α -PiHP, 18+19 = (R/S)-MDPHP, 21+22 = (R/S)-4Cl-pentedrone, 23+24 = (R/S)-3-CMC, 25+26 = (R/S)-3-MMC, 27+28 = (R/S)-NEH) with 3.5 % HS- β -CD in 50 mM phosphate buffer (pH2.3), short-end injection (-50 mbar \times 5 s), +16 kV, detection wavelength 230 nm, sample concentration of 50 mg/L in water/phosphate buffer (2:8), * indicates internal standard

The enantiomers of MDBD, methylone and ethylone were no longer separated. Different BGE concentrations (25-100 mM) and HS- β -CD concentrations were tested (1.5-3.5 %, (w/v)) to improve resolution. Optimal resolution and peak shape were obtained at 3.5 % HS- β -CD in 50 mM phosphate buffer (pH 2.3) with all enantiomer pairs separated within 6.2 min, see Figure 6-2. Several synthetic cathinone derivatives comigrate including the enantiomer pairs of regioisomers (3-CMC, 4-CMC, 3-MMC and 4-MMC) or other synthetic cathinone derivatives like methedrone and methylone, α -PiHP and DMC, ethylone and 3-MMC and NEC and buphedrone (Table 6-2). All enantiomers of the substances were baseline separated except mephedrone and ethylone, which were only partially separated.

6.4.2 Selection of internal standard

The use of internal standards is sufficient to ensure the necessary precision and accuracy. Only a few forensic publications on CE thematise the use of suitable standards explicitly. Moini et al. applied amphetamine as internal standard with a BGE of formic acid and HS- γ -CD in conjunction with (+)-18-crown-6-tetracarboxylic acid as chiral selectors.¹⁶⁰ Li et al. described the separation 24 regioisomers of synthetic cathinone derivatives in a 80 mM phosphate buffer with HP- β -CD within 18 min with nicotineamide as internal standard.³²¹ In this study, several internal standards were tested with structural similarities to the investigated synthetic cathinone derivatives. These included phentermine, phenethylamine, chinin, pCPP and oCPP). Phentermine and phenethylamine had insufficient absorption at the detection wavelength of 230 nm due to their λ_{max} of 260 and 250 nm. In addition, both substances migrated at 11-13 min in the screening method and thus interfered with several analytes (see Table 6-2). Chinin was detectable at 230 nm but impaired the analysis of MDBD. In case of CPP derivatives, only pCPP and oCPP were considered for analysis. mCPP is classified as a controlled substance in some European countries (Germany, Switzerland, Belgium, Denmark, Finland, Hungary and Netherlands). oCPP showed best performance with a migration time of 10 min where no comigration with analytes occurred.

6.4.3 Figures of merit

Both methods were validated in terms of linearity, intraday and interday precision, sensitivity (LOD and LOQ) and accuracy using Valistat 2.0 (Avercon, Walldorf, Germany). All data are summarised in Table 6-3 and Table 6-4. The validation software was constructed for blood or urine analysis in GC-MS according to the guidelines of the Society of Toxicological and Forensic Chemistry (GTFCh) in consideration of DIN EN ISO 17025.

Linearity of the method was confirmed via a 6-point calibration curve in the range of 5 to 50 mg/L ($n = 6$) with correlation coefficients ranging between 0.9901 and 0.9981 for the screening method and 0.9900 to 0.9995 for the high-throughput method. All substances passed the outlier test (Grubbs-test), the variance homogeneity (Cochran-test) and linearity

test (Mandel-F-test). The sensitivity of the developed methods was investigated by the slope of the calibration curves according to DIN 32646. LODs and LOQs ranged from 1.04-2.38 mg/L and 5.23-10.54 mg/L for the screening method and for the high-throughput method from 0.54-2.60 mg/L and 2.85-10.57 mg/L.

The analytical intra-day ($n = 6$) and inter-day ($8d/n = 3$) precision were estimated with two quality control samples (QC1 and QC2) of each synthetic cathinone derivative covering the specified linear range of the procedure with 2 different concentration levels (0.01 and 0.05 mg/L). The use of the internal standard oCPP improved precision for both methods from $\leq 5.0\%$ for intra-day and $\leq 17.6\%$ for inter-day precision to 1.72% for intra- and interday precision. The same applied to RSD values for the peak area of each compound signal which were improved from 1.9-16.4% for intra-day and 3.7-27.5% for inter-day precision to $RSD \leq 6.0\%$ (screening method) and $\leq 7.0\%$ (high-throughput method) for intra- and inter-day experiments (see Table 6-3 and Table 6-4). The trueness was determined with a bias that ranged from -4.6 to 4.6% for both methods (Table 6-4). In the State Office of Criminal Investigation Rhineland-Palatinate (Germany), a general measurement uncertainty of 10% was stated to be acceptable for quantification results. This value stems from empirical values of quantifications of classical drugs which allow a maximum deviation of 5% during measurements. Consequently, the scope of uncertainty was established to be a twofold deviation of 5%.

Table 6-3 Validation of screening method with the usage of the internal standard in terms of linearity, sensitivity, precision and trueness (QC1 = 0.01 mg/L and QC2 = 0.05 mg/L) evaluated for each enantiomer of synthetic cathinone derivatives

Substance	Linearity		Sensitivity in mg/L		Precision						Trueness	
	slope	R ²	LOD	LOQ	RSD time in %		QC1		QC2		Bias in %	
					intra-day	inter-day	intra-day	inter-day	intra-day	inter-day	QC1	QC2
3-CMC	8.142	0.9952	2.03	9.28	0.08	1.69	0.24	4.60	0.30	4.30	2.00	2.00
	8.625	0.9932	1.96	9.04	0.30	1.76	0.76	3.39	1.00	3.32	1.57	1.90
3-MMC	9.495	0.9913	2.23	10.12	0.39	1.98	0.34	4.95	1.00	1.36	0.05	-2.50
	9.777	0.9925	2.07	9.43	0.46	1.11	1.31	4.31	0.27	4.23	4.70	2.00
4-Cl-pentedrone	7.514	0.9941	1.83	8.56	0.64	1.26	1.65	5.06	1.90	2.00	0.69	2.60
	7.432	0.9974	1.29	5.89	0.89	1.32	1.44	4.59	1.52	2.58	0.27	2.00
α -PiHP	3.676	0.9922	2.11	9.56	0.06	0.15	2.07	3.16	3.49	3.50	1.45	-1.10
	4.725	0.9951	1.67	7.88	0.43	0.45	1.59	2.94	2.00	2.76	-3.47	1.2.0
buphedrone	7.193	0.9928	2.02	9.23	0.31	0.35	1.13	4.38	1.80	2.80	-1.85	1.6.0
	7.997	0.9917	2.17	9.82	0.45	0.47	2.30	4.99	3.10	3.13	0.74	1.00
dibutylone	14.49	0.9939	1.86	8.64	0.13	0.16	1.37	2.75	1.00	1.30	1.77	0.70
	15.78	0.9922	2.11	9.57	0.06	0.11	1.14	2.76	4.55	4.60	3.46	-1.00
DMC	4.112	0.9901	2.38	10.54	0.24	0.28	2.01	5.83	0.35	1.30	4.54	1.40
	4.166	0.9923	2.10	9.53	0.51	0.98	0.40	5.66	2.60	2.61	1.35	-0.80
ethylone	22.35	0.9925	2.07	9.43	0.06	0.11	1.62	4.02	1.16	1.20	3.03	1.40
	21.98	0.9924	2.07	9.45	0.04	0.11	1.47	3.83	1.20	1.58	1.90	0.10
MDBD	12.98	0.9978	1.11	5.55	0.25	0.27	1.10	5.98	0.40	3.03	0.89	1.20
	13.51	0.9978	1.11	5.55	0.26	0.28	1.50	4.11	1.40	1.49	1.37	1.80
MDPHP	14.94	0.9981	1.04	5.23	0.14	0.21	0.40	4.89	0.96	4.91	-0.05	1.00
	15.23	0.9977	1.14	5.67	0.30	0.35	0.56	4.32	2.60	4.56	0.16	0.60

Substance	Linearity		Sensitivity in mg/L		Precision						Trueness	
	slope	R ²	LOD	LOQ	RSD time in %		RSD area in %				Bias in %	
					intra-day	inter-day	QC1		QC2		QC1	QC2
					intra-day	inter-day	intra-day	inter-day	intra-day	inter-day	QC1	QC2
methylone	23.01	0.9966	1.68	7.96	0.06	1.60	0.76	5.47	1.71	2.43	1.66	0.30
	23.18	0.995	1.65	7.8	0.03	1.67	0.22	2.09	1.10	3.10	2.22	0.11
methedrone	14.83	0.9976	1.71	5.81	0.12	1.65	0.24	4.60	2.30	3.33	1.72	2.00
	15.33	0.9966	1.39	6.76	0.09	1.62	0.93	5.32	1.10	5.10	1.39	0.20
NEC	17.64	0.9937	1.89	8.75	0.38	1.18	0.22	5.54	3.18	3.20	-0.58	0.70
	16.97	0.9967	1.36	6.64	0.48	1.19	0.25	4.54	2.70	2.89	0.50	1.80
NEH	8.74	0.993	2.31	9.64	1.03	1.42	1.10	3.78	1.24	3.25	0.87	0.20
	8.3355	0.9905	2.33	10.3	1.23	1.59	1.99	4.99	0.80	3.79	0.35	1.40

Table 6-4 Validation data of the high-throughput method with the use of internal standard in terms of linearity, sensitivity, precision and trueness (QC1 = 0.01 mg/L and QC2 = 0.05 mg/L) determined for each enantiomer of synthetic cathinone derivatives

Substance	Linearity		Sensitivity in mg/L		Precision				Trueness			
	slope	R ²	LOD	LOQ	RSD time in %		RSD area in %		Bias in %			
					intra-day	inter-day	intra-day	inter-day	QC1	QC2		
3-CMC	7.596	0.9966	1.87	8.57	0.25	0.18	0.55	4.59	1.4	4.32	-0.41	4.00
	8.745	0.9936	2.60	10.43	0.25	0.19	1.65	3.46	0.32	3.11	-3.74	-2.50
3-MMC	9.628	0.9944	1.71	8.15	0.42	0.36	5.24	6.41	3.58	4.58	-0.99	4.24
	9.309	0.9936	1.19	8.82	0.41	0.35	2.17	5.24	2.71	6.86	0.59	-4.10
4-Cl-pentedrone	6.115	0.9966	1.38	6.72	0.46	0.44	2.56	3.56	0.50	2.93	3.34	0.40
	6.936	0.9900	2.39	10.57	0.44	0.48	0.40	1.40	1.70	4.14	2.52	2.40
α -PiHP	4.111	0.9986	2.31	10.32	0.36	0.40	2.48	4.24	0.90	5.66	-4.6	2.30
	4.999	0.9950	1.69	7.98	0.51	0.50	1.51	3.03	0.20	3.56	1.28	2.80
buphedrone	12.713	0.9929	2.01	9.21	0.46	0.47	0.83	1.76	1.20	2.40	1.72	-0.60
	13.193	0.9901	2.37	10.52	0.49	0.48	0.82	2.35	1.20	4.22	-1.40	-1.40
dibutylone	13.525	0.9979	1.08	5.43	0.37	0.44	1.51	6.88	0.50	5.55	4.21	-4.40
	13.827	0.9989	0.80	4.11	0.22	0.23	1.51	6.88	0.50	5.55	0.13	-4.40
DMC	8.007	0.9965	1.40	6.80	0.24	0.30	1.24	2.34	0.40	2.88	4.08	1.80
	9.55	0.9905	2.32	10.35	0.30	0.36	0.70	1.63	0.40	2.88	4.08	1.70
ethylone	5.786	0.9944	1.78	8.32	0.82	0.92	1.02	2.03	0.98	1.24	1.56	2.60
	5.136	0.9953	1.63	7.71	0.88	1.03	1.32	2.56	1.54	2.90	1.09	1.40
MDBD	16.416	0.9952	1.65	7.82	1.00	0.24	1.82	2.34	1.90	2.50	0.30	2.30
	17.17	0.9928	2.02	9.23	0.96	0.27	1.72	2.22	1.62	3.10	1.40	1.70
MDPHP	15.342	0.9993	0.64	3.35	0.38	0.41	1.61	6.96	1.20	2.66	1.65	2.00
					0.34	0.36	1.49	4.65	0.80	3.47	-2.22	1.20

Substance	Linearity		Sensitivity in mg/L		Precision						Trueness	
	slope	R ²	LOD	LOQ	RSD time in %		RSD area in %		Bias in %			
					intra-day	inter-day	QC1	QC2	QC1	QC2		
methyldone	8.035	0.9952	1.65	7.83	0.32	0.40	0.26	1.27	0.80	2.84	1.31	-1.60
	9.934	0.9971	1.28	6.30	0.40	0.48	2.16	3.16	0.10	3.95	-2.40	-3.00
methedrone	7.904	0.9913	2.22	9.99	0.67	0.70	2.43	3.44	2.02	3.00	1.60	1.68
	7.103	0.9936	1.90	8.81	0.70	0.77	4.32	4.98	4.56	4.87	1.30	-1.30
NEC	7.160	0.9926	2.05	9.35	1.00	1.51	2.32	4.92	1.78	3.01	2.50	1.50
	9.460	0.9928	2.02	9.26	1.13	1.72	2.45	3.93	1.40	3.09	-2.09	-3.00
NEH	8.085	0.9950	1.69	7.97	0.44	0.27	5.52	3.27	3.50	6.68	-3.09	3.60
	8.116	0.9953	1.63	7.76	0.49	0.31	1.68	4.83	1.10	6.47	2.96	-0.30

6.4.4 Applications

6.4.4.1 Extension to other synthetic cathinone derivatives

The range of substances was extended by analysing 22 further synthetic cathinone derivatives from seizures by separate injections of 3,4-DMC, 4-BMC, 4-CL-PVP, 4-CMC, 4M- α -PPP, 4-MEC, 4-MMC, α -PHP, butylone, ephylone, methcathinone, NEHP, NEMNP, 4-CBC, 4-CEC, α -PBP, α -PVP, flephedrone, MDPV, mexedrone, pentedrone (for structures see Table 6-1). These samples were exclusively white powders without cutting agents present. The samples were analysed by both methods, migration time and resolution data are given in Table 6-5.

Table 6-5 Enantiomeric excess *ee*, migration times and their corresponding chiral resolution *R* of synthetic cathinone derivatives in 22 seized samples for screening and high-throughput method

Substance	ee in %	Screening method			high throughput		
		Time in min		R enantiomers	Time in min		R enantiomers
3,4-DMC	0.86	11.43	14.15	8.48	2.46	2.76	2.86
4-BMC	2.74	11.31	11.48	2.39	2.94	3.00	0.71
4-Cl-PVP	0.27	14.14	14.62	2.00	4.32	4.48	1.02
4-CMC	0.34	13.17	13.96	9.32	3.58	3.88	3.01
4-M- α -PPP	1.63	12.51	13.95	14.13	2.83	3.24	2.94
4-MEC	0.00	14.09	15.53	5.38	3.53	4.02	2.91
4-MMC	2.89	13.56	14.20	4.79	3.35	3.58	2.14
α -PHP	0.29	15.63	18.16	22.02	4.96	6.29	7.40
α -PPP	0.40	14.66	16.18	12.79	5.02	6.32	10.94
butylone	0.42	11.21	11.83	3.59	2.54	2.74	1.58
ephylone	0.69	13.81	15.83	21.51	3.18	3.62	2.88
methcathinone	0.30	15.31	16.61	7.67	3.80	4.18	2.72
NEHP	2.20	18.43	20.53	19.53	5.93	7.01	4.50
NEMNP	0.03	14.96	19.97	46.73	4.16	6.21	15.10
4-CBC	0.98	14.99	15.15	1.75	4.02	4.22	1.04
4-CEC	0.58	16.12	16.37	1.76	3.71	3.96	1.45
α -PBP	1.86	12.31	12.81	4.83	2.76	2.88	1.17
α -PVP	0.43	15.20	16.05	7.09	3.42	3.63	2.20
flephedrone	1.08	17.95	22.72	39.02	4.57	6.07	10.04
MDPV	1.93	11.44	11.89	5.56	2.62	2.73	1.79
mexedrone	1.19	21.79	29.40	39.55	5.13	7.26	13.02
pentedrone	0.40	17.97	23.67	43.90	4.32	6.03	14.86

Every racemate was separated into its enantiomers with a migration time window of 11.1-29.4 min for the screening method and 2.4-7.2 min for the high-throughput method. The reduction of migration times in case of short-end injection is accompanied with a loss in resolution by a factor of 3 (0.7-15.1 compared to 1.7-46.7 for the screening method). The high-throughput method shows limitations with regard to the simultaneous analysis of more than one synthetic cathinone derivative. Here, the screening method is the analytical technique of choice: In Figure 6-3, successful separation of the chiral separation of regioisomers is demonstrated including 3-CMC, 4-CMC and 3-MMC and 4-MMC.

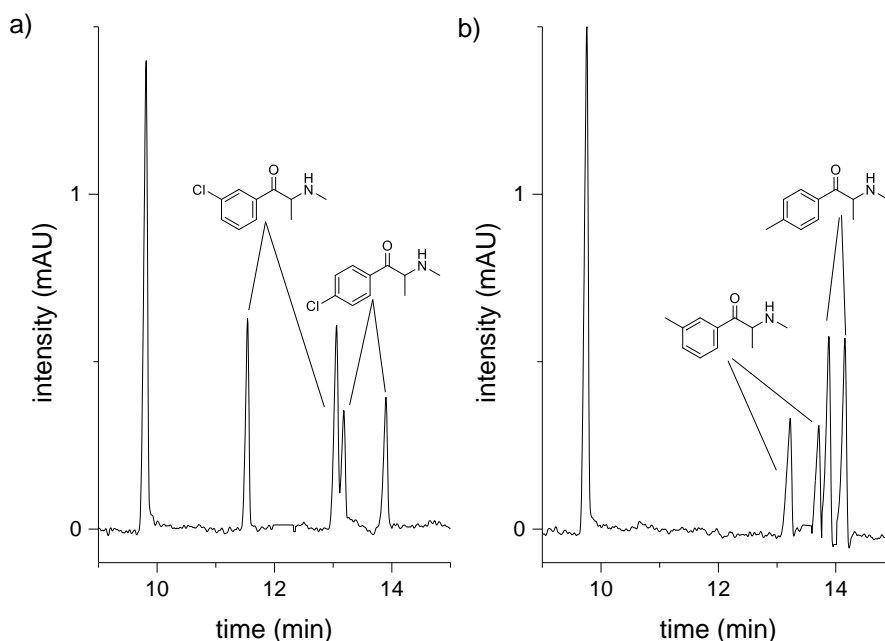


Figure 6-3 Electropherograms of a) (R/S)-3- and (R/S)-4 CMC and b) (R/S)-3- and (R/S)-4-MMC with screening method; long end-injection (50 mbar \times 5 s), -20 kV, detection wavelength 230 nm, sample concentration of 50 mg/L in water/phosphate buffer (2:8)

6.4.4.2 Exclusion of matrix effects by cutting agents

Most cathinones are seized as powders and some of them contain cutting agents, mostly lidocaine, benzocaine and caffeine.^{21,112,113,309} Both, the screening method and the high-throughput method were not impaired by these compounds as demonstrated by spiking experiments (see Figure 6-4). Migration times of lidocaine and benzocaine were 36 and 21 min so that they could be identified with the same method. In contrast, caffeine, being neutral in the BGE chosen, was detected at 54 min. Presumably, the complexation with CD is very weak for this very polar compound. The possibility of analysing synthetic cathinone derivatives simultaneously with their cutting agents was proven by the analysis of three mixtures which were taken from criminal cases: Figure 6-4 shows the electropherograms of Mixture 1 (methyldone and α -PBP), Mixture 2 (methyldone, MDPV) both with benzocaine as cutting agents and Mixture 3 (methyldone, α -PIHP, MDPHP). Clearly the identification of all

synthetic cathinone derivatives was possible via their migration times without interference from cutting agents.

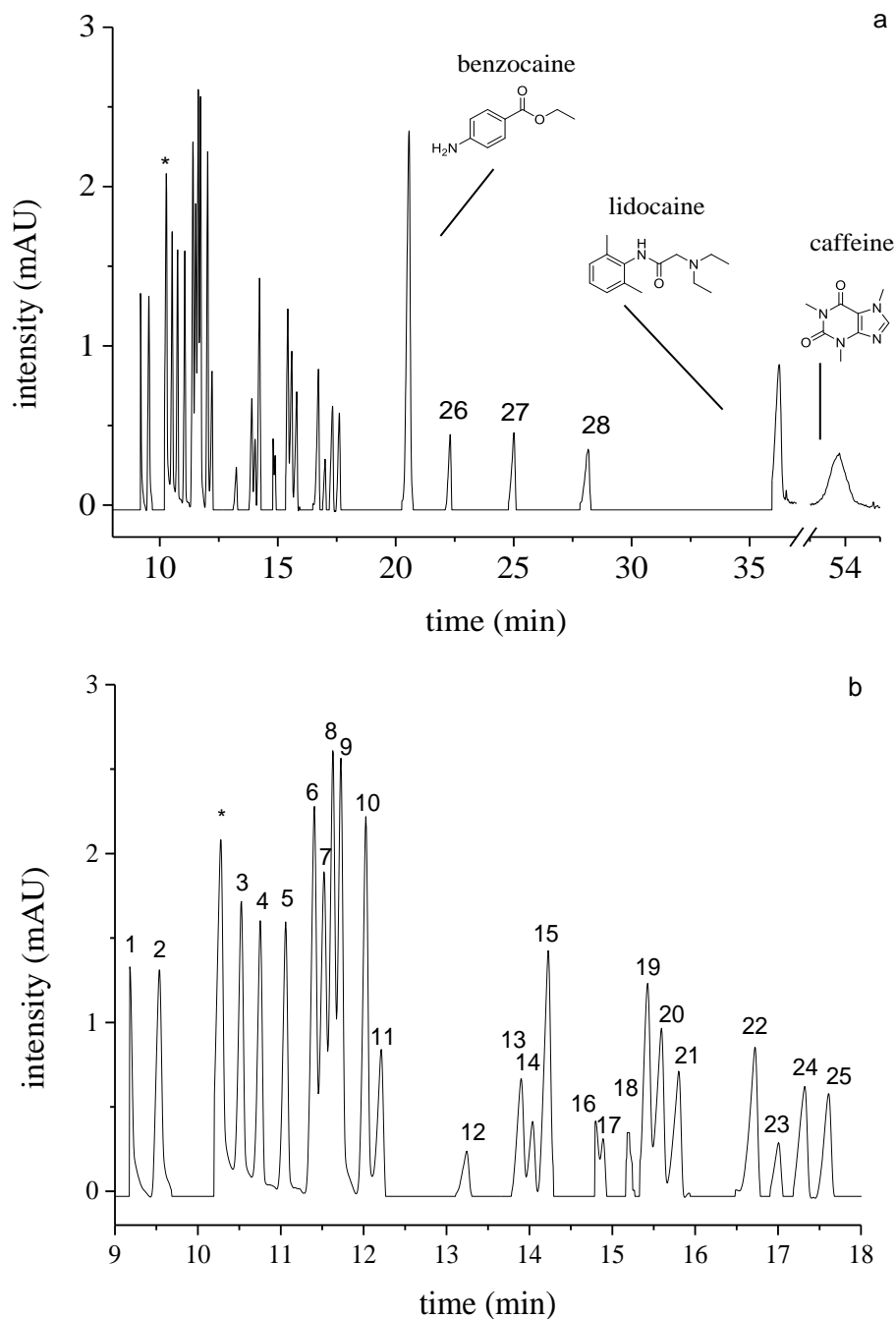


Figure 6-4 Electropherogram of a) 14 racemic mixtures of synthetic cathinone derivatives using screening method (1+2 = (R/S)-MDBD, 3+6 = (R/S)-dibutylone, 4+5 = (R/S)-mephedrone, 7+10 = (R/S)-methytlone, 8+9 = (R/S)-ethylone, 11+13 = (R/S)-3-CMC, 12+23 = (R/S)- α -PiHP, 14+17 = (R/S)-DMC, 15+19 = (R/S)-MDPHP, 16+18 = (R/S)-3-MMC, 20+22 = (R/S)-NEC, 21+24 = (R/S)-buphedrone, 25+26 = (R/S)-4-Cl-pentedrone, 27+28 = (R/S)-NEH) with possible cutting agents benzocaine, lidocaine and caffeine with following running conditions: 25 mM phosphate buffer (pH 2.3) with 2.5 % HS- β -CD with * internal standard oCPP and b) detailed view of migration time window 9-18 min. long end-injection(50 mbar \times 5 s), -20 kV, detection wavelength 230 nm, sample concentration of 50 mg/L in water/phosphate buffer (2:8)

6.4.4.3 Applicability to other substance classes

The developed screening method represents a versatile analytical tool for chiral separation of racemic mixtures of substances. In forensic investigation, the suitability of a screening method for more than one substance class is preferable. For this reason the enantioselective separation of further substance classes including piperazines and other phenethylamines was successfully tested also for methamphetamine, ephedrine and pseudoephedrine in less than 14 min, as well as for regioisomers of mCPP including pCPP and oCPP in 11 min. The corresponding electropherograms are shown in Figure 6-5. Thus, due to the use of highly charged CDs, the developed method has a very broad application range for forensic drug analytics.

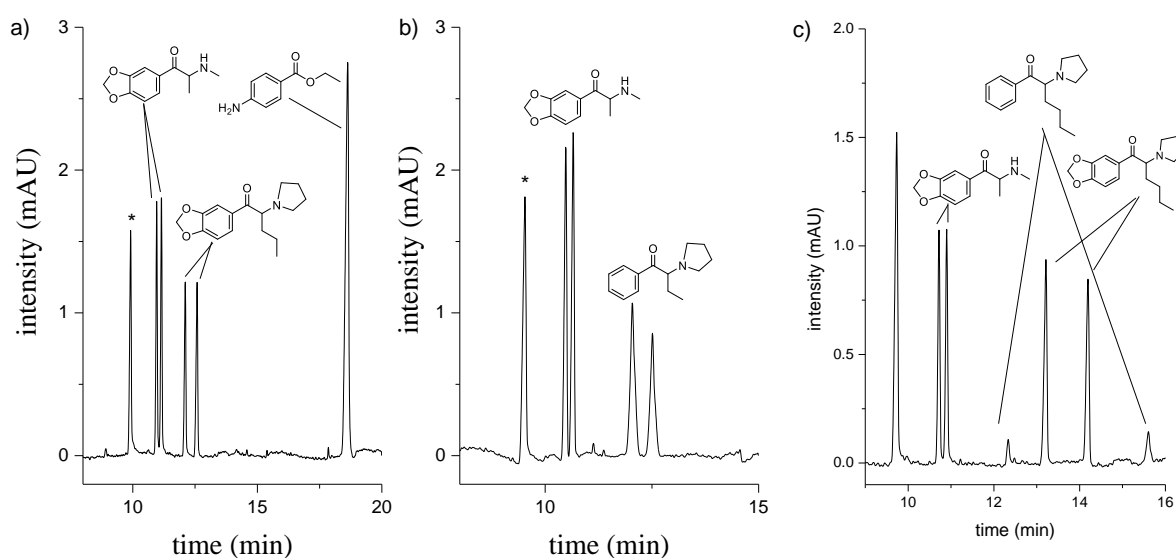


Figure 6-5 Electropherograms of seized samples measured with the screening method including a) Mixture 1 ((*R/S*)-methyldone, (*R/S*)-MDPV and benzocaine), b) Mixture 2 ((*R/S*)-methyldone and (*R/S*)- α -PBP) and c) Mixture 3 ((*R/S*)-methyldone, (*R/S*)- α -PIHP, (*R/S*)-MDPHP) with * internal standard, long end-injection (50 mbar \times 5 s), -20 kV, detection wavelength 230 nm, sample concentration of 50 mg/L in water/phosphate buffer(2:8)

6.5 Discussion

6.5.1 Interaction of synthetic cathinone derivatives with HS- β -CD

With an understanding of the interaction of specific structural elements of the cathinones, hints on the identification can be gained from migration times. β -CDs are cyclic oligosaccharides consisting of seven glucopyranose units with a truncated cone providing a hydrophobic cavity.³²² The glucose units are arranged in chair conformations leading to special arrangement of functional groups in the CD molecule. The secondary hydroxyl groups are located on the interior, the primary hydroxyl groups on the exterior of the cavity.³²³ Thus, the outer cavity is hydrophilic, making the CDs soluble in aqueous solution, while the inside cavity is apolar and hydrophobic (compared to water). Modifications of the CDs induce

different selectivity in enantiomeric separation. Highly sulphated β -cyclodextrins are negatively charged in aqueous buffers. The interaction of synthetic cathinone derivatives with HS- β -CD is often based on the insertion of their benzene ring into the CD cavity.³²⁴ Among all 36 chiral cathinones studied here, MDBD, an MDMA derivate with a 3,4-methylenedioxy substitution on the benzene ring, shows the strongest interaction with the chiral selector and thus the shortest migration time (see Figure 6-2). Next, the structurally related synthetic cathinone derivatives butylone, dibutylone, methylone, ethylone and ephylone are detected, also with a 3,4-methylenedioxy substitution on the benzene ring. The substance 3,4-DMMC shows similar migrations times with a 3,4-dimethyl substitution on the benzene ring (Table 6-2 and Table 6-5). Obviously, both the degree and the position of substitution is decisive for the interaction with the CD. Substances with 1,4-chloro- and 1,4-methyl-substituted benzene rings migrate after 3,4-di-substituted substances (Figure 6-2). Another interesting point is the consideration of different halogenated substitutions on the benzene ring. In case of bromo, chloro and fluoro substituents, the molecular size seems to play a role as visible in the migration order 4-BMC (bromo) < 4-CMC (chloro) < flephedrone (fluoro) with otherwise similar structures (see Table 6-2 and Table 6-5). Longest migration times and thus comparatively weak interaction with CDs were observed for synthetic cathinone derivatives without a substitution on the benzene (see Figure 6-2).

Regarding the substitution on the α -carbon atom (see position R4 in Table 6-1) it can be observed that the longer the alkyl-chain on the α -carbon the lower is the interaction strength between the CD and the analyte with migrations times of NEH (23.5 and 27.1 min), 4-Cl-pentredone (16.9 and 21.1 min) and NEHP (18.4 and 20.5 min). 4-Cl-pentredone represents the only substance with a propyl group on the α -carbon (see Table 6-1). Mexedrone and methedrone have a similar chemical structure with an ether group on the position R4 (mexedrone) and R3 (methedrone) and mexedrone migrates twice as long as methedrone. Substances with 1,3-substituted benzene rings such as 3-CMC or 3-MMC migrate faster than their 1,4-substituted counterparts such as 4-CMC and 4-MMC (see Figure 6-3). Whether the nitrogen atom is present in a pyrrolidino ring or not does not seem to influence CD interaction as related cathinones can be observed over the whole migration time window (see Table 6-2 and Table 6-5).

Regarding the interaction between enantiomer pairs and HS- β -CD on the basis of their resolution values, several factors were involved such as hydrophobicity, configuration on the β -carbon, configuration of the benzene ring, hydrogen bonding, dipole interactions and Van der Waals forces. Maximum apparent mobility differences and hence maximum resolution between the enantiomer pairs were investigated for benzene-cathinones, methylphenyl-cathinones and chloro-phenyl-cathinones which possess an alkyl substitution ($\geq C_2H_5$) on the β -carbon atom (see Table 6-1). NEMNP ($R = 46.7$), mexedrone ($R = 39.5$), 4Cl-pentredone ($R = 39.2$) pentredone ($R = 43.9$) and α -PIHP ($R = 35.7$) show the highest resolution values

due to alky-chain and thus increased lipophilicity (see Table 6-2 and Table 6-5). These substances show also the highest migration times thus, the migration time is directly connected to enantiomeric pairs resolution (see Table 6-2 and Table 6-5). Iwata et al. discussed the influence of ring-substitution and configuration that occurs on the β -carbon on the basis of amphetamine type stimulants. α -PIHP ($R = 35.7$) and α -PHP ($R = 22.0$) represent stereoisomers with different alkyl substituents on the β -carbon. The higher the observed degree of branching the higher the resolution of an enantiomeric pair. Resolution values decrease to $R = 5.5-22.02$ with synthetic cathinone derivatives differing in the substitution on the β -carbon $\geq C_2H_5$ in combination with a pyrrolidino ring including MDPV, α -PVP, MDPHP and α -PHP. The lowest resolution values were achieved for synthetic cathinone derivatives which possess an hydrogen atom on the β -carbon. Especially chloro-ring-substituted substances show resolutions < 2 followed by methyl-, methylenedioxy- and substances without ring-substitution ($R = 3.5-8.5$ when only one methyl-group is attached to the nitrogen-atom). In case of methyl-substitution on R1 and R2 like in dibutylone and DMC, resolution values rise to ~ 10 . Thus, configuration on R1 and R2 change the lipophilicity of the substance and the inclusion of the molecules in the HS- β -CD.

To summarise, the substitution on the benzene ring of synthetic cathinone derivatives seems to be most important for the interaction strength with the CD visible in high migration times, whereas the substitution on the β -carbon atom has more strongly influences chiral separation selectivity.

6.5.2 Comparison of the screening method and high-throughput method with literature methods

In this study, chiral separation of synthetic cathinone derivatives (Table 6-1) was performed with two different methods in CE-DAD, first, using conventional long-end injection in a screening method (Figure 6-1 and Figure 6-4) and second, a short-end injection method in a high-throughput method (Figure 6-2) for the fast determination of the enantiomeric excess. The results for both methods are summarised in Table 6-2. Optimal resolution and peak shape for all investigated synthetic cathinone derivatives was obtained with an additive concentration of 2.5 % HS- β -CD in 25 mM phosphate buffer (pH 2.3) with an analysis time of 27 min using the screening method. A slightly higher concentration of HS- β -CD of 3.5 % and in 50 mM phosphate electrolyte (pH 2.3) in combination with the short-end injection mode revealed a strongly reduced analysis time of only 6 min and thus gave rise to a high-throughput for chiral analysis of single enantiomer pairs.

The screening method has benefits in its improved chiral resolution and the possibility to simultaneously analyse more than one synthetic cathinone derivative. In addition, the chiral separation of enantiomers of structurally closely related substances like regioisomers which differ only in the C4 or C5 position of a halogen-atom in a pentyl-chain was achieved. The

number of theoretical plates was about a factor 21 smaller with the screening method to the high-throughput method.

The advantages of the high-throughput method lie in the possibility to use a BGE of higher ionic strength and reduction of the EOF resulting in a faster analysis time, improved peak symmetry by enhanced stacking effects and by minimisation of sorption to the capillary wall and in decreased buffer depletion effects leading to higher precision. Both CE-DAD methods were able to determine the enantiomeric excess but the high throughput method allowed faster analysis (5.3 fold) and superior peaks symmetries. In Table 6-2 and Table 6-5 the migrations times and the resolution are given for various enantiomer pairs. The current stayed nearly constant during analysis, whereas in long-end injection, the current continuously increased by up to 10 μA over prolonged injection sequences (> 5 measurements).

The use of an internal standard was shown to greatly improve migration time and peak area precision by a factor of 10 and 5, respectively. Regarding method validation, the calculated peak area and migration time precisions were nearly equal for both methods (see Table 6-4 and Table 6-5). Reliable results were also achieved for peak areas with $\text{RSD} \leq 7.0\%$ for intra- and inter-day experiments in both CE-DAD methods. Likewise, LODs and LOQs were nearly equal for both methods (see Table 6-3 and Table 6-4).

The broad applicability of the developed methods was proven by the successful analysis of 22 casework samples (results given in Table 6-5). In case of samples with only one active ingredient, the high-throughput method is preferred for qualitative analysis with migration times below 7.3 min and enantiomeric resolutions of 0.7-15.1. The high-throughput method, however, requires a prior identification of the cathinone as comigration of different cathinones are possible (see Table 6-2 and Table 6-5). Especially, overlapping signals were observed for the regioisomers 3-CMC, 4-CMC, 3-MMC and 4-MMC and also other synthetic cathinone derivatives like methedrone and methylone, α -PiHP and DMC, ethylone and 3-MMC and NEC and buphedrone (Table 6-2 and Table 6-5). Thus, the analysis of unknown casework samples with more than one active ingredient or the presence of a cutting agent is only possible with long-end injection (Figure 6-4 and Figure 6-5). With this method, the regioisomers of 3-CMC, 4-CMC, 3-MMC and 4-MMC were well separated. To the best of our knowledge, no further publication demonstrated a method capable of the simultaneous chiral separation of 14 or more different racemic mixtures of synthetic cathinone derivative. Only Merola et al.¹⁵⁸ showed the chiral separation of 12 synthetic cathinones within 18 min using CE-DAD. In our study, we also demonstrated that the method's selectivity is high enough to enable the analysis of casework samples with bulking agents.

The broad applicability of the newly developed screening method was demonstrated not only for synthetic cathinone derivatives but also for other substance classes including the chiral separation of methamphetamine, ephedrine, pseudoephedrine and oCPP, mCPP and pCPP is possible (see Figure 6-6).

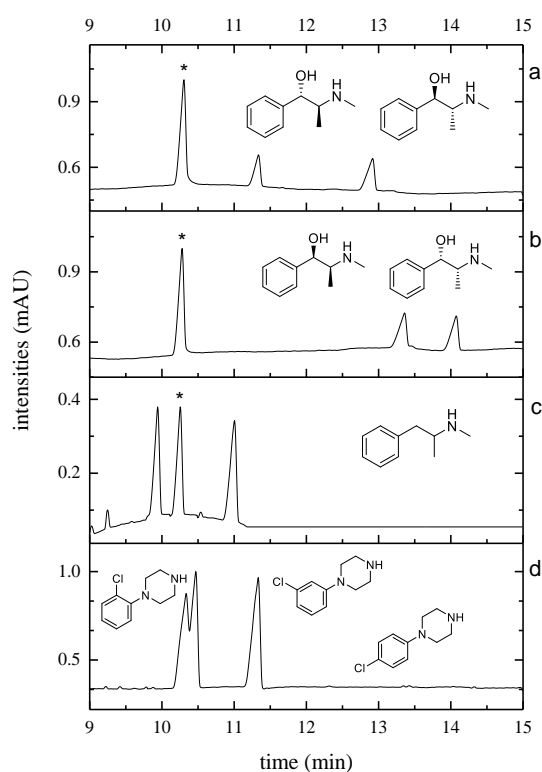


Figure 6-6 Stacked electropherograms of the enantioselective separation of a) (R/S)-pseudoephedrine, b) (R/S)-ephedrine, c) (R/S)-methamphetamine and d) mCPP, oCPP, pCPP with * internal standard using the screening method, long end-injection (50 mbar \times 5 s), -20 kV, detection wavelength 230 nm, sample concentration of 50 mg/L in water/phosphate buffer (2:8)

Usually, methods are published for single substance classes, only. The simultaneous chiral separation of methamphetamine, ephedrine and pseudoephedrine was reported using CD as chiral selector for CE-DAD analysis with migration times from 15 to 32 min.³²⁵⁻³²⁸ or within 13-17 min using a cationic coating.³²¹ Chiral GC-MS analysis after derivatisation to diastereomer or with chiral stationary phases was shown with retention times of up to 15 min, however with higher needs for sample preparation than in our CE-UV method.^{329,330} Puetz et al. described baseline-separation of the three positional isomers of 1-chlorophenylpiperazine by CE-ESI-MS utilising the chiral selector 2-hydroxypropyl-beta-cyclodextrin with migration times of 10-13 min. The application of non-volatile chiral selectors as additives in CE-ESI-MS contributes to loss of sensitivity due to ion suppression during the electrospray process and cause contamination of the mass spectrometer.³³¹ With the broad applicability and selectivity, it was possible to characterise 20 synthetic cathinone derivative enantiomers pairs not covered by any other publication. In this study the ease of sample treatment and preparation of chiral buffer solutions without disturbing effects during detection makes the procedure highly effective for large sample cohorts. The advantage of the high throughput method compared to other chiral methods published is the possibility to estimate the enantiomeric excess of enantiomer pairs in less than 6 minutes

when the identity of the cathinone is known. Other publications reported migration times for synthetic cathinone derivatives between 10-20 min with CE applications^{154,157,158,160} and 12-85 min for LC methods (studies including more than one substance) and 12-40 min for GC applications. In addition, with the CD just added to the BGE, the CE-DAD method is comparatively cheap without the need for chiral stationary phases. Direct analysis without the need for derivatisation as necessary for GC is possible.

The need to use an internal standard was demonstrated by the determination of precision: RSD-values for inter-day precision rose by a factor of 5 for area values and by a factor of 10 for migration time values without the usage of oCPP. Overall, acceptable figures of merit were obtained. The enantiomeric excess was determined for all seized or purchased synthetic cathinone derivatives, which demonstrated that they all exist as (near-)racemic mixtures (see Table 6-2 and Table 6-5) with an enantiomeric excess (ee) in the range of 0.01-3.16 %. Considering the production conditions of synthetic cathinone derivatives, the formation of racemic or enantiopure products is possible. Enantiomeric excess values < 4 % represent a negligible deviation mainly caused by random errors.

6.6 Conclusion

In this study, the successful development of a screening and a high-throughput method for the chiral separation of 36 synthetic cathinone derivatives was demonstrated. Optimal separation conditions were achieved with 2.5 % HS- β -CD in 25 mM phosphate buffer (pH 2.3) for the screening method and 3.5 % HS- β -CD in 50 mM phosphate buffer (pH 2.3) for the high-throughput method. The latter allowed ee determination in less than 6 min, due to the use of short-end injection. The reliability of both methods was proven by figures of merit on linearity, intraday and interday precision, sensitivity, LOD and LOQ, and accuracy. Not only the inclusion of newly emerged synthetic cathinone derivatives but also the structural diversity within this substance class was in the focus of this study. The utility of the approach was demonstrated by the successful analysis of 3 seized samples with mixtures of synthetic cathinone derivatives as active ingredients in the presence of bulking agents. The high-throughput method was constructed for the fast analysis of samples with only one identified active ingredient in the sample. The time reduction was obtained at the cost of separation efficiency and resolution. The screening method had a longer analysis time but is better suited for the analysis of seized samples containing more than one active ingredient or cutting agents. The interaction of HS- β -CD with possible substituents concerning the benzene ring, the β -carbon or the nitrogen atom was discussed. The substitution on the benzene ring was shown to be a decisive parameter for the strength of the interaction of the analyte with the chiral selector. In forensic applications, this represents a helpful tool to characterise an unknown substance in order to predict the approximate structure of the substance by its migration behaviour.

7 Comparison of all analytical techniques applied

7.1 On site analysis - best choice for a presumptive test

The rapid emergence of novel NPS products requires the development of rapid and simple drug detection methods.³⁴ There is a growing number of police agencies, prisons or other institutions being interested in on-site drug testing techniques.^{34,250} The choice of a suitable analytical technique depends on the application field. For the forensic sector, the advantages and limitations of different presumptive tests were described on the basis of defined criteria including analysis time, handling and work safety, sensitivity, specificity and identification power, selectivity, matrix tolerance, costs and the successful application.

The main challenge for presumptive drug tests is the dynamically changing NPS-market and the resulting high diversity of new substances with similar chemical structures. To ensure the actuality of those tests, a constant production of new rapid drug tests and the maintenance of analytical databases are inevitable.

Table 7-1 shows the analytical techniques and summarises their performance with regard to different criteria. In general, colour coding tests, immunoassays or Raman and IR spectroscopy were applied for roadside drug controls or drug controls in public institutions like airports.^{87,137} TLC is frequently used in laboratories of criminal investigation institutions. In Chapters 2 and 4, ion mobility and THz spectroscopy was introduced as an alternative presumptive test for NPS, which is rarely applied in drug testing and is limited to the detection of classical drugs. For NPS analytics, there are no publications and experimental data on the application of THz radiation. In this work, a novel approach for uncovering drug trafficking was tested: the detection of synthetic cannabinoids in postal packages using THz spectroscopy. The time domain and frequency domain spectra of 15 synthetic cannabinoids were tested (Table 4-3). The spatial distribution of the illicit drugs concealed in an envelope was obtained from terahertz multispectral transillumination images. To avoid imaging the whole packaging material, a pre-screening step was proposed, by first detecting the presence of powders in the envelopes and then defining the grid of measurement points.

Table 7-1 Properties of field devices for presumptive drug testing

Immuno-assays	Colour coding	TLC	IMS	Raman	IR	THz
Analysis time (including sample preparation)						
★★★★	★★★★★	★	★★★★★	Pure powders Matrices: ★★★	★★★★	Pure powders ★★
Handling and work safety						
★★★★★	★★★★★	★	★★★★	★★★★ Laser application		★ Not portable
Sensitivity						
★★★★ ~ng/mL	★★★★ ~ng/mL	★★★★ ng range	★★★★★ ng-pg range	★★ Several mg	★★★ Several mg	★ Several mg
Specificity (Need of reference standards)						
★★	★	★★	★★★	★★★★★	★★★★	★★
Selectivity						
★★★★	★	★★★★	★★★★	★★★	★★★	★
Matrix tolerance						
★★ Body fluids	★ Pure powders	★★ Herbal mixtures, body fluids	★★★★ Herbal mixtures, papers, foods, cosmetic, several fluids	★★★ Analysis through packaging material like glass or plastics; Pure powders, liquids	★★ Pure powders, liquids	★ Pure powders
Identification – applicability to closely related substances						

Immuno-assays	Colour coding	TLC	IMS	Raman	IR	THz
★	★	★	★★★	★★★★★	★★★★★	★★
Cost of the device						
3-10 €	5-10 €	-	40.000 €	70.000 €	50.000 €	250.000 €
Successful application						
Preliminary testing; Body fluids	Preliminary testing; Only powders	Suitable for laboratories Purification step for subsequent analysis e.g. NMR	Analysis in/on several matrices especially papers, herbal mixtures	Powders; Analysis of unknowns, Hazardous materials	Powders; Analysis of unknowns	Powders; Benchtop device, not for on-site analysis

The portable IMS was shown to be a powerful analytical method for the application in prisons to uncover NPS drug trafficking. The new IMS approach presented is an effective and non-destructive presumptive test with a direct indication of the presence of synthetic cannabinoids. IMS was shown to allow a fast operation with a simple sample application by wiping the surface of a sample with a swab without any further sample preparation, even when rather complex matrices are present. In this study, all synthetic cannabinoids in demand were successfully detected by IMS when present as single substances, independent of the matrix. In contrast to other presumptive tests, the developed database is easily expendable to newly occurring narcotics.

What opportunities or limitations do THz spectroscopy and IMS offer for the analysis of NPS in comparison to other presumptive tests like, immunoassays, colour coding tests, TLC, IR or Raman? As summarised in Table 7-1, the techniques previously mentioned are all easy to handle and thus, they do not require special analytical expertise and skills and can be applied by e.g. prison or police officers. An exception is given by the performance of TLC due to the need of basic analytical skills and specific laboratory equipment and chemicals. All techniques are portable and suitable for on-site analysis except for TLC and the THz spectrometer which is not portable and thus bound to firmly installed workplaces like the laboratory or mail distribution centre. Regarding health and safety, laser-based devices like Raman could include class 3b or 4 lasers which are notifiable and require a laser protection officer. Here, further technical instruction is inevitable to avoid health risks. Some portable

IMS use radioactive sources for the ionisation process which requires a radiation protection commissioner. In contrast, in this study, the portable IMS used a corona ionisation with battery systems to maintain the attractiveness of the IMS as a handheld device.

The analysis time is another important aspect for selecting the most suitable presumptive test. Colour coding tests and IMS have the shortest analysis times with a direct indication of the presence of analyte. IMS enables a fast operation (10 sec) with a simple sample application by wiping the surface of a sample with a swab without any further sample preparation.²⁴⁸ For immunoassays, the reaction of a single antibody binding site with the antigen takes 8-10 min to reach equilibrium.¹⁷⁵ In TLC, the sample preparation steps and the separation process take 15-30 min depending on the solvent and the plate material.^{2,27} For Raman, IR or THz spectroscopy, the direct measurement of a powder is possible and takes only a few minutes including a subsequent library search. Some matrices may necessitate a further extraction process.^{2,62,63}

The presumptive tests discussed cover a wide range in terms of sensitivity (see Table 7-1): Immunoassays, colour coding tests and TLC are very sensitive and detect analytes in extracts at concentrations of 10-50 ng/mL. IMS is also a sensitive technique and the LODs estimated for the synthetic cannabinoids in this study are in the range of 0.7-3.6 ng. The high sensitivity also provides some limitations including 1) a limited dynamic response range, 2) the ease of contaminations with long residence times in the spectrometer, and 3) concentration-dependent response characteristics (Chapter 2.4.2).

In comparison, spectroscopic methods require several milligrams of the sample to produce spectroscopic data with an acceptable S/N-ratio. IR is more sensitive than Raman spectroscopy followed by THz spectroscopy. However, IR and Raman devices are very specific due to spectral fingerprinting which allow the approximate elucidation of a chemical substance.⁴⁵ According to the recommendations of the scientific working group for the analysis of seized drugs (SWGDRUG), Raman and IR spectroscopy are category A analytical techniques with maximum discriminating power.⁴⁵ THz-spectroscopy is limited in the applicableness regarding the detection of known substances and the identification of a new substance. In Chapter 4 in Table 4-3, limitations of THz spectroscopy become visible in conjunction with the distinction of structurally closely related substances. Small changes in the structure of NPS do not significantly change the spectra (Figure 4-2).

With regard to specificity, IMS performance is between the one of spectroscopic techniques and colour coding tests and immunoassays. In Chapter 2, it was shown that all synthetic cannabinoids of this study were successfully detected by IMS when present as single substances, independent of the matrix, although some publications reported that analytes with nearly the same chemical structure like the synthetic cannabinoids cannot be distinguished.^{2,181} An unambiguous assignment is not possible with IMS, because it is a preliminary test which gives a hint to a possible active ingredient based on the size and shape of the ion with the reduced mobility as the only parameter available for identification. Colour

coding tests or immunoassays are rapid, sensitive, inexpensive and easy but they lack specificity. There is a risk of false positive results due to cross-reactivity with other non-targeted drugs of similar chemical structure including plant materials, flavours or bulking agents.^{41,43,332} Immunoassays are more specific than colour coding tests due to the antigen-antibody recognition. Moreover, the differences in the chemical structure within one substance class caused by the increasingly diverse NPS-market would require the constant production of new rapid drug tests.³³ There are also practical limitations to these tests, including the risk to produce false positive results due to wrong reagents and a misinterpretation of the resulting colour.

The techniques discussed have one thing in common: the need for reference material. The presumptive tests require information on a substance like its chemical structure, R_f-value, colour changes, K₀-values to guarantee a substance-specific detection. Raman and IR spectroscopy are the only technologies which are able to characterise the chemical structure according to specific bands in a spectrum as shown by the frequency tables in Chapter 3.4.3.

With regard to selectivity, the IMS approach is the most suitable method to analyse mixtures of more than 3 substances (Figure 2-2). Here, the necessary resolution $R > 0.75$ of mobile IMS for identification was estimated to require differences in drift times and reduced mobility values of > 0.15 ms (> 0.013 cm²V⁻¹s⁻¹) (Chapter 2.4.2.2). Smaller differences led to a positive identification only for the substance present at higher concentration. The analysis of mixtures with more than two constituents is challenging for spectroscopic techniques due to overlaying bands in the spectra. TLC is also quite specific and selective and but many of the standards show the same or similar responses (R_f-value and colour) by applying same running conditions.⁴⁴ Some immunoassays or colour coding tests were designed to detect a selection of substances simultaneously. In case of mixtures, immunoassays show different bands of the defined substance. For colour coding tests, the analysis of mixtures is difficult because the resulting colour is not well defined.

Another important point is the matrix tolerance and the resulting applicability of the techniques: Immunoassays are designed to analyse NPS in body fluids like blood,¹²⁷ serum⁴¹ or urine⁴⁰ whereas colour coding tests are dedicated to analyse pure powders. Both techniques are suitable for e.g. police roadside presumptive testing to determine on the one hand if an individual is operating a vehicle while under the influence of a controlled substance or the direct analysis of suspicious substances.³⁴ TLC is applicable to different matrices like herbal mixtures or body fluids after extraction, thus it is often used as a purification step for subsequent identification with e.g. NMR.^{57,58}

Spectroscopic techniques are less matrix tolerant and are primarily applied to powders or liquids. Powders or liquids can be analysed directly provided that there is a relative high concentration of the active ingredient in the sample matrix. The analysis of specific matrices like herbal mixtures requires a further extraction steps. IR-spectroscopy is more sensitive than Raman spectroscopy and with a further extraction step with methanol or acetone, it is possible

to obtain a good IR spectrum after evaporating the extract directly on the ATR diamond cell.^{2,62,63} In Chapter 3.3.2.1, a simple sample preparation technique was developed to extract synthetic cannabinoids from only 100 mg of the plant material using a solid/liquid extraction with dichloromethane followed by precipitation of the active ingredient by the addition of water. Recoveries proved sufficient for subsequent Raman analysis down to a content of 0.5 % synthetic cannabinoid in the herbal matrix. To the best of our knowledge, sample preparation strategies to purify synthetic cannabinoids from the herbal matrix to avoid disturbance of fluorescence in Raman spectroscopy have not been published. The applicability of the presented approach was proven by the analysis of 60 casework samples. A large number of herbal mixtures were investigated to demonstrate the high matrix tolerance of the overall procedure. The extraction process developed is intended to be applied in the laboratory and not for on field drug testing.

In contrast, the low sensitivity of THz analysis was shown to impede the analysis of NPS in different matrices like herbal mixtures, e-liquids or papers as discussed in Chapter 4.4.3. Due to the low amount of active ingredient in the matrix, the generation of spectral features was impossible. THz spectroscopy is better suitable for the detection of pure powders when available in sufficient quantity, e.g. for the security inspection in public institutions like postal facilities to avoid potential health risk by contaminations. But THz spectroscopy show some more limitations including influences of different packaging materials and therefore the attenuation properties of the covering layers,^{291,292} the scattering effects related to the morphology and inhomogeneity of the substance surface,^{288,293} changes in the atmospheric humidity due to strong attenuation properties of water vapor during the measurements²⁹⁴ lead to low reliability of identification of this method.

In comparison to spectroscopic techniques, portable IMS showed high matrix tolerance. In Chapter 2.4.2.3, the successful analysis of synthetic cannabinoids in herbal mixtures, papers, foods and cosmetics was successful, independent of the matrix. The analysis of active ingredients in highly viscous matrices (toothpaste or liquid soap) and medicinal products was challenging due to the poor solubility and inhomogeneous distribution of the NPS in the cosmetic products with their high viscosity. In general, it seems that only liquids with a low viscosity are amenable to the detection of synthetic cannabinoids. To the best of our knowledge, no other presumptive test is able to detect NPS which were impregnated onto a paper in less than 10 seconds. It can easily be used by non-scientists like prison or police officers as no special analytical expertise and skills are required. In contrast to other presumptive tests, the databases of spectroscopic techniques and IMS are easily expendable to newly occurring narcotics and therefore suitable for the detection of NPS.

When selecting a presumptive technique for a specific application area, the costs have to be considered. Immunoassays and colour coding tests are quite cheap with 2-10 € but they are produced for a single use. The costs of the other devices used in this study were (in increasing order): IMS (~30.000 €) < IR spectrometer (~50.000 €) < Raman spectrometer

(~70.000 €) < THz spectrometer (~250 000 €) (data derived from the acquisitions of those techniques by State Office of Criminal Investigation Rhineland-Palatinate).

There are no presumptive tests which can cover all application areas, so that the choice of a suitable technique depends on the criteria discussed above and in Table 7-1. For the rapid identification of unknown chemicals in a field setting e.g. a crime scene or drug and explosive detection in e.g. airports the combination of IMS and Raman spectroscopy fulfils most of the criteria which are essential for on-site analysis. IMS is a suitable presumptive test for different matrices especially herbal mixtures, tobaccos, papers or diverse liquids and gives a hint on possible drug trafficking in prison. Suspicious objects can be analysed by wiping the surface of a sample with a swab without any further sample preparation. A more detailed characterisation of a substance is achieved using Raman spectroscopy. Here, the analysis of powders or liquids is preferred and the direct analysis through packaging materials like glass or plastics is possible. This is an important aspect when analysing hazardous materials.

7.2 Identification strength: the characterisation of unknowns

The dynamic NPS market and the resulting availability of a large number of structurally related substances, requires effective tools that provide the necessary structural information for their differentiation. According to the recommendations of the SWGDRUG, spectroscopic methods like NMR, Raman and IR spectroscopy as well as mass spectrometry are category A analytical techniques with maximum discriminating power.⁴⁵

NMR is the most important technique for structure elucidation and enables unambiguous identification of unknown and novel substances like synthetic cannabinoids or synthetic cathinone derivatives.² Even the absolute configuration of closely related substances, e.g. stereoisomers is determined by ¹H NMR and ¹³C NMR. The occurrence of specific isomers is another way to circumvent the level of legal penalties that conforms to a specific isomer which is listed in drug laws.³³ Except for some rare cases it is not possible to interpret complex molecular structures with MS, IR and Raman spectroscopy alone. Major disadvantages of this technique are the cost of NMR spectroscopy and the required technical expertise, which leads to a limited applicability in routine analysis.²

As a consequence, the benefits of the other techniques have to be fully exhausted. Mass spectrometry is not able to distinguish between isomers of a compound having the same charge-to-mass (m/z) ratio but it gives information about the molecular weight of a compound which is useful in determining a molecular formula for the substance of interest. Additionally, MS can tell you if the compound contains certain elements such as bromine and chlorine, based on the abundance of their isotopes.

In comparison to NMR, IR and Raman spectroscopy have a lower identification power but due to the fingerprint region in the spectra, the active substances in seizures can be classified

according to their specific structural components. Closely related substances were differentiated in this study (Figure 3-5).

In general, a prerequisite for the field application of spectroscopic techniques is the actuality and quality of the reference library. In Chapter 3.4.1, the analysis of synthetic cannabinoids and synthetic cathinone derivatives was carried out using three different Raman spectrometers including one benchtop device and two portable devices. We showed that the Raman spectra generated by different spectrometers were very similar using instrument in-built correlation algorithms to estimate the hit qualities. Thus, the maintenance of the database can be executed centrally and under uniform conditions, so that field analysis is possible with updated libraries. Furthermore, the identification power of Raman spectroscopy was demonstrated in various applications with a new approach especially for the challenging analysis of unknown samples, which were not part of the reference library (Chapter 3.4.4). A PCA model was developed to predict the NPS subgroup (synthetic cathinone derivatives and cannabinoids) of pure powders or seized samples (herbal mixtures). In Figure 3-2 and Figure 3-3, the formation of clusters according to characteristic main vibrational group frequencies visible from the loadings plots was observed. The prediction of NPS subclasses was quite accurate. In addition, not only the class of a substance but also the possibility to discriminate typical structural elements of the NPS including core, linker and linked group was examined. Comparing this approach to literature, nearly all other PCA models presented, focus on the discrimination of substance classes but not on the distinction of substances within one substance class.^{71,84,91} Based on the PCA loadings, specific group frequencies of NPS with high identification power were summarised in tables (see Table 3-3-Table 3-7) that enable the assessment of a possible chemical structure. Currently, spectral information on specific structural vibrations of NPS are limited and, to the best of our knowledge, have not yet been published in detail for synthetic cannabinoids (except for the synthetic cannabinoid 5F-AMB⁹⁵).

It has been shown that Raman spectroscopy is broadly applicable: Raman spectroscopy is not only suitable as a preliminary tests (discussed in Chapter 3) but also the combination of Raman spectroscopy with the resulting vibrational frequency tables and a PCA model are useful for the characterisation of the chemical structure of unknown samples.

7.3 Quantification of NPS

After identification, one of the main analytical tasks in forensic toxicology is the quantification of the active ingredient due to the correlated penalties that are regulated in specific drug laws. Nearly every analytical technique affords time consuming calibration and requires that reference standards with a known purity are available.³² Due to dynamic NPS market, reference material is not always available. In Chapter 5, a new and unique alternative was demonstrated for the determination of active ingredients in casework samples, analysed

for the first time: The need for reference standards is circumvented by evaluation of possible cross calibrations between different but structurally related synthetic cannabinoids, some of which are readily available as reference material. Therefore, a quantitative screening analysis of 20 synthetic cannabinoids was developed using UPLC-DAD with maximal retention times of 10 min. First, the figures of merit of the method were investigated including linearity, sensitivity and precision for all substances (see Chapter 5.4.2.2). For cross calibration between synthetic cannabinoids, the accuracy and the corresponding bias values were determined by evaluating QC-samples of one substance with calibration curves from other synthetic cannabinoids. For quantification of casework samples in forensic applications, some general rules were deducted: The most important prerequisite for possible cross calibration are same core- and linker-groups present in the synthetic cannabinoids leading to a similar sensitivity given by the slope of the calibration curve. Similarities in the tail-group can be advantageous but are not a precondition. Overall, only five synthetic cannabinoids standards were shown to be necessary for the precise quantification via cross calibration, which also considerably reduces the effort and working time. For these substances, reference material is commercially available. In case of unknown samples, which were not further characterised, the UV_{max} values gave a first hint to the presence of an indazole, indole or carbazole-core synthetic cannabinoid (see Chapter 5.4.2.1).

Compared to literature, hyphenated techniques dominate quantitative analysis of NPS in different matrices mainly including LC-MS^{101,111,114-136} and GC-MS,^{36,44,47,54-58,62,100-114} followed by LC-UV.^{2,140} Several techniques were described in literature using reference standards that are suitable for the quantification of NPS. However, these methods fail, when an appropriate reference material is not available as in the case of the dynamic NPS market. Then, only NMR can be regarded as a suitable method due to absolute concentration determinations that can be assessed with calibrating on a reference substance that gives resonance signals in the excited frequency range. As the number of 1H atoms present is directly proportional to the signal intensity, other substances can be used for referencing.⁴⁹ This provides a very high flexibility in the choice of reference substances. As mentioned in previous chapters, the availability of NMR spectrometers is limited for routine analysis due to the high cost and requirement of technical expertise.²

The lowest cost-variant for quantification of substances is LC-UV but none the less, LC-MS is the technique of choice which is proven by the large number of publications. The usage of LC-MS offers higher identification strength towards LC-UV due to the resulting mass fragmentation patterns. What are the advantages of UV detection? There are two criteria, which have to be fulfilled using LC-UV, but not LC-MS: First the molecule must possess a chromophore or be tagged with a UV absorbing group and the target compound and co-elutant must absorb at different wavelengths. Regardless of the type of NPS, every subclass, especially synthetic cathinone derivatives and synthetic cannabinoids are UV active.

Reported LODs and LOQs of the UPLC-DAD method were significantly higher than for chromatographic techniques coupled to mass spectrometry. In the presented study in Chapter 5, LODs and LOQs ranged from 0.49-4.17 mg/L and 1.57-10.1 mg/L, respectively. This is sufficient for the analysis of powdered samples or herbal mixtures.

LC-DAD shows some benefits for quantification: It is difficult to determine component purity from a chromatogram but a DAD detector can easily analyse peak purity by comparing spectra within a peak. DAD detectors are equipped with the software to perform peak purity assessment, thus providing an extra level of quality control to the LC-DAD analysis. In addition, LC-DAD measurements are well reproducible and precise which was proven by the low RSD values in the UPLC-DAD method developed in this thesis (Table 5-2).

Method development for LC-MS is more sophisticated due to the more complex technical principle concerning the ionisation mechanism. Ion suppression by matrix components (e.g. salts, ion pairing agents) may impair quantification and reduce precision, if isotopically labelled standards are not available.

7.4 Chiral discrimination of NPS

The availability and development of stereoselective analytical methods gain in importance in clinical chemistry and forensic toxicology. Many synthetic cathinone derivatives are on the market as racemic mixtures due to the use of racemic precursors during the manufacturing process. Often, the R and S enantiomers show significant differences in their pharmacological activity.^{144,145}

We developed an effective and fast method for the enantioselective separation and detection of racemic mixtures of 36 synthetic cathinone derivatives using capillary electrophoresis with diode array detection and HS- β -CD as chiral selector. The choice of HS- β -CD in this study and the frequent application of CD is based on the beneficial properties such as UV transparency, availability, wide application range (polar, nonpolar, charged, uncharged analytes), and reasonable solubility in water.³³³ In addition, with the CD just added to the BGE, the CE-DAD method is comparatively cheap, as no chiral stationary phases is required. Moreover, improved chiral selectivity was observed many times with charged CDs compared with neutral ones as a result of an enhanced stability of host-guest complexes due to additional electrostatic (Coulomb) interactions of oppositely charged functional groups of complexing partners.^{165,334} At the acidic pH (2.3) chosen, the EOF is negligible and with the reversed separation polarity the anionic chiral selector migrates towards the anode, while the free synthetic cathinone derivatives migrate towards the cathode.

In this study, two analytical methods were developed for different applications: First, a screening method for the simultaneous chiral analysis of synthetic cathinone derivatives was developed using reversed polarity and long-end injection mode with a maximum migration time of 26 min. To the best of our knowledge, no further publication demonstrated the

simultaneous separation of a large number of 36 analytes including the discrimination of enantiomers of structurally closely related substances like regioisomers which differ only in the C4 or C5 position of a halogen-atom in a pentyl-chain. Furthermore, almost no publication thematises the analyses of seized samples with possible bulking agents, demonstrated in this study. Silva et al. described the analysis of real samples containing bulking agents but without demonstrating that the selectivity is high enough to discriminate between bulk and active agent.¹⁵²

The second method allowed the fast determination of the enantiomeric excess of synthetic cathinone derivatives (present as single active agent) using normal polarity and short-end injection mode with an overall migration time of only 6 min. The advantage of the high throughput method compared to other chiral methods published is the possibility to estimate the enantiomeric excess of enantiomer pairs in less than 6 minutes when the identity of the cathinone is known. Other publications reported migration times for synthetic cathinone derivatives between 10-20 min in CE applications^{154,157,158,160} and 12-85 min for LC methods¹⁴⁶⁻¹⁵³ (studies including more than one substance) and 12-40 min for GC methods^{150,154-156}.

In general, CE is better suitable for chiral analysis than GC: The direct analysis is possible without the need for derivatisation as necessary for GC, which requires (i) the need of a functional group that can be derivatised, (ii) a high purity of the derivatization reagent and (iii) additional time-consuming sample preparation steps with the risk of racemisation under the reaction conditions.

Comparing chiral LC and CE, CE offers a high separation efficiency, versatility, simplicity, short analysis time and good compatibility with aqueous samples.^{335,336} Benefits and limitations of LC and CE are discussed comparing the screening UPLC-DAD method in Chapter 5 with the chiral screening method using CE-DAD presented in Chapter 6. The efficiency of CE is higher than in LC with detected theoretical plates of 210°000 for the analysis of synthetic cathinone derivatives. Thus, chiral resolution is better in CE due to differences in molecular interactions and the electrically driven separation mechanism giving rise to the separation of the diastereomeric complexes, which is not possible in LC with chiral stationary phases. The overall sensitivity was nearly equal with LODs and LOQs ranged from 0.49-4.17 mg/L and 1.57-10.1 mg/L for UPLC-DAD and 1.04-2.38 mg/L and 5.23-10.54 mg/L for CE-DAD. In some research works, sensitivity of LC-DAD is higher as a consequence of the small volumes injected and the short detector path-length in CE compared with HPLC.³³⁷ The precision of both methods is nearly the same. The precision was determined with two quality control samples (QC) of high and low concentration, which were analysed daily (n = 2) on eight consecutive days. The intraday and interday imprecision was ≤ 5.1 % for UPLC-DAD and ≤ 6.0 % for CE-DAD.

Some advantages of CE-DAD emerged during the method development in this work: A series of different BGEs was tested since there is no need for a long equilibration time when

switching to a different chiral BGE. Furthermore, multiple chiral selectors were screened at a lower cost compared to the cost for the purchase of one or more chiral LC columns. Not only the overall expenses for the method development were reduced but also the low solvent and solute consumption makes CE more environmentally friendly.

8 Conclusion

In this thesis, the portfolio of new analytical methods was expanded to face the challenges given by the dynamically and constantly changing drug market of synthetic cannabinoids and synthetic cathinone derivatives, the most frequently seized NPS. These substances pose serious risks to public health and raised prominent challenges in law enforcement, executive apparatus, public health authorities and forensic and toxicology laboratories.

One of the main difficulties is the limited availability for actual reference material of new emerging drugs in order to verify their identification and especially to enable their quantification by routine laboratory methods. Therefore, analytical data for various recently launched NPS are lacking which impedes the analysis of casework samples. Using seized material, analytical data and reference spectral libraries were updated to facilitate identification and to keep up with characterisation of newly emerged synthetic cannabinoids and cathinone derivatives using IMS, THz and Raman spectroscopy and UV/VIS-detection.

A new approach was introduced for the characterisation and also identification of unknowns using Raman spectroscopy in Chapter 3: Tables with specific group frequencies were developed and used to discriminate typical structural elements of NPS in combination with a PCA model. Some of these NPS were characterised for the first time. We successfully identified synthetic cannabinoids in herbal seizures using a simple solid/liquid extraction of only 100 mg herbal material.

For quantitative analysis, a possibility to reduce the need for reference material for quantification by UPLC-DAD: A similar slope of the calibration curve was present for synthetic cannabinoids with high structural similarity was observed, which allow quantification via cross calibration using a small set of only five substances, for which commercial reference standards are available (Chapter 5).

The combination of the Raman spectroscopic method presented here with the cross calibration approach using UPLC-DAD is a powerful tool for both identification and subsequent quantification of NPS in different matrices. Thus, the low identification strength of DAD compared to MS or NMR could be balanced.

The relevance of regioisomers and enantiomers has been increasingly recognised in NPS analysis, which requires special analytical methods. In Chapter 6, the successful development and validation of a screening and a high-throughput method for the chiral separation of 36 synthetic cathinone derivatives was demonstrated using HS- β -CD as chiral selector in CE-DAD.

Another important issue is the detection of NPS in public institutions to minimise serious risks to staff when handling NPS from drug trafficking. This requires analytical technique to be fast, simple to operate also by non-scientists and non-destructive for covert investigations. We here show that Raman and IMS are suitable for different aspects of NPS analysis:

Raman spectroscopy was shown to be suitable for both the application in the laboratory but for on-site analysis in public institutions (Chapter 3). According to chemometric evaluations, only one spectral reference library proved to be necessary for the discrimination of unknown substances, which can be transferred to other portable Raman systems independent of the vendor. This is a great advantage for field analytics at border controls or in for policing when centralised databases are available and maintained.

In addition, two different presumptive tests were applied to detect NPS in different matrices or packaging material: A portable IMS was used to successfully characterise 25 different synthetic cannabinoids with regard to substance-specific K_0 values and drift times which were reported for the first time. The IMS method was shown to be highly matrix tolerant. It was successfully applied to the analysis of herbal mixtures and paper impregnated with synthetic cannabinoids, as well as different cosmetics and liquid food samples (Chapter 2).

For the first time, the analysis of synthetic cannabinoids was investigated using a THz-TDS spectrometer (Chapter 4). We here show that with the instrumentation used, the sensitivity only allows to analyse pure powders, however also packed in plastic bags and in envelopes. Monitoring was simplified and accelerated using transillumination images of packed materials, and then a suitable grid of measurement points for detailed analysis was chosen. Here, the importance of interfering parameters such as humidity in air, medium, salt form, etc should be tested by performing further in-field analysis with a large number of different samples. In addition, technical investigations have to be developed to avoid influences of atmospheric conditions.

What is the impact of the presented laboratory and portable methods for the future NPS analytics for the criminal investigation institutions?

Since October 2018, the IMS method developed in this thesis has been applied in a prison by trained prison officers in Rhineland-Palatinate and has guaranteed a fast and non-destructive analysis of suspicious samples with a direct indication of the presence of NPS. This became feasible because the IMS software was programmed to generate alarms and the actuality of the database is constantly updated centrally by the criminal investigation of Rhineland Palatinate. Due to the reliable measuring results, the project has expanded to all other prisons in Rhineland-Palatinate to analyse suspicious samples. In 2019, more than 200 samples were analysed.

The Raman spectroscopic method as well as the chiral CE-DAD methods were developed inter alia for the EU-project ADEBAR. Within this project, the identification, the collection of analytical data and the distribution of reference material of newly occurring NPS is organised among criminal institutes in the EU. The spectral libraries of the Raman spectrometers used in this study were internally published on platforms for Criminal Investigations Offices in Germany. In addition, all spectra recorded with different devices were collected in an external database (KnowItAll software), which enables the analysis of casework samples in different institutions independent of the Raman spectrometer used.

Both chiral methods using CE-DAD were applied in the Federal Criminal Police Office (Wiesbaden, Germany) for the analysis of casework samples and for the characterisation of the samples from the ADEBAR project.

The quantitative analysis of synthetic cannabinoids via cross calibrations using UPLC-DAD was incorporated into the routine analysis in the State Office of Criminal Investigation (Rhineland-Palatinate). Based on these results, the possibility to cross-calibrate NPS by a small set of commercially available reference standards will further be extended in upcoming EU-Project “ADEBAR *plus*”, which started in October 2019 as a follow up-project of ADEBAR.

References

1. United Nations Office on Drugs and Crime. NPS-new psychoactive substances 2013; https://www.unodc.org/documents/scientific/NPS_leaflet_E.pdf. Accessed January 22, 2019.
2. United Nations Office on Drugs and Crime. Recommended methods for the identification and analysis of synthetic cannabinoid receptor agonists in seized materials. 2013; https://www.unodc.org/documents/scientific/STNAR48_Synthetic_Cannabinoids_EN_G.pdf. Accessed March 08, 2019.
3. European Monitoring Centre for Drug and Drug Addiction. <http://www.emcdda.europa.eu/publications/drug-profiles/synthetic-cannabinoids/de>. 2018. Accessed March 23, 2019.
4. United Nations Office on Drugs and Crime. Single Convention on Narcotic Drugs. 1961; https://www.unodc.org/pdf/convention_1961_en.pdf. Accessed February 01, 2018.
5. United Nations Office on Drugs and Crime. Convention on Psychotropic Substances. 1971; https://www.unodc.org/pdf/convention_1971_en.pdf. Accessed February 01, 2018.
6. United Nations Office on Drugs and Crime. The challenge of new psychoactive substances. 2013; https://www.unodc.org/documents/scientific/NPS_2013_SMART.pdf. Accessed March 07, 2019.
7. European Monitoring Centre for Drug and Drug Addiction. Health responses to new psychoactive substances. 2016; <http://www.emcdda.europa.eu/system/files/publications/2812/TD0216555ENN.pdf>. Accessed March 10, 2019.
8. European Monitoring Centre for Drug and Drug Addiction. European Drug Report 2019: Trends and Developments. 2019; <http://www.emcdda.europa.eu/publications/edr/trends-developments/2019>. Accessed August 17, 2019.
9. Neue-psychoaktive-Stoffe-Gesetz (NpSG) *Bundesministerium der Justiz und für Verbraucherschutz*. 2016, Germany.
10. Bonnet U, Mahler H. Synthetische Cannabinoide: Verbreitung, Suchtbiologie und aktuelle Perspektiven der persönlichen Gesundheitsgefährdung. *Fortschritte der Neurologie*. 2015;83(4):221-231.
11. Hohmann N, Mikus G, Czock D. Effects and risks associated with novel psychoactive substances. *Dtsch Arztebl International*. 2014;111(9):139-147.
12. Hess C, Schoeder CT, Pillaiyar T, Madea B, Müller CE. Pharmacological evaluation of synthetic cannabinoids identified as constituents of spice. *Forensic Toxicol*. 2016;34(2):329-343.
13. European Monitoring Centre for Drug and Drug Addiction. Early warning system - national profiles. 2012; <http://www.emcdda.europa.eu/thematic-papers/ews>. Accessed March 01, 2018.
14. Krecke J. Council Decision 2005/387/JHA of 10 May 2005 on the information exchange, risk-assessment and control of new psychoactive substances. *Official Journal of the European Union*. 2005.

15. European Monitoring Centre for Drug and Drug Addiction. Perspectives on drugs-Synthetic cannabinoids in Europe. 2017; http://www.emcdda.europa.eu/system/files/publications/2753/POD_Synthetic%20cannabinoids_0.pdf. Accessed July 28, 2019.
16. European Monitoring Centre for Drug and Drug Addiction. Understanding the spice phenomenon. 2009; <http://www.emcdda.europa.eu/system/files/publications/537/Spice-Thematic-paper-final-version.pdf>. Accessed June 03, 2019.
17. Dresen S, Ferreirós N, Pütz M, Westphal F, Zimmermann R, Auwärter V. Monitoring of herbal mixtures potentially containing synthetic cannabinoids as psychoactive compounds. *J Mass Spectrom.* 2010;45(10):1186-1194.
18. European Monitoring Centre for Drug and Drug Addiction. Synthetic cathinones drug profile. 2019; <http://www.emcdda.europa.eu/publications/drug-profiles/synthetic-cathinones>. Accessed July 08, 2019.
19. European Monitoring Centre for Drug and Drug Addiction. Europol–EMCDDA Joint Report on a new psychoactive substance: 4-methylmethcathinone (mephedrone). 2010. Accessed June 24, 2019.
20. Gregg RA, Rawls SM. Behavioral pharmacology of designer cathinones: A review of the preclinical literature. *Life Sci.* 2014;97(1):27-30.
21. European Monitoring Centre for Drug and Drug Addiction. EMCDDA–Europol Joint Report on a new psychoactive substance: MDPV (3,4-methylenedioxypropylone). 2014; http://www.emcdda.europa.eu/publications/joint-report/MDPV_en. Accessed July 15, 2019.
22. Martínez-Clemente J, Escubedo E, Pubill D, Camarasa J. Interaction of mephedrone with dopamine and serotonin targets in rats. *Eur Neuropsychopharmacol.* 2012;22(3):231-236.
23. Schifano F, Albanese A, Fergus S, et al. Mephedrone (4-methylmethcathinone; ‘meow meow’): chemical, pharmacological and clinical issues. *Psychopharmacology.* 2011;214(3):593-602.
24. Meyer MR, Wilhelm J, Peters FT, Maurer HH. Beta-keto amphetamines: studies on the metabolism of the designer drug mephedrone and toxicological detection of mephedrone, butylone, and methylone in urine using gas chromatography–mass spectrometry. *Anal Bioanal Chem.* 2010;397(3):1225-1233.
25. Pedersen AJ, Reitzel LA, Johansen SS, Linnet K. In vitro metabolism studies on mephedrone and analysis of forensic cases. *Drug Test Anal.* 2013;5(6):430-438.
26. Valente MJ, Guedes de Pinho P, de Lourdes Bastos M, Carvalho F, Carvalho M. Khat and synthetic cathinones: a review. *Arch Toxicol.* 2014;88(1):15-45.
27. United Nations Office on Drugs and Crime. Recommended methods for the identification and analysis of synthetic cathinones in seized materials. 2015; <https://www.unodc.org/unodc/en/scientists/recommended-methods-for-the-identification-and-analysis-of-synthetic-cathinones-in-seized-materials.html>. Accessed March 10, 2019.
28. Patona T, Kónya K, Juhász-Tóth E. Syntheses and transformations of alpha-azido ketones and related derivatives. *Chem Soc Rev.* 2011;40:2797–2847.
29. Collins M. Some new psychoactive substances: Precursor chemicals and synthesis-driven end-products. *Drug Test Anal.* 2011;3(7-8):404-416.
30. United Nations Office on Drugs and Crime. Recommended methods for the identification and analysis of amphetamine, methamphetamine, and their ring-substituted analogues in seized materials: manual for use by national drug testing laboratories. 2006.

31. Saem de Burnaga Sanchez J. Sur un Homologue de L'ephedrine (On an Analogue of Ephedrine). *Bull Soc Chim Fr.* 1929:284-286.
32. Archer RP, Treble R, Williams K. Reference materials for new psychoactive substances. *Drug Test Anal.* 2011;3(7-8):505-514.
33. Brandt SD, King LA, Evans-Brown M. The new drug phenomenon. *Drug Test Anal.* 2014;6(7-8):587-597.
34. Manili BA, Connors EF, Stephens DW, Stedman JR. Police drug testing. *National Institute of Justice* 1987; <https://www.ncjrs.gov/pdffiles1/Digitization/157668NCJRS.pdf>. Accessed March 29, 2018.
35. Isaacs RCA. A structure–reactivity relationship driven approach to the identification of a color test protocol for the presumptive indication of synthetic cannabimimetic drugs of abuse. *Forensic Sci Int.* 2014;242:135-141.
36. Zaitso K, Katagi M, Nakanishi K, et al. Comprehensive analytical methods of the synthetic cannabinoids appearing in the illicit drug market. *Jpn J Forensic Sci Tech.* 2011;16(2):73-90.
37. Wood DM, Dargan PI. Mephedrone (4-methylmethcathinone): What is new in our understanding of its use and toxicity. *Prog Neuro-Psychopharmacol Biol Psychiatry.* 2012;39(2):227-233.
38. Uchiyama N, Kawamura M, Kamakura H, Kikura-Hanajiri R, Goda Y. Analytical data of designated substances (Shitei-Yakubutsu) controlled by the Pharmaceutical Affairs Law in Japan, part II: Color test and TLC. *Yakugaku zasshi : J Pharmaceutical Soc Japan.* 2008;128(6):981-987.
39. Dal Cason TA. The characterization of some 3,4-methylenedioxyecathinone (MDCATH) homologs. *Forensic Sci Int.* 1997;87(1):9-53.
40. Arntson A, Ofsa B, Lancaster D, Simon JR, McMullin M, Logan B. Validation of a novel immunoassay for the detection of synthetic cannabinoids and metabolites in urine specimens. *J Anal Toxicol.* 2013;37(5):284-290.
41. Swortwood MJ, Hearn WL, DeCaprio AP. Cross-reactivity of designer drugs, including cathinone derivatives, in commercial enzyme-linked immunosorbent assays. *Drug Test Anal.* 2014;6(7-8):716-727.
42. Ellefsen KN, Anizan S, Castaneto MS, et al. Validation of the only commercially available immunoassay for synthetic cathinones in urine: randox drugs of abuse V biochip array technology. *Drug Test Anal.* 2014;6(7-8):728-738.
43. Penders TM, Gestring RE, Vilensky DA. Intoxication delirium following use of synthetic cathinone derivatives. *Am J Drug AB.* 2012;38(6):616-617.
44. Logan BK, Reinhold LE, Xu A, Diamond FX. Identification of synthetic cannabinoids in herbal incense blends in the United States. *J Forensic Sci.* 2012;57(5):1168-1180.
45. Scientific working group for the analysis of seized drugs (SWGDRUG). Recommendations Version 7.0. 2014; <http://www.swgdrug.org/approved.htm>. Accessed June 15, 2019.
46. Ernst L, Schiebel H-M, Theuring C, Lindigkeit R, Beuerle T. Identification and characterization of JWH-122 used as new ingredient in “Spice-like” herbal incenses. *Forensic Sci Int.* 2011;208(1):e31-e35.
47. Westphal F, Sönnichsen FD, Thiemt S. Identification of 1-butyl-3-(1-(4-methyl)naphthoyl)indole in a herbal mixture. *Forensic Sci Int.* 2012;215(1):8-13.
48. Moosmann B, Kneisel S, Girreser U, Brecht V, Westphal F, Auwärter V. Separation and structural characterization of the synthetic cannabinoids JWH-412 and 1-[(5-fluoropentyl)-1H-indol-3yl]-(4-methylnaphthalene-1-yl)methanone using GC–MS,

- NMR analysis and a flash chromatography system. *Forensic Sci Int.* 2012;220(1):e17-e22.
49. Schoenberger T. Determination of standard sample purity using the high-precision ¹H-NMR process. *Anal Bioanal Chem.* 2012;403:247-254.
 50. Jankovics P, Váradi A, Tölgyesi L, Lohner S, Németh-Palotás J, Balla J. Detection and identification of the new potential synthetic cannabinoids 1-pentyl-3-(2-iodobenzoyl)indole and 1-pentyl-3-(1-adamantoyl)indole in seized bulk powders in Hungary. *Forensic Sci Int.* 2012;214(1):27-32.
 51. Marino MA, Voyer B, Cody RB, Dane AJ, Veltri M, Huang L. Rapid identification of synthetic cannabinoids in herbal incenses with DART-MS and NMR. *J Forensic Sci.* 2016;61(S1):82-91.
 52. Fowler F, Voyer B, Marino M, et al. Rapid screening and quantification of synthetic cannabinoids in herbal products with NMR spectroscopic methods. *Anal Methods.* 2015;7(18):7907-7916.
 53. Dunne SJ, Rosengren-Holmberg JP. Quantification of synthetic cannabinoids in herbal smoking blends using NMR. *Drug Test Anal.* 2017;9(5):734-743.
 54. Uchiyama N, Shimokawa Y, Kawamura M, Kikura-Hanajiri R, Hakamatsuka T. Chemical analysis of a benzofuran derivative, 2-(2-ethylaminopropyl)benzofuran (2-EAPB), eight synthetic cannabinoids, five cathinone derivatives, and five other designer drugs newly detected in illegal products. *Forensic Toxicol.* 2014;32(2):266-281.
 55. Uchiyama N, Kawamura M, Kikura-Hanajiri R, Goda Y. Identification of two new-type synthetic cannabinoids, N-(1-adamantyl)-1-pentyl-1H-indole-3-carboxamide (APICA) and N-(1-adamantyl)-1-pentyl-1H-indazole-3-carboxamide (APINACA), and detection of five synthetic cannabinoids, AM-1220, AM-2233, AM-1241, CB-13 (CRA-13), and AM-1248, as designer drugs in illegal products. *Forensic Toxicol.* 2012;30(2):114-125.
 56. Uchiyama N, Matsuda S, Wakana D, Kikura-Hanajiri R, Goda Y. New cannabimimetic indazole derivatives, N-(1-amino-3-methyl-1-oxobutan-2-yl)-1-pentyl-1H-indazole-3-carboxamide (AB-PINACA) and N-(1-amino-3-methyl-1-oxobutan-2-yl)-1-(4-fluorobenzyl)-1H-indazole-3-carboxamide (AB-FUBINACA) identified as designer drugs in illegal products. *Forensic Toxicol.* 2013;31(1):93-100.
 57. Uchiyama N, Shimokawa Y, Matsuda S, Kawamura M, Kikura-Hanajiri R, Goda Y. Two new synthetic cannabinoids, AM-2201 benzimidazole analog (FUBIMINA) and (4-methylpiperazin-1-yl)(1-pentyl-1H-indol-3-yl)methanone (MEPIRAPIM), and three phenethylamine derivatives, 25H-NBOMe 3,4,5-trimethoxybenzyl analog, 25B-NBOMe, and 2C-N-NBOMe, identified in illegal products. *Forensic Toxicol.* 2014;32(1):105-115.
 58. Uchiyama N, Matsuda S, Kawamura M, Kikura-Hanajiri R, Goda Y. Two new-type cannabimimetic quinolinyl carboxylates, QUPIC and QUCHIC, two new cannabimimetic carboxamide derivatives, ADB-FUBINACA and ADBICA, and five synthetic cannabinoids detected with a thiophene derivative α -PVT and an opioid receptor agonist AH-7921 identified in illegal products. *Forensic Toxicol.* 2013;31(2):223-240.
 59. Jones LE, Stewart A, Peters KL, et al. Infrared and Raman screening of seized novel psychoactive substances: a large scale study of >200 samples. *Analyst.* 2016;141(3):902-909.
 60. Tsujikawa K, Yamamuro T, Kuwayama K, et al. Application of a portable near infrared spectrometer for presumptive identification of psychoactive drugs. *Forensic Sci Int.* 2014;242:162-171.

61. Risoluti R, Materazzi S, Gregori A, Ripani L. Early detection of emerging street drugs by near infrared spectroscopy and chemometrics. *Talanta*. 2016;153:407-413.
62. Kneisel S, Westphal F, Rösner P, et al. Cannabinoidmimetika: Massenspektren und IR-ATR-Spektren neuer Verbindungen aus den Jahren 2009/2010. *Toxichem Krimtech*. 2011;78:23-35.
63. Langer N, Lindigkeit R, Schiebel HM, Papke U, Ernst L, Beuerle T. Identification and quantification of synthetic cannabinoids in "spice-like" herbal mixtures: Update of the German situation for the spring of 2016. *Forensic Sci Int*. 2016;269(1):31-41.
64. Willis JJN, Cook RB, Jankowa R. Raman spectrometry of some common barbiturates. *Anal Chem*. 1972;44(7):1228-1234.
65. Lin L, Lv J, Ji Y, et al. Characterization of barbiturates by Infrared and Raman microscopy. *Anal Lett*. 2013;46(18):2890-2898.
66. Moreno VM, López-López M, Atoche J-C, García-Ruiz C. Raman identification of drug of abuse particles collected with colored and transparent tapes. *Sci Justice*. 2014;54(2):164-169.
67. Neville GA, Beckstead HD, Shurvell HF. A Fourier Transform-Raman and Infrared vibrational study of delorazepam, fludiazepam, flurazepam, and tetrazepam. *DARU J Pharm Sci*. 1994;83(2):143-151.
68. Carter JC, Brewer WE, Angel SM. Raman spectroscopy for the in situ identification of cocaine and selected adulterants. *Appl Spectrosc*. 2000;54(12):1876-1881.
69. Ali EMA, Edwards HGM, Hargreaves MD, Scowen IJ. Raman spectroscopic investigation of cocaine hydrochloride on human nail in a forensic context. *Anal Bioanal Chem*. 2008;390(4):1159-1166.
70. Eliasson C, Macleod NA, Matousek P. Non-invasive detection of cocaine dissolved in beverages using displaced Raman spectroscopy. *Anal Chim Acta*. 2008;607(1):50-53.
71. Hargreaves MD, Page K, Munshi T, Tomsett R, Lynch G, Edwards HGM. Analysis of seized drugs using portable Raman spectroscopy in an airport environment—a proof of principle study. *J Raman Spectrosc*. 2008;39(7):873-880.
72. West MJ, Went MJ. The spectroscopic detection of drugs of abuse in fingerprints after development with powders and recovery with adhesive lifters. *Spectrochim Acta A*. 2009;71(5):1984-1988.
73. Burnett AD, Edwards HGM, Hargreaves MD, Munshi T, Page K. A forensic case study: the detection of contraband drugs in carrier solutions by Raman spectroscopy. *Drug Test Anal*. 2011;3(9):539-543.
74. Weyermann C, Mimoune Y, Anglada F, Massonnet G, Esseiva P, Buzzini P. Applications of a transportable Raman spectrometer for the in situ detection of controlled substances at border controls. *Forensic Sci Int*. 2011;209(1):21-28.
75. Hargreaves MD, Burnett AD, Munshi T, et al. Comparison of near infrared laser excitation wavelengths and its influence on the interrogation of seized drugs-of-abuse by Raman spectroscopy. *J Raman Spectrosc*. 2009;40(12):1974-1983.
76. Katainen E, Elomaa M, Laakkonen U-M, et al. Quantification of the amphetamine content in seized street samples by Raman Spectroscopy. *J Forensic Sci*. 2007;52(1):88-92.
77. Stewart SP, Bell SEJ, Fletcher NC, et al. Raman spectroscopy for forensic examination of β -ketophenethylamine "legal highs": Reference and seized samples of cathinone derivatives. *Anal Chim Acta*. 2012;711:1-6.
78. Ali EMA, Edwards HGM, Scowen IJ. Rapid in situ detection of street samples of drugs of abuse on textile substrates using microRaman spectroscopy. *Spectrochim Acta A*. 2011;80(1):2-7.

79. Bell SEJ, Thorburn Burns D, Dennis AC, Matchett LJ, Speers JS. Composition profiling of seized ecstasy tablets by Raman spectroscopy. *Analyst*. 2000;125(10):1811-1815.
80. Weston RG. Quick screening of crystal methamphetamine/methyl sulfone exhibits by Raman spectroscopy. *J Forensic Sci*. 2010;55(4):1068-1075.
81. Triplett JS, Hatfield JA, Kaeff TL, Ramsey CR, Robinson SD, Standifer AF. Raman spectroscopy as a simple, rapid, nondestructive screening test for methamphetamine in clandestine laboratory liquids. *J Forensic Sci*. 2013;58(6):1607-1614.
82. Bell SEJ, Fido LA, Sirimuthu NMS, Speers SJ, Peters KL, Cosbey SH. Screening tablets for DOB using surface-enhanced Raman spectroscopy. *J Forensic Sci*. 2007;52(5):1063-1067.
83. Rana V, Cañamares MV, Kubic T, Leona M, Lombardi JR. Surface-enhanced Raman spectroscopy for trace identification of controlled substances: morphine, codeine, and hydrocodone. *J Forensic Sci*. 2011;56(1):200-207.
84. Omar J, Slowikowski B, Guillou C, Reniero F, Holland MV, Boix A. Identification of new psychoactive substances (NPS) by Raman spectroscopy. *J Raman Spectrosc*. 2018.
85. Calvo-Castro J, Guirguis A, Samaras EG, Zloh M, Kirton SB, Stair Jacqueline L. Detection of newly emerging psychoactive substances using Raman spectroscopy and chemometrics. *RSC Advances*. 2018;8(56):31924-31933.
86. Guirguis A, Girotto S, Berti B, Stair JL. Identification of new psychoactive substances (NPS) using handheld Raman spectroscopy employing both 785 and 1064nm laser sources. *Forensic Sci Int*. 2017;273:113-123.
87. Assi S, Guirguis A, Halsey S, Fergus S, Stair JL. Analysis of 'legal high' substances and common adulterants using handheld spectroscopic techniques. *Anal Methods*. 2015;7(2):736-746.
88. Assi S, Wallis B, Osselton D. The evaluation of dual laser handheld Raman spectroscopy for identifying novel psychoactive substances. *Am Pharm Rev*. 2016;19.
89. Christie R, Horan E, Fox J, et al. Discrimination of cathinone regioisomers, sold as 'legal highs', by Raman spectroscopy. *Drug Test Anal*. 2014;6(7-8):651-657.
90. Harkai S, Pütz M. Comparison of rapid detecting optical techniques for the identification of New Psychoactive Substances in 'Legal High' preparations. *Toxichem Krimtech*. 2015;82:229-238.
91. Muhamadali H, Watt A, Xu Y, et al. Rapid detection and quantification of novel psychoactive substances (NPS) using Raman spectroscopy and surface-enhanced Raman scattering. *Front Chem*. 2019;7(412).
92. Mabbott S, Correa E, Cowcher DP, Allwood JW, Goodacre R. Optimization of parameters for the quantitative surface-enhanced Raman scattering detection of mephedrone using a fractional factorial design and a portable Raman spectrometer. *Anal Chem*. 2013;85(2):923-931.
93. Lee WWY, Silverson VAD, Jones LE, et al. Surface-enhanced Raman spectroscopy of novel psychoactive substances using polymer-stabilized Ag nanoparticle aggregates. *Chem Commun*. 2016;52(3):493-496.
94. Mostowtt T, McCord B. Surface enhanced Raman spectroscopy (SERS) as a method for the toxicological analysis of synthetic cannabinoids. *Talanta*. 2017;164:396-402.
95. Lobo Vicente J, Chassaing H, Holland MV, et al. Systematic analytical characterization of new psychoactive substances: A case study. *Forensic Sci Int*. 2016;265:107-115.
96. Ali EMA, Edwards HGM, Cox R. Forensic and security applications of a long-wavelength dispersive Raman system. *J Raman Spectrosc*. 2015;46(3):322-326.

97. Favretto D, Pascali JP, Tagliaro F. New challenges and innovation in forensic toxicology: Focus on the “New Psychoactive Substances”. *J Chromatogr A*. 2013;1287:84-95.
98. Meyer MR, Peters FT, Maurer HH. Automated mass spectral deconvolution and identification system for GC-MS screening for drugs, poisons, and metabolites in urine. *Clin Chem*. 2010;56(4):575-584.
99. Nic Daeid N, Savage KA, Ramsay D, Holland C, Sutcliffe OB. Development of gas chromatography–mass spectrometry (GC–MS) and other rapid screening methods for the analysis of 16 ‘legal high’ cathinone derivatives. *Sci Justice*. 2014;54(1):22-31.
100. Choi H, Heo S, Choe S, et al. Simultaneous analysis of synthetic cannabinoids in the materials seized during drug trafficking using GC-MS. *Anal Bioanal Chem*. 2013;405(12):3937-3944.
101. Hudson S, Ramsey J. The emergence and analysis of synthetic cannabinoids. *Drug Test Anal*. 2011;3(7-8):466-478.
102. Cox AO, Daw RC, Mason MD, et al. Use of SPME-HS-GC–MS for the analysis of herbal products containing synthetic cannabinoids. *J Anal Toxicol*. 2012;36(5):293-302.
103. Kneisel S, Westphal F, Bisel P, Brecht V, Broecker S, Auwärter V. Identification and structural characterization of the synthetic cannabinoid 3-(1-adamantoyl)-1-pentylindole as an additive in ‘herbal incense’. *J Mass Spectrom*. 2012;47(2):195-200.
104. Harris DN, Hokanson S, Miller V, Jackson GP. Fragmentation differences in the EI spectra of three synthetic cannabinoid positional isomers: JWH-250, JWH-302, and JWH-201. *Int J Mass Spectrom*. 2014;368:23-29.
105. DeRuiter J, Smith FT, Abdel-Hay K, Clark CR. Analytical differentiation of 1-alkyl-3-acylindoles and 1-acyl-3-alkylindoles: isomeric synthetic cannabinoids. *Anal Chem*. 2014;86(8):3801-3808.
106. Shevyrin V, Melkozerov V, Nevero A, Eltsov O, Morzherin Y, Shafran Y. 3-Naphthoylindazoles and 2-naphthoylbenzimidazoles as novel chemical groups of synthetic cannabinoids: Chemical structure elucidation, analytical characteristics and identification of the first representatives in smoke mixtures. *Forensic Sci Int*. 2014;242:72-80.
107. Ibáñez M, Bijlsma L, van Nuijs ALN, et al. Quadrupole-time-of-flight mass spectrometry screening for synthetic cannabinoids in herbal blends. *J Mass Spectrom*. 2013;48(6):685-694.
108. Zaitso K, Katagi M, Kamata HT, et al. Determination of the metabolites of the new designer drugs bk-MBDB and bk-MDEA in human urine. *Forensic Sci Int*. 2009;188(1):131-139.
109. Westphal F, Junge T. Ring positional differentiation of isomeric N-alkylated fluorocathinones by gas chromatography/tandem mass spectrometry. *Forensic Sci Int*. 2012;223(1):97-105.
110. Gwak S, Arroyo-Mora LE, Almirall JR. Qualitative analysis of seized synthetic cannabinoids and synthetic cathinones by gas chromatography triple quadrupole tandem mass spectrometry. *Drug Test Anal*. 2015;7(2):121-130.
111. Zuba D. Identification of cathinones and other active components of ‘legal highs’ by mass spectrometric methods. *TrAC*. 2012;32:15-30.
112. Brandt SD, Sumnall HR, Measham F, Cole J. Analyses of second-generation ‘legal highs’ in the UK: Initial findings. *Drug Test Anal*. 2010;2(8):377-382.
113. Brandt SD, Freeman S, Sumnall HR, Measham F, Cole J. Analysis of NRG ‘legal highs’ in the UK: identification and formation of novel cathinones. *Drug Test Anal*. 2011;3(9):569-575.

114. Fornal E. Identification of substituted cathinones: 3,4-Methylenedioxy derivatives by high performance liquid chromatography–quadrupole time of flight mass spectrometry. *J Pharm Biomed Anal.* 2013;81-82:13-19.
115. Kneisel S, Auwärter V. Analysis of 30 synthetic cannabinoids in serum by liquid chromatography-electrospray ionization tandem mass spectrometry after liquid-liquid extraction. *J Mass Spectrom.* 2012;47(7):825-835.
116. Scheidweiler KB, Huestis MA. Simultaneous quantification of 20 synthetic cannabinoids and 21 metabolites, and semi-quantification of 12 alkyl hydroxy metabolites in human urine by liquid chromatography–tandem mass spectrometry. *J Chromatogr A.* 2014;1327:105-117.
117. Wohlfarth A, Scheidweiler KB, Chen X, Liu H-f, Huestis MA. Qualitative confirmation of 9 synthetic cannabinoids and 20 metabolites in human urine using LC–MS/MS and library search. *Anal Chem.* 2013;85(7):3730-3738.
118. Kneisel S, Auwärter V, Kempf J. Analysis of 30 synthetic cannabinoids in oral fluid using liquid chromatography-electrospray ionization tandem mass spectrometry. *Drug Test Anal.* 2013;5(8):657-669.
119. Kneisel S, Speck M, Moosmann B, Corneillie TM, Butlin NG, Auwärter V. LC/ESI-MS/MS method for quantification of 28 synthetic cannabinoids in neat oral fluid and its application to preliminary studies on their detection windows. *Anal Bioanal Chem.* 2013;405(14):4691-4706.
120. Hutter M, Kneisel S, Auwärter V, Neukamm MA. Determination of 22 synthetic cannabinoids in human hair by liquid chromatography–tandem mass spectrometry. *J Chromatogr B.* 2012;903:95-101.
121. Teske J, Weller J-P, Fieguth A, Rothämel T, Schulz Y, Tröger HD. Sensitive and rapid quantification of the cannabinoid receptor agonist naphthalen-1-yl-(1-pentylindol-3-yl)methanone (JWH-018) in human serum by liquid chromatography–tandem mass spectrometry. *J Chromatogr B.* 2010;878(27):2659-2663.
122. Xu A, Warrington DM, Homan JW, McMullin MM, Kacinko SL, Logan BK. Development and validation of a liquid chromatography-tandem mass spectrometry method for the identification and quantification of JWH-018, JWH-073, JWH-019, and JWH-250 in human whole blood. *J Anal Toxicol.* 2011;35(7):386-393.
123. Dresen S, Kneisel S, Weinmann W, Zimmermann R, Auwärter V. Development and validation of a liquid chromatography–tandem mass spectrometry method for the quantitation of synthetic cannabinoids of the aminoalkylindole type and methanandamide in serum and its application to forensic samples. *J Mass Spectrom.* 2011;46(2):163-171.
124. Chimalakonda KC, Moran CL, Kennedy PD, et al. Solid-phase extraction and quantitative measurement of omega and omega-1 metabolites of JWH-018 and JWH-073 in human urine. *Anal Chem.* 2011;83(16):6381-6388.
125. de Jager AD, Warner JV, Henman M, Ferguson W, Hall A. LC–MS/MS method for the quantitation of metabolites of eight commonly-used synthetic cannabinoids in human urine – An Australian perspective. *J Chromatogr B.* 2012;897:22-31.
126. Yanes EG, Lovett DP. High-throughput bioanalytical method for analysis of synthetic cannabinoid metabolites in urine using salting-out sample preparation and LC–MS/MS. *J Chromatogr B.* 2012;909:42-50.
127. Hermanns-Clausen M, Kneisel S, Hutter M, Szabo B, Auwärter V. Acute intoxication by synthetic cannabinoids – Four case reports. *Drug Test Anal.* 2013;5(9-10):790-794.
128. Hutter M, Broecker S, Kneisel S, Auwärter V. Identification of the major urinary metabolites in man of seven synthetic cannabinoids of the aminoalkylindole type

- present as adulterants in 'herbal mixtures' using LC-MS/MS techniques. *J Mass Spectrom.* 2012;47(1):54-65.
129. Terrell AR, Dahn T, Shanks KG. Detection of JWH-018 and JWH-073 by UPLC-MS-MS in postmortem whole blood casework. *J Anal Toxicol.* 2012;36(3):145-152.
130. Saito T, Namera A, Miura N, et al. A fatal case of MAM-2201 poisoning. *Forensic Toxicol.* 2013;31(2):333-337.
131. Meroueh C, Lynch CF, Jaskierny DJ, et al. Four postmortem case reports with quantitative detection of the synthetic cannabinoid, 5F-PB-22. *J Anal Toxicol.* 2014;38(8):559-562.
132. Mazzarino M, Torre Xdl, Botrè F. A liquid chromatography-mass spectrometry method based on class characteristic fragmentation pathways to detect the class of indole-derivative synthetic cannabinoids in biological samples. *Anal Chim Acta.* 2014;837:70-82.
133. Jankovics P, Váradi A, Tölgyesi L, Lohner S, Németh-Palotás J, Kőszegi-Szalai H. Identification and characterization of the new designer drug 4'-methylethcathinone (4-MEC) and elaboration of a novel liquid chromatography-tandem mass spectrometry (LC-MS/MS) screening method for seven different methcathinone analogs. *Forensic Sci Int.* 2011;210(1):213-220.
134. Swortwood MJ, Boland DM, DeCaprio AP. Determination of 32 cathinone derivatives and other designer drugs in serum by comprehensive LC-QQQ-MS/MS analysis. *Anal Bioanal Chem.* 2013;405(4):1383-1397.
135. Sørensen LK. Determination of cathinones and related ephedrines in forensic whole-blood samples by liquid-chromatography-electrospray tandem mass spectrometry. *J Chromatogr B.* 2011;879(11):727-736.
136. Wohlfarth A, Weinmann W, Dresen S. LC-MS/MS screening method for designer amphetamines, tryptamines, and piperazines in serum. *Anal Bioanal Chem.* 2010;396(7):2403-2414.
137. Namera A, Kawamura M, Nakamoto A, Saito T, Nagao M. Comprehensive review of the detection methods for synthetic cannabinoids and cathinones. *Forensic Toxicol.* 2015;33(2):175-194.
138. Uchiyama N, Kikura-Hanajiri R, Kawahara N, Goda Y. Identification of a cannabimimetic indole as a designer drug in a herbal product. *Forensic Toxicol.* 2009;27(2):61-66.
139. Uchiyama N, Kikura-Hanajiri R, Kawahara N, Haishima Y, Goda Y. Identification of a cannabinoid analog as a new type of designer drug in a herbal product. *Chem Pharm Bull.* 2009;57(4):439-441.
140. Uchiyama N, Kikura-Hanajiri R, Ogata J, Goda Y. Chemical analysis of synthetic cannabinoids as designer drugs in herbal products. *Forensic Sci Int.* 2010;198(1):31-38.
141. Auwärter V, Dresen S, Weinmann W, Müller M, Pütz M, Ferreirós N. 'Spice' and other herbal blends: harmless incense or cannabinoid designer drugs? *J Mass Spectrom.* 2009;44(5):832-837.
142. Bijlsma L, Sancho JV, Hernández F, Niessen WMA. Fragmentation pathways of drugs of abuse and their metabolites based on QTOF MS/MS and MSE accurate-mass spectra. *J Mass Spectrom.* 2011;46(9):865-875.
143. Sekuła K, Zuba D, Stanaszek R. Identification of naphthoylindoles acting on cannabinoid receptors based on their fragmentation patterns under ESI-QTOFMS. *J Mass Spectrom.* 2012;47(5):632-643.

144. Gregg RA, Baumann MH, Partilla JS, et al. Stereochemistry of mephedrone neuropharmacology: enantiomer-specific behavioural and neurochemical effects in rats. *Br J Pharmacol*. 2015;172(3):883-894.
145. Rentsch KM. The importance of stereoselective determination of drugs in the clinical laboratory. *J Biochem Biophys Methods*. 2002;54(1):1-9.
146. Aboul-Enein HY, Serignese V. Direct chiral resolution of phenylalkylamines using a crown ether chiral stationary phase. *Biomed Chromatogr*. 1997;11(1):7-10.
147. Aboul-Enein HY, Serignese V. Direct enantiomeric separation of cathinone and one major metabolite on cellobiohydrolase (CBH-I) chiral stationary phase. *Biomed Chromatogr*. 1997;11(1):47-49.
148. Perera RWH, Abraham I, Gupta S, et al. Screening approach, optimisation and scale-up for chiral liquid chromatography of cathinones. *J Chromatogr A*. 2012;1269:189-197.
149. Albals D, Heyden YV, Schmid MG, Chankvetadze B, Mangelings D. Chiral separations of cathinone and amphetamine-derivatives: comparative study between capillary electrochromatography, supercritical fluid chromatography and three liquid chromatographic modes. *J Pharm Biomed Anal*. 2016;121:232-243.
150. Weiß JA, Taschwer M, Kunert O, Schmid MG. Analysis of a new drug of abuse: Cathinone derivative 1-(3,4-dimethoxyphenyl)-2-(ethylamino)pentan-1-one. *J Sep Sci*. 2015;38(5):825-828.
151. Wolrab D, Frühauf P, Moulisová A, et al. Chiral separation of new designer drugs (Cathinones) on chiral ion-exchange type stationary phases. *J Pharm Biomed Anal*. 2016;120:306-315.
152. Silva B, Fernandes C, Tiritan ME, et al. Chiral enantioresolution of cathinone derivatives present in “legal highs”, and enantioselectivity evaluation on cytotoxicity of 3,4-methylenedioxypropylvalerone (MDPV). *Forensic Toxicol*. 2016;34(2):372-385.
153. Taschwer M, Seidl Y, Mohr S, Schmid MG. Chiral separation of cathinone and amphetamine derivatives by HPLC/UV using sulfated β -cyclodextrin as chiral mobile phase additive. *Chirality*. 2014;26(8):411-418.
154. Taschwer M, Weiß JA, Kunert O, Schmid MG. Analysis and characterization of the novel psychoactive drug 4-chloromethcathinone (clephedrone). *Forensic Sci Int*. 2014;244:e56-e59.
155. Weiß JA, Mohr S, Schmid MG. Indirect chiral separation of new recreational drugs by gas chromatography-mass spectrometry using trifluoroacetyl-L-prolyl chloride as chiral derivatization reagent. *Chirality*. 2015;27(3):211-215.
156. Mohr S, Weiß JA, Spreitz J, Schmid MG. Chiral separation of new cathinone- and amphetamine-related designer drugs by gas chromatography-mass spectrometry using trifluoroacetyl-L-prolyl chloride as chiral derivatization reagent. *J Chromatogr A*. 2012;1269:352-359.
157. Baciú T, Borrull F, Calull M, Aguilar C. Enantioselective determination of cathinone derivatives in human hair by capillary electrophoresis combined in-line with solid-phase extraction. *Electrophoresis*. 2016;37(17-18):2352-2362.
158. Merola G, Fu H, Tagliaro F, Macchia T, McCord BR. Chiral separation of 12 cathinone analogs by cyclodextrin-assisted capillary electrophoresis with UV and mass spectrometry detection. *Electrophoresis*. 2014;35(21-22):3231-3241.
159. Mohr S, Pilaj S, Schmid MG. Chiral separation of cathinone derivatives used as recreational drugs by cyclodextrin-modified capillary electrophoresis. *Electrophoresis*. 2012;33(11):1624-1630.
160. Moini M, Rollman CM. Compatibility of highly sulfated cyclodextrin with electro spray ionization at low nanoliter/minute flow rates and its application to

- capillary electrophoresis/electrospray ionization mass spectrometric analysis of cathinone derivatives and their optical isomers. *Rapid Commun Mass Spectrom.* 2015;29(3):304-310.
161. Makino Y, Ohta S, Hirobe M. Enantiomeric separation of amphetamine by high-performance liquid chromatography using chiral crown ether-coated reversed-phase packing: application to forensic analysis. *Forensic Sci Int.* 1996;78(1):65-70.
162. Ho Hyun M, Tan G, Cho YJ. Liquid chromatographic enantioseparation of aryl α -amino ketones on a crown ether-based chiral stationary phase. *Biomed Chromatogr.* 2005;19(3):208-213.
163. Brunnenberg M, Kovar K-A. Stereospecific analysis of ecstasy-like N-ethyl-3,4-methylenedioxyamphetamine and its metabolites in humans. *J Chromatogr B : Biomedical Sciences and Applications.* 2001;751(1):9-18.
164. Mohr S, Taschwer M, Schmid MG. Chiral separation of cathinone derivatives used as recreational drugs by HPLC-UV using a CHIRALPAK® AS-H column as stationary phase. *Chirality.* 2012;24(6):486-492.
165. Vespalec R, Boček P. Chiral separations in capillary electrophoresis. *Chemical Reviews.* 2000;100(10):3715-3754.
166. Armstrong DW, Rundlett K, Reid GL. Use of a macrocyclic antibiotic, Rifamycin B, and indirect detection for the resolution of racemic amino alcohols by CE. *Anal Chem.* 1994;66(10):1690-1695.
167. Nishi H, Nakamura K, Nakai H, Sato T. Enantiomer separation by capillary electrophoresis using DEAE-dextran and aminoglycosidic antibiotics. *Chromatographia.* 1996;43(7):426-430.
168. Europäische Beobachtungsstelle für Drogen und Drogensucht. Europäischer Drogenbericht 2018 - Trends und Entwicklungen. http://www.emcdda.europa.eu/system/files/publications/8585/20181816_TDAT18001_DEN_PDF.pdf. Accessed November 10, 2018.
169. European Monitoring Centre for Drug and Drug Addiction. Fentanils and synthetic cannabinoids: driving greater complexity into the drug situation. An update from the EU Early Warning System (June 2018). 2018; <http://www.emcdda.europa.eu/system/files/publications/8870/2018-2489-td0118414enn.pdf>. Accessed August 23, 2018.
170. European Monitoring Centre for Drug and Drug Addiction. New psychoactive substances in prison. 2018; <http://www.emcdda.europa.eu/system/files/publications/8869/nps-in-prison.pdf>. Accessed March 30, 2019.
171. Schulte L, Dammer E, Pfeiffer-Gerschel T, Bartsch G, Friedrich M. *Deutschland Bericht 2017 des nationalen REITOX-Knotenpunkts an die EBDD (Datenjahr 2016 / 2017)*. Vol Gefängnis: European Monitoring Centre for Drugs and Drug Addiction; 2017.
172. Øiestad EL, Karinen R, Haugland K, Øiestad ÅML. Screening of synthetic cannabinoids. In: *Handbook of cannabis and related pathologies*. San Diego: Academic Press; 2017:981-997.
173. Ewald AH, Jacobsen-Bauer A, Klein B, Uhl M. Gemeinsamer Vorschlag des Arbeitskreises Analytik der Suchtstoffe der GTFCh zur besseren analytischen Bewältigung der großen Anzahl und Vielfalt von „Kräutermischungen“ *Toxichem Krimtech.* 2013;80(1):3-7.
174. Musshoff F, Hokamp EG, Bott U, Madea B. Performance evaluation of on-site oral fluid drug screening devices in normal police procedure in Germany. *Forensic Sci Int.* 2014;238:120-124.

175. Barnes AJ, Young S, Spinelli E, Martin TM, Klette KL, Huestis MA. Evaluation of a homogenous enzyme immunoassay for the detection of synthetic cannabinoids in urine. *Forensic Sci Int.* 2014;241(1):27-34.
176. Hutter M. Synthetische Cannabinoide in der forensischen Toxikologie: Metabolismus und Nachweis in unterschiedlichen Matrices. *Toxichem Krimtech.* 2015;82(3):307-310.
177. Ewing RG, Atkinson DA, Eiceman GA, Ewing GJ. A critical review of ion mobility spectrometry for the detection of explosives and explosive related compounds. *Talanta.* 2001;54:515-529.
178. Eiceman GA, Karpas Z. *Ion Mobility Spectrometry.* 2nd ed. Boca Raton: Taylor Francis Group; 2005.
179. Mäkinen MA, Anttalainen OA, Sillanpää MET. Ion mobility spectrometry and its application in detection of chemical warfare agents. *Anal Chem.* 2010;82:9594-9600.
180. Armenta S, Alcalá M, Blanco M. A review of recent, unconventional applications of ion mobility spectrometry (IMS). *Anal Chim Acta.* 2011;703(2):114-123.
181. Verkouteren JR, Staymates JL. Reliability of ion mobility spectrometry for qualitative analysis of complex, multicomponent illicit drug samples. *Forensic Sci Int.* 2011;206(1-3):190-196.
182. Hilton CK, Krueger CA, Midey AJ, Osgood M, Wu J, Wu C. Improved analysis of explosives samples with electrospray ionization-high resolution ion mobility spectrometry (ESI-HRIMS). *Int J Mass Spectrom.* 2010;298:64-71.
183. Karpas Z. Ion mobility spectrometry: A tool in the war against terror. *Bull Isr Chem Soc.* 2009;24:26-30.
184. Kanu AB, E. Haigh P, H. Hill H. *Surface detection of chemical warfare agent simulants and degradation products.* Vol 5532005.
185. Strege MA, Kozerski J, Juarbe N, Mahoney P. At-line quantitative ion mobility spectrometry for direct analysis of swabs for pharmaceutical manufacturing equipment cleaning verification. *Anal Chem.* 2008;80:3040-3044.
186. Dwivedi P, Wu C, Matz LM, Clowers BH, Siems WF, Hill Jr HH. Gas-phase chiral separations by ion mobility spectrometry. *Anal Chem.* 2006;78(24):8200-8206.
187. Dwivedi P, Bendiak B, Clowers BH, Hill Jr HH. Rapid resolution of carbohydrate isomers by electrospray ionization ambient pressure ion mobility spectrometry-time-of-flight mass spectrometry (ESI-APIMS-TOFMS). *J Am Soc Mass Spectrom.* 2007;18(7):1163-1175.
188. Zhu M, Bendiak B, Clowers BH, Hill Jr HH. Ion mobility- mass spectrometry analysis of isomeric carbohydrate precursor ions. *Anal Bioanal Chem.* 2009;394(7):1853-1867.
189. Vautz W, Baumbach JI, Uhde E. Detection of emissions from surfaces using ion mobility spectrometry. *Anal Bioanal Chem.* 2006;384(4):980-986.
190. Myles L, Meyers TP, Robinson L. Atmospheric ammonia measurement with an ion mobility spectrometer. *Atmos Environ.* 2006;40(30):5745-5752.
191. Borsdorf H, Rämmler A. Continuous on-line determination of methyl tert-butyl ether in water samples using ion mobility spectrometry. *J Chromatogr A.* 2005;1072(1):45-54.
192. Alizadeh N, Jafari M, Mohammadi A. Headspace-solid-phase microextraction using a dodecylsulfate-doped polypyrrole film coupled to ion mobility spectrometry for analysis methyl tert-butyl ether in water and gasoline. *J Hazard Mater.* 2009;169(1):861-867.
193. Du Y, Zhang W, Whitten W, Li H, Watson DB, Xu J. Membrane-Extraction Ion Mobility Spectrometry for in Situ Detection of Chlorinated Hydrocarbons in Water. *Anal Chem.* 2010;82(10):4089-4096.

194. Aguilera-Herrador E, Lucena R, Cárdenas S, Valcárcel M. Ionic liquid-based single drop microextraction and room-temperature gas chromatography for on-site ion mobility spectrometric analysis. *J Chromatogr A*. 2009;1216(29):5580-5587.
195. Walendzik G, Baumbach JI, Klockow D. Coupling of SPME with MCC/UV-IMS as a tool for rapid on-site detection of groundwater and surface water contamination. *Anal Bioanal Chem*. 2005;382(8):1842-1847.
196. Tadjimukhamedov FK, Stone JA, Papanastasiou D, et al. Liquid chromatography/electrospray ionization/ion mobility spectrometry of chlorophenols with full flow from large bore LC columns. *Int J Ion Mobility Spectrom*. 2008;11(1):51-60.
197. Jafari MT. Determination and identification of malathion, ethion and dichlorovos using ion mobility spectrometry. *Talanta*. 2006;69(5):1054-1058.
198. Jafari MT, Azimi M. Analysis of sevin, amitraz, and metalaxyl pesticides using ion mobility spectrometry. *Anal Lett*. 2006;39(9):2061-2071.
199. Nousiainen M, Peräkorpä K, Sillanpää M. Determination of gas-phase produced ethyl parathion and toluene 2,4-diisocyanate by ion mobility spectrometry, gas chromatography and liquid chromatography. *Talanta*. 2007;72(3):984-990.
200. Mohammadi A, Ameli A, Alizadeh N. Headspace solid-phase microextraction using a dodecylsulfate-doped polypyrrole film coupled to ion mobility spectrometry for the simultaneous determination of atrazine and ametryn in soil and water samples. *Talanta*. 2009;78(3):1107-1114.
201. Jafari MT, Khayamian T. Direct determination of ammoniacal nitrogen in water samples using corona discharge ion mobility spectrometry. *Talanta*. 2008;76(5):1189-1193.
202. Kunz RR, Leibowitz FL, Downs DK. Ultraviolet photolytic vapor generation from particulate ensembles for detection of malathion residues in aerosols. *Anal Chim Acta*. 2005;531(2):267-277.
203. Viitanen A-K, Saukko E, Virtanen A, et al. Ion mobility distributions during the initial stages of new particle formation by the ozonolysis of α -pinene. *Environ Sci Technol*. 2010;44(23):8917-8923.
204. Vautz W, Zimmermann D, Hartmann M, Baumbach JI, Nolte J. Ion mobility spectrometry for food quality and safety. *Food Addit Contam*. 2006;23(11):1064-1073.
205. Vautz W, Baumbach JI, Jung J. Beer fermentation control using ion mobility spectrometry — results of a pilot study. *J Institute of Brewing*. 2006;112(2):157-164.
206. Vautz W, Baumbach JI. Analysis of bio-processes using ion mobility spectrometry. *Eng Life Sci*. 2008;8(1):19-25.
207. Gursoy O, Somervuo P, Alatossava T. Preliminary study of ion mobility based electronic nose MGD-1 for discrimination of hard cheeses. *J Food Eng*. 2009;92(2):202-207.
208. Karpas Z, Tilman B, Gdalevsky R, Lorber A. Determination of volatile biogenic amines in muscle food products by ion mobility spectrometry. *Anal Chim Acta*. 2002;463(2):155-163.
209. Bota GM, Harrington PB. Direct detection of trimethylamine in meat food products using ion mobility spectrometry. *Talanta*. 2006;68(3):629-635.
210. Menéndez M, Garrido-Delgado R, Arce L, Valcárcel M. Direct determination of volatile analytes from solid samples by UV-ion mobility spectrometry. *J Chromatogr A*. 2008;1215(1):8-14.

211. Vestergaard JS, Martens M, Turkki P. Analysis of sensory quality changes during storage of a modified atmosphere packaged meat product (pizza topping) by an electronic nose system. *J Food Sci Technol*. 2007;40(6):1083-1094.
212. Jafari MT, Khayamian T, Shaer V, Zarei N. Determination of veterinary drug residues in chicken meat using corona discharge ion mobility spectrometry. *Anal Chim Acta*. 2007;581(1):147-153.
213. Sheibani A, Tabrizchi M, Ghaziaskar HS. Determination of aflatoxins B1 and B2 using ion mobility spectrometry. *Talanta*. 2008;75(1):233-238.
214. Khalesi M, Sheikh-Zeinoddin M, Tabrizchi M. Determination of ochratoxin A in licorice root using inverse ion mobility spectrometry. *Talanta*. 2011;83(3):988-993.
215. Alonso R, Rodríguez-Estévez V, Domínguez-Vidal A, Ayora-Cañada MJ, Arce L, Valcárcel M. Ion mobility spectrometry of volatile compounds from Iberian pig fat for fast feeding regime authentication. *Talanta*. 2008;76(3):591-596.
216. Wolfgang V, Jürgen N, Rita F, Jörg Ingo B. Breath analysis—performance and potential of ion mobility spectrometry. *J Breath Res*. 2009;3(3):036004.
217. Perl T, Carstens E, Hirn A, et al. Determination of serum propofol concentrations by breath analysis using ion mobility spectrometry. *Br J Anaesth* 2009;103(6):822-827.
218. Ruzsanyi V, Baumbach JI. Analysis of human breath using IMS. *Int J Ion Mobility Spectrom*. 2005;8:5-7.
219. Westhoff M, Litterst P, Freitag L, Urfer W, Bader S, Baumbach JI. Ion mobility spectrometry for the detection of volatile organic compounds in exhaled breath of patients with lung cancer: results of a pilot study. *Thorax*. 2009;64(9):744.
220. Bunkowski A, Bödeker B, Bader S, Westhoff M, Litterst P, Baumbach JI. MCC/IMS signals in human breath related to sarcoidosis—results of a feasibility study using an automated peak finding procedure. *J Breath Res*. 2009;3(4):046001.
221. Reynolds JC, Blackburn GJ, Guallar-Hoyas C, et al. Detection of volatile organic compounds in breath using thermal desorption electrospray ionization-ion mobility-mass spectrometry. *Anal Chem*. 2010;82(5):2139-2144.
222. Garrido-Delgado R, Arce L, Pérez-Marín CC, Valcárcel M. Use of ion mobility spectroscopy with an ultraviolet ionization source as a vanguard screening system for the detection and determination of acetone in urine as a biomarker for cow and human diseases. *Talanta*. 2009;78(3):863-868.
223. Isailovic D, Kurulugama RT, Plasencia MD, et al. Profiling of human serum glycans associated with liver cancer and cirrhosis by IMS-MS. *J Proteome Res*. 2008;7(3):1109-1117.
224. Dwivedi P, Schultz AJ, Jr HHH. Metabolic profiling of human blood by high-resolution ion mobility mass spectrometry (IM-MS). *Int J Mass Spec*. 2010;298(1):78-90.
225. Kaplan K, Dwivedi P, Davidson S, et al. Monitoring dynamic changes in lymph metabolome of fasting and fed rats by electrospray ionization-ion mobility mass spectrometry (ESI-IMMS). *Anal Chem*. 2009;81(19):7944-7953.
226. Alizadeh N, Mohammadi A, Tabrizchi M. Rapid screening of methamphetamines in human serum by headspace solid-phase microextraction using a dodecylsulfate-doped polypyrrole film coupled to ion mobility spectrometry. *J Chromatogr A*. 2008;1183(1-2):21-28.
227. Mercer J, Shakleya D, Beli S. Applications of ion mobility spectrometry (IMS) to the analysis of gamma-hydroxybutyrate and gamma-hydroxyvalerate in toxicological matrices *J Anal Toxicol*. 2006;30:539-544.
228. O'Donnell R, Xiaobo S, Harrington P. Pharmaceutical applications of ion mobility spectrometry *Trends Anal Chem*. 2008;27:44-53.

229. Lu Y, O'Donnell RM, Harrington PB. Detection of cocaine and its metabolites in urine using solid phase extraction-ion mobility spectrometry with alternating least squares. *Forensic Sci Int.* 2009;189(1):54-59.
230. Lokhnauth JK, Snow NH. Solid phase micro-extraction coupled with ion mobility spectrometry for the analysis of ephedrine in urine. *J Sep Sci.* 2005;28(7):612-618.
231. Karimi A, Alizadeh N. Rapid analysis of captopril in human plasma and pharmaceutical preparations by headspace solid phase microextraction based on polypyrrole film coupled to ion mobility spectrometry. *Talanta.* 2009;79(2):479-485.
232. Wang Y, Nacson S, Pawliszyn J. The coupling of solid-phase microextraction/surface enhanced laser desorption/ionization to ion mobility spectrometry for drug analysis. *Anal Chim Acta.* 2007;582(1):50-54.
233. Keller T, Regenscheit P, Dirnhofer R, et al. Analysis of psilocybin and psilocin in *Psilocybe subcubensis* GUZMAN by ion mobility spectrometry and gas chromatography-mass spectrometry. *Forensic Sci Int.* 1999;99:93-105.
234. Miki A, Keller T, Regenscheit P, et al. Application of ion mobility spectrometry to the rapid screening of methamphetamine incorporated in hair. *J Chromatogr B.* 1997;692:319-328.
235. Keller T, Miki A, Regenscheit P, Dirnhofer R, Schneider A, Tsuchihashi H. Detection of designer drugs in human hair by ion mobility spectrometry (IMS). *Forensic Sci Int.* 1998;94:55-63.
236. Zeeuw RA, Kode A, Kim L, Cacciaccaro L. Hair analysis by ion mobility spectrometry. *International Conference and Workshop For Hair Analysis in Forensic Toxicology.* 1995:334-350.
237. Lai H, Corbin I, Almirall JR. Headspace sampling and detection of cocaine, MDMA, and marijuana via volatile markers in the presence of potential interferences by solid phase microextraction-ion mobility spectrometry (SPME-IMS). *Anal Bioanal Chem.* 2008;392(1-2):105-113.
238. Lawrence AH. Characterization of benzodiazepine drugs by ion mobility spectrometry. *Anal Chem.* 1989;51:343-349.
239. Kanu AB, Brandt SD, Williams MD, Zhang N, Hill HH. Analysis of psychoactive cathinones and tryptamines by electrospray ionization atmospheric pressure ion mobility time-of-flight mass spectrometry. *Anal Chem.* 2013;85(18):8535-8542.
240. Sysoev AA, Poteshin SS, Chernyshev DM, et al. Analysis of new synthetic drugs by ion mobility time-of-flight mass spectrometry. *Eur J Mass Spectrom.* 2014;20(2):185-192.
241. Gwak S, Almirall JR. Rapid screening of 35 new psychoactive substances by ion mobility spectrometry (IMS) and direct analysis in real time (DART) coupled to quadrupole time-of-flight mass spectrometry (QTOF-MS). *Drug Test Anal.* 2015;7(10):884-893.
242. Armenta S, Garrigues S, de la Guardia M, et al. Detection and characterization of emerging psychoactive substances by ion mobility spectrometry. *Drug Test Anal.* 2015;7(4):280-289.
243. Kanu AB, Wu C, Hill HH. Rapid pre-separation of interferences for ion mobility spectrometry. *Analytica chimica acta.* 2008;610(1):125-134.
244. Kanu AB, Leal A. Identity Efficiency for High-Performance Ambient Pressure Ion Mobility Spectrometry. *Analytical Chemistry.* 2016;88(6):3058-3066.
245. DIN-Norm. *DIN 32645:2008-11 Chemische Analytik - Nachweis-, Erfassungs- und Bestimmungsgrenze unter Wiederholbedingungen - Begriffe, Verfahren, Auswertung.* 2008.

246. DIN-Norm. *DIN32646:2003-12 Chemische Analyse - Erfassungs- und Bestimmungsgrenze als Verfahrenskenngrößen - Ermittlung in einem Ringversuch unter Vergleichsbedingungen; Begriffe, Bedeutung, Vorgehensweise* 2003.
247. Borka WR, Dahlenburg R, Fritsch R, et al. Herleitung von Grenzwerten der "nicht geringen Menge" im Sinne des BtMG bei "neuen psychoaktiven Stoffen". *Toxichem Krimtech.* 2016;84:1-28.
248. Metternich S, Zörntlein S, Schönberger T, Huhn C. Ion mobility spectrometry as a fast screening tool for synthetic cannabinoids to uncover drug trafficking in jail via herbal mixtures, paper, food, and cosmetics. *Drug Test Anal.* 2019;11(6):833-846.
249. Yanini A, Esteve-Turrillas FA, de la Guardia M, Armenta S. Ion mobility spectrometry and high resolution mass-spectrometry as methodologies for rapid identification of the last generation of new psychoactive substances. *J Chromatogr A.* 2018;1574:91-100.
250. European Monitoring Centre for Drug and Drug Addiction. European Drug Report 2018: Trends and Developments. 2018; <http://www.emcdda.europa.eu/publications/edr/trends-developments/2018>. Accessed February 14, 2019.
251. European Monitoring Centre for Drug and Drug Addiction. Internet and drug markets. 2018; http://www.emcdda.europa.eu/publications/insights/internet-drug-markets_en. Accessed February 15, 2019.
252. Photonics H. Terahertz Spectrometer. 2019; <https://www.hubner-photonics.com/products/terahertz-technology/terahertz-spectrometers/t-cognition/>. Accessed March 01, 2019.
253. Bumbrah GS, Sharma RM. Raman spectroscopy – Basic principle, instrumentation and selected applications for the characterization of drugs of abuse. *Egyptian Journal of Forensic Sciences.* 2016;6(3):209-215.
254. CAMO Software AS. The Unscrambler User Manual. <https://www.camo.com/downloads/user-manuals.html>. Accessed August 23, 2019.
255. Metternich S, Fischmann S, Münster-Müller S, et al. Discrimination of synthetic cannabinoids in herbal matrices and of cathinone derivatives by portable and laboratory-based Raman spectroscopy. *Forensic Chem.* 2020;19:100241.
256. Takeuchi H, Harada I. Normal coordinate analysis of the indole ring. *Spectrochim Acta A.* 1986;42(9):1069-1078.
257. Miura T, Takeuchi H, I. H. Tryptophan raman bands sensitive to hydrogen bonding and side-chain conformation. *J Raman Spectrosc.* 1989;20:667-671.
258. Masayo N, Shin-ichi N, Noboru H. Electron paramagnetic resonance and optical detection of magnetic resonance studies of the lowest excited triplet states of purine, benzimidazole, and indazole in benzoic acid host crystals. *Bull Chem Soc Jpn.* 1984;57(9):2376-2382.
259. Anandhi R, Umapathy S. Resonance Raman spectroscopic studies on the conducting state of polyvinylcarbazole and its model compounds. *J Raman Spectrosc.* 1998;29(10-11):901-906.
260. Socrates G. *Infrared and Raman characteristic group frequencies.* Vol 3. West Sussex, England: John Wiley & Sons Ltd; 2001.
261. Jenkins TE, Lewis J. A Raman study of adamantane (C₁₀H₁₆), diamantane (C₁₄H₂₀) and triamantane (C₁₈H₂₄) between 10 K and room temperatures. *Spectrochim Acta A.* 1980;36(3):259-264.
262. Mayo DW, Miller FA, Hannah RW. *Course notes on the interpretation of infrared and raman spectra.* New Jersey: John Wiley & Sons; 2003.

263. Moosmann B, Angerer V, Auwärter V. Inhomogeneities in herbal mixtures: a serious risk for consumers. *Forensic Toxicology*. 2015;33(1):54-60.
264. Langer N, Lindigkeit R, Schiebel H-M, Papke U, Ernst L, Beuerle T. Identification and quantification of synthetic cannabinoids in “spice-like” herbal mixtures: update of the German situation for the spring of 2015. *Forensic Toxicology*. 2016;34(1):94-107.
265. Angerer VK. Neue psychoaktive Substanzen in der forensischen Toxikologie : synthetische Cannabinoide – eine unendliche Geschichte? *Universität Freiburg*. 2017(DOI:10.6094/UNIFR/13534).
266. Kawase K, Ogawa Y, Watanabe Y, Inoue H. Non-destructive terahertz imaging of illicit drugs using spectral fingerprints. *Opt Express*. 2003;11(20):2549-2554.
267. Davies AG, Burnett AD, Fan W, Linfield EH, Cunningham JE. Terahertz spectroscopy of explosives and drugs. *Mater Today*. 2008;11(3):18-26.
268. Kemp MC. Detecting hidden objects: Security imaging using millimetre-waves and terahertz. Paper presented at: 2007 IEEE Conference on Advanced Video and Signal Based Surveillance; 5-7 Sept. 2007, 2007.
269. Wilmink GJ, Grundt JE. Invited review article: current state of research on biological effects of Terahertz radiation. *J Infrared Millim Te*. 2011;32(10):1074-1122.
270. Akyildiz IF, Jornet JM, Han C. Terahertz band: Next frontier for wireless communications. *PhyCom*. 2014;12:16-32.
271. O. AlNabooda M, Shubair R, Rishani N, Aldabbagh G. *Terahertz Spectroscopy and imaging for the detection and identification of illicit drugs*. 2017.
272. Zeitler JA, Taday PF, Newnham DA, Pepper M, Gordon KC, Rades T. Terahertz pulsed spectroscopy and imaging in the pharmaceutical setting - a review. *J Pharm Pharmacol*. 2007;59(2):209-223.
273. McGoverin CM, Rades T, Gordon KC. Recent pharmaceutical applications of raman and terahertz spectroscopies. *J Pharm Sci*. 2008;97(11):4598-4621.
274. Jha KR, Singh G. Terahertz planar antennas for future wireless communication: A technical review. *Infrared Phys Technol*. 2013;60:71-80.
275. Siegel PH. Terahertz technology in biology and medicine. *IEEE Journal of Transactions on Microwave Theory and Techniques*. 2004;52:2438-2447.
276. Kim H, Kim KW, Park J, Han JK, Son J-H. Terahertz tomographic imaging of topical drugs. Paper presented at: Conference on Lasers and Electro-Optics 2012; 2012/05/06, 2012; San Jose, California.
277. Shen Y-C. Terahertz pulsed spectroscopy and imaging for pharmaceutical applications: A review. *J Pharm Policy Pract*. 2011;417(1):48-60.
278. Pivonka DE, Claybourn, M. , Yang, H. , Gradinarsky, L. , Johansson, J. and Folestad, S. Terahertz Spectroscopy for pharmaceutical applications. In: *Handbook of Vibrational Spectroscopy*. 2007.
279. HWU SU, SeSilva K, Jih CT. *IEEE Sensors Applications Symposium Proceedings*. 2013:171-175.
280. Federici JF, Schulin B, Huang F, et al. THz imaging and sensing for security applications—explosives, weapons and drugs. *Semicond Sci Technol*. 2005;20:266-280.
281. Hakey PM, Allis DG, Ouellette W, Korter TM. Cryogenic Terahertz spectrum of (+)-methamphetamine hydrochloride and assignment using solid-state density functional theory. *J Phys Chem A*. 2009;113(17):5119-5127.
282. Ning L, Jingling S, Jinhai S, et al. Study on the THz spectrum of methamphetamine. *Opt Express*. 2005;13(18):6750-6755.

283. Sun J-H, Shen J-L, Liang L-S, Xu X-Y, Liu H-B, Zhang C-L. Experimental investigation on Terahertz spectra of amphetamine type stimulants. *Chin Phys Lett*. 2005;22(12):3176.
284. Lu M, Shen J, Li N, et al. *Detection and identification of illicit drugs using terahertz imaging*. Vol 1002006.
285. Guangqin W, Jingling S, Yan J. Vibrational spectra of ketamine hydrochloride and 3, 4-methylene-dioxymethamphetamine in THz range. Paper presented at: 2007 Joint 32nd International Conference on Infrared and Millimeter Waves and the 15th International Conference on Terahertz Electronics; 2-9 Sept. 2007, 2007.
286. Fischer B, Hoffmann M, Helm H, Modjesch G, Jepsen P. *Chemical recognition in terahertz time-domain spectroscopy and imaging*. Vol 202005.
287. Dreizler RM, Lüdde CS. Theoretische Physik 4. In: *Statistische Mechanik und Thermodynamik*. Berlin, Heidelberg: Springer Spektrum; 2016:288-299.
288. Zurk LM, Sundberg G, Schecklman S, Zhou Z, Chen A, Thorsos EI. *Scattering effects in terahertz reflection spectroscopy*. Vol 6949: SPIE; 2008.
289. Jepsen PU, Clark SJ. Precise ab-initio prediction of terahertz vibrational modes in crystalline systems. *Chem Phys Lett*. 2007;442(4):275-280.
290. Kemp MC. Explosives detection by Terahertz Spectroscopy—A bridge too far? *IEEE Transactions on Terahertz Science and Technology*. 2011;1(1):282-292.
291. Gatesman AJ, Danylov A, Goyette TM, et al. *Terahertz behavior of optical components and common materials*. Vol 6212: SPIE; 2006.
292. Baker C, Tribe WR, Lo T, Cole BE, Chandler S, Kemp MC. *People screening using terahertz technology*. Vol 5790: SPIE; 2005.
293. Xiong W, Shen J. Fingerprint extraction from interference destruction terahertz spectrum. *Opt Express*. 2010;18(21):21798-21803.
294. Giertzuch P-L, Khodaei Y, Schubert M-H, et al. *Measuring tryptophan concentrations of aqueous solutions for cancer research using terahertz time-domain spectroscopy with metal parallel-plate waveguides*. Vol 10072: SPIE; 2017.
295. Cheville RA, Grischkowsky D. Far-infrared terahertz time-domain spectroscopy of flames. *Opt Letters*. 1995;20(15):1646-1648.
296. Day GM, Zeitler JA, Jones W, Rades T, Taday PF. Understanding the influence of polymorphism on phonon spectra: Lattice dynamics calculations and Terahertz spectroscopy of carbamazepine. *J Phys Chem B*. 2006;110(1):447-456.
297. Strachan CJ, Taday PF, Newnham DA, et al. Using Terahertz pulsed spectroscopy to quantify pharmaceutical polymorphism and crystallinity. *J Pharm Sci*. 2005;94(4):837-846.
298. King LA, Kicman AT. A brief history of ‘new psychoactive substances’. *Drug Testing and Analysis*. 2011;3(7-8):401-403.
299. Grigoryev A, Kavanagh P, Melnik A, Savchuk S, Simonov A. Gas and Liquid Chromatography-Mass Spectrometry Detection of the Urinary Metabolites of UR-144 and Its Major Pyrolysis Product. *J Anal Toxicol*. 2013;37(5):265-276.
300. Tsujikawa K, Yamamuro T, Kuwayama K, Kanamori T, Iwata YT, Inoue H. Thermal degradation of a new synthetic cannabinoid QUPIC during analysis by gas chromatography–mass spectrometry. *Forensic Toxicology*. 2014;32(2):201-207.
301. Houlihan WJ, Remers WA, Brown RK. *Indoles part one*. Canada: John Wiley & Sons, Inc.; 1972.
302. Trivedi M, Tallapragada RM, Branton A, et al. Biofield Treatment: A Potential Strategy for Modification of Physical and Thermal Properties of Indole. 2015;2.
303. Simmler L, Buser T, Donzelli M, et al. Pharmacological characterization of designer cathinones in vitro. *Br J Pharmacol*. 2013;168(2):458-470.

304. Liechti M. Novel psychoactive substances (designer drugs): overview and pharmacology of modulators of monoamine signalling *Swiss Medical Weekly*. 2015;145(w14043).
305. Majchrzak M, Celiński R, Kuś P, Kowalska T, Sajewicz M. The newest cathinone derivatives as designer drugs: an analytical and toxicological review. *Forensic Toxicol*. 2018;36(1):33-50.
306. Baumann MH, Ayestas Jr MA, Partilla JS, et al. The designer methcathinone analogs, mephedrone and methylone, are substrates for monoamine transporters in brain tissue. *Neuropsychopharmacology*. 2011;37:1192.
307. López-Arnau R, Martínez-Clemente J, Pubill D, Escubedo E, Camarasa J. Comparative neuropharmacology of three psychostimulant cathinone derivatives: butylone, mephedrone and methylone. *Br J Pharmacol*. 2012;167(2):407-420.
308. Dargan PI, Sedefov R, Gallegos A, Wood DM. The pharmacology and toxicology of the synthetic cathinone mephedrone (4-methylmethcathinone). *Drug Test Anal*. 2011;3(7-8):454-463.
309. European Monitoring Centre for Drug and Drug Addiction. Alpha-PVP. Report on the assessment of 1-phenyl-2-(pyrrolidin-1-yl)pentan-1-one (alpha-pyrrolidinovalerophenone, alpha-PVP) in the framework of the council decision on new psychoactive substances. 2016; <http://www.emcdda.europa.eu/system/files/publications/2934/>.
310. Aturki Z, Schmid MG, Chankvetadze B, Fanali S. Enantiomeric separation of new cathinone derivatives designer drugs by capillary electrochromatography using a chiral stationary phase, based on amylose tris(5-chloro-2-methylphenylcarbamate). *Electrophoresis*. 2014;35(21-22):3242-3249.
311. Dieckmann S, Pütz M, Dahlenburg R. Chiral profiling of illicit meth- amphetamine samples by capillary electrophoresis. *Toxichem Krimtech*. 2005.
312. Süß F, Sängler-van de Griend CE, Scriba GKE. Migration order of dipeptide and tripeptide enantiomers in the presence of single isomer and randomly sulfated cyclodextrins as a function of pH. *Electrophoresis*. 2003;24(6):1069-1076.
313. Stalcup AM, Gahm KH. Application of sulfated cyclodextrins to chiral separations by capillary zone electrophoresis. *Anal Chem*. 1996;68(8):1360-1368.
314. Gahm K-H, Stalcup AM. Sulfated cyclodextrins for the chiral separations of catecholamines and related compounds in the reversed electrophoretic polarity mode. *Chirality*. 1996;8(4):316-324.
315. Jain AC, Adeyeye MC. Hygroscopicity, phase solubility and dissolution of various substituted sulfobutylether β -cyclodextrins (SBE) and danazol-SBE inclusion complexes. *Int J Pharm*. 2001;212(2):177-186.
316. Nagase Y, Hirata M, Wada K, et al. Improvement of some pharmaceutical properties of DY-9760e by sulfobutyl ether β -cyclodextrin. *Int J Pharm*. 2001;229(1):163-172.
317. Rudaz S, Calleri E, Geiser L, Cherkaoui S, Prat J, Veuthey J-L. Infinite enantiomeric resolution of basic compounds using highly sulfated cyclodextrin as chiral selector in capillary electrophoresis. *Electrophoresis*. 2003;24(15):2633-2641.
318. Bergholdt AB, Jørgensen KW, Wendel L, Lehmann SV. Fast chiral separations using sulfated β -cyclodextrin and short-end injection in capillary electrophoresis. *J Chromatogr A*. 2000;875(1):403-410.
319. Altria KD, Kelly MA, Clark BJ. The use of a short-end injection procedure to achieve improved performance in capillary electrophoresis. *Chromatographia*. 1996;43(3):153-158.

320. Perrin C, Heyden YV, Maftouh M, Massart DL. Rapid screening for chiral separations by short-end injection capillary electrophoresis using highly sulfated cyclodextrins as chiral selectors. *Electrophoresis*. 2001;22(15):3203-3215.
321. Li L, Lurie IS. Regioisomeric and enantiomeric analyses of 24 designer cathinones and phenethylamines using ultra high performance liquid chromatography and capillary electrophoresis with added cyclodextrins. *Forensic Sci Int*. 2015;254:148-157.
322. Gübitz G, Schmid MG. Recent progress in chiral separation principles in capillary electrophoresis. *Electrophoresis*. 2000;21(18):4112-4135.
323. Chi L, Li Z, Dong S, He P, Wang Q, Fang Y. Simultaneous determination of flavonoids and phenolic acids in Chinese herbal tea by beta-cyclodextrin based capillary zone electrophoresis. *Microchim Acta*. 2009;167(3):179.
324. Wood DJ, Hruska FE, Saenger W. Proton NMR study of the inclusion of aromatic molecules in alpha-cyclodextrin. *J Am Chem Soc*. 1977;99(6):1735-1740.
325. Liao A-S, Liu J-T, Lin L-C, et al. Optimization of a simple method for the chiral separation of methamphetamine and related compounds in clandestine tablets and urine samples by β -cyclodextrin modified capillary electrophoresis: a complementary method to GC-MS. *Forensic Sci Int*. 2003;134(1):17-24.
326. Tagliaro F, Manetto G, Bellini S, Scarcella D, Smith FP, Marigo M. Simultaneous chiral separation of 3,4-methylenedioxymethamphetamine (MDMA), 3,4-methylenedioxyamphetamine (MDA), 3,4-methylenedioxyethylamphetamine (MDE), ephedrine, amphetamine and methamphetamine by capillary electrophoresis in uncoated and coated capillaries with native β -cyclodextrin as the chiral selector: Preliminary application to the analysis of urine and hair. *Electrophoresis*. 1998;19(1):42-50.
327. Iwata YT, Inoue H, Kuwayama K, et al. Forensic application of chiral separation of amphetamine-type stimulants to impurity analysis of seized methamphetamine by capillary electrophoresis. *Forensic Sci Int*. 2006;161(2):92-96.
328. Chinaka S, Tanaka S, Takayama N, Komai K, Ohshima T, Ueda K. Simultaneous chiral analysis of methamphetamine and related compounds by capillary electrophoresis. *Journal of Chromatography B: Biomedical Sciences and Applications*. 2000;749(1):111-118.
329. LeBelle MJ, Savard C, Dawson BA, et al. Chiral identification and determination of ephedrine, pseudoephedrine, methamphetamine and metecathinone by gas chromatography and nuclear magnetic resonance. *Forensic Sci Int*. 1995;71(3):215-223.
330. Armstrong DW, Rundlett KL, Nair UB. Enantioresolution of amphetamine, methamphetamine, and deprenyl (selegiline) by LC, GC, and CE. 1996:57-61.
331. Pütz M, Martin N. *Application of CE-ESI-MS in forensic toxicology: Identification of piperazine-derived designer drugs in Ecstasy tablets and of food colorants in illicit drugs*. 2007.
332. Elliott S. Cat and mouse: the analytical toxicology of designer drugs. *Bioanalysis*. 2011;3(3):249-251.
333. Scriba GKEV. Cyclodextrins in capillary electrophoresis enantioseparations – Recent developments and applications. *J Sep Sci*. 2008;31(11):1991-2011.
334. Wenz G, Strassnig C, Thiele C, Engelke A, Morgenstern B, Hegetschweiler K. Recognition of ionic guests by ionic β -cyclodextrin derivatives. *Chemistry – A European Journal*. 2008;14(24):7202-7211.
335. Altria K, Marsh A, Sanger-van de Griend C. Capillary electrophoresis for the analysis of small-molecule pharmaceuticals. *ELECTROPHORESIS*. 2006;27(12):2263-2282.

336. Chankvetadze B. Enantioseparations by using capillary electrophoretic techniques: The story of 20 and a few more years. *J Chromatogr A*. 2007;1168(1):45-70.
337. Vanhoenacker G, De Villiers A, Lazou K, De Keukeleire D, Sandra P. Comparison of high-performance liquid chromatography — Mass spectroscopy and capillary electrophoresis— mass spectroscopy for the analysis of phenolic compounds in diethyl ether extracts of red wines. *Chromatographia*. 2001;54(5):309-315.

Supervision and Project partners

Sonja Metternich- State Office of Criminal Investigation Rhineland-Palatinate, Forensic Science Institute, Dez. 33 Chemistry/Toxicology (Mainz, Germany) and Institute for Physical and Theoretical Chemistry, Faculty of Science, Eberhard Karls Universität (Tübingen, Germany):

I conducted all analytical measurements, method developments, sample preparation steps and evaluation of analytical data presented in this thesis. Ideas for development and optimisation of the following methods and procedures stem from me: i) solid/liquid extraction of herbal mixtures with synthetic cannabinoids as active ingredient and the PCA model together with frequency tables by Raman spectroscopy, ii) THz measurements and sample preparation, iii) all measurements of reference samples and ideas for analysis of casework samples of different matrices by Ion mobility spectrometry, iv) methods for the chiral discrimination of synthetic cathinone derivatives by CE-DAD and v) cross calibrations using UPLC-DAD. During the project I was responsible for project management and communication. Finally, I summarised the work conducted in the framework of the presented thesis. Details on the contribution in the different chapter are given below.

EU-project ADEBAR (IZ25-5793-2016-27).

Results presented in Chapter 2, 3 and 6 were achieved in the EU-project ADEBAR which was co-funded by the Internal Security Fund of the European Union (IZ25-5793-2016-27).

Almost all reference materials were provided by the EU-project ADEBAR, which were used for the development of different techniques including, Raman spectroscopy and CE-DAD.

Prof. Carolin Huhn – Institute of Physical and Theoretical Chemistry, Faculty of Science, Eberhard Karls University, (Tübingen Germany):

Prof. Carolin Huhn was the supervisor of my PhD project and conducted basic ideas, expertise, the scoping review, contributed to conceptual framework development and made revisions to all chapters.

Dr. Siegfried Zörntlein - State Office of Criminal Investigation Rhineland-Palatinate, Forensic Science Institute, Dez. 33 Chemistry/Toxicology (Mainz, Germany):

Dr. Siegfried Zörntlein was the local supervisor of my PhD project due to the external performance of my thesis at the State Office of Criminal Investigation Rhineland-Palatinate. He contributed basic ideas, scientific network for new innovations and techniques and made revisions to chapters.

Michael Pütz - Federal Criminal Police Office, Forensic Science Institute (Wiesbaden, Germany):

Michael Pütz was the local supervisor of my PhD project for the CE-DAD and Raman spectroscopy part due to the external performance of my thesis at the Federal Criminal Police Office. He contributed discussions, ideas for method development presented in this thesis and scoping review.

Dr. Torsten Schoenberger, Federal Criminal Police Office, Forensic Science Institute (Wiesbaden, Germany):

Dr. Torsten Schoenberger carried out all $^1\text{H-NMR}$ measurements for the determination of the purity of casework samples which were used as reference standards in all projects that are presented in this thesis. All sections describing details of NMR measurements stem from Dr. Schoenberger.

Dr. Svenja Fischmann, State Office of Criminal Investigation Schleswig-Holstein, Section Narcotics/Toxicology (Kiel, Germany):

Dr. Svenja Fischmann was one of the EU project leaders ADEBAR and measured all Raman spectra using the portable Raman spectrometer from BW-tech (Newark, USA).

Maren Lyczkowski, State Office of Criminal Investigation Rhineland-Palatinate, Forensic Science Institute, Dez. 33 Chemistry/Toxicology (Mainz, Germany):

The basic idea of the solid/liquid extraction for herbal mixtures for the analysis with Raman spectroscopy stems from me, Maren Lyczkowski carried out the advancement and the application of this procedure under my supervision.

Julia Schaper, State Office of Criminal Investigation Rhineland-Palatinate, Forensic Science Institute, Dez. 33 Chemistry/Toxicology (Mainz, Germany):

Julia Schaper has developed the screening method for synthetic cannabinoids using UPLC-DAD under my supervision and carried out validations for five analytes. Subsequently, I used the method for cross calibrations of synthetic cannabinoids.

Dr. Georgia Moody, Smiths Detection (London, UK):

Dr. Georgia Moody and his company provided the portable IMS (IONSCAN600) for several months and the appropriate expertise while handling the software with regard to the detection of NPS in different matrices.

Dr. Korbinian Hens, Hübner Photonics (Kassel, Germany)

Dr. Korbinian Hens and his company provided the THz spectrometer (T-COGNITION) for 2 months and the appropriate expertise while handling the software. The ability to detect NPS in packaging material was examined using this technique.

Jörn Patzak, Kilian Letzas, Günther Müller, Wittlich Prison, (Germany):

Jörn Patzak and the employees of the Wittlich prison (Germany) provided samples for the analysis by portable IMS and enabled the application of a portable IMS in prison setting to uncover drug trafficking in jail.

Own contribution in the chapters

Reference samples and casework samples

The majority of the reference materials and the casework samples (herbal mixtures) were provided by the State Office of Criminal Investigation Rhineland-Palatinate (Germany) and by the EU project “ADEBAR” which was co-funded by the Internal Security Fund of the European Union (IZ25-5793-2016-27).

Chapter 2: „Ion mobility spectrometry as a fast screening tool for synthetic cannabinoids to uncover drug trafficking in jail via herbal mixtures, paper, food, and cosmetics“

Sonja Metternich, Georgia Moody, Siegfried Zörntlein, Torsten Schönberger, Carolin Huhn

The literature search, performance of the measurements (reference samples and casework samples in different matrices), validation and construction of the database and writing of the manuscript was my contribution (100 %). The expertise in handling the IONSCAN600 software to subsequently construct a database was provided by Dr. Gerogia Moody. Torsten Schönberger carried out the quantifications of the samples (powders) which were used as reference material using NMR analysis. The project was supervised by Siegfried Zörntlein and Carolin Huhn.

Chapter 3: „Discrimination of synthetic cannabinoids in herbal matrices and of synthetic cathinone derivatives by portable and laboratory-based Raman spectroscopy“

Sonja Metternich, Svenja Fischmann, Sascha Münster-Müller, Michael Pütz, Folker Westphal, Torsten Schönberger, Maren Lyczkowski, Siegfried Zörntlein, Carolin Huhn

The literature search, performance of the measurements, evaluation of the measurement results, and writing of the manuscript was my contribution (100 %). Ideas for the solid/liquid extraction procedure development and optimization are to 100 % my own work. Maren Lyczkowski carried out the advancement and the application of this procedure including the analysis of 60 herbal mixtures using Raman spectroscopy in her Master Thesis under my supervision. Dr. Svenja Fischmann provides the Raman spectra of all substances using the portable Raman spectrometer from BW-Tech (Newark, USA). Sascha Münster-Müller provided his expertise in working with the software Unscrambler to develop a PCA model for characterisation of unknown NPS samples. Folker Westphal is responsible for the scientific leadership of the EU project ADEBAR which provide the reference material. The project was supervised by Carolin Huhn, Michael Pütz, and Siegfried Zörntlein.

Chapter 4: “Terahertz spectroscopy for the contactless and non-destructive detection of synthetic cannabinoids to uncover drug trafficking“

Sonja Metternich, Korbinian Hens, Torsten Schönberger, Carolin Huhn

The literature search, performance of the measurements and writing of the manuscript was done to 100% by me. Evaluation of the measurement results were carried out with a specified matlab script by Dr. Korbinian Hens (100%) and the interpretation of the results was my contribution (100%). Torsten Schönberger carried out the quantifications of the samples (powders) which were used as reference material using NMR analysis. The project was supervised by Siegfried Zörntlein and Carolin Huhn.

Chapter 5: „Structural similarity of synthetic cannabinoids in herbal mixtures allows to cross-calibrate analytes without reference material by UPLC-DAD“

Sonja Metternich, Julia Schaper, Siegfried Zörntlein, Carolin Huhn

The method development, the analysis of reference samples and the validation of five synthetic cannabinoids were performed by Julia Schaper during her Bachelor Thesis under my supervision. Further validations (for 15 synthetic cannabinoids) that were used for cross calibration investigation, sample analysis; data evaluation and writing of the chapter were performed by me (100%). The project was supervised by Siegfried Zörntlein and Carolin Huhn.

Chapter 6: “Chiral discrimination of NPS using CE-DAD: Enantioselective separation of synthetic cathinone derivatives by capillary electrophoresis with UV“

Sonja Metternich, Michael Pütz, Nathalie Martin, Carolin Huhn

The development of the CE-DAD methods, performance of all analyses, evaluation of data and writing were done to 100 % by me. Ideas for development of the analytical methods were based on further studies which were carried out by Michael Pütz and Nathalie Martin. The project was supervised by Michael Pütz and Carolin Huhn.

Abbreviations

ADEBAR	Aufbau analytischer Datenbanken, Erhebung und bundesweite Bereitstellung von analytischen Daten und Referenzmaterialien im Bereich neuer psychoaktiver Stoffe
APCI	Atmospheric pressure chemical ionization
BSA	Bovine serum albumin
CB1	Cannabinoid receptor type 1
CB2	Cannabinoid receptor type 2
CD	Cyclodextrin
CE	Capillary electrophoresis
DAD	Diode-array-detector
DAT	Dopamine transporter
EMCDDA	European Monitoring Centre for Drugs and Drug Addiction
EOF	Electroosmotic flow
ESI	Electrospray ionisation
EU	European Union
Fast blue BB	4-benzamido-2,5-diethoxybenzene diazonium chloride hemi zinc salt
FWHM	Full width at half maximum
GC	Gas chromatographie
HMQC	Heteronuclear Multiple-Quantum Correlation
HPLC	High-performance liquid chromatography
HP- γ -CD	(2-hydroxypropyl)- γ -cyclodextrin
HP- β -CD	(2-hydroxypropyl)- β -cyclodextrin
HQI	Hit Quality Index
HQ	Hit Quality
HS- β -CD	Highly sulfated
IC	Internal calibrant
IMS	Ion mobility spectrometry
IR	Infrared
JWH	John William Huffman (professor at Clemson University who first synthesised novel cannabinoids)
LC	Liquid chromatographie
LOD	Limit of detection
LOQ	Limit of quantification
LSD	Lysergic acid diethylamide
mCPP	1-(3-chlorophenylpiperazin)

MDMA	3,4-Methylenedioxyamphetamine
MeOH	Methanol
MS	Thin layer chromatography
NAT	Noradrenaline transporter
NMR	Nuclear magnetic resonance
NOESY	Nuclear Overhauser Effect Spectroscopy
NPS	New psychoactive substances
oCPP	1-(2-chlorophenylpiperazine)
PCA	Principal component analysis
pCPP	1-(4-chlorophenylpiperazine)
QC	Quality Control
qNMR	Quantitative nuclear magnetic resonance
R _f	Retention factor
ROI	Region of interest
rpm	Revolutions per minute
S/N	Signal-to-noise
SERS	Surface enhanced Raman spectroscopy
SERT	Serotonin transporter
SNV	Standard normal variate
SPE	Solid Phase extraction
SWGDRUG	scientific working group for the analysis of seized drugs
TDS-THz	Terahertz-Time domain spectroscopy
THC	delta 9-tetrahydrocannabinol
TLC	Thin layer chromatography
UNODC	United Nations Office on Drugs and Crime
UPLC	Ultra-Performance Liquid Chromatography
UV-Vis	ultraviolet-visible

Acknowledgement

The work conducted in the presented thesis was done at the State Office of Criminal Investigation Rhineland-Palatinate, Forensic Science Institute, Dez. 33 Chemistry/Toxicology (Mainz, Germany) and the external supervision was carried out at the Eberhard Karls University at the Institute for Physical and Theoretical Chemistry in the working group for effect-based environmental analysis.

At first, I would like to express my deep gratitude to Professor Carolin Huhn, my main supervisor, for their patient guidance, enthusiastic encouragement and useful critiques of this research work. I would like to thank her for the helpful revisions to all chapters, the brilliant scientific and methodical ideas that pave my way through the thesis and her confidence in external performing my practical work. Without her guidance and persistent help this dissertation would not have been possible.

Further I would like to thank Dr. Siegfried Zörntlein and Michael Pütz, my co-supervisors, for their valuable and constructive suggestions during the planning, development and elaboration of this research work and for the possibility to get a deep insight into the world of forensic science.

I would also like to extend my thanks to the technicians, especially Ellinor Schneider and Simone Racké, of the laboratory of department 33 of the Forensic Science Institute of the State Office of Criminal Investigation Rhineland-Palatinate and the KT 45 of the Forensic Science Institute of the Federal Criminal Police Office department for their help in handling the different techniques and the support in every aspect.

This study might have never happened without the financial aid of EU-project ADEBAR and I wish to express my gratitude to the members for discussion, cooperation and financial support during my thesis. I would like to give special thanks to Dr. Svenja Fischmann, Dr. Folker Westphal and Sascha Münster Müller for the support in the Raman spectroscopy part and Dr. Torsten Schoenberger for the NMR measurements and comments.

I want to thank my working group AG Huhn who accompanied and supported me during my processing of my dissertation via skype.

I also express my thanks to the Minister of Justice of Rhineland-Palatinate and the Wittlich Prison, especially Jörn Patzak, Kilian Letzas and Günther Müller for their trust, the reliable participation and the opportunity to implement the portable IMS to uncover drug trafficking in jail. I wish to thank Dr. Georgia Moody and Dr. Korbinian Hens for their contribution to this project and for their valuable technical support.

The completion of this thesis would not have been possible without the support of my parents and my sister for their tireless strengthening and motivation, as well as for the always open ear for mine thoughts. They encouraged me in all of my pursuits and they never stopped believing in me.

Thanks, Max.

List of Publications and scientific contributions

Talks

- Doktorandenseminar Hohenroda (2019)
„Ionenmobilitätsspektrometrie als portable Analysentechnik zur Detektion von synthetischen Cannabinoiden in unterschiedlichen Matrices wie Kräutermischungen, Papiere, Lebensmittel und Kosmetika zur Aufdeckung des Drogenhandels in Gefängnissen“
- XXI Mosbacher Symposium (2019)
“Ion mobility spectrometry as a fast screening tool for synthetic cannabinoids to uncover drug trafficking in jail via herbal mixtures, papers, food and cosmetics”
- Pressekonferenz Justizministerium “Pressekeller” (2018)
“Einsatz des IONSCAN 600 in der Justizvollzugsanstalt Wittlich“

Posters

- Analytica conference, München, Germany (2016)
- XX Mosbacher Symposium, Mosbach, Germany (2017)
“Application of Raman spectroscopy for the direct identification of synthetic cannabinoids in herbal mixtures”
- Anakon, Tübingen, Germany (2017)
“Application of Raman spectroscopy for the identification of regioisomers of Cl-MDMB-CHMICA in herbal mixtures”
- Symposium 70 Jahre Polizei, Koblenz, Germany (2017)
“Neue psychoaktive Substanzen”
- Kriminaltechnik-Messe Rheinland-Pfalz, Mainz, Germany (2018)
„Ionenmobilitätsspektrometrie als neue Methode zur Detektion von NPS“

Publications (not published)

- Sonja Metternich, Michael Pütz; Nathalie Martin, Siegfried Zörntlein, Carolin Huhn. Research article: Enantioselective separation of synthetic cathinone derivatives by capillary electrophoresis with UV detection using both normal and short-end injection mode
- Sonja Metternich, Korbinian Hens, Siegfried Zörntlein, Torsten Schönberger, Carolin Huhn. Technical note: Terahertz Spectroscopy for the contactless and non-destructive detection of synthetic cannabinoids to uncover drug trafficking

Publications (published)

- Sonja Metternich, Siegfried Zörntlein, Torsten Schönberger, Carolin Huhn. Research article: Ion mobility spectrometry as a fast screening tool for synthetic cannabinoids to uncover drug trafficking in jail via herbal mixtures, paper, food, and cosmetics. *Drug Test Anal.* 2019; 11: 833– 846. <https://doi.org/10.1002/dta.2565>
- Sonja Metternich, Svenja Fischmann, Sascha Münster-Müller, Michael Pütz, Folker Westphal, Torsten Schönberger, Maren Lyczkowski, Siegfried Zörntlein, Carolin Huhn. Research article: Discrimination of synthetic cannabinoids in herbal matrices and of cathinone derivatives by portable and laboratory-based Raman spectroscopy. *Forensic Chem.* 2020; 19: 100241. <https://doi.org/10.1016/j.forc.2020.100241>
- Sonja Metternich, Jörn Patzak. Article: Der neue IONSCAN 600: Drogenscanner der JVA Wittlich zum Aufspüren von Neuen Psychoaktiven Stoffen (NPS), *Forum Strafvollzug.* 2019, 3: 211-213. ISSN 1865-1534